

NASA/TM—2002—210005



## **SIMBIOS Project 2001 Annual Report**

*G.S. Fargion and C.R. McClain*

National Aeronautics and  
Space Administration

**Goddard Space Flight Center**  
Greenbelt, Maryland 20771

---

March 2002

## The NASA STI Program Office ... in Profile

Since its founding, NASA has been dedicated to the advancement of aeronautics and space science. The NASA Scientific and Technical Information (STI) Program Office plays a key part in helping NASA maintain this important role.

The NASA STI Program Office is operated by Langley Research Center, the lead center for NASA's scientific and technical information. The NASA STI Program Office provides access to the NASA STI Database, the largest collection of aeronautical and space science STI in the world. The Program Office is also NASA's institutional mechanism for disseminating the results of its research and development activities. These results are published by NASA in the NASA STI Report Series, which includes the following report types:

- **TECHNICAL PUBLICATION.** Reports of completed research or a major significant phase of research that present the results of NASA programs and include extensive data or theoretical analysis. Includes compilations of significant scientific and technical data and information deemed to be of continuing reference value. NASA's counterpart of peer-reviewed formal professional papers but has less stringent limitations on manuscript length and extent of graphic presentations.
- **TECHNICAL MEMORANDUM.** Scientific and technical findings that are preliminary or of specialized interest, e.g., quick release reports, working papers, and bibliographies that contain minimal annotation. Does not contain extensive analysis.
- **CONTRACTOR REPORT.** Scientific and technical findings by NASA-sponsored contractors and grantees.
- **CONFERENCE PUBLICATION.** Collected papers from scientific and technical conferences, symposia, seminars, or other meetings sponsored or cosponsored by NASA.
- **SPECIAL PUBLICATION.** Scientific, technical, or historical information from NASA programs, projects, and mission, often concerned with subjects having substantial public interest.
- **TECHNICAL TRANSLATION.** English-language translations of foreign scientific and technical material pertinent to NASA's mission.

Specialized services that complement the STI Program Office's diverse offerings include creating custom thesauri, building customized databases, organizing and publishing research results . . . even providing videos.

For more information about the NASA STI Program Office, see the following:

- Access the NASA STI Program Home Page at <http://www.sti.nasa.gov/STI-homepage.html>
- E-mail your question via the Internet to [help@sti.nasa.gov](mailto:help@sti.nasa.gov)
- Fax your question to the NASA Access Help Desk at (301) 621-0134
- Telephone the NASA Access Help Desk at (301) 621-0390
- Write to:  
NASA Access Help Desk  
NASA Center for Aerospace Information  
7121 Standard Drive  
Hanover, MD 21076-1320

NASA/TM—2002—210005



## **SIMBIOS Project 2001 Annual Report**

*Giulietta S. Fargion, Science Applications International Corporation, Beltsville, Maryland*  
*Charles R. McClain, Goddard Space Flight Center, Greenbelt, Maryland*

National Aeronautics and  
Space Administration

**Goddard Space Flight Center**  
Greenbelt, Maryland 20771

---

March 2002

Available from:

NASA Center for AeroSpace Information  
7121 Standard Drive  
Hanover, MD 21076-1320  
Price Code: A17

National Technical Information Service  
5285 Port Royal Road  
Springfield, VA 22161  
Price Code: A10

*Preface*

The purpose of this technical report is to provide current documentation of the Sensor Intercomparison and Merger for Biological and Interdisciplinary Oceanic Studies (SIMBIOS) Project activities, NASA Research Announcement (NRA) research status, satellite data processing, data product validation, and field calibration. This documentation is necessary to ensure that critical information is related to the scientific community and NASA management. This critical information includes the technical difficulties and challenges of validating and combining ocean color data from an array of independent satellite systems to form consistent and accurate global bio-optical time series products. This technical report is not meant as a substitute for scientific literature. Instead, it will provide a ready and responsive vehicle for the multitude of technical reports issued by an operational project.

The SIMBIOS Science Team Principal Investigators (PIs) original contributions to this report are in chapters four and above. The purpose of these contributions is to describe the current research status of the SIMBIOS-NRA-96 funded research. The contributions are published as submitted, with the exception of minor edits to correct obvious grammatical or clerical errors.



*Table of Contents*

1. AN OVERVIEW OF SIMBIOS PROJECT ACTIVITIES AND ACCOMPLISHMENTS DURING FY01 .....	1
2. SIMBIOS: SCIENCE TEAM AND CONTRACTS.....	5
3. SIMBIOS PROJECT DATA PROCESSING AND ANALYSIS RESULTS .....	8
4. ADAPTATION OF A HYPERSPECTRAL ATMOSPHERIC CORRECTION ALGORITHM FOR MULTI-SPECTRAL OCEAN COLOR DATA IN COASTAL WATERS .....	28
5. BIO-OPTICAL MEASUREMENTS IN UPWELLING ECOSYSTEMS IN SUPPORT OF SIMBIOS.....	31
6. SATELLITE OCEAN-COLOR VALIDATION USING SHIPS OF OPPORTUNITY .....	40
7. MERGING OCEAN COLOR DATA FROM MULTIPLE MISSIONS.....	50
8. BIO-OPTICAL AND REMOTE SENSING OBSERVATIONS IN CHESAPEAKE BAY.....	52
9. REFINEMENT OF PROTOCOLS FOR MEASURING THE APPARENT OPTICAL PROPERTIES OF SEAWATER .....	63
10. OPTIMIZATION OF OCEAN COLOR ALGORITHMS: APPLICATION TO SATELLITE AND IN SITU DATA MERGING.....	73
11. AEROSOL OPTICAL PROPERTIES OVER THE OCEANS: A SUMMARY OF THE FRSR DATABASE, CALIBRATION PROTOCOL AND MEASUREMENT UNCERTAINTIES.....	77
12. BIO-OPTICAL MEASUREMENT AND MODELING OF THE CALIFORNIA CURRENT AND SOUTHERN OCEANS .....	84
13. VARIABILITY IN OCEAN COLOR ASSOCIATED WITH PHYTOPLANKTON AND TERRIGENOUS MATTER: TIME SERIES MEASUREMENTS AND ALGORITHM DEVELOPMENT AT THE FRONT SITE ON THE NEW ENGLAND CONTINENTAL SHELF. ....	92
14. OCEAN OPTICS PROTOCOLS AND SIMBIOS PROTOCOL INTERCOMPARISON ROUND ROBIN EXPERIMENTS (SPIRREX). 99	
15. BERMUDA BIO OPTICS PROJECT .....	101
16. PLUMES AND BLOOMS: MODELING THE CASE II WATERS OF THE SANTA BARBARA CHANNEL .....	108
17. ALGORITHMS FOR PROCESSING AND ANALYSIS OF OCEAN COLOR SATELLITE DATA FOR COASTAL CASE 2 WATERS... 112	
18. FACTORS AFFECTING, AND IMPACT OF, DIAZOTROPHIC MICROORGANISMS IN THE WESTERN EQUATORIAL ATLANTIC 121	
19. HPLC PIGMENT MEASUREMENTS FOR ALGORITHM DEVELOPMENT AND VALIDATION IN SUPPORT OF THE SIMBIOS SCIENCE TEAM.....	125
20. ASSESSMENT, VALIDATION, AND REFINEMENT OF THE ATMOSPHERIC CORRECTION ALGORITHM FOR THE OCEAN COLOR SENSORS .....	130
21. MEASUREMENTS OF THE VERTICAL STRUCTURE OF AEROSOLS AND CLOUDS OVER THE OCEAN USING MICRO-PULSE LIDAR SYSTEMS.....	136
22. MEASUREMENTS AND MODELING OF APPARENT OPTICAL PROPERTIES OF OCEAN WATERS IN SUPPORT TO OCEAN COLOR DATA CALIBRATION, VALIDATION, AND MERGING.....	140

SIMBIOS Project Annual Report

23. CONTRIBUTION TO A GLOBAL CLIMATOLOGY OF SURFACE PIGMENTS FROM OCEAN COLOR SENSORS .....	147
24. CNES CONTRIBUTION TO OCEAN COLOR CALIBRATION : MULTI-SENSOR CROSS-CALIBRATION OVER DESERT SITES..	159
25. SUMMARY OF THE OSMI RADIOMETRIC CALIBRATION EFFORTS .....	164
26. EVALUATION AND IMPROVEMENT OF THE ATMOSPHERIC CORRECTION AND BIO-OPTICAL ALGORITHMS FOR THE BLACK AND BARENTS SEAS .....	170
27. VALIDATION OF SEAWIFS OCEAN AND ATMOSPHERIC PRODUCTS IN THE MEDITERRANEAN SEA .....	176

## Chapter 1

# An Overview of SIMBIOS Project Activities and Accomplishments During FY01

Charles R. McClain

*NASA Goddard Space Flight Center, Greenbelt, Maryland*

Giulietta S. Fargion

*Science Applications International Corporation (SAIC), Beltsville, Maryland*

In FY01, the SIMBIOS Project brought a number of activities to fruition and laid the groundwork for FY02 initiatives. With SeaWiFS continuing to perform well, the Terra platform and MODIS launched in December 1999, and several other global missions scheduled for launch (e.g., the Aqua platform with MODIS in 2002, the ENVISAT mission with MERIS in 2002, and ADEOS-II with GLI and POLDER in 2002), the first real opportunities to merge global data sets can be pursued. NASA HQ approved a three-year continuation of the science team (2001-2003) under an NRA and the Project Office. As it is taking some time for the MODIS team to work through the initial on-orbit processing issues, data merger-related activities within the Project Office have been in the development of data merging algorithms and software to read MODIS, development of capabilities for working with multiple global data sets in the future (i.e., OCTS-GAC reprocessing) and supporting the characterization of OSMI. These activities and accomplishments are described below.

### *SIMBIOS Science Team Support*

- a. The fifth science team meeting was held in Baltimore in January 2002 with a substantial US (SIMBIOS and MODIS PIs) and international participation, with official representation from OCTS, POLDER-I and II, MOS, MERIS, GLI, and VIIRS missions. During the meeting the team addressed atmospheric correction and bio-optical algorithms, a MODIS data merging plan for 2002, uncertainty budget and sources from in situ observation, SeaWiFS re-processing, protocols updates and international collaborations. The agenda, presentations, minutes and recommendations are posted at <http://simbios.gsfc.nasa.gov/Info/>
- b. Under a SIMBIOS NRA released in late 1999, a new science team was selected and has been funded under contracts or interagency agreements (2000-2003). The initial team consists of 19 U.S. and 12 international

investigations with additional international investigations to be added as post-NRA proposals are received and accepted (i.e., Australian and Korean proposals). Agreements with the international team members were initiated by NASA/HQ in Fall 2000 and most of them have now been signed.

- c. In October 2001 the SIMBIOS Project management conducted team performance evaluations on all investigations. Formal evaluations of investigations funded through contracts are required by the NASA Procurement Office. All investigations, with the exclusion of one, were renewed for the second year (2002).

### *Satellite Data Characterization*

- a. KOMPSAT/OSMI characterization work was done in collaboration with KARI. Joint scientific papers were presented at the Fall AGU meeting in San Francisco (Franz and Kim, 2002; Kim et al. 2002). In addition, KARI requested assistance from the Project to identify a schedule to record onboard OSMI data. Our recommendation is now implemented.
- b. The Project is hosting a NASDA representative (Mr. Tanaka) for one year (June 2001-June 2002) at NASA Goddard Space Flight Center to assist in the GLI preparations. The Project worked on a document entitled "Instrument characterization of the GLI", delivered at the GLI science team meeting in Tokyo (November 2001).

### *Satellite Data Analyses*

- a. OCTS GAC data reprocessing was completed. This was a very productive collaboration effort with NASDA and Japanese scientists. A scientific presentation was given at the Fall 2001 AGU meeting in San Francisco (Tanaka et al. 2001). OCTS-GAC data is available through the

GSFC DAAC, the SIMBIOS Project and NASDA. Descriptions of the data processing stream, OCTS-specific modification to the algorithms, and statistical comparison between OCTS & SeaWiFS can be found at: [http://seawifs.gsfc.nasa.gov/SEAWIFS/RECAL/OCTS\\_Repro1/](http://seawifs.gsfc.nasa.gov/SEAWIFS/RECAL/OCTS_Repro1/)

- b. In collaboration with KARI, SIMBIOS Project worked on: 1) evaluating the of TRW pre-launch calibration of OSMI; 2) adapting SIMBIOS software (MSL12) to process OSMI data and retrieve oceanic optical properties; 3) developing OSMI vicarious calibration using in situ (MOBY) and/or another sensor; 4) evaluating the quality of derived ocean color products. Scientific presentations were given at the Fall 2001 AGU meeting in San Francisco (Kim et al., 2001; Franz and Kim, 2001).
- c. Reception, processing, distribution of IRS-P3 MOS data continued operationally. The data is a realtime broadcast as captured at Wallops Flight Facility using a subsystem purchased from a firm in India. Therefore, the coverage is the western North Atlantic and eastern continental U.S. and Canada. When the spacecraft is configured for MOS data collection (periods of space data collection using another instrument precludes MOS operations), the data is captured, networked to the Project Office, processed, and distributed on-line via a browse capability. Presentations on long-term intercomparison on MOS and SeaWiFS were given at the MOS workshop in Berlin and at the Fall AGU in San Francisco (Franz and Gales, 2001; Gales and Franz 2001).
- d. The calibrations of the OCTS and POLDER using MOBY comparisons and the SeaWiFS atmospheric correction scheme were completed and published (Wang et al. In press).

#### *Sunphotometer Data Acquisition*

- a. A total of 14 coastal and island SIMBIOS CIMEL stations (1998-2001) were contributed to the NASA AERONET network. This year marks the end of Project supported AERONET coastal and island CIMEL sites. Starting from January 2002, the SIMBIOS CIMELs will be operated and be maintained by AERONET.
- b. This year, SIMBIOS CIMEL sun photometer data were used by the community in more than 20 scientific papers.
- c. PREDE characterization and instrument hardening are ongoing. PREDE and MPL were deployed during ACE-ASIA international campaign.
- d. All sun photometer calibrations are done at GSFC. A consistent end-to-end data processing procedure was developed for the suite of sun photometers that provide data to the Project. The different instruments include the Microtops hand-held instrument, CIMEL, the Brookhaven shadow-band radiometer, SIMBAD, and PREDE. The analysis procedures include calibration, derived product generation, quality control, archival in SeaBASS, and

satellite match-up analyses. The procedures are documented in a NASA technical memorandum published in early 2001 (Fargion, Barnes and McClain 2001) and scientific papers presented at the Fall 201 AGU meeting in San Francisco (Pietras et al. 2001; Knoelspiesse et al. 2001).

- e. Global Marine Atmosphere Database: The Project began work with Dr. Frouin (SIO), Dr. Miller (BNL) and AERONET to create an AOT database in order to develop alternative atmospheric models from those of Shettle and Fenn.

#### *Bio-Optical Data Evaluation And Synthesis*

- a. Multisensor in-situ bio-optical and atmospheric match-up analysis routines are in place for MOS, SeaWiFS, OCTS-GAC, OSMI and MODIS (Bailey et al. 2001).
- b. The SeaBASS data volume continues to grow steadily as Science Team members and others submit new data sets. A new SeaBASS data archive and relational database were developed (Werdell et al. 2001). We now have password-protected and public SeaBASS archive versions. Public data is currently from 1975 to 1999 and includes all data collected by the first SIMBIOS Team. An agreement is in place between the National Oceanographic Data Center (NODC) and the Project for the distribution of the SeaBASS CD-ROM and data archive depository. All SeaBASS data collected prior to 31 December 1999 has been submitted to NODC.
- c. The sun photometer data from the coastal CIMEL sites and the shipboard observations are also being ingested into the archive. Data quality control tests are being refined and automated in order to keep up with the increasing volume of new data. In order to make SeaBASS more efficient and easier to use, the archive was redesigned and rebuilt over the past year.
- d. The *in situ* measurement protocols were updated, expanded (*version 3*) and are in press (Mueller and Fargion, 2002). The format of this protocol manual was changed so that specific topics were included as chapters with different groups of authors for each chapter.

#### *Data Merging*

- a. Algorithms for combined extraction and processing of MODIS and SeaWiFS bins have been developed. The Project has collaborated with University of Miami (Dr. Evans) on the comparison of MODIS and SeaWiFS ocean color retrievals for overlapping bins with water-leaving radiance and chlorophyll products.
- b. A Neural Network (NN) merging technique was applied to SeaWiFS-MODIS (level 3), and a wavelet merging technique was applied to SeaWiFS-MOS (level 2). A scientific presentation was given at the Fall 2001 AGU meeting in San Francisco (Kwiatkowska-Ainsworth, 2002).

- c. A diagnostic data set was implemented at different ocean sites and is intended to facilitate future data merging activities. The regions were discussed at several SIMBIOS Team and IOCCG meetings. Approximately 30 SeaWiFS ocean sites were implemented for this purpose as a collaboration of SeaWiFS and SIMBIOS Projects. We had constant and large browse and data download traffic of these ocean sites. MOS and OCTS-GAC diagnostic data sets will be made available in winter 2002.
- a. The Project organized a special session at the Fall AGU meeting (13-14 December, 2001) on "Calibration and Validation Efforts Under Way by the Ocean Color Missions". We had a full day oral session and a ½ day poster session. A substantial number of US and international SIMBIOS investigators participated. For more information see: <http://agu.org/meetings>
- b. Project staff provided technical support for MODIS and OSMI processing in the SeaWiFS Data Analysis System (SeaDAS). The SIMBIOS and SeaWiFS Projects also provided system administration, software maintenance, and hardware upgrade support to the SeaDAS program.

### Radiometric Data Quality Assurance

- a. SIMBIOS Radiometric Intercomparison (SIMRIC-1) was performed as a round robin in which radiance was measured at 5 laboratories and at 3 companies (Satlantic Inc., Biospherical Instruments Inc., HOBI Labs) with the NIST-calibrated SXR-II. Agreement was always (with one exception) within combined uncertainties (about +/- 2%). Spectralon bi-directional reflectance factors are an important source of uncertainty. A scientific presentation was given at the Fall 2001 AGU meeting in San Francisco (Meister et al., 2002).
- b. SeaWiFS transfer Radiometer (SXR-II) was calibrated with SIRCUS at NIST in December 2000 and December 2001.
- c. The SXR-IIx was monitored from November 2000 to December 2001 by a portable light source, the SQM-II (~ 50 HiBank and ~ 50 LoBank mode measurements).
- d. SXR-II measurements were made of the following sources: NIST NPR, GSFC Hardy and Code 916 sphere (6 times or more).
- e. The Project participated in EOS and NIST radiometric intercomparison round robin at GSFC (April 2001).
- c. This year, the SIMBIOS Project sent representatives to 12 national and international conferences and workshops, in addition to MODIS and NIST workshops.

With these accomplishments, the SIMBIOS Project is well positioned to undertake a number of new initiatives in 2002. These include, but are not limited to, the following:

- Continuing work on MODIS with the MODIS Oceans Team and GSFC DAAC: match-up in situ parameter comparison (L2); MODIS/SeaWiFS comparison (L3) and coordination of the MODIS diagnostic data set.
- Continuing work on data merger by Project staff (L3): Neural Networks and other techniques including implementation of code from the Maritorena and Gregg merging activities.
- Begin preparations for the ADEOS-II/GLI/POLDER and ENVISAT/MERIS missions: sensor characterization and data format information and planning of international cruises.
- Conclude the collaboration with KARI on the KOMPSAT/OSMI calibration data and sensor characterization
- Conclude the work with the MOS Science Team on the use of MOS for linking the SeaWiFS with the ADEOS-I OCTS and POLDER time series
- Rebuild and release the SeaBAM data set
- First release of the Global Marine Atmosphere Database: QC and uncertainty
- Assist the NASA SeaDAS group with incorporating OSMI processing capabilities into SeaDAS
- SIMBIOS NODC CD-ROM release in spring 2002.

### Support Services

- a. The Project Office provided cruise support (satellite coverage information, near-realtime data products, instrument pool, etc.) to 282 cruises to date (not all by Science Team members) including ACE-Asia (2-month) and a SIMBIOS Validation Study (6-month) in the Atlantic Ocean and Antarctic on the R/V Akademik Ioffe. This campaign is in collaboration with Russian scientists. The Project provides to the ocean color community satellite over-flight prediction support for SeaWiFS, MODIS, MOS, OCI, OCM and OSMI, in addition to near real-time SeaWiFS Level-1, 2 images in support of on-going cruises.
- b. Image browser may be used with SeaWiFS, MOS, OCTS-GAC or OSMI data sets.
- c. Sun photometer instrument pool deployments were made for 14 MicroTops, 2 PREDE, 1 SIMBAD and 2 SIMBADA.

### Outreach

## REFERENCES

- Bailey, S. W., J. Werdell and C. R. McClain, 2001: Validation of Satellite-Derived Ocean Color: Theory and Practice, *EOS. Trans. AGU*, 82(47), Fall Meet., Suppl., Abstract OS52A-0520, 2001.
- Fargion, G. S., and J. L. Mueller, 2000: Ocean Optics for Satellite Ocean Color Sensor Validation, Revision 2,

- NASA/TM-2000-209966, NASA Goddard Space Flight Center, Greenbelt, MD, 184 pp.
- Franz B. A. and J. M. Gales, 2001: A Long Term Intercomparison of MOS and SeaWiFS, 4<sup>th</sup> Berlin Workshop on Remote Sensing "5Years of MOS-IRS", 9-16.
- Gales J., B. Franz and M. Wang, 2001: A Three Year Intercomparison of Oceanic Optical Properties from MOS and SeaWiFS, *EOS. Trans. AGU*, **82(47)**, Fall Meet., Suppl., Abstract OS52A-0513, 2001.
- Knobelspiesse K., C. Pietras and G.S. Fargion, 2001: MicroTops II Hand-held Sun Photometers Sun Pointing Error Correction for Sea Deployment, *EOS. Trans. AGU*, **82(47)**, Fall Meet., Suppl., Abstract OS52A-0532, 2001.
- Kwiatwska-Ainsworth, 2001; Merger of Ocean Color Information of Different Spatial Resolution: SeaWiFs and MOS, *EOS. Trans. AGU*, **82(47)**, Fall Meet., Suppl., Abstract OS52A-0514, 2001.
- Mueller J.L., and G.S Fargion, 2002: Ocean Optics for Satellite Ocean Color Sensor Validation, Revision 3, NASA/TM-2002, NASA Goddard Space Flight Center, Greenbelt, MD, in press.
- Pietras C. et al. 2001: Aerosol Properties Derived from the PREDE POM-01 Mark II Sun Photometer, *EOS. Trans. AGU*, **82(47)**, Fall Meet., Suppl., Abstract OS52A-0531, 2001.
- Wang, M., A. Isaacman, B.A. Franz, and C.R. McClain, 2002: Ocean Color Optical Property Data Derived from OCTS and POLDER: A Comparison Study, *Appl. Opt.* (in press).
- Werdell P. J., S. W. bailey and G.S. Fargion, 2001: The Architecture and Utility of SeaBASS: the SeaWiFS Bio-Optical Archive and storage System, *EOS. Trans. AGU*, **82(47)**, Fall Meet., Suppl., Abstract OS52A-0533, 2001.

Table 1.1 SIMBIOS Project Personnel

Ewa Ainsworth	SAIC
Sean Bailey*	FutureTech Corporation
Robert Barnes *	SAIC
Patty Clow *	NASA
Giulietta Fargion	SAIC
Gene Feldman *	NASA
Bryan Franz *	SAIC
Joel Gales*	FutureTech Corporation
Lynne Hoppel *	NASA
Kirk Knobelspiesse*	SSAI Corporation
Sung Lee *	SAIC
Kathy Lingerfelt*	NASA
Charles McClain *	NASA
Gerhard Meister	FutureTech Corporation
Kevin Miller*	FutureTech Corporation
Fred Patt *	SAIC
Christophe Pietras	SAIC
India Robinson *	NASA
Paul Smith *	SAIC
Judy Stubblefield*	SAIC
Tamara Tucker *	SAIC
Jeremy Werdell*	SSAI
Bill Woodford*	FutureTech Corporation

\* shared with SeaWiFS Project

## Chapter 2

# SIMBIOS: Science Team and Contracts

Giulietta S. Fargion

*Science Applications International Corporation (SAIC), Beltsville, Maryland*

### 2.1 SCIENCE TEAM

The Science Team is selected through a NASA Research Announcement (NRA). Presently, NASA has had two NRA's, in 1996 and 1999. NASA HQ manages the process of team selection, but the Goddard Space Flight Center (GSFC) NASA Procurement Office handles the team contracts, work statements and, if necessary, budget negotiations. The Project funds numerous US investigators and collaborates with several international investigators, space agencies (e.g., NASDA, CNES, KARI, etc.) and international organizations (e.g., IOCCG, JRC). US investigators under contract provide *in situ* atmospheric and bio-optical data sets, and develop algorithms and methodologies for data merger schemes. NASA GSFC Procurement requires formal evaluations for all contracts at the end of each contract year. These evaluations are to go into a database and are shared with the PI's institution or upper management.

The locations of specific SIMBIOS team investigations (i.e., NRA-99) are shown in Figures 2.1. The international ocean color community response for the NRA-99 was overwhelming, with a total of 75 PI's attempting to collaborate with the Project group in twelve proposals. The twelve international proposals cover topics ranging from protocols, calibration-validation activities, atmospheric-biological algorithms, and data merging.

The SIMBIOS Science Team (NRA-96) meetings were held in August 1997 at Solomons Island (Maryland), in September 1998 at La Jolla (California) and in September 1999 at Annapolis (Maryland). Meanwhile, the SIMBIOS Science Team's (NRA-99) meeting will be held in January 2001 at GSFC in Greenbelt, Maryland and in January 2002 at the Marriott (BWI), Baltimore, Maryland.

In general, all Science Team members, US and international, were in attendance or were represented by one of their staff. Also, the IOCCG and MODIS Teams are invited, and most attended or sent representatives. During each year the Project Office has fostered international collaborations by hosting visiting scientists at GSFC. These visits lasted from one week to several months. For international participants, the Project provided partial or as-needed travel support to team meetings or to collaborate with the project on specific topics such as calibration, and product evaluations.

The fifth science team meeting (January 2002) was the most attended, participation reached over 90 scientists (Figure 2.2). The team had a substantial US (SIMBIOS and MODIS PIs) and international participation, with official representation from OCTS, POLDER-I and II, MOS, MERIS, GLI, and VIIRS missions. During the meeting the team addressed atmospheric correction and bio-optical algorithms, a MODIS data merging plan for 2002, uncertainty budget and sources from *in situ* observation, SeaWiFS re-processing, protocols updates and international collaborations. The agenda, presentations, minutes and recommendations are posted at <http://simbios.gsfc.nasa.gov/Info/>

Chapters 4 to 21 contain the individual PI's contributions and describe the funded research topics, field studies activities, and results of concluded research. These chapters are reproduced as submitted with minimal editing by the Project Office.

### 2.2 CONTRACT OVERVIEW

The second-year of the SIMBIOS NRA-99 contracts ended on November 30, 2000. The SIMBIOS Project scheduled a telephone conference (telecon), of about 30-45 minutes, with each PI and other appropriate staff during the month of October. Prior to the telecon, the SIMBIOS Project reviewed each contract, the statement of work, and the agreed to deliveries. The Project Office followed the same procedure used in 1999 and coordinated an inside panel with key contract and project personnel to perform an across-the-board evaluation of all funded contracts (Table 2.1).

Table 2.1 Contract evaluation key personnel

Contracting Officer:	Lynne Hoppel
Contracting Assistant:	Kathy Lingerfelt
Resource/Financial Officer:	Patty Clow
Manager, SIMBIOS Project:	Giulietta Fargion
Manager, Office for Global Carbon Studies:	Charles McClain

The four categories to be evaluated are suggested in the "Evaluation of Performance" from the Federal Acquisition Regulation (FAR) 42.15 and NASA FAR Supplement (NSF)

SIMBIOS Project Annual Report

1842.15 or NASA form 1680 used by GSFC. Under the “quality” category the following are considered:

- data quality and completeness;
- ancillary information provided on the data (metadata);
- the data's usefulness in relation to SIMBIOS goals, i.e., calibration, validation, and algorithm development; and
- quality of technical reports.

The “time” category is a mixed bag, but is viewed with respect to data and documentation (monthly and year-end reports, and special topic publications) and delivery times. Under the “other” category is considered:

- scientific publications and scientific achievements;
- science team collaboration and involvement; and
- other significant events occurring during the contract period evaluated.

As a result of the formal evaluation and telecon with the SIMBIOS PIs, all but two investigators were evaluated as good or very good. The GSFC Procurement Office implemented and executed 12 second-year options, closed one contract, and gave a 1-month no cost extension to one contract. Presently, the Project has in place 12 contracts, 3 interagency agreements and 2 NASA investigations. Further details on the research status and progress reports can be found on our web site at <http://simbios.gsfc.nasa.gov/status.html>.

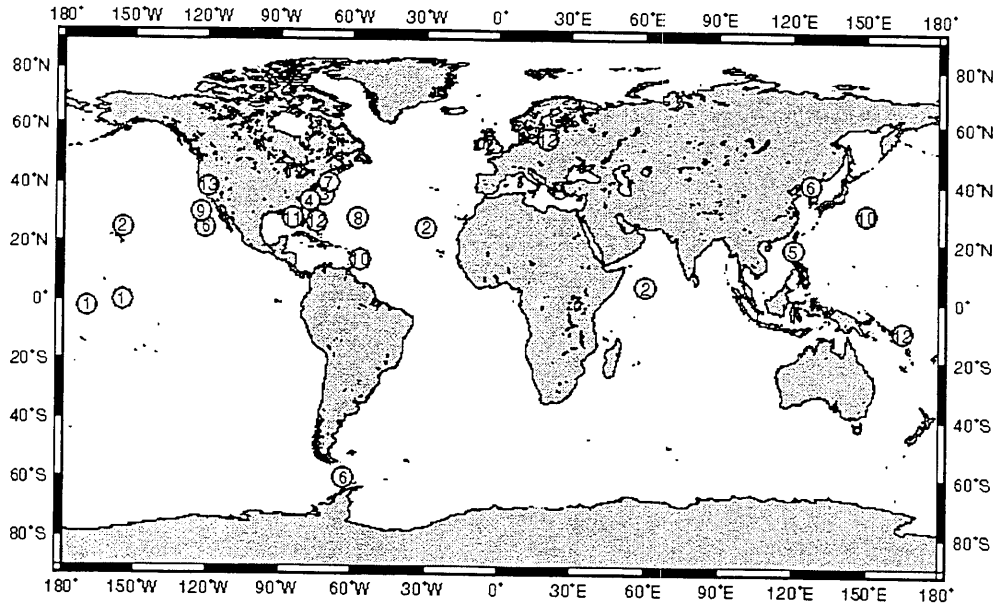


Figure 2.1: Global distribution of the NRA-99 selected SIMBIOS studies. United States (field): (1) Chavez; (2) Frouin; (3) Gao; (4) Harding; (5) Miller; (6) Mitchell; (7) Morrison; (8) Nelson; (9) Siegel; (10) Spinhirne; (11) Stumpf; (12) Subramaniam; (13) Zalewski. United States (theoretical, protocols, or team support): Gregg; Hooker; Maritorena; Mueller; Trees and Wang. International: Antoine; Bohm; Chen; Deschamps; Fougne; Fukushima; He; Li; Ishizaka; Kim; Kopelevich; Lynch; Tang and Zibordi.



Figure 2.2: SIMBIOS Science Team Meeting in Baltimore (January 15-16-17, 2002).

## Chapter 3

# SIMBIOS Project Data Processing and Analysis Results

Giulietta Fargion, Bryan Franz, Ewa Kwiatkowska-Ainsworth, Christophe Pietras and Paul Smith  
*Science Applications International Corporation (SAIC), Beltsville, Maryland*

Sean Bailey, Joel Gales and Gerhard Meister  
*FutureTech Corporation, Greenbelt, Maryland*

Kirk Knobelspiesse and Jeremy Werdell  
*Science Systems and Applications Inc., Greenbelt, Maryland*

Charles McClain and Gene Feldman  
*NASA Goddard Space Flight Center, Greenbelt, Maryland*

### 3.1 INTRODUCTION

The SIMBIOS Project is concerned with ocean color satellite sensor data intercomparison and merger for biological and interdisciplinary studies of the global oceans (Barnes et al., 2000). Imagery from different ocean color sensors (OCTS, POLDER, SeaWiFS, MOS and OSMI) can now be processed by a single software package using the same algorithms, adjusted by different sensor spectral characteristics, and the same ancillary meteorological and environmental data. This enables cross-comparison and validation of the data derived from satellite sensors and, consequently, creates continuity in ocean color information on both the temporal and spatial scale. The next step in this process is the integration of *in situ* ocean and atmospheric parameters to enable cross-validation and further refinement of the ocean color methodology. The SIMBIOS Project Office accomplishments during 2001 year are summarized under (a) satellite data processing, (b) data merging (c) SeaBASS database, (d) supporting services, (e) sun photometers and calibration activities and (f) calibration round robins. These accomplishments are described below.

### 3.2 SATELLITE DATA PROCESSING

#### 3.2.1 Satellite Characterization

The SIMBIOS Project has worked closely with our colleagues in the OSMI Program and with the instrument manufacturer to define and assemble the instrument performance characteristics required for the lookup tables for the algorithms that determine OSMI top-of-the-atmosphere radiances. Of special importance in this regard are the spectral responses of the OSMI bands and the spatial co-registration of

the detectors. In addition, the Project has opened a collaboration with the GLI Program. GLI is scheduled for launch no sooner than November 2002. The GLI/SIMBIOS collaboration has centered on the characteristics of the GLI scan mirror as a function of scan angle and the normalization of detector-to-detector gain differences in the GLI bands. Plans are underway for a cross-calibration of the GLI and SeaWiFS near infrared bands, which are used for the determination of the aerosol type and amount for the atmospheric correction algorithms.

#### 3.2.2 MOS Data Collection, Processing, and Distribution

Since February of 1999, the SIMBIOS project has been operating a receiving station at NASA's Wallops Flight Facility (WFF) to acquire data from the German Modular Optoelectronic Scanner (MOS) onboard the Indian IRS-P3 spacecraft. When a pass is acquired at Wallops, the raw files are transferred to the SIMBIOS project at NASA's Goddard Space Flight Center via an automated FTP process. The raw files are then converted to Level-0 format through a software package provided by the Indian Space Research Organization (ISRO). The resulting Level-0 files are made available to the German Remote Sensing Data Centre (DLR-DFD) for archive and distribution. In addition, the SIMBIOS project is processing the data through Level-1B using the standard software provided by the German Institute for Space Sensor Technology (DLR-ISST) (Neumann et al., 1995). All data processed by the SIMBIOS project is made available through the MOS browse system at <http://simbios.gsfc.nasa.gov/oceancolor.html>. The Level-1B data can be processed to Level-2 using SIMBIOS-developed software tools distributed through SeaDAS.

### Comparison with SeaWiFS

The SIMBIOS project developed an automated process to perform sensor-to-sensor intercomparisons using the online archive of MOS data from Wallops and the SeaWiFS HRPT data from the GSFC groundstation. MOS scenes are first reprocessed to Level-1B to ensure the latest calibration has been applied, and then the meta-data of each 200 x 200 km scene segment is examined to determine the observation time, geographic area, and percentage of visible ocean pixels. If the scene segment contains at least 80% ocean pixels and no more than 20% cloud pixels, the process proceeds to perform a database search for potential SeaWiFS file matchups. Once a valid SeaWiFS match is located, the area corresponding to the MOS scene segment is identified in terms of pixel and scan limits within the SeaWiFS scene, and both subscenes are processed to Level-2 using MSL12.

Match-up results from this automated analysis are shown in Figure 3.1. Each point in the scatter plot represents the

average water-leaving reflectance of MOS versus SeaWiFS within each match-up scene, for the spectral channels near 412, 443, 490, 510, and 555 nm. The selected scenes represent various locations off of the U.S. East Coast, for various times throughout the years 1999 through 2001. These results demonstrate that the Gordon and Wang atmospheric correction scheme (Gordon and Wang, 1994), in conjunction with a sensor cross-calibration, can provide comparable water-leaving reflectance retrievals from two independent sensors observing at different times within the day. The last panel of Figure 3.1 is a color-color diagram comparing a typical ocean color band ratio between the two sensors. The band ratios are in good agreement with an  $r^2$  of 0.72, indicating that comparable ocean color retrievals can be derived.

This work was presented at the 4th Berlin Workshop on Ocean Remote Sensing in June of 2001, and a poster presentation was made at the Fall meeting of the American Geophysical Union in December of 2001.

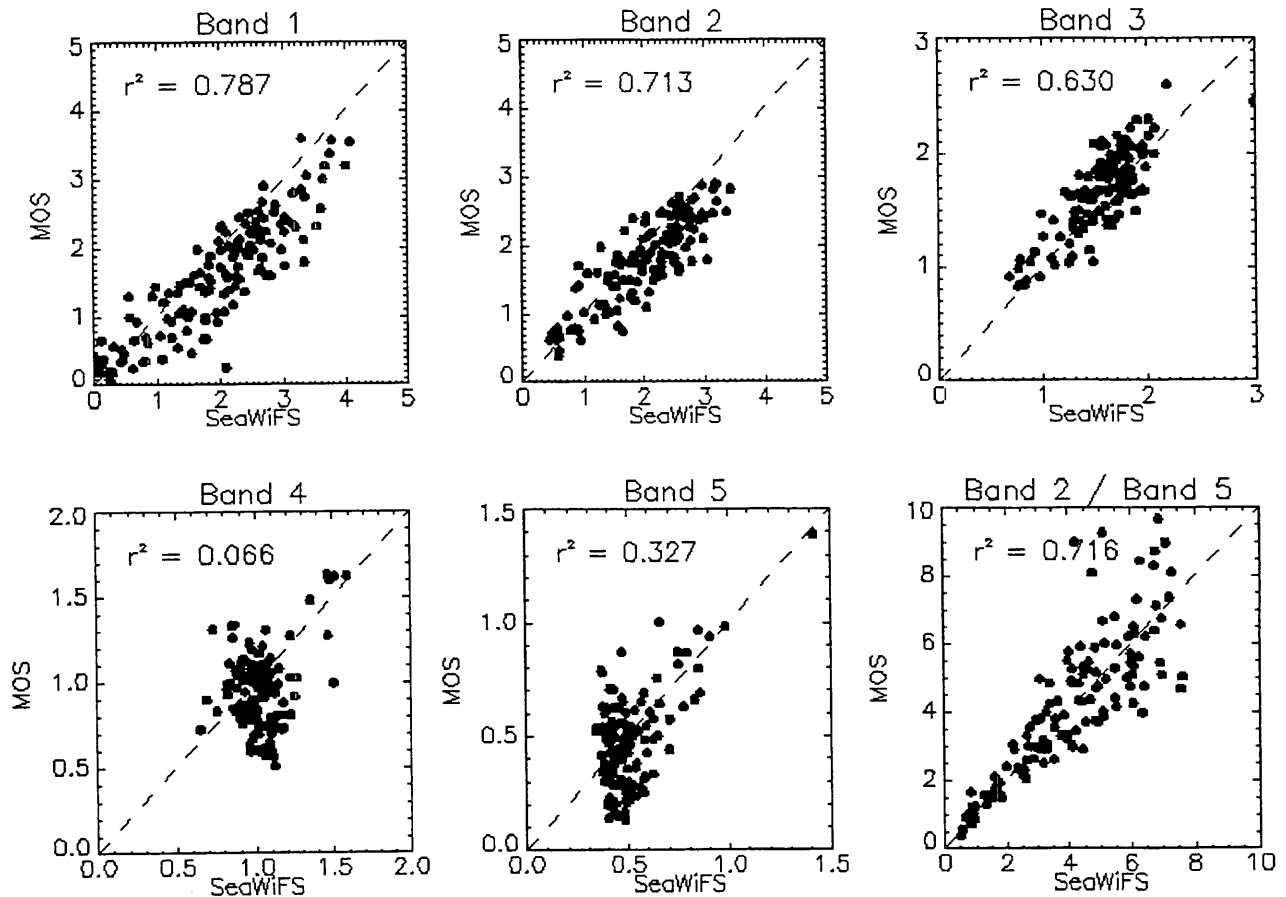


Figure 3.1: Scene-averaged match-up results for MOS versus SeaWiFS, at each SeaWiFS band. The last panel shows the comparison of band ratios, for a typical ratio used to characterize ocean color.

### 3.2.3 OCTS Calibration and Processing

On request by and in collaboration with NASDA, the SIMBIOS Project acquired the entire OCTS GAC Level-1A archive and processed the data through Level-3 using the same software employed for SeaWiFS processing. The goal of this effort was to enhance the consistency of the OCTS and SeaWiFS global datasets by minimizing calibration and processing algorithm differences between the two missions. Like SeaWiFS, the OCTS data was vicariously calibrated to MOBY (Wang et al., 2001). The Level-2 processing was performed using MSL12, with algorithms and output formats nearly identical to standard SeaWiFS processing, and Level-3 processing was performed using standard SeaWiFS space and time binning software. The OCTS products generated by SIMBIOS have been distributed to the Goddard DAAC.

Figure 3.2 shows a comparison of global monthly chlorophyll concentration for both the NASDA and SIMBIOS-derived products. The results indicate that, relative to NASDA processing, the SIMBIOS-retrieved chlorophyll concentrations are lower in high chlorophyll waters and higher in low chlorophyll waters. This is primarily due to the change in chlorophyll algorithms (NASDA's OCTS-C versus an OCTS variant of O'Reilly's OC4 algorithm) and the use of an iterative correction for non-zero water-leaving radiances in the near infrared.

### Comparison to SeaWiFS and Future Activities

Comparative studies of OCTS and SeaWiFS products were performed at several, relatively homogenous ocean regions. A comparison of seasonal variability between the two missions for two such regions in the northern and southern Pacific is shown in Figure 3.3. The SeaWiFS results show very good annual repeatability in the seasonal cycle, suggesting that these regions are not significantly influenced by inter-annual events such as El Niño/La Niña. The OCTS results for the same region show similar trends, but the chlorophyll concentrations are generally about 30% lower than SeaWiFS. This may be due to differences in the vicarious calibration, as the MOBY dataset from the OCTS mission time-frame was limited in quantity and quality.

One possible solution to the vicarious calibration differences between OCTS and SeaWiFS is to simply cross-calibrate the two instruments. This could be done by selecting one or more regions of the ocean where the optical properties are expected to be stable from year to year, and forcing the retrieved OCTS water-leaving radiances to match the average seasonal variability observed by SeaWiFS.

Another possible approach to cross-calibration or cross-mission validation is to make use of the MOS instrument, which spans the lifetimes of both the OCTS and SeaWiFS missions. The MOS instrument has already been cross-calibrated to SeaWiFS (Wang & Franz, 2000), so it would be interesting to see how well the oceanic optical properties

retrieved from MOS compare with OCTS. The SIMBIOS Project has acquired a large set of MOS data from 1997, and the Project has been collecting MOS data directly from the spacecraft since February 1999 (Franz, 2000), so the data is available and it is expected that this multi-instrument comparison will be performed in the near future.

### 3.2.4 OSMI Calibration and Processing

On request by and in collaboration with the Korea Aerospace Research Institute (KARI), the SIMBIOS Project began an evaluation of the calibration and data quality of the Ocean-Scanning Multi-Spectral Imager (OSMI), which is currently flying on KOMPSAT. OSMI is a whisk-broom scanning Charge Coupled Device (CCD) with 192 detectors oriented along track and six programmable spectral channels in the visible and near infrared. The instrument has a ground resolution of approximately 1 km with a swath width of 800 km. OSMI was launched on 21 December 1999 into a 685 km sun-synchronous polar orbit with an ascending equatorial crossing near 11:00 a.m. local time.

Using the pre-launch calibration and standard atmospheric correction software developed for OSMI, it was found that the sensor was not able to retrieve reasonable ocean optical properties. To allow for meaningful comparisons between OSMI and SeaWiFS, it was necessary to first modify the SIMBIOS atmospheric correction software, MSL12, to accept and process the OSMI data, thereby ensuring consistent and proven algorithms. The SeaWiFS normalized water-leaving radiance measurements and aerosol optical thickness retrievals from a clear scene over Hawaii were then used as truth data to enable a vicarious calibration of the 192 independent CCD elements of each OSMI spectral band.

### Comparison with SeaWiFS and Future Activities

Figure 3.4 shows averaged water-leaving radiance, chlorophyll, and aerosol optical thickness retrievals from both OSMI and SeaWiFS, for a 1-deg square region near Hawaii. The black symbols are the four-year SeaWiFS record, and the red symbols are the available OSMI scenes. These results show that, using the standard SIMBIOS atmospheric correction approach (Gordon and Wang, 1994) in conjunction with an instrument cross-calibration, it is possible to retrieve oceanic optical properties from OSMI which are in good agreement with SeaWiFS, on average.

It remains to be seen whether the OSMI instrument is stable over time. Artifacts such as detector striping and banding are visible in the OSMI scenes, and they appear to vary over time. A more detailed analysis will be required to better characterize and remove these effects. The software and calibration files created by the SIMBIOS Project have been supplied to KARI, and it is expected that they will be able to use these tools to advance their understanding of the OSMI instrument and further improve the calibration.

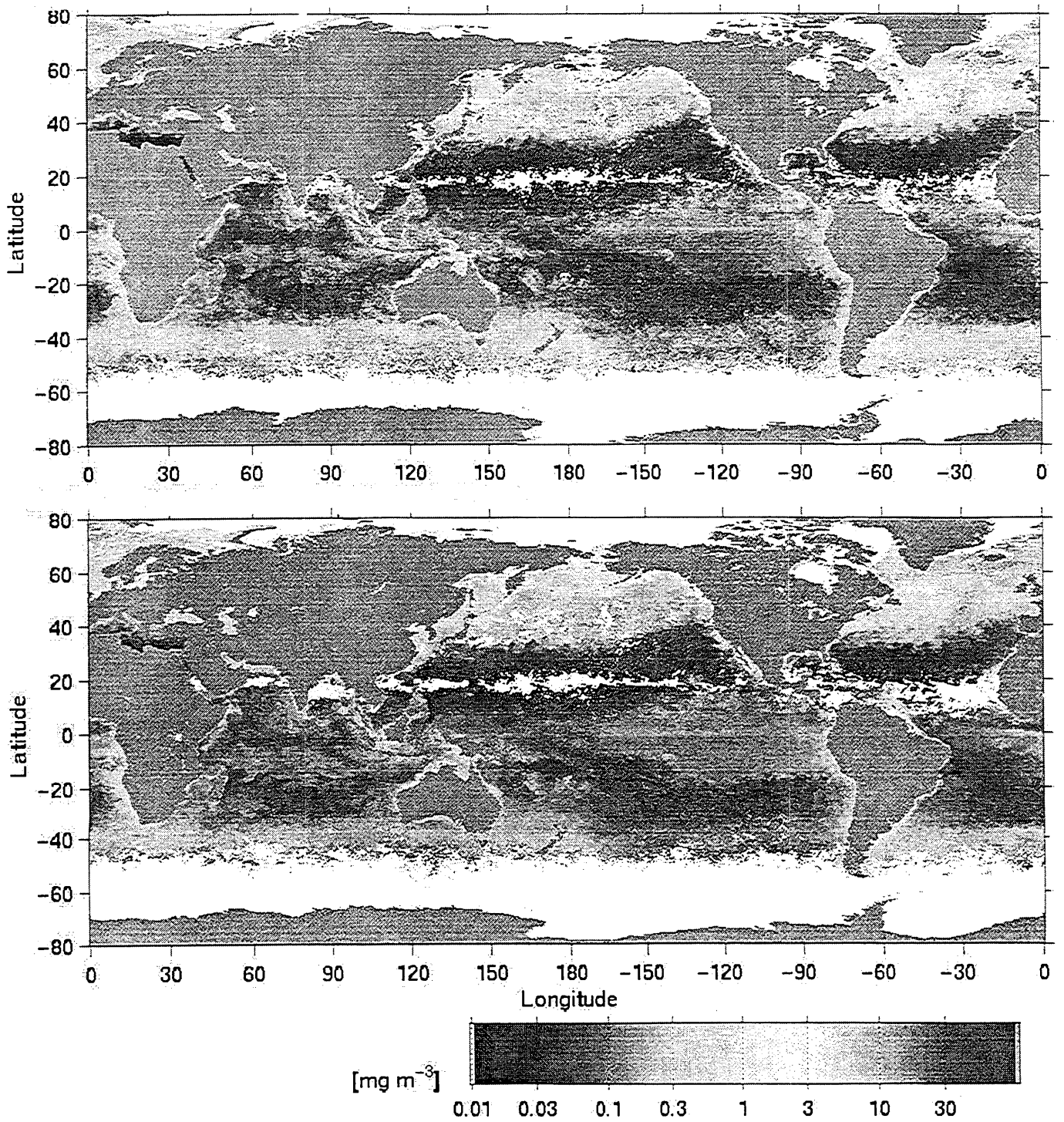


Figure 3.2: May 1997 global monthly chlorophyll retrievals from NASDA version 4 (top) and SIMBIOS processing (bottom).

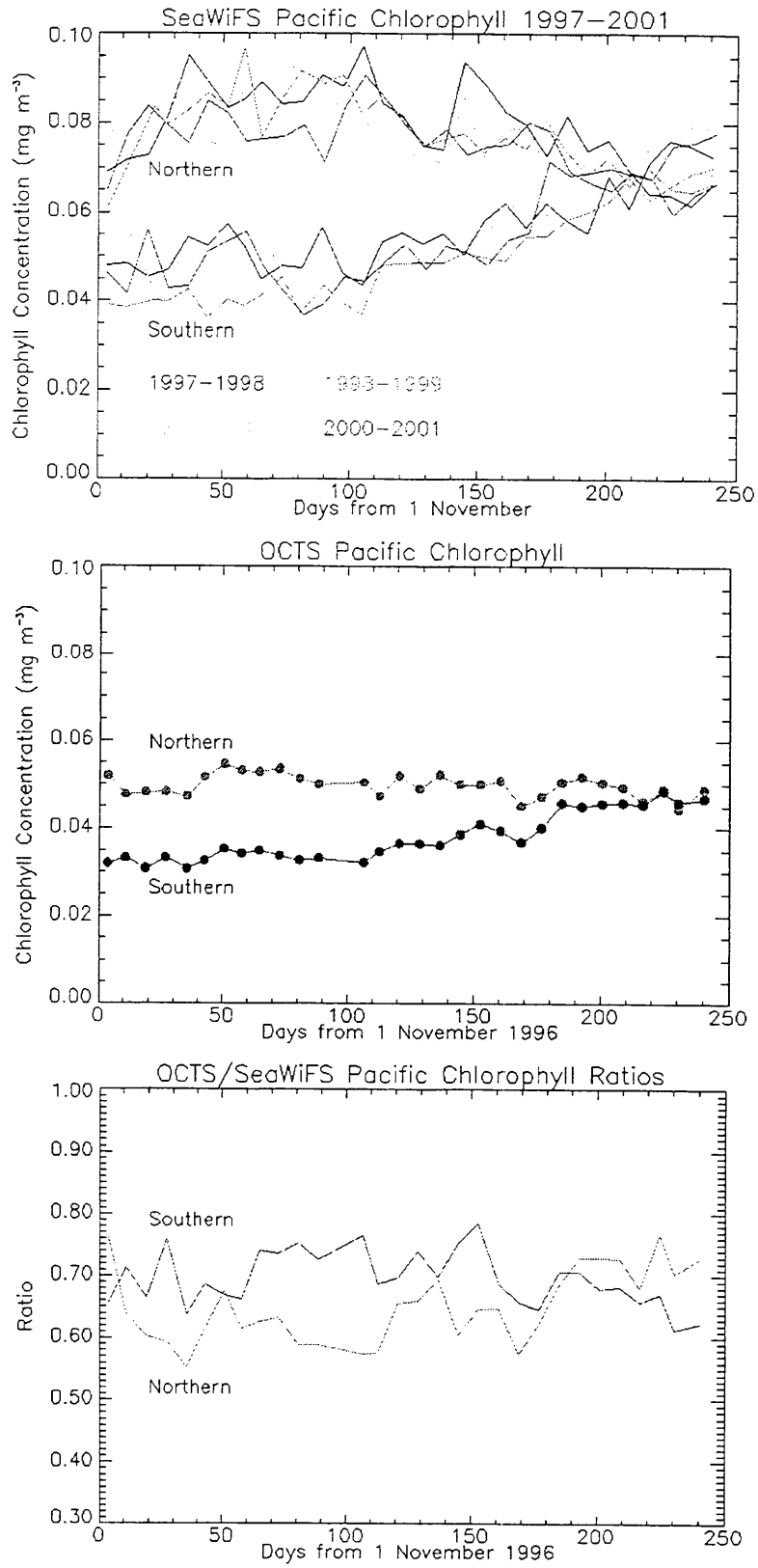


Figure 3.3: Temporal variability of retrieved chlorophyll concentrations from OCTS and SeaWiFS in the northern and southern Pacific.

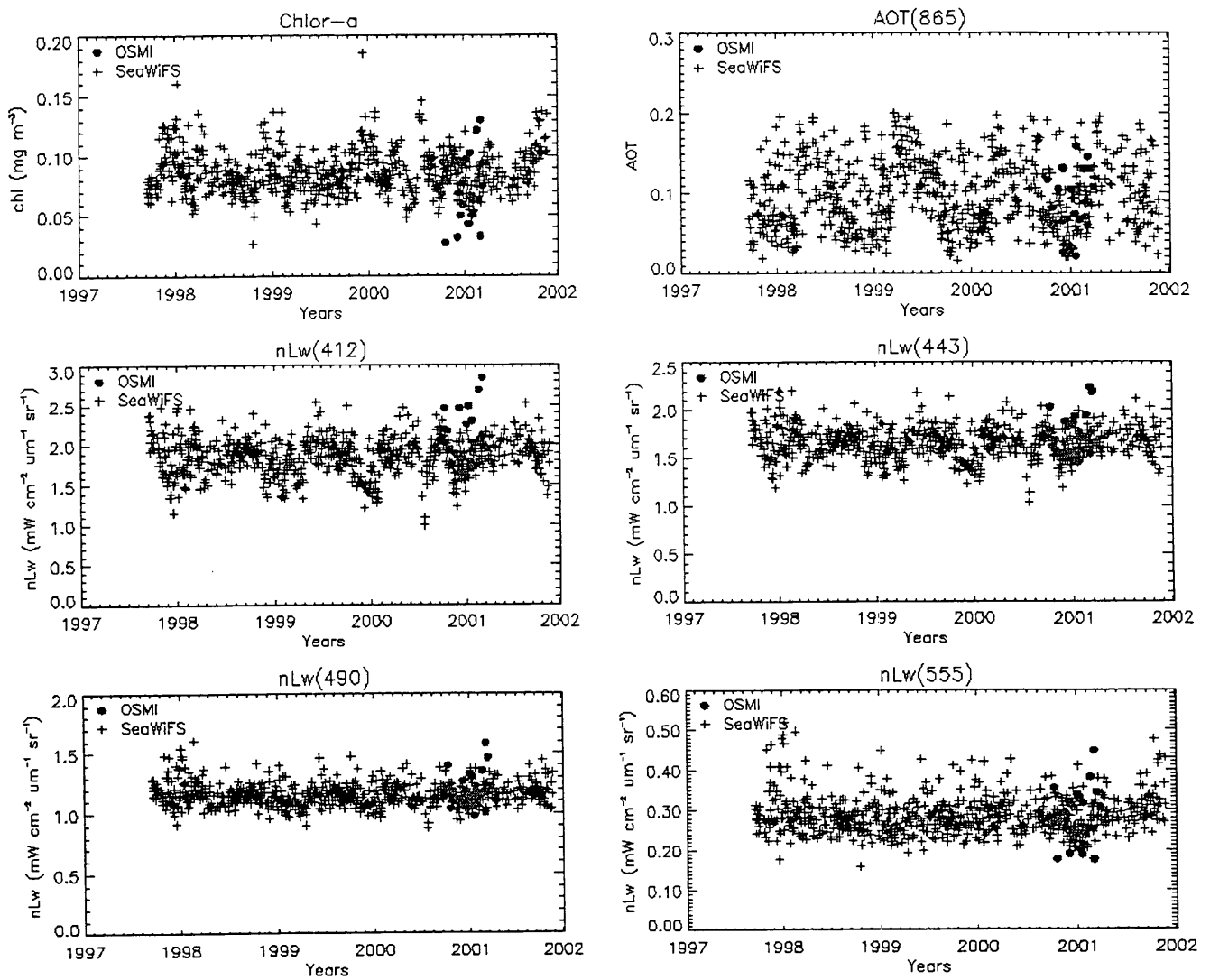


Figure 3.4: OSMI (red) and SeaWiFS (black) mean oceanic optical property retrievals from a 1x1-deg square box in the vicinity of Hawaii.

### 3.3 DATA MERGING

The purpose of data merger activities undertaken by the SIMBIOS Project is to create scientific quality ocean color data sets encompassing measurements from past, present and any future satellite missions. The most obvious benefit of the data merger is improvement in spatial and temporal ocean color coverage (Gregg et al., 1998) and increased statistical confidence in extracted bio-optical parameters (Thiebaut and Pedder, 1987; Thiebaut, 1973). A large variety of useful multi-sensor applications can be implemented which will take advantage of sensor-varying calibration/validation accuracies and spectral, spatial, temporal, and ground coverage characteristics. The Project already has experience with sensor cross-calibrations; SeaWiFS nLw and aerosol optical

thickness were used to calibrate MOS Level-1B radiances (Wang and Franz, 2000). In the near future a number of merged ocean color products are expected to be produced, including daily global chlorophyll maps at the highest feasible spatial resolution using MODIS and SeaWiFS (initially, using 36km mapped data); regional and local products for a variety of local applications; long-term time series using CZCS, OCTS/POLDER, MOS and SeaWiFS/MODIS data; and climatological data sets.

There are many difficulties associated with ocean color data merger. Sensors have varying designs and characteristics. They rely on different calibration approaches, processing algorithms, and means of vicarious calibration. With new sensors, like MODIS-AM, and the planned MODIS-PM, MERIS, GLI, and POLDER-II, the science community needs

to rely on the calibration/validation quality of data products generated by the respective science teams. However, before merging data, the differences in standard products among sensors need to be assessed. The same products can be derived using different spectral bands which may or may not cause noticeable incompatibilities. Data acquisition and retrieval are not straightforward between the missions because of differences in file formats, geometric projections, and limited availability of subsampled data sets.

Fortunately, over the last year the SIMBIOS Project Office has been addressing the data merger difficulties. It has acquired expertise with ingesting and analyzing data formats from different missions, including recent MODIS-AM data sets. Software for uniform calibration and processing of selected ocean color missions has been made available to improve the level of compatibility among products. For example, the entire data set of OCTS GAC has been reprocessed and made available to the user community through DAAC; MOS has been cross-calibrated with SeaWiFS; SeaWiFS, CZCS, OCTS, and MOS are available for processing and display via SeaDAS; and MODIS-AM data can be also displayed in SeaDAS. The Project has been operating a thorough ocean color validation program to quantify the accuracies of the missions' products in comparison to *in situ* measurements. Cross-sensor comparisons have been performed to evaluate mission product differences. The most recent efforts concentrated on MODIS and SeaWiFS matchups. Finally, the Project Office has initiated research and development of methodologies for generating merged multi-sensor ocean color products. The main emphasis has been placed on defining the algorithms which can uniformly overcome mission-specific parameters and be applied to different products and sensors.

#### *Data Merger Achievements*

In the last year, the SIMBIOS Project Office has developed a number of image processing and data fusion methodologies and algorithms to gain expertise and meet the goals of data merger. Three major issues which concern the generation of multi-sensor ocean color products have been addressed:

- Improvement of ocean color global coverage (MODIS and SeaWiFS).
- Merger of ocean color data of different spatial resolutions (MOS and SeaWiFS).
- Merger of satellite and *in situ* measurements (SeaWiFS and CalCOFI).

#### *Improvement of ocean color global coverage (MODIS and SeaWiFS)*

Common data formats and products have been identified for MODIS and SeaWiFS. For comparisons and to perform an initial merger of data from both missions, L3 binned daily global products were used at 4.63km resolution. For

chlorophyll comparisons, the MODIS chlor\_a\_2 product was applied because this represents the OC3M algorithm which is most similar to the SeaWiFS OC4v4 algorithm (chlor\_a product). A number of comparisons between SeaWiFS and MODIS nLw, chlorophyll, nLw ratios, AOT, and K490 were made using MODIS version 3 data from DAAC and SeaWiFS data processed by the Project using the operational algorithm. Also, MODIS data were made available from the University of Miami Remote Sensing Group which were processed using upgraded algorithms and new MOBY stray light correction values. To match the MODIS processing, SeaWiFS data sets for these comparisons were compiled from the results of the unofficial fourth reprocessing which also included stray light corrections for MOBY. Software was developed for the combined extraction and analysis of binned MODIS and SeaWiFS files. MODIS and SeaWiFS comparisons were made for overlapping bins for each day. Product differences were evaluated using density scatter plots and statistics. The matchups were made using both total global coverage data and open-ocean/clear-atmosphere data. The open-ocean/clear-atmosphere observations were analyzed separately to eliminate ambiguous case 2 water and high AOT conditions.

Preliminary daily global matchups (December 4, 2000; April 4, 2001; and June 10, 2001) show that recent MODIS processing does not exhibit time-dependent trends. SeaWiFS and MODIS products compare relatively well for nLw, nLw ratios, K\_490, and chlorophyll concentration. When considered exclusively, open ocean and clear atmosphere conditions show the same statistical trends as the entire global data set. To better evaluate product correlations and differences between the two missions, more analyses are necessary with global and local coverage ranges and cross-seasonal temporal scales. This work will continue in cooperation with the MODIS Oceans Team, MODIS group at GSFC and the University of Miami.

Over the last year, both the SIMBIOS Science Team and the SIMBIOS Project Office have investigated a number of merger methodologies which would increase ocean color coverage (Maritorena et al., 2000). MODIS and SeaWiFS daily global sets have been used in these investigations. The algorithm proposed by the SIMBIOS Project Office is aimed at producing global merged products of consistent accuracy for all data bins or pixels (Reynolds, 1988; Barnes, 1964). The method has to be effective in circumstances where there are only a limited number of sensors with patchy global distributions. The approach should alleviate sensor-to-sensor differences in instrument design, characteristics, calibration peculiarities, and data processing. The merger will incorporate product accuracy levels defined by matchups with *in situ* measurements. In practice, one of the goals is to eliminate discontinuities in product values in areas where individual and joint satellite coverages meet. Since algorithms which smooth out the coverage conversions would produce uneven accuracies for distant pixels or bins, an alternate method has been proposed which reproduces the missing sensor data for regions where only a single sensor coverage exists. This

approach consists of the mapping of one sensor's data so as to imitate data from the other sensor. Although the mapping can be performed using linear or non-linear regression, the use of an artificial neural network is preferred because any complex mapping functions can be approximated using such a neural network methodology. The mapping can be obtained using data from overlapping bins from both sensors, e.g. MODIS and SeaWiFS bins used in the matchups. The neural network will map chlorophyll values from one sensor into chlorophyll values from the other sensor given additional information on nLw, quality control parameters, spatial and temporal chlorophyll distributions, and possibly other products. The neural network scheme can also be used to map nLw and other data from one sensor into the other. The methodology enables uniform processing irrespective of sensor and product characteristics. The largest effort associated with this method is the determination of an optimal set of input products and parameters for the neural network (data mining) as well as training the network on representative global and temporal data sets so as to cover the widest range of chlorophyll conditions. Once trained, the neural network mapping will be efficient. The merger can then be performed as a weighted average for each pixel/bin between the two sensor data sets where the weights will be defined by confidence levels attributed to both sensors by the matchups with *in situ* measurements. The neural network mapping research is ongoing.

#### *Merger of ocean color data of different spatial resolutions (MOS and SeaWiFS)*

During the last year, the SIMBIOS Project Office has examined the feasibility of merging chlorophyll concentration products from ocean color sensors of different spatial resolutions for cases where there is overlapping ground coverage for individual scenes. The prospect of enhancing oceanic features in lower resolution imagery through the use of higher resolution data has also been studied. This algorithm is based on a signal processing approach—wavelet multiresolution analysis—which enables an image to be examined at different frequency or scale intervals (Mallat, 1989). The resolution of an image, which is a measure of detail information in the scene, can be defined and changed by a combination of high pass and low pass filtering operations. The scale of an image is changed by downsampling and upsampling operations. The high frequency, low-scale spatial detail in higher resolution scenes is extracted using the high pass filters of the wavelet transform and is combined with the complete lower resolution image (Nunez et al., 1999). Reversal of the transform increases the resolution and adds high frequency variation to the lower resolution scene. This process enables spatial resolution enhancement without altering the average magnitudes of the ocean color values. Because of this, the wavelet method is particularly useful when the sensor qualities are different and the measurement accuracy of the lower resolution sensor should be preserved.

The wavelet algorithm has been tested on SeaWiFS and MOS imagery—a rare opportunity as these two missions have been cross-calibrated, uniformly processed, and analyzed for overlapping concurrent ground-coverage within the SIMBIOS Project. SeaWiFS Level-2 scenes are binned at 1km and MOS Level-2 scenes at 0.5km resolution. Bins are then projected onto a rectangular latitude/longitude grid map to facilitate image processing and to preserve spatial resolution of the bins in the mapped image. Any missing grid points caused by the mapping of spherical coordinates onto a flat grid are approximated. The approximation uses a wavelet-based iterative algorithm that minimizes high frequency anomalies associated with the missing data. This preprocessing provides data with the desired size and resolution for the wavelet analysis. A single wavelet filtering of the MOS image then extracts pixel-to-pixel spatial detail from MOS data and subsamples the MOS scene by 2. The entire preprocessed SeaWiFS scene then replaces the output of the MOS low pass filter (which is at 1km resolution). An inverse wavelet transform is applied to this result which produces an enhanced, 0.5km resolution SeaWiFS image. To merge the data sets, a weighted addition of the enhanced SeaWiFS image and the original MOS scene is produced which depends on the established relative accuracies of the products from each instrument.

To validate the wavelet algorithm, the original MOS scenes were compared against wavelet-enhanced SeaWiFS scenes and SeaWiFS scenes which were bi-linearly interpolated to the MOS resolution. The bi-linear interpolation does not provide the benefits of the higher resolution feature extraction which enabled SeaWiFS imagery to acquire spatial detail inherent in MOS data. Quantitatively, the correlation of interpolated SeaWiFS imagery with original MOS imagery is considerably smaller (~10%) than the correlation for the wavelet-enhanced SeaWiFS scenes. Qualitatively, the gain in spatial detail obtained by the wavelet approach is consequential and unique.

There have been some difficulties associated with the application of the wavelet approach. Although the wavelet-merged scenes appear sharper, there is a degree of high-frequency noise introduced from MOS which is peculiar to this sensor's data. As it happens, wavelets also provide a means for denoising speckled imagery and this has been implemented as an option in the algorithm (Dondro, 1995). This option is based on the soft-thresholding of wavelet coefficients and is equivalent to removing Gaussian noise from an arbitrary image. Manipulation of wavelet coefficients causes undesirable ringing effects in images because of the high frequency features. To limit this ringing, a selected number of transformed solutions based on different wavelet functions is averaged. Flags and masks of the ocean color products from both sensors are also merged in the final product.

In the future, it would be interesting to apply the wavelet algorithm to the merger of overlapping scenes of MODIS and SeaWiFS data so that SeaWiFS imagery could be enhanced by

the spatial detail contained in MODIS data. Also, a useful experiment would be to combine MODIS ocean color products at 1km resolution with high frequency spatial information contained in MODIS high-resolution bands, such as 500m or 250m.

#### *Merger of satellite and in situ measurements (SeaWiFS and CalCOFI)*

An approach has been developed to merge Level-2 ocean color data with *in situ* measurements. The major purpose is to provide a utility to expose changes in remotely sensed chlorophyll range and distribution when collected *in situ* chlorophyll measurements are overlaid. The algorithm can be used for specialized local applications and when merging data from multiple sources, as for climatological data sets. The method is based on the application of the wavelet transform which spatially spreads *in situ* data point values onto corresponding areas in satellite imagery. These areas are defined by a radius of influence and depend on the *in situ* measurement localization. The effect of *in situ* data points changes with their distance from the center of the areas and the scaling uses the Hann window function. Lower frequency coefficients of the original ocean color subscenes are replaced with the lower frequency coefficients of these subscenes updated with the *in situ* data points (Starck and Murtagh, 1994). The wavelet forces the resulting satellite pixels to be interpolations of *in situ* data points which, at the low resolution, are distributed smoothly around their areas of influence. Leaving the higher frequency coefficients associated with the image unchanged preserves the original high-resolution spatial variations within the areas of influence and protects pixel-to-pixel data variabilities.

The radius of area of influence can be defined using texture extraction. The more irregular the texture around the *in situ* measurement point, the smaller the radius; the smoother the texture, the bigger the radius. The merger is dependent on the established relative accuracies assigned to *in situ* and satellite data. A condition for merger is set as the maximum time difference between the satellite and *in situ* observations.

Results of the satellite and *in situ* measurement merger algorithm have been analyzed for the years 1997 and 1998 using SeaWiFS and California Cooperative Oceanic Fisheries Investigation (CalCOFI) data sets. Although the largest time difference between the SeaWiFS overflight and *in situ* data collection ranges from  $\pm 3$  hours to  $\pm 12$  hours, there were just 13 SeaWiFS files for which the merger could have been performed, with a single maximum of three points per scene. The low number of matchups was principally caused by the presence of cloud cover. To limit the cases where small clouds (a few pixels long) and other conditions cause ocean color pixels to be masked out from the imagery, a gap-filling algorithm has been designed and implemented. The algorithm is based on the iterative reduction of total high frequency content corresponding to missing pixels in the analyzed scene. The frequency content of a pixel is established by inverting a

wavelet transform of a scene where the inversion is limited only to the higher frequencies extracted by the forward transform. The iterations are initialized by filling the gaps with values corresponding to the lower frequency representation of the scene. To eliminate local minima, a random perturbation is introduced to the best gap pixel values which have been found so far in the course of the algorithm. The gap-filling algorithm has been implemented in combination with the satellite and *in situ* measurement merger to eliminate small clouds within the areas of influence of *in situ* data points. This contributed an increase in matchups of around 10%.

#### *Future Activities*

In the last year, the SIMBIOS Project Office has gained experience in a variety of different approaches to ocean color data merger. For the next year, it is looking forward to cooperating with the SIMBIOS Science Team, MODIS Team, and DAAC on sensor intercomparisons, data merger, and algorithm implementation. The merger emphasis will now be placed on global ocean color missions such as MODIS and SeaWiFS. The Project Office will work on defining an optimal mapping algorithm for MODIS and SeaWiFS and creating daily merged global chlorophyll products. In the future, other products can also be considered like nLw at different spectral bands and aerosol optical thickness. MODIS-PM, MERIS, GLI and POLDER II data will also be investigated once they become available from their respective ocean color teams.

### 3.4 SEABASS INTERFACE

The SeaWiFS Bio-optical Archive and Storage System (SeaBASS) serves as a local repository for *in situ* data used in a variety of scientific analyses, for example, satellite data product validation, bio-optical algorithm development, and data merger studies. Archived data include measurements of apparent and inherent optical properties, phytoplankton pigment concentrations, aerosol optical thickness, and other related oceanographic and atmospheric data collected on ships, moorings, and drifters. Additional information on SeaBASS is provided in Werdell et al. (2000) and via the World Wide Web at: <http://seabass.gsfc.nasa.gov>.

SeaBASS contains data from over 750 cruises, encompassing more than 25,000 data files. The volume of archived data is rapidly increasing, as SIMBIOS US Science Team members are contractually obligated to provide data (McClain and Fargion 1999a and 1999b).

SeaBASS data files are flat (two-dimensional) ASCII text with data presented in columns. Each file includes a series of predefined metadata headers, which provide descriptive information about the data, such as the names of the contributor and experiment, the date and location, and other ancillary data. All data files and related documents are stored in a directory tree organized by contributor affiliation, experiment, and specific cruise. Data are further archived

using a relational database management system (RDBMS). The RDBMS is used to catalog and archive metadata and data information from each data file, and to locate and retrieve specific metadata and geophysical data information from the full bio-optical data set. The standard file format and the storage protocols did not change significantly during the past year of the SIMBIOS effort. The SIMBIOS Project maintains software, named FCHECK, to validate the format of SeaBASS data files. Contributors are requested to use either the electronic mail or File Transfer Protocol (FTP) version of FCHECK to evaluate their data files prior to submission. Once the files meet SeaBASS format requirements, the contributor may submit their data and related documentation, such as cruise reports and instrument calibration files, to the SeaBASS Administrator via FTP. Additional information regarding FCHECK and data submission protocols is available online at <[http://seabass.gsfc.nasa.gov/seabass\\_submit.html](http://seabass.gsfc.nasa.gov/seabass_submit.html)>.

Protocols for format validation and data submission have not been altered over the past year. The full bio-optical data set is available online via the SeaBASS Web site. Data are located and retrieved using a series of online search engines, listed and described in detail at:

<<http://seabass.gsfc.nasa.gov/dataordering.html>>.

Each search engine allows users to limit queries to particular experiment, contributors, dates, locations, and data types. Several additional search engines were developed during the past year. In February 2001, a utility for retrieving geophysical pigment values from the bio-optical data set, named the SeaBASS Pigment Locator, was put online. Similarly, in May 2001, a tool for retrieving geophysical sun photometer data, named the SeaBASS Aerosol Locator, was put online. To protect the publication rights of contributors' data, full access to SeaBASS is limited to members of the SIMBIOS Science Team and other NASA-funded researchers. In July 2001, however, all data collected prior to 31 December 1999 were made available to the public. A password is required to access more recent data. In December 2001, the public data were released to NOAA's National Oceanographic Data Center. The development of a CD-ROM version of the full public bio-optical data set is planned for Spring 2002.

The procedures for the water-leaving radiance, chlorophyll *a*, and aerosol optical thickness satellite-to-*in situ* match-up analyses changed little during the past year of the SIMBIOS effort. Information on these analyses may be found in the SeaWiFS Postlaunch Technical Report Series Volume 10 (Bailey et al. 2000).

### 3.5 SUPPORT SERVICES

In an effort to improve the quality and quantity of calibration and validation data sets, the SIMBIOS Project offers several support services to field investigators. These services include; scheduling of on-board LAC recording for SeaWiFS; overflight predictions for operational sensors (currently SeaWiFS, OCTS, MOS-B, MODIS, OCI, OCM and

OSMI); near real time SeaWiFS imagery for cruise locations; and sunphotometer instrumentation from a pool of project-owned instruments. These services may be requested via the World Wide Web at <http://simbios.gsfc.nasa.gov>. In return for these services, the SIMBIOS Project requests that the field investigators provide in situ validation data to the Project's bio-optical archive, SeaBASS. Since January of 2001, the SIMBIOS Project has supported 76 cruises (Table 3.1).

#### *Scheduling SeaWiFS On-board LAC Recording*

Since much of the world's oceans are not covered by a SeaWiFS HRPT station, high-resolution data may be recorded onboard the SeaWiFS sensor. As a service to the scientific community, the SIMBIOS Project in conjunction with the SeaWiFS Project can schedule SeaWiFS onboard LAC for cruises that occur outside HRPT coverage. SeaWiFS has the ability to record a maximum of 10 minutes of high-resolution data per downlink. Typically, a 30-second interval is allotted for LAC target, which corresponds to 180 scan lines or approximately 200 km along track at nadir. Detailed information on LAC scheduling is available on the SIMBIOS web site.

#### *Overflight Predictions for Operational Sensors*

For calibration and validation purposes, in situ measurements should be made as close to the sensor overflight time as is possible. To aid investigators in determining when sampling should occur, the SIMBIOS Project offers overflight predictions for all operational ocean color remote sensors. Currently, the sensors supported are SeaWiFS, MOS-B, OCI, MODIS, OSMI and OCM. Detailed information on overflight predictions is available on the SIMBIOS web site.

#### *Near Real Time SeaWiFS Imagery*

In addition to providing predictions for satellite overflight times, the SIMBIOS Project offers near real time imagery of the operational SeaWiFS products in JPEG or GIF format to cruises at sea. 'True color' images are in JPEG format, all other products are in GIF format. These images provide field investigators with additional information with which they may maximize *in situ* sampling of transient oceanographic features. The default specifications for the images provided include:

- available LAC, HRPT, and GAC;
- chlorophyll-*a* and pseudo-true color images;
- 2-degree box about a designated location or the entire designated region;
- image width of 600 pixels;
- minimum percent valid chlorophyll pixels: 5%;
- images may be customized to best accommodate individual investigator needs.

Detailed information on near real-time imagery is available on the SIMBIOS web site.

## SIMBIOS Project Annual Report

Table 3.1: SIMBIOS supported cruises with services provided.

Experiment name	Investigator	Period	Services
Railroad_Valley	Edward Zalewski	Jan 6 2001	Jan 8 2001 overflight
Poseidon_2001	Thomas Martin	Jan 8 2001	Feb 23 2001 image
Bering_Sea_Coccc	Peter Miller	Jan 11 2001	Feb 18 2001 image, LAC
Poseidon_2001	Thomas Martin	Jan 13 2001	Feb 13 2001 image
jan01sj	Ajit Subramaniam	Jan 23 2001	Feb 24 2001 image, LAC, overflight
HOM3	Mike Mickelson	Feb 1 2001	Jan 1 2002 image
Bahamas_2001	Stanford Hooker	Feb 1 2001	Mar 4 2001 image, overflight
ANTXVIII_5	Andre Belem	Feb 7 2001	May 7 2001 overflight
AMLR2001	Mati Kahru	Feb 8 2001	Mar 5 2001 LAC, overflight
GasEx1	Francisco Chave	Feb 10 2001	Mar 3 2001 LAC, image, overflight
GASPROD	Francis Gohin	Feb 12 2001	Mar 6 2001 image
ACE_ASIA	Philip A. Durke	Feb 20 2001	Feb 28 2001 image
Lake_Tahoe	Edward Zalewski	Feb 20 2001	Mar 1 2001 overflight
WestMed2001	Emanuele Bohm	Feb 27 2001	Mar 22 2001 image
SBC_LTER_01	Dave Siegel	Mar 1 2001	Mar 29 2001 image, overflight
WRISCS_Project	Samantha Lavend	Mar 1 2001	Sep 30 2001 image
GasEx2	Francisco Chavez	Mar 3 2001	Mar 10 2001 LAC, overflight
htob	Francisco Chavez	Mar 13 2001	Mar 29 2001 LAC
SF6_Eastern_Med	Steve Groom	Apr 1 2001	May 21 2001 image
Railroad_Valley	Edward Zalewski	Apr 8 2001	Apr 12 2001 overflight
Palmer_2001	Andre Belem	Apr 12 2001	Apr 30 2001 image
Bluefin_Gulf_of	Andreas Walli	Apr 12 2001	May 15 2001 image
EN355_test	Ru Morrison	Apr 19 2001	Apr 23 2001 image
IsoFix_II	Mark Altabet	Apr 25 2001	May 30 2001 image
CLAMS_test	William Smith	Apr 26 2001	Apr 28 2001 image
MBARI_ESP2001	Brian Schlining	Apr 30 2001	May 30 2001 image, overflight
ALKOR_159	Thomas Martin	May 1 2001	May 13 2001 image
Meteor_50_1	Thomas Martin	May 1 2001	May 31 2001 image
CoOP_WEST_Spring_2001	Raphael Kudela	May 1 2001	Jun 19 2001 image
NC_Ferry	Varis Ransibrah	May 10 2001	Jun 1 2001 overflight
W0105C	Ricardo Letelier	May 15 2001	Jun 15 2001 image
EN355	Ru Morrison	May 30 2001	Jun 15 2001 image, overflight
CLAMS	William Smith	Jun 7 2001	Aug 6 2001 image
CLT2001	Glenn Cota	Jun 11 2001	Aug 31 2001 overflight
NC_monthly_ferr	Varis Ransi	Jun 11 2001	Jun 30 2001 overflight
TAG_A_GIANT_200	Andreas Walli	Jun 15 2001	Apr 25 2002 image
Mucillagine_200	Vittorio Barale	Jun 15 2001	Sep 15 2001 image
DYNAS	Thomas Ohde	Jun 17 2001	Jun 23 2001 overflight
Belgica_2001	Kevin Ruddick	Jun 17 2001	Jun 23 2001 overflight
jun01kn_1	Ajit Subramania	Jun 26 2001	Jul 7 2001 overflight
Pacific_Bluefin	Kevin Weng	Jun 27 2001	Aug 5 2001 image
SedTrap2	Aurea Ciotti	Jul 1 2001	Jul 10 2001 overflight
NC_ferry_July	Varis Ransi	Jul 1 2001	Jul 31 2001 overflight
SLAswarm	Ru Morrison	Jul 3 2001	Jul 15 2001 image
CLT2001_1	Glenn Cota	Jul 4 2001	Aug 14 2001 image
jun01kn_2	Ajit Subramania	Jul 6 2001	Jul 16 2001 LAC, overflight
MELEE_V_CCGS	Steven Wilhelm	Jul 6 2001	Jul 20 2001 image, overflight
Cornell_Worksho	Bruce Monger	Jul 7 2001	Jul 17 2001 image, overflight
jun01kn_leg2	Ajit Subramania	Jul 20 2001	Aug 18 2001 image, LAC, overflight
COAS_COAST	Ricardo Letelie	Aug 1 2001	Aug 31 2001 image
Cerebrus	Will Aicken	Aug 6 2001	Sep 14 2001 image
PDC_Japan	Craig Laben	Aug 8 2001	Jan 31 2002 image
PDC_Hawaii	Craig Laben	Aug 8 2001	Jan 31 2002 image
PDC_Taiwan	Craig Laben	Aug 8 2001	Jan 31 2002 image
PDC_Malaysia	Craig Laben	Aug 8 2001	Jan 31 2002 image
PDC_Indonesia	Craig Laben	Aug 8 2001	Jan 31 2002 image
PDC_Philippines	Craig Laben	Aug 8 2001	Jan 31 2002 image
AFMA_Sulu_Sea	Kathleen M. Sil	Aug 10 2001	Aug 25 2001 LAC, overflight
Zeeleeuw_2001	Kevin Ruddick	Aug 17 2001	Sep 14 2001 overflight
AMBITION	Peter Miller	Aug 23 2001	Oct 5 2001 image
CLT2001	Glenn Cota	Sep 1 2001	Dec 31 2001 overflight
Lake_Tahoe_Sep2	Edward Zalewski	Sep 7 2001	Nov 30 2001 overflight
Post_CLAMS	William Smith	Sep 11 2001	Oct 5 2001 image
CT010912	Ru Morrison	Sep 12 2001	Sep 25 2001 image
MERIS_Prof_Penc	Herbert Siegel	Sep 12 2001	Sep 19 2001 overflight
BPA_NMFS_Septem	Pablo Clemente-	Sep 18 2001	Sep 30 2001 overflight
EN361	Ru Morrison	Sep 28 2001	Oct 20 2001 image, overflight
McGillicuddy_Eddies_2001	Norm Nelson	Oct 1 2001	Oct 16 2001 image
CT011004	Ru Morrison	Oct 4 2001	Oct 22 2001 overflight
Russian_Cruise	Oleg Kopelevich	Oct 6 2001	Mar 6 2002 LAC, overflight
DIAPALIS_1	Cecile DUPOUY	Oct 22 2001	Nov 1 2001 image
MELEE_VI	Steven Wilhelm	Nov 2 2001	Nov 11 2001 image
Chalk-Ex_A	Barney Balch	Nov 9 2001	Nov 14 2001 image
PACSEA_2_and_3	Kathleen Silvan	Nov 13 2001	Nov 25 2001 LAC
Chalk-Ex_B	Barney Balch	Nov 14 2001	Nov 18 2001 image
DIAPALIS_2	Cecile Dupouy	Nov 26 2001	Dec 23 2001 LAC, image

### 3.6 SIMBIOS SUNPHOTOMETERS AND CALIBRATIONS

Atmospheric correction of satellite radiances and, in particular, estimation of aerosol effects on the upwelling radiance at the top of the atmosphere is one of the most difficult aspects of satellite remote sensing. Merging of aerosol properties obtained from *in situ* observations with those derived by sensor algorithms creates exceptional opportunities to validate and improve the atmospheric correction. There are many uncertainties associated with *in situ* measurements themselves. These uncertainties include sun photometer or radiometer calibration and operational problems, inadequate manual handling, and cloud contamination. When matching against atmospheric properties obtained by a satellite sensor, additional uncertainties come into play. These uncertainties may be caused by different satellite and surface instrument viewing angles and by observation acquisition time discrepancies. In the case of the atmosphere, these uncertainties are considerable. Therefore, exact calibration of sun photometers and radiometers is essential, as well as the best possible (and uniform from instrument to instrument) correction of obtained measurements. Finally, in order to cross-validate the quality of *in situ* data, as well as extract measurements of high stability and confidence, and compare them against satellite sensor estimates with the largest degree of certainty, having multiple observations from different sun photometers and radiometers is essential. An extended group of ground stations from AERONET is now available for product validation. These instruments are located at either coastal or island stations and were operational for a reasonable length of time after SeaWiFS went into operation. Table 3.2 provides the AERONET station name, location (latitude and longitude), and the corresponding responsible AERONET PIs. In 2000, match-ups analysis between AOT data obtained from *in situ* observations and satellite-derived AOT levels were conducted using some of the sites listed in Tables 3.2. Match-ups have been obtained for the SeaWiFS-derived aerosol properties and AOT levels calculated from AERONET and SIMBIOS sun and sky radiometer data. The study showed the need to improve the cloud-screening algorithms. Efforts have been made to refine the protocols and the cloud-screening algorithms. Extensive efforts have been also made to associate uncertainties with aerosol optical thickness measured by various sun photometers that compose the SIMBIOS pool of sun photometers. Based on Russel *et al.* (1993) and Eck *et al.* (1999), the uncertainties for the Microtops and SIMBAD sun photometers were estimated and are summarized on Table 3.3.

#### Pointing Error Screening

Once AOT values have been calculated, points representing erroneous measurements must be removed. It can be difficult to point a hand held sun photometer at the sun

accurately from a moving platform, like a boat at sea. Measurements that were taken when the instrument was not pointed at the sun will produce erroneous AOT values. A poorly pointed instrument mistakenly records less than the full direct solar radiance, so the computed AOT is much higher than reality. This is a significant problem with the Microtops II sun photometer, as its measurement cycle of about 3Hz is not always fast enough to avoid ship motion (Porter *et al.* 2001). Figure 3.5 is an example of the manifestation of this pointing error.

Table 3.2: AERONET sites used for aerosol matchups analyses.

Station	Latitude	Longitude	AERONET PI
Arica	-18.47	-70.31	B. Holben
Ascension Isl.	-7.98	-14.41	C. McClain*
Azores	38.53	-28.63	C. McClain*
Bahrain	26.32	50.50	C. McClain*
Bermuda	32.37	-64.70	B. Holben
Chinae	35.67	-117.74	B. Holben
Coconut Island	21.433	-157.79	C. McClain*
Dry Tortugas	24.60	-82.80	K. Voss & H. Gordon
Kaashidhoo	4.97	73.47	B. Holben
Lanai	20.83	-156.99	C. McClain*
Midway Island	28.21	-177.38	B. Holben
Nauru	-0.52	166.92	M. Miller
Puerto Madryn	-42.79	-65.01	C. McClain*
Rottneest Island	-32.00	115.30	C. McClain*
SanNicolas	33.26	-119.49	R. Frouin
Tahiti	-17.58	-149.61	C. McClain*
Erdemli	36.56	34.25	C. McClain*
Wallops	37.94	-75.47	C. McClain* & B. Holben
* SIMBIOS Project Office			

Table 3.3: Calibration and AOT uncertainties for various sun photometers. The master cimels are used to transfer the calibration to other sun photometers. The uncertainties given for the Cimel are from Holben *et al.* 1998 and Eck *et al.* 1999

	$\frac{\delta v_0}{v_0}$	$\delta\tau$
Master Cimel	0.002-0.005	0.005
Standard Cimel	0.01	0.01-0.02
MicroTops	0.015	0.015-0.02
SIMBAD	0.015	0.015-0.02

Two steps were taken to reduce the possibility of recording erroneous measurements with the Microtops. First, the measurement protocol was changed. Unlike the default protocol, which saves the average of the 4 largest (out of 32)

voltage values, the new protocol logs the largest single value of 20 measurements. This has several advantages. The largest voltage is the only value recorded, so the chance of keeping a contaminated point is minimized. In addition, the total time needed to make this measurement is smaller than with the default protocol, so more measurements can be taken in a short period of time. After the experiment, a post-processing algorithm is applied. This algorithm calculates the coefficient of variation (standard deviation divided by the mean, or CoV) for each set of measurements in each band. If the CoV is above an arbitrary threshold of 0.05 (expressed in terms of optical thickness), the lowest voltage (highest AOT) value is removed, and the CoV recalculated. This is repeated until it is less than 0.05 or there are not enough points left to calculate the standard deviation. The passed points are those that passed this iterative process in all bands. Figure 3.6 is an example of data gathered with this protocol, and which points remained after the post-processing algorithm. A post processing protocol was also developed to remove erroneous measurements due to pointing problems from data that were already collected with the old (4 out of 32) protocol. One of the fields in a raw Microtops data file is the standard deviation of the four largest measurements used for each data point. Data whose standard deviation, in any band, is larger than the instrument error (0.015, in optical thickness) is simply removed from the data set. While this severely limits the data available for analysis, it reduces the need for manual data screening. The improved pointing error screening was presented at the Fall AGU meeting in December 2001 (Knobelspiesse *et al.*, 2001).

### Cloud Screening

Several methods for removing cloud contaminated measurements from sun photometer data have been established. (Reynolds *et al.* 2000, Smirnov *et al.* 2000) These cloud screening algorithms are based upon the assumption that cloud contaminated data contains higher temporal frequencies than cloud free data. Screening is performed using various statistical or signal processing techniques that remove data with high temporal frequencies. Established screening algorithms are intended for specific instrument types, and often utilize measurement characteristics unique to that instrument. The SIMBIOS project gathers data from a variety of sun photometer types, and is therefore interested in cloud screening methods that perform universally for data from all sun photometers. In 2001, software to perform two types of cloud screening was written. Screening results from three sun photometer data sets taken during ACE-Asia 2001 will be compared during 2002, with the hope that a uniform SIMBIOS cloud screening method will be found. Software was written to perform the cloud screening established in Smirnov *et al.* (2000) for the Cimel land based sun photometer. This approach uses a mix of statistically based criteria and a second derivative based smoothness criteria to remove cloud contaminated data. The SIMBIOS project wrote software to perform this type cloud screening on data from any sun photometer. It is not known if this screening method will work equally on data with different sampling rates than that measured by the Cimel sun photometer.

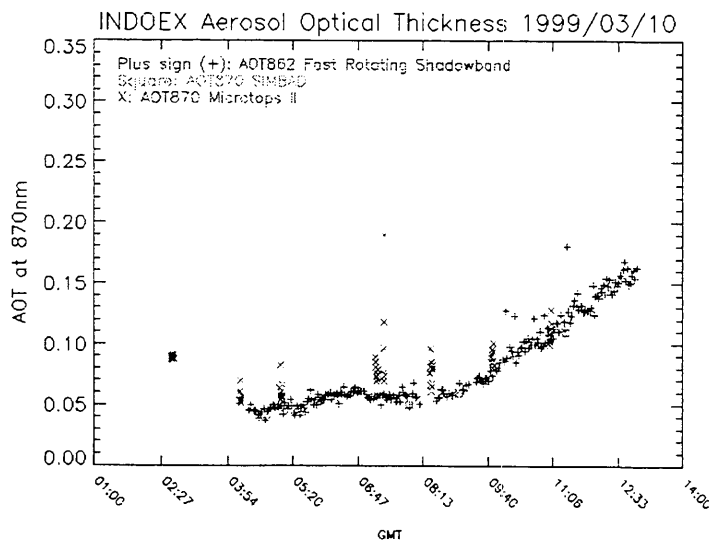


Figure 3.5 is a plot of AOT values at 870nm gathered by three sun photometers during the INDOEX cruise in the Indian Ocean on March 10<sup>th</sup>, 1999. Data in blue are from the Fast Rotating Shadowband Radiometer. Data in green were gathered with the SIMBAD hand held sun photometer. Data in red were gathered with the Microtops II hand held sun photometer. Note how much of the Microtops II values are higher than measurements made with other instruments at the same time. This is due to pointing errors.

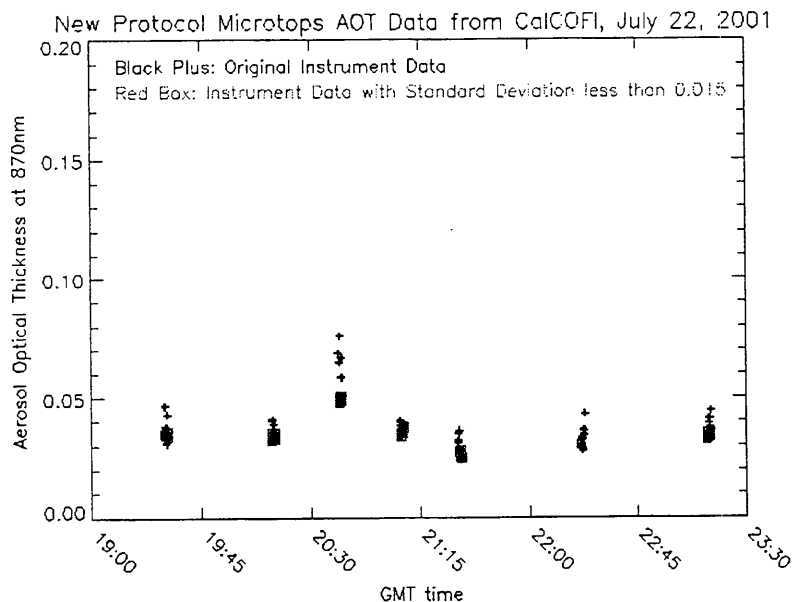


Figure 3.6 shows data gathered during the CalCOFI cruise off California on July 22<sup>nd</sup>, 2001 with the new Microtops II measurement protocol. Points in black are the results of the largest of 20 data gathering protocol. Points with red boxes around them remained after the post processing routine. Note that the unnaturally large AOT values have been removed.

Wavelet based signal processing has the potential to provide a screening method that directly addresses the main cloud screening assumption – that cloud contaminated data has higher temporal frequencies than cloud free data. Clouds, as expressed in optical thickness signals, are non-stationary (non-repeating) high frequencies. Wavelet analysis is intended for non-stationary signals. Therefore, wavelets are potentially more useful than other frequency analysis techniques, such as Fourier or statistical analysis, that are intended for stationary signals. (Ainsworth *et al.* 2001) However, the proper frequencies to remove has yet to be established. Software was written to perform wavelet screening using a given frequency threshold. Software was also written to iteratively determine the proper threshold frequency by comparing results with the Cimel screening by Smirnov *et al.* (2000). Results from this parameterization process are not yet validated.

The ACE-Asia cruise in the spring of 2001 provided ideal data for validation and comparison of the above screening algorithms. During this cruise, simultaneous measurements were made with the Fast Rotating Shadowband Radiometer, the SIMBAD hand held sun photometer and the Microtops II hand held sun photometer. In addition, measurements were made with a Micro-Pulse LIDAR (MPL). Normalized Relative Backscatter (NRB) data from this instrument could provide a valuable verification of the existence of clouds. Therefore, MPL NRB data were archived in SeaBASS. In 2002, the

above data sets will be used to determine and verify a SIMBIOS cloud screening routine.

#### Data Tracking Software

As the SIMBIOS instrument pool grows, tracking the shipping, calibration and data processing has become increasingly difficult. Several steps were taken to streamline the management of the above tasks. First, the voltage to AOT data processing was consolidated to use the same software on data from various instruments. This insures that the calibration coefficients and ancillary data are applied in a uniform manner. Next, routines were created to automatically update the calibration constants shown on the SIMBIOS web page, so that the same set of current values are always used. To reduce miscommunication, an email account was created to provide a single sun photometry contact point for PI's. Finally, a management software package was created so track the instrument requests, shipping, calibration and data processing. This software produces plots on the SIMBIOS web site so that everybody can see the instrument schedules.

#### Sensor Calibration

Seven Cimel sun photometers have been re-designed to help the site managers and the Aeronet group maintain the

instruments. The new design includes a new robot, new connectors, and cables that make easier the exchange of parts. Two new Cimels were bought and delivered to handle and perform gradually the modifications to every sun photometer. Fourteen Cimel sun photometers compose the SIMBIOS Pool of instruments at this time; ten are deployed in the field of which five need to be refitted; two are expected to be back for calibration and redesign; the last four are ready to be deployed. The Aeronet group is now in charge of the maintenance and shipping of the SIMBIOS pool of Cimel sun photometers.

Twelve Microtops, two SIMBADs and two PREDE Mark II sun photometers were deployed in several cruises between 1998 and 2001. The data collected by the Project is available at <http://seabass.gsfc.nasa.gov/>, where an interactive mapping tool is provided to public users. Two new Microtops were bought to support the expected growth of cruise experiments and the expected filter degradation of some Microtops. Two SIMBADAs, new versions of the SIMBAD with 11 channels, have been delivered to the project in late 2001, calibrated at GSFC, and are ready for deployment in 2002.

In 2000, the PREDE Company upgraded our pair of land version PREDE to ship versions. The ship versions were checked at Goddard Space Flight center in 2001. The PREDE PS1000111 was used at GSFC and several modifications were performed to improve the instrument water proofing. The instrument was deployed during the ACE-ASIA experiment in March and April 2001, while the PREDE PS110611 was shipped back to Japan to repair the optical alignment. The data analysis algorithm was delivered to the SIMBIOS Project in March 2001 and great efforts were made to implement and test the code with the data collected at GSFC. The data collected during ACE-ASIA and at GSFC have been analyzed and presented at the AGU meeting in San Francisco in December 2001 (Pietras *et al.* 2001).

#### *Sun Photometer Calibration: Non-Polarized Channels*

The calibration of the sun photometers was described in McClain and Fargion (1999). Details on operating the sun photometers, calibration and the theoretical principles are posted at <http://simbios.gsfc.nasa.gov/Sunphotometers/calibration.html>.

Twelve Microtops, two SIMBADs and two PREDES compose the SIMBIOS instrument pool. Two new Microtops were added to account for the filter degradation noticed in some instruments. Two SIMBADAs, new versions of the SIMBAD with 11 channel were delivered in late 2001 to support the growth of the SIMBIOS PIs requests for above water instruments. Each instrument is calibrated before and after every cruise deployment. The processing code is common to all sun photometers and is under development to account for the two new SIMBADAs. This code allows the cross calibration with a master Cimel instrument based on the time to time voltage ratios ( $V_0$ ). Only clear days that show a

variation  $\Delta V_0/V_0$  less than 1% are retained as calibration days. The time series of the cross calibration is reported in Table 3.4 for the Microtops #3773, the SIMBAD #972306 and the PREDE #PS1000111 returned from the ACE-ASIA experiment.

#### *Sun Photometer Calibration: Polarized Channels*

Two polarized Cimel sun photometers are still deployed in the field. The Aeronet group is now in charge of the calibration of the polarized sun photometers. Instrument #162 has been refitted and deployed in Coconut Island (Hawaii). Instrument #191 has been refitted and is ready to be deployed.

#### *Above Water Radiometer Calibration*

The SIMBAD and SIMBADA radiometers are also designed to do above water measurements (in addition to being a sun photometer). The optics and filters are the same but the electronic gain is different. The calibration is generally performed at GSFC using a 6' or a 42" integrated sphere at GSFC. Table 3.5 shows the reflectances per count obtained for various calibrations performed since 1999 with two SIMBAD instruments. Efforts are underway to estimate uncertainties of the calibration coefficient determination based on the standard deviation obtained from the measurements and based on the accuracy of the integrated sphere calibration. The integrated spheres are maintained and calibrated monthly by the Calibration Facility group at Goddard Space Flight Center (<http://spectral.gsfc.nasa.gov>). The two SIMBADA were also calibrated since July 2001 using the 42" sphere. The analysis code that process the sphere calibration is under development to account for the new channels of SIMBADA and various levels of lamps or various spheres.

New techniques have been also implemented to monitor the behavior of the radiometers over time. The SeaWiFS Quality Monitor (SQM) has been used used in 2001 to monitor the SIMBAD 09; the time series is reported on Table 3.5. Although the SQM is not a source as bright as the 6' sphere, the relative comparison is easy to obtain and is useful between two sphere absolute calibrations. In addition, a Spectralon plaque has been bought and has been delivered to the SIMBIOS Project in early spring 2001. The plaque is used as a relative and absolute calibration device for the SIMBAD and SIMBADA radiometers. The relative calibration consists of determining the gain ratio (low/high) in each channel of the two SIMBADA looking at the plaque illuminated by the sun during a clear day. The results are summarized in Table 3.6. The gain ratios time serie is helpful to observe a change in some channels during a field experiment. Absolute calibration that requires a precise estimate of the solar flux illuminating the plaque needs to be developed.

Table 3.4: Top of Atmosphere (TOA) signals (digital counts) and standard deviations for the sun photometers determined by transfer calibration from a calibrated Cimel at GSFC between August 1998 and September 2000.

MicroTops	Cimel#	440 nm	500 nm	675 nm	870 nm	
03773						
8/21/1998	37	1244	988	1218	824	
6/9/1999	101	1238	987	1198	827	
9/20/2000	37	1242	984	1194	817	
7/6/2001	101	1224	980	1202	831	
12/6/2001	101	1202	984	1208	825	
SIMBAD		440 nm	490 nm	560 nm	675 nm	870nm
932706						
8/21/1998	37	388591	479121	406870	421086	304820
12/14/1998	94	388269	473101	394874	410455	311944
9/23/1999	94	376205	464224	391526	416182	300000
10/28/1999	101	376820	462637	387034	410887	302475
3/6/2000	37	382815	465574	382168	408538	301005
PREDE		440 nm	500 nm	675 nm	870 nm	1020 nm
PS1000111						
7/6/2001	101	1.480E-04	2.866E-04	3.643E-04	2.743E-04	1.530E-04
8/2/2001	101	1.446E-04	2.874E-04	3.668E-04	2.767E-04	1.530E-04
9/6/2001	94	1.451E-04	2.873E-04	3.646E-04	2.796E-04	1.552E-04
9/7/2001	94	1.460E-04	2.907E-04	3.635E-04	2.777E-04	1.542E-04
10/28/2001	94	1.817E-04	2.820E-04	3.557E-04	2.721E-04	1.533E-04

Table 3.5: Calibration coefficients (relectance/counts) for SIMBAD # 06 and 09 between 1999 and 2001.

SIMBAD #972306	443nm	490nm	560nm	675nm	870nm
08-12-1999	3.8181	2.1922	2.4319	4.2292	8.0289
01-14-2000	3.7650	2.1339	2.3894	4.1096	7.6506
03-06-2000	3.6442	2.1186	2.4042	4.1324	7.7366
08-18-2000	3.7942	2.2376	2.5963	4.3958	8.2380
SIMBAD #972309					
08-12-1999	4.931	2.425	2.695	4.312	8.277
01-14-2000	5.0134	2.3451	2.6511	4.2599	7.9370
03-06-2000	4.7363	2.2771	2.6234	4.2219	8.0104
03-28-2001	4.6895	2.2732	2.6727	4.2406	8.5264

Table 3.6: Time series of the SIMBAD #972309 signals (digital counts) measured with the SeaWiFS Quality Monitor.

SIMBAD #972309	443nm	490nm	560nm	675nm	870nm
7/18/2001	1807.59	8038.90	7202.52	8959.86	16838.10
7/19/2001	1836.44	8189.62	7318.16	8891.35	16508.60
7/20/2001	1830.41	8176.76	7287.21	8846.80	16527.40
8/10/2001	1819.62	8189.30	7336.47	8880.20	16363.50
8/21/2001	1822.99	8185.61	7308.21	8874.63	16321.60
8/22/2001	1814.30	8165.62	7332.26	8891.08	16260.50
8/23/2001	1814.40	8188.15	7328.14	8890.44	16267.90
1/8/2002	1789.77	8278.85	7399.86	8786.97	15088.30

Table 3.7: Gain ratios (Low/High) retrieved with both SIMBADA aiming the Spectralon plaque during a clear day.

SIMBADA #	350nm	380nm	410nm	443nm	490nm	510nm	565nm	620nm	675nm	750nm	870nm
SIMBADA #09 Spectralon plaque	99.5	101.6	219.2	229.2	202.5	224.0	204.2	219.9	213.7	211.3	203.5
SIMBADA #07 Spectralon plaque	100.6	100.4	226.5	220.0	205.5	230.3	219.8	213.9	219.0	230.2	228.3

### 3.7 CALIBRATION ROUND ROBIN

Calibration round-robin intercomparison experiments are conducted by the SIMBIOS Project. The specific goals are to:

- verify that all laboratories are on the same radiometric scale
- detect and correct problems at any individual laboratory in a timely fashion
- enforce the common use of calibration protocols
- identify areas where the calibration protocols need to be improved
- document the calibration procedures specific to each laboratory.

The participating laboratories include academic institutions, government agencies and instrument manufacturers that either directly or indirectly contribute to SeaWiFS (see section 3.4). In the year 2001, the participating laboratories of the first SIMBIOS Radiometric Intercomparison SIMRIC-1 include:

- Naval Research Laboratory (NRL), Optical Sensing Section, Washington, DC
- Scripps Institution of Oceanography, University of California, San Diego, California
- Biospherical Instruments Inc., San Diego.
- The Institute for Computational Earth System Science (ICESS), University of California at Santa Barbara, California.
- HOBI Labs, Watsonville, California
- NASA Code 920.1 Calibration Facility, Greenbelt, Maryland
- Satlantic Inc., Halifax, Canada

The above laboratories were visited by SIMBIOS staff with a NIST designed and calibrated radiometer, the SeaWiFS Transfer Radiometer II (SXR-II), described in Johnson et al., 1998a. The radiances produced by the laboratories for calibration were measured in six channels from 411 nm to 777 nm and compared to the radiances expected by the laboratories. A NASA-TM (Meister et al., 2002) documents the various calibration procedures in these laboratories, evaluates the comparison results, and discusses areas where the calibration protocols should be improved. Furthermore, several characteristics of the SXR-II (e.g. its radiometric stability and its field of view) and of the SQM-II (e.g. the stability of its light output and the stability of its

internal detector) are described. The major result of the SIMRIC-1 is that typically the SXR-II measured radiances were higher than the expected radiances by 0 to 2 %, see Figure 3.7. This level of agreement is satisfactory. Furthermore, several issues were identified where the calibration protocols need to be improved:

- the reflectance calibration of the reference plaques
- the possible use of an effective distance correction when using the irradiance standards at distances greater than the original 50 cm calibration distance
- all laboratories should adopt the new NIST 2000 irradiance scale as soon as possible.

The SXR-II was calibrated by NIST using SIRCUS in December 2000. SIRCUS (Spectral Irradiance and Radiance Calibrations with Uniform Sources) is a new calibration facility that combines the use of tunable lasers and integrating spheres. The radiometric stability of the SXR-II from November 2000 to December 2001 was monitored by a commercial portable light source, the Satlantic SeaWiFS Quality Monitor II (SQM-II). A 2 % decrease was found for the responsivity of the SXR-II channel 1 at 411 nm. Also, a decrease of about 1 % is likely for SXR-II channel 6 at 777 nm. Both changes will be proved or disproved by the second calibration of the SXR-II at NIST in December 2001. The intensity of the SQM-II light output for the HiBank mode increased by about 1 %, for a burning time of 113 hours, which is a very good result. The internal detector of the SQM-II measured an increase of about 9 %, the reason for this discrepancy is unknown.

### 3.8 SIMBIOS COMPUTING RESOURCES

The SIMBIOS computing facility consists of a variety of equipment types. The main goal of the facility is to provide computational support for the Project in the following areas:

- routine bulk data processing,
- large scale analysis and match-up between sensors,
- focused analysis on data subsets, and
- storage of large sensor data sets.

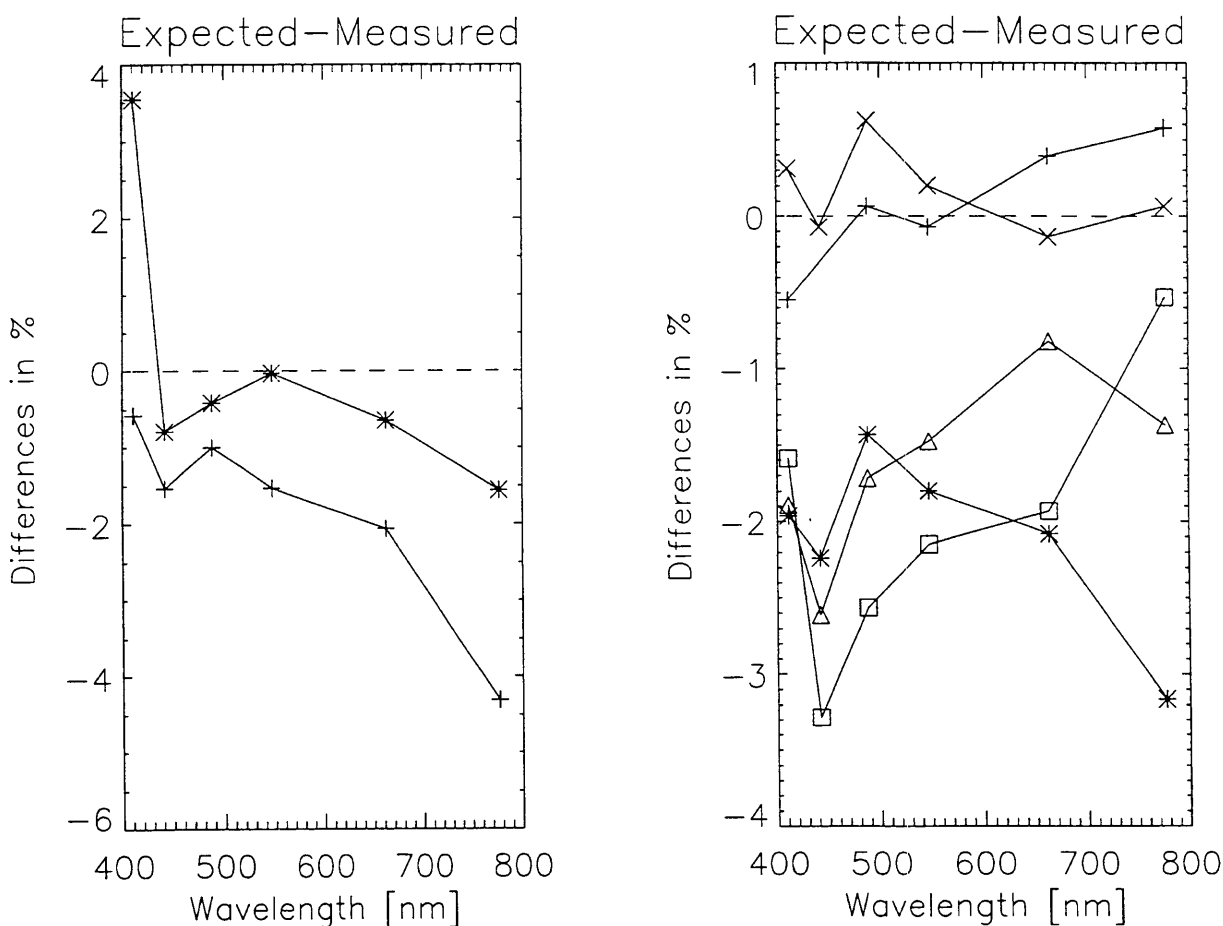


Figure 3.7.: Comparison of the radiances measured by the SXR-II at the laboratories participating in the SIMRIC-1 and the radiances expected by the laboratories. The differences (expected radiance minus measured radiance) are plotted in % as a function of wavelength. The plot on the left shows the two laboratories on the NIST 2000 irradiance scale ('\*' symbols for NASA Code 920.1, '+' symbols for ICESS UCSB). The right plot shows the laboratories referenced to older NIST irradiance scales ('\*' symbols for NRL, '+' symbols for Biospherical, '+' symbols for Scripps, triangles for HOBi Labs, squares for Satlantic). The difference at 411 nm for NASA Code 920.1 is due to the low responsivity of the Code 920.1 transfer radiometer at that wavelength used to transfer the calibration from the NIST calibrated FEL to the Hardy integrating sphere, which was measured by the SXR-II. At ICESS UCSB, calibrations are only performed up to 680 nm, so the strong disagreement at 777 nm does not affect their calibrations. At HOBi Labs, 2 further lamp standards were measured that showed disagreements of more than 5 % (not shown). These 2 lamps were recalibrated after the SIMRIC-1; the new calibrations are in much better agreement with the SXR-II measurements. The SXR-II measurements at Satlantic are affected by the decreases of responsivity at 411 nm and 777 nm and are not corrected for in this plot.

The facility is co-located with the SeaWiFS Project on-site at the NASA Goddard Space Flight Center. This arrangement benefits both projects, allowing sharing of resources and costs for supporting equipment, network infrastructure and the physical facility. Bulk data processing and large-scale analysis tasks are performed by two Silicon Graphics (SGI) Origin 2000 servers. Each system has 6 processors and approximately 3 gigabytes (GB) of RAM. The influx of large data sets for additional sensors requires increasing amounts of disk space, especially when performing comparative analysis. The Data Processing server has nearly

100 GB of disk space and the Data Analysis server has almost 400 GB of total disk space. Long-term storage of data sets is handled by the 6 TB tape library attached to the Data Analysis server. Silicon Graphics O2 workstations now share software development and focused analysis tasks with high performance PCs running the Red Hat distribution of the Linux operating system. The sizing of the workstations varies with the task requirements. SIMBIOS is connected to the Internet via a 100-megabit link, making network transfer of large data sets more feasible. Internal connections are also 100 megabit for rapid transfer of data between the servers and

the workstations. Data ingest for SIMBIOS is also done via removable media including CD-ROM, 8 millimeter tape, 4 millimeter (DAT) tape, and DLT media up through DLT 7000. Off-line media storage space is shared with the SeaWiFS Project.

The group's work covered a variety of sensors over the year, with a significant effort covering the OCTS data set. Late in the year planning began on handling larger datasets from other sensors. The ground station at Wallops Flight Facility continues to receive MOS data downlinks, and the facility continues to perform routine processing of MOS data at the Greenbelt site. In support of these efforts, the facility has experienced moderate growth over the past year. PC workstations were added to the Project. Storage was maintained at its current level, with tape archival used to make room for additional data. With larger data sets on the horizon for next year, the Project will be increasing its storage capacity to meet the demand for space. Most space needs will be addressed using relatively low cost network attached storage (NAS) devices. Each server's FibreChannel interface was upgraded again to incorporate new functionality in FibreChannel hardware. The new interfaces were required to allow the servers to participate in the SeaWiFS Project Storage Area Network (SAN). While the implementation of the SeaWiFS high availability SGI server project has been shelved, manual fail-over of hardware components has been greatly enhanced with the use of SAN technology. Future growth in server-based computing power will be required to deal with large data set sensors. The Project will address these requirements with rack-mounted Linux clusters, a method which has proven highly successful for the SeaWiFS Data Processing System.

## REFERENCES

- Ainsworth, E.J., C. Pietras, M. Miller, R. Frouin, and S.W. Bailey, 2001: SIMBIOS Project Protocols for Processing In Situ Aerosol Optical Thickness Measurements, *National Aeronautics and Space Administration, Goddard Space Flight Center, Greenbelt, MD, Tech. Memo. 2001-209982*, 43-69.
- Barnes, S.L. J., 1964: A Technique for Minimizing Details in Numerical Weather Map Analysis, *Applied Meteorology*, vol. 3, 396-410.
- Bailey, S.W., C.R. McClain, P.J. Werdell, and B.D. Schieber, 2000: Normalized water-leaving radiance and chlorophyll *a* match-up analyses, In SeaWiFS Postlaunch Calibration and Validation Analyses, Part 2, *NASA Tech. Memo. 2000-206892*, S.B. Hooker and E.R. Firestone, Eds. NASA Goddard Space Flight Center, Greenbelt, Maryland, 45-52.
- Donoho, D.L., 1995: De-Noising by Soft-Thresholding, *IEEE Trans. on Information Theory*, vol. 41, no. 3, 613-627.
- Eck, T.F., B.N.Holben, J.S.Reid, O.Dubovik, A.Smirnov, N.T.O'Neill, I.Slutsker, and S.Kinne, 1999: The wavelength dependence of the optical depth of biomass burning, urban and desert dust aerosols, *J. Geophys. Res.*, 104, 31 333-31 350
- Franz, Bryan A. 2000: Status of the MOS Ground Station at NASA/Wallops, *Proc. 3rd International Workshop on MOS-IRS and Ocean Colour*, Berlin, Germany, 21-23 April 1999.
- Holben B.N., T.F.Eck, I.Slutsker, D.Tanre, J.P.Buis, A.Setzer, E.Vermote, J.A.Reagan, Y.Kaufman, T.Nakajima, F.Lavenu, I.Jankowiak, and A.Smirnov, 1998: AERONET - A federated instrument network and data archive for aerosol characterization, *Rem. Sens. Environ.*, 66, 1-16
- Gordon, H. R., and Wang, M., 1994: Retrieval of water-leaving radiance and aerosol optical thickness over the oceans with SeaWiFS: a preliminary algorithm, *Appl. Opt.* 33, 443-452.
- Gregg, W.W., W.E. Esaias, G.C. Feldman, R. Frouin, S.B. Hooker, C.R. McClain, R.H. Woodward, 1998: Coverage Opportunities for Global Ocean Color in a Multimission Era, *IEEE Trans. Geosci. and Remote Sens.*, vol. 36, no. 5, 1620-1627.
- Knobelspiesse, K.D., C. Pietras, and G.S. Fargion, 2001: Microtops II Hand-Held Sun Photometer Sun Pointing Error Correction for Sea Deployment, *Eos. Trans. AGU*, 82(47), Fall Meet. Suppl., Abstract OS52A-0532.
- Mallat, S.G., 1989: A Theory for Multiresolution Signal Decomposition: The Wavelet Representation, *IEEE Trans. on Pattern Analysis and Machine Intelligence*, vol. 11, no. 7, pp. 674-693.
- Maritorena, S., D.A. Siegel, A.R. Peterson and M. Lorenzi-Kayser, 2000: Tuning of a Pseudo-analytical Ocean Color Algorithm for Studies at Global Scales, AGU, OS12M-05, Jan. 2000, San Antonio, Texas.
- McClain, C.R. and G.S. Fargion, 1999a: SIMBIOS Project 1998 Annual Report. *NASA Tech. Memo. 1999-208645*, NASA Goddard Space Flight Center, Greenbelt, Maryland, 105 pp.

- McClain, C.R. and G.S. Fargion, 1999b: SIMBIOS Project 1999 Annual Report. *NASA Tech. Memo. 1999-209486*, NASA Goddard Space Flight Center, Greenbelt, Maryland, 128 pp.
- Núñez, J., X. Otazu, O. Fors, A. Prades, V. Palà, R. Arbiol, 1999: Multiresolution-Based Image Fusion with Additive Wavelet Decomposition, *IEEE Trans. Geosci. and Remote Sens.*, vol. **37**, no.3, 1204-1211.
- Pietras, C., R. Frouin, T. Nakajima, M. Yamano, K.D. Knobelspiesse, J. Werdell, G. Meister, G. Fargion, C. McClain, 2001: Aerosol Properties Derived from the PREDE POM-01 Mark II Sun Photometer, *Eos. Trans. AGU*, 82(47), Fall Meet. Suppl., Abstract OS52A-0531.
- Porter, J.N., M.A. Miller, C. Pietras, and G. Motell, 2001: Ship-based sun photometer measurements using Microtops sun Photometers, *J. Atmos. Ocean. Tech.*, **18**, 765-774.
- Reynolds R.W. 1988: A Real-Time Global Sea Surface Temperature Analysis, *Climate*, vol. **1**, 75-86.
- Reynolds, R.M., M.A. Miller, and M.J. Bartholomew, 2000: Design, operation, and calibration of a shipboard fast rotating shadowband spectral radiometer. *J. Atmos. Ocean. Tech.*, **18**, 200-214.
- Russell, P. B., J.M. Livingston, E.G. Dutton, R.F. Pueschel, J.A. Reagan, T.E. Defour, M.A. Box, D. Allen, P. Pilewskie, B.M. Herman, S.A. Kinne, and D.J. Hofmann, 1993: Pinatubo and pre-Pinatubo optical depth spectra: Mauna Loa measurements, comparisons, inferred particle size distributions, radiative effects, and relationship to lidar data, *J. Geophys. Res.*, **98**, 22,969-22,985.
- Smirnov, A., B.N.Holben, T.F.Eck, O.Dubovik, and I.Slutsker, 2000: Cloud screening and quality control algorithms for the AERONET data base. *Rem. Sens. Environ.*, **73**, 337-349.
- Starck J. L. and F. Murtagh, 1994: Image Restoration with Noise Suppression Using The Wavelet Transform, *Astron. Astrophys.*, vol. **288**, pp. 342-348.
- Thiebaux H.J and Pedder, 1987: *Spatial Objective Analysis*, Academic Press.
- Thiebaux, H. J., 1973: Maximally Stable Estimation of Meteorological Parameters at Grid Points, *J. Atmospheric Science*, vol. **30**, 1710-1714.
- Wang M. , S. Bailey, C. Pietras, C.R. McClain, and T. Riley, 2000: SeaWiFS Aerosol Optical Thickness Matchup Analysis, *NASA Tech. Memo. 2000-206892*. In McClain, C.R., E.J. Ainsworth, R.A. Barnes, R.E. Eplee, Jr., F.S. Patt, W.D. Robinson, M. Wang, and S.W. Bayley, SeaWiFS Postlaunch Calibration and Validation analyses, Part 1, S.B. Hooker and E.R. Firestone, Eds, NASA Goddard Space Flight Center, Greenbelt, Maryland.
- Wang, M., Isaacman, A, Franz, B. A. 2001: Ocean Color Optical Property Data Derived from OCTS and POLDER: A Comparison Study, *Appl. Opt.*, in press.
- Wang, M. and Franz, B. A., 2000: Comparing the ocean color measurements between MOS and SeaWiFS: A vicarious intercalibration approach for MOS, *IEEE Trans. Geosci. Remote Sensing*, Vol. **38**, No 1, 184-197.
- Werdell, P.J., S.W. Bailey, and G.S. Fargion, 2000: SeaBASS data protocols and policy, In Ocean Optics Protocols for Satellite Ocean Color Sensor Validation, Revision 2, *NASA Tech. Memo. 2000-209966*, G.S. Fargion and J.L. Mueller, Eds. NASA Goddard Space Flight Center, Greenbelt, Maryland, 170-172.

## Chapter 4

# Adaptation of a Hyperspectral Atmospheric Correction Algorithm for Multi-spectral Ocean Color Data in Coastal Waters

Bo-Cai Gao, Marcos J. Montes, and Curtiss O. Davis

*Remote Sensing Division, Naval Research Laboratory, Washington, D.C.*

### 4.1 INTRODUCTION

This SIMBIOS contract supports several activities over its three-year time-span. These include certain computational aspects of atmospheric correction, such as the modification of our hyperspectral atmospheric correction algorithm for various multi-spectral instruments, such as SeaWiFS, MODIS, and GLI. Additionally, since absorbing aerosols are becoming common in many coastal areas, this grant supports the calculation and incorporation of various absorbing aerosol models into tables used by our atmospheric correction algorithm. Finally, we will use MODIS data to characterize thin cirrus effects on aerosol retrieval.

### 4.2 RESEARCH ACTIVITIES

The research activities during the first year of this contract were mostly concerned with modifications of our hyperspectral atmospheric correction algorithm (Gao et al. 2000; Montes et al. 2001) to versions compatible with MODIS and SeaWiFS. Our first concern was getting the algorithms to compile and run successfully; a secondary concern was to ensure that they are executing in a reasonable time. Each version was compiled on both SGI and Linux workstations. The Linux version is at the SeaWiFS project office for further testing. Some testing has been done as part of an AVIRIS/MODIS/MOBY intercalibration. In preparation for calculating lookup-tables with various dust aerosol models, we applied for and received computer time on the Naval Research Laboratory's High Performance Computer system.

### 4.3 RESEARCH RESULTS

The modification of the algorithms has proceeded along two lines. For hyperspectral data using normal platforms, in the past it has been sufficient to assume single solar and observational geometries. This allows us to perform one major interpolation over all the geometrical quantities in our lookup tables before performing atmospheric correction. This is not

practical with both MODIS and SeaWiFS since their ground swath widths are very large. For these versions, we have currently implemented averaging over a user-specified box when calculating the angular values used for the atmospheric correction. The box sizes can be specified in both the x and y directions, and the solar and view angles are averaged. These averaged angles are used to interpolate the look-up tables. Finally, the atmospheric correction is performed for each pixel in the box. We have also investigated a pure pixel-by-pixel atmospheric correction code. This necessarily executes more slowly than the box versions because a separate interpolation across the angular directions of the lookup tables must be performed for each pixel.

We have processed a few scenes of MODIS and SeaWiFS with the box versions of the atmospheric correction code. Some studies have been done for areas near the MOBY buoy. In particular, we have analyzed some scenes from April, 2000 when AVIRIS flew under MODIS and SeaWiFS. We developed software to navigate the AVIRIS scene in order to find locations in the AVIRIS and MODIS scenes with similar view and solar geometry. Additionally, it was necessary to correct the AVIRIS measurements for both absorption and scattering effects from AVIRIS' approximately 20 km altitude to the top of the atmosphere. We find that near 0.47 micron, the observed reflectance (corrected to the top of the atmosphere) for AVIRIS is 9% greater than that measured by MODIS; at 0.747 micron the difference is about 8%, with the MODIS values being greater than those of AVIRIS (see Figures 4.1 and 4.2).

A final comparison is performed between the water-leaving reflectance from MOBY (Clark & Flora 2000) and that calculated by atmospheric correction for AVIRIS and MODIS. We find that MOBY agrees quite well with MODIS. However, the aforementioned differences between AVIRIS and MODIS lead to large differences in the derived water-leaving reflectance for AVIRIS and MOBY. There appear to be two reasons for this effect. First, the 0.747 micron band was used to determine the aerosol model and type. The lower AVIRIS value implies a different aerosol model is being chosen for the AVIRIS atmospheric correction – one with

lower optical depth, and therefore less aerosol scattering to remove than was indicated by the MODIS measurements. Second, AVIRIS's greater signal in the blue is subtracted out less. Thus, the atmospherically corrected signal from AVIRIS is much different than that of MODIS. Having said all this, we are still working with only this single AVIRIS underflight of MODIS, and with the initial calibration information we received for MOBY, MODIS, and AVIRIS. These results may change somewhat as we continue the testing of our software and as we obtain better calibration information for each of the instruments.

#### 4.4 CONCLUSIONS

We have made progress in modifying our atmospheric correction algorithm to be used with multi-spectral data from MODIS and SeaWiFS. "Box" versions of these algorithms have been successfully compiled and run on two platforms. Initial results are promising, but in some instances we need to

determine final calibrations status for MOBY, MODIS, and SeaWiFS data as we continue our testing. In the following year we intend to begin calculations of tables with various dusts, in addition to finishing continuing intercomparisons of data from MOBY, MODIS, SeaWiFS, and AVIRIS.

#### REFERENCES

Clark, D. and S. Flora, 2000. Personal communication.

Gao, B.-C., M.J. Montes, Z. Ahmad, and C.O. Davis, 2000. Atmospheric correction algorithm for hyperspectral remote sensing of ocean color from space. *Appl Opt.*, **39**(6), 887-896.

Montes, M.J., B.-C. Gao, and C.O. Davis. 2001: A new algorithm for atmospheric correction of hyperspectral remote sensing data. *SPIE*, **4383**, 23-30.

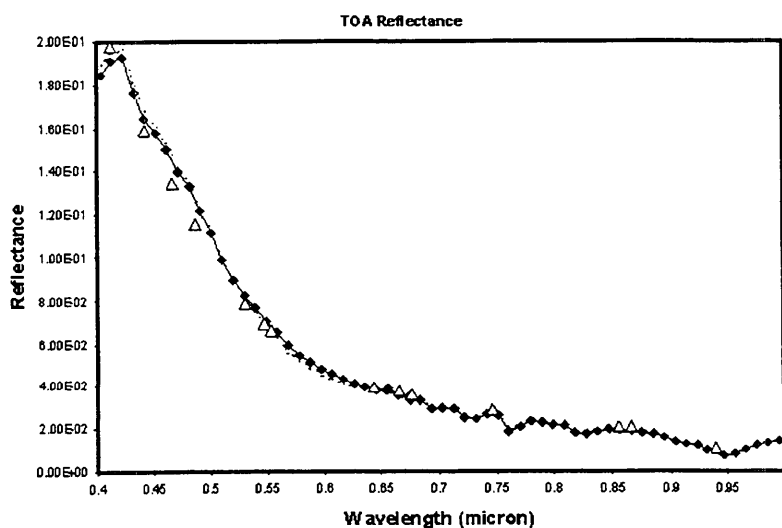


Figure 4.1: Top of the atmosphere reflectance observed near the MOBY site by AVIRIS (dashed line) and MODIS (open triangles). Note that while the radiance measurements are generally in good agreement, the AVIRIS radiance near 0.4 micron is significantly less than radiance observed by MODIS. The AVIRIS radiance at 0.747 micron is also about 10% less than that measured by MODIS. The solid line with solid diamonds is the observed atmospheric reflectance before being transferred to the top of the atmosphere.

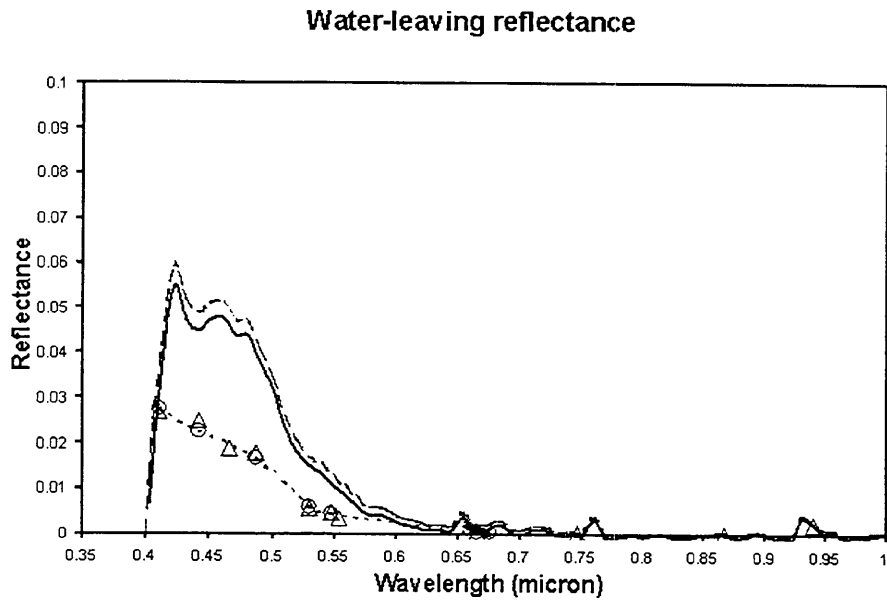


Figure 4.2: Derived water-leaving reflectance spectra from AVIRIS and MODIS (open triangles), compared to MOBY (open circles, small dashes) measurements. The solid line is AVIRIS corrected using the two MODIS bands near 0.75 micron and 0.865 micron to determine the atmospheric correction. The long-dashed line is the atmospheric correction derived using four window channels longer than 1 micron.

*This research was supported by the SIMBIOS NASA interagency agreement # S-44797-X*

## PRESENTATIONS

Gao, B. C., M.J. Montes, and C.O. Davis, 2001: Development of an atmospheric correction algorithm for remote sensing of coastal waters. Presented at the SIMBIOS Science Team Meeting, Greenbelt.

Davis, C.O., B.-C. Gao, M.J. Montes, G. Feldman, B. Franz, F. Patt, and R. Stumpf, 2001: Atmospheric Correction of Ocean Color Data at the MOBY site in Hawaiian Waters. Presented at the Tenth JPL AVIRIS Science and Applications Workshop, Pasadena.

## Chapter 5

# Bio-Optical Measurements in Upwelling Ecosystems in Support of SIMBIOS

Francisco P. Chavez, Peter G. Strutton, Victor S. Kuwahara and Eric Drake  
*Monterey Bay Aquarium Research Institute, Moss Landing, California*

### 5.1 INTRODUCTION

The equatorial Pacific strongly influences global biogeochemistry, due to the upwelling which spans more than a quarter of the earth's circumference. This upwelling system has significant implications for global CO<sub>2</sub> fluxes (Tans *et al.*, 1990; Takahashi *et al.*, 1997; Feely *et al.*, 1999), as well as primary and secondary production (Chavez and Barber, 1987; Chavez and Toggweiler, 1995; Chavez *et al.*, 1996; Dugdale and Wilkerson, 1998; Chavez *et al.*, 1999; Strutton and Chavez, 2000). In addition, this region represents a large oceanic province over which validation data for SeaWiFS are necessary. This project consists of a mooring program and supporting cruise-based measurements aimed at quantifying the spectrum of biological and chemical variability in the equatorial Pacific and obtaining validation data for SeaWiFS. Since 1997, the MBARI equatorial Pacific program has demonstrated ability to:

- obtain high quality, near real time measurements of ocean color from moored platforms in the equatorial Pacific.
- process these data into files of the required format for routine ftp to the SeaBASS database.
- obtain supporting ship-based optical profiles (including water leaving radiance,  $L_{wn}$ ) and pigment concentration measurements, also for submission to SeaBASS.
- process and interpret the time series, satellite and ship-based data in order to quantify the biogeochemical processes occurring in the equatorial Pacific on time scales of days to years (Chavez *et al.*, 1998; Chavez *et al.*, 1999; Strutton & Chavez, 2000; Strutton *et al.*, 2001).

### 5.2 RESEARCH ACTIVITIES

#### *Moorings*

Chavez *et al.* (1998; 1999) and McClain and Fargion (1999, p.44) describe the configuration of the MBARI bio-optical and chemical instruments deployed at 0°, 155°W and

2°S, 170°W; two of the 70 moorings which form the Tropical Atmosphere Ocean (TAO) array.

From these locations daily local 10 am and noon (ie approximate time of MODIS and SeaWiFS overpasses, respectively) bio-optical and chemical data are transmitted via service ARGOS in near real time to MBARI, and then displayed on the web at:

<http://bog.shore.mbari.org/~bog/oasis.html>.

Higher frequency, publication-quality data (15-minute intervals) are recovered at approximately six month intervals, and sent to the SeaBASS database after processing and quality control. Derived products, such as water leaving radiance ( $L_w$ ), and remote sensing reflectance ( $R_{rs}$ ) are included in these data files for validation efforts. In the past,  $L_w$  has been calculated via three different methods (McLain and Fargion, 1999b), but is currently calculated only as follows. The diffuse attenuation coefficient ( $K_\lambda$ ) over the upper 20m of the water column is calculated using  $Ed_{3m+}$  and  $Ed_{20m-}$ , then using this  $K_\lambda$ ,  $Lu_{20m}$  is extrapolated back to just below the surface. This parameter ( $Lu_{0m-}$ ) is then multiplied by 0.544 to account for transmission across the air-water interface to obtain  $Lu_{0m+}$ . Of the three methods previously used, this has been shown to be the most reliable, because the 3m+ and 20m- instruments are less susceptible to fouling than the OCR-100s moored at ~1.5m. However, the efficacy of this method is currently being assessed, and we hope to make improvements in the near future.

During 2001 our data processing, quality control and data provision capabilities have improved, and the majority of the mooring data can now be viewed on the web at:

[http://www.mbari.org/bog/Projects/EQPAC/eqpac\\_qc/eqpac\\_qc.htm](http://www.mbari.org/bog/Projects/EQPAC/eqpac_qc/eqpac_qc.htm)

The following quality control procedures are currently applied to our data:

- Measured surface-incident irradiance ( $E_s$ ) must be less than 1.15 times modeled, clear-sky  $E_s$  (Frouin, 1989).
- $K_\lambda$  must be greater than that of pure water (Morel, 1988).
- OC2V2 chlorophyll is calculated for the  $R_{rs}$  ratios of 412/555, 443/555, 490/555, and 510/555 and the

coefficient of variance is calculated for each sample. *In situ measurements*  
Coefficients of variance less than 0.4 are acceptable.

- Time series of all parameters at all wavelengths for all individual instrument deployments are plotted together as one long time series to identify discontinuities between deployments, due to problems such as poor calibrations. This is sometimes identified by normalizing specific wavelengths against others. In coming years we hope to continue improvement of these criteria and use the results to perhaps modify mooring and instrument configurations.

With the buoy design and data acquisition protocols now proven in the field, we are making significant improvements to the quantity and quality of optical data collected during this funding period. This will amount to augmenting the discrete wavelength instruments with hyperspectral, optical fiber packages. We anticipate these configuration changes will produce data of significantly higher quality for almost the same cost as the existing discrete-wavelength instruments. In 2000 we deployed a HOBILabs HydroRad 4 (HR4) system at the M1 mooring in Monterey Bay. In October 2001, we deployed a HOBILabs HR3 at both equatorial Pacific moorings: 0° 155°W and 2°S 170°W. This instrument will provide hyperspectral data consisting of:

- downwelling irradiance above the surface (3m)
- downwelling irradiance and upwelling radiance at 10m depth.

The Hydrorad data are available in programmable bin sizes (highest resolution 0.37nm), over the range ~300 to 850nm, but for deployment in the equatorial Pacific we have binned the data to ~2nm resolution. We also anticipate improved fluorescence measurements with newly deployed HOBILabs Hydrosat 2 (HS2) instruments fitted with new copper anti-fouling shutters. The HS2 measures backscatter and fluorescence at two wavelengths. With the deployment of these new instruments, in particular the hyperspectral radiometers, we can better support new and forthcoming ocean color missions such as MODIS and GLI and the development of ocean color algorithms that will go beyond chlorophyll.

#### *Optical profiling measurements*

On mooring maintenance cruises, optical profiles of the upper 100 to 200 m of the water column are performed, daily when possible, close to local noon. The instrument used is the Satlantic SeaWiFS Profiling Multispectral Radiometer (SPMR). Profile data are processed using Satlantic's ProSoft software, and a suite of derived products, including diffuse attenuation coefficients, water leaving radiances ( $L_{wn}$ ) and light penetration depths are obtained. Parameters of interest (mostly  $L_{wn}$ ) are provided to NASA post-cruise, and the profile data are archived at MBARI along with existing optical profiles from almost every oceanic province.

Table 5.1 summarizes the cruises undertaken by MBARI this fiscal year in support of SIMBIOS. Essentially, the cruise-based measurements consist of chlorophyll (using the fluorometric method described by Chavez *et al.* (1995) and nutrient profiles (8 depths, 0-200m) obtained at CTD stations between 8°N and 8°S across the Pacific from 95°W to 165°E. On selected cruises (the 155°W and 170°W meridional transects), HPLC samples are collected and productivity ( $^{14}\text{C}$ ,  $^{15}\text{N}$ ) measurements are also performed. These data are archived at MBARI and the pigment data provided to the SeaBASS database for algorithm development. More recently we have measured colored dissolved organic matter (CDOM) on our cruises.

## 5.3 RESEARCH RESULTS

#### *Biogeochemical cycles*

Several publications describing ecosystem variability in the equatorial Pacific have been produced under MBARI's SIMBIOS funding. Chavez *et al.* (1998) used mooring data from 0°, 155°W to describe the biological-physical coupling observed in the central equatorial Pacific during the onset of the 1997-98 El Niño. Chavez *et al.* (1999) combined the physical, biological and chemical data from moorings, ships and SeaWiFS to provide a comprehensive view of the ecosystem's response to the extreme physical forcings experienced during the 1997-98 El Niño. Strutton and Chavez (2000) summarized the *in situ* cruise measurements spanning the period from November 1996 to December 1998, and used these data to describe the perturbations to chlorophyll, nutrients and productivity during the same time period. Strutton *et al.* (2001) used time series from smaller Satlantic bio-optical packages and SeaWiFS imagery, to quantify the extreme anomalies in chlorophyll associated with the passage of tropical instability waves (TIWs) during the second half of 1998 and 1999. These data not only quantified the magnitude of the chlorophyll anomalies observed, but also helped to elucidate the mechanisms potentially responsible for the concentration of chlorophyll in association with TIWs.

In addition to the manuscripts just described, Chavez *et al.* (2000) documented the design, and demonstrated the efficacy of the shutter mechanism which protects the 20m radiometer on the moorings from fouling. Further, we have submitted two abstracts to 2001 Fall AGU and are working on the mooring chapter for the 3<sup>rd</sup> revision of the Mueller protocols TM. Other manuscripts currently in preparation include a book chapter for submission to a CRC Press publication (Strutton *et al.* In prep), a paper describing the evolution of the 1998 La Niña blooms (Ryan *et al.*, in revision), and a manuscript describing the biological component of the equatorial Pacific heat budget (Strutton and Chavez, in revision).

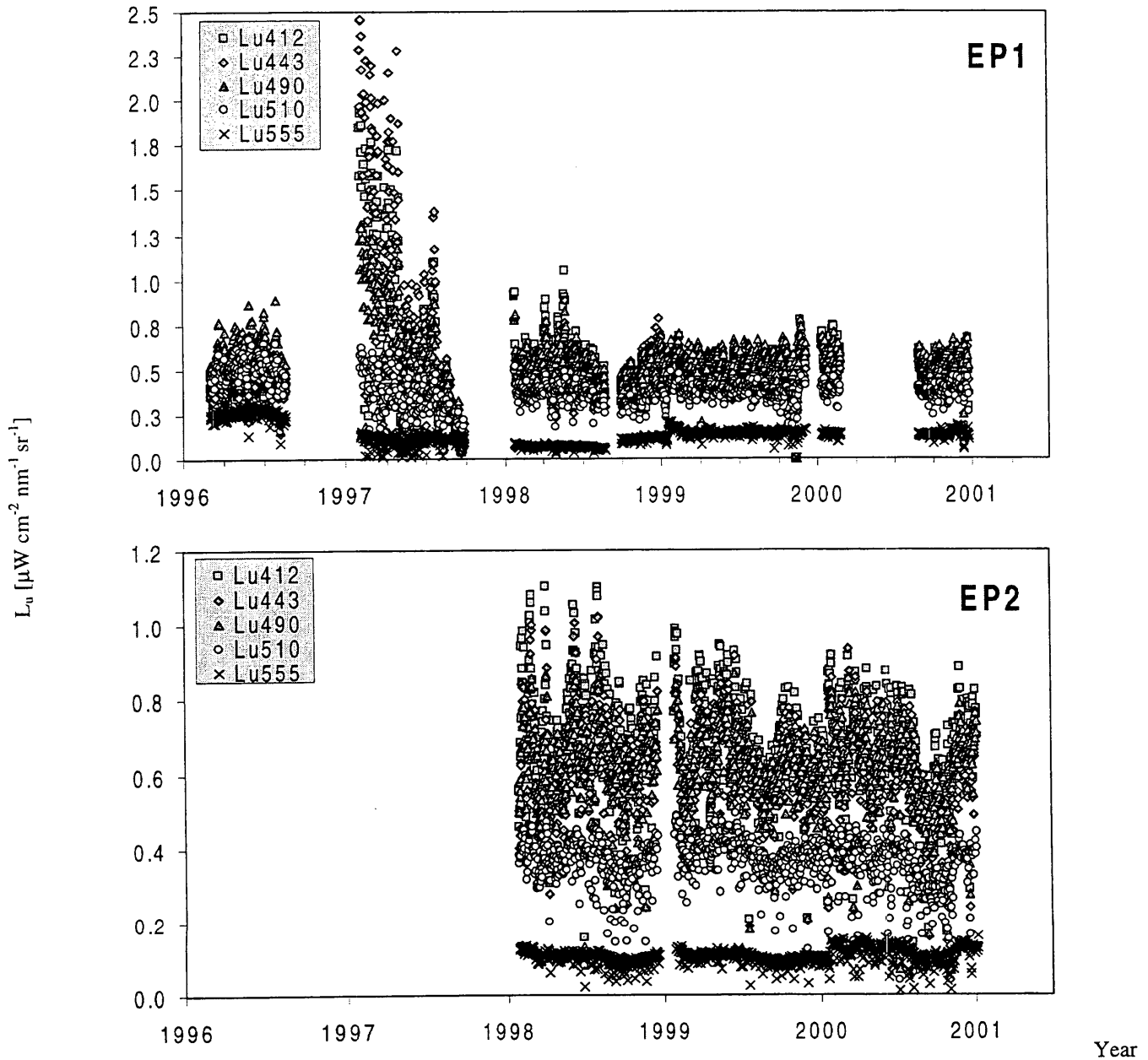


Figure 5.1: The time series of the upwelling radiance,  $L_u$  [ $\mu\text{W cm}^{-2} \text{ nm}^{-1} \text{ sr}^{-1}$ ], derived from the MBARI optical instruments on the TAO moorings at  $0^\circ$   $155^\circ\text{W}$  (EP1) and  $2^\circ\text{S}$   $170^\circ\text{W}$  (EP2).

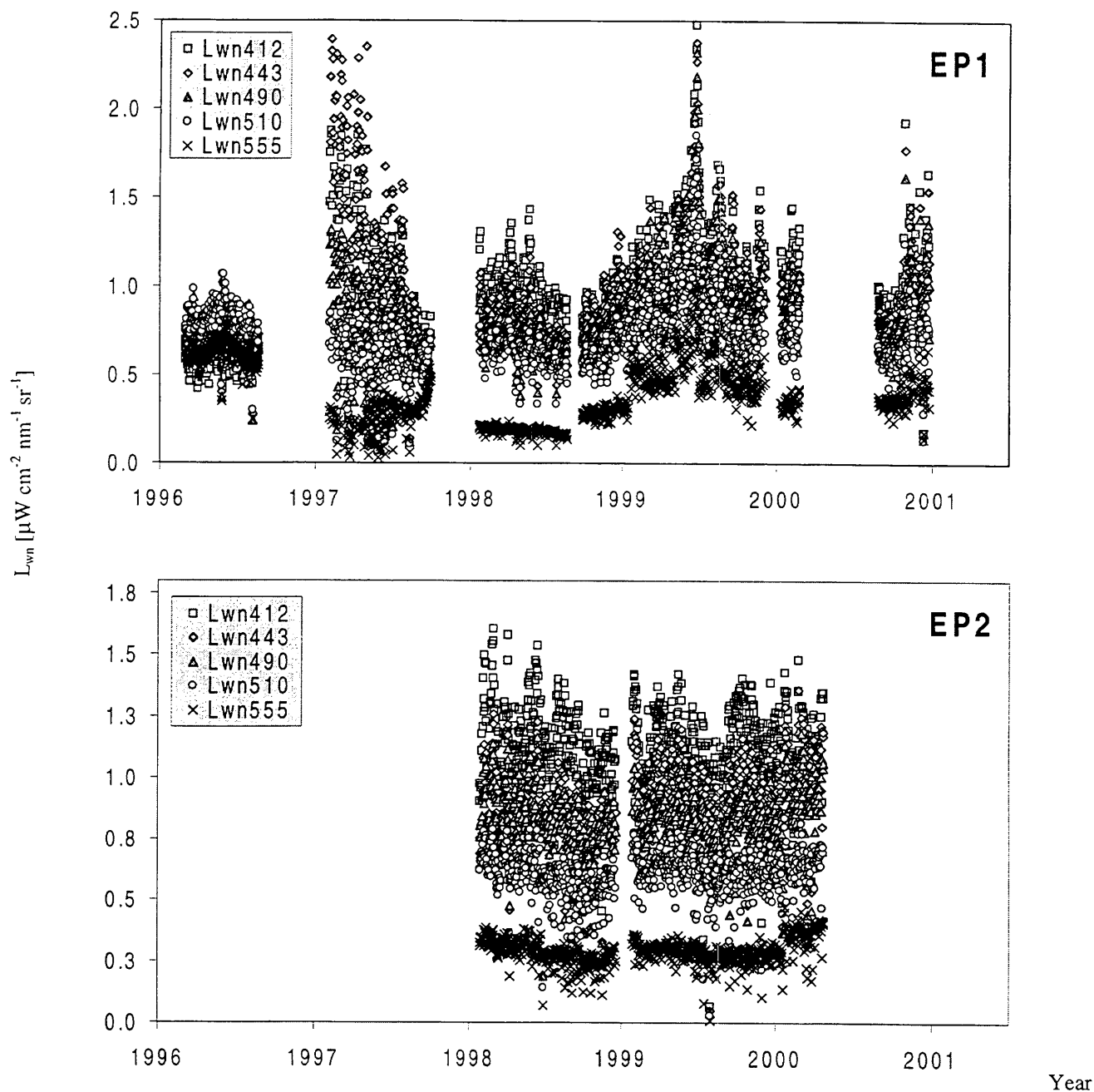


Figure 5.2: The time series of normalized water-leaving radiance,  $L_{wn}$  [ $\mu\text{W cm}^{-2} \text{ nm}^{-1} \text{ sr}^{-1}$ ], derived from the  $L_u$  and  $K_d$  data obtained from MBARI optical instruments on the TAO moorings at  $0^\circ 155^\circ\text{W}$  (EP1) and  $2^\circ\text{S } 170^\circ\text{W}$  (EP2). The data have been subject to quality control as described in methods. Note: Although EP2  $L_{wn}$  data from 01-Feb-01 to present is available, data are not included in graph because post-calibration of the above water radiometer is required.

#### SeaWiFS Calibration/Validation

Over the last 3 months we have rigorously reprocessed the full mooring records (1996-2001) for EP1 ( $0^\circ$ ,  $155^\circ\text{W}$ ) and EP2 ( $2^\circ\text{S}$ ,  $170^\circ\text{W}$ ) to further improve our data quality control methods. Analysis and improvements to quality control

continue on the reprocessed data. These data have been uploaded to SeaBass. Figures 5.1 and 5.2 show the time series of  $L_u$  and  $L_{wn}$ , respectively. Figure 5.3 shows the time series products based on  $K_d$  and  $L_{wn}$ . The two methods in Figure 5.3 agree particularly well over a range of chlorophyll concentrations from  $\sim 0.05$  to  $>1 \mu\text{g l}^{-1}$ . This agreement is

further quantified in Figure 5.4a, which directly shows the comparison of the two methods for EP1.

McClain and Fargion (1999b) showed matchup data derived from optical profiles of the SPMR in the equatorial Pacific. These data indicated excellent agreement between the satellite- and profile-derived water-leaving radiance values. Similarly, Figure 4b compares the surface chlorophyll values obtained from SPMR casts with the extracted chlorophyll samples obtained at the same location.

## 5.4 FUTURE WORK

None recent setbacks related to hardware failures and vandalism, the two major mooring installations at 0°, 155°W and 2°S, 170°W are now operating relatively well. The recent deployment of hyperspectral instruments at both moorings will better support validation efforts for future ocean color missions.

This year alone we have conducted over 50 SPMR profile casts, analyzed more than 2500 shipboard chlorophyll measurements, and collected close to 500 HPLC samples. In the near future we intend to analyze these HPLC data in conjunction with the optical profile data in order to better understand the pigment distribution in the euphotic zone and its relationship to water leaving radiance. Further, we are now in the process of updating our analysis of nutrient samples. The program of cruise-based measurements as described above will continue on eight equatorial Pacific cruises during 2002-2003, with scheduled SeaWiFS LAC where applicable, to enhance the probability of obtaining valid matchups.

## REFERENCES

- Chavez, F.P., and R.T. Barber, 1987: An estimate of new production in the equatorial Pacific, *Deep-Sea Research*, **34**, 1229-1243.
- Chavez, F.P., K.R. Buck, R.R. Bidigare, D.M. Karl, D. Hebel, M. Latasa, L. Campbell and J. Newton, 1995: On the chlorophyll a retention properties of glass-fiber GF/F filters. *Limnology and Oceanography*, **40**, 428-433.
- Chavez, F.P. and J. R. Toggweiler, 1995: in *Upwelling in the Ocean: Modern Processes and Ancient Records* C. P. Summerhayes, K. C. Emeis, M. V. Angel, R. L. Smith, B. Zeitzschel, Eds. (J. Wiley & Sons, Chichester, 1995) 313-320.
- Chavez, F.P., K.R. Buck, S.K. Service, J. Newton and R.T. Barber 1996: Phytoplankton variability in the central and eastern tropical Pacific. *Deep-Sea Research*, **43**(4-6), 835-870.
- Chavez, F.P., P.G. Strutton, and M.J. McPhaden, 1998: Biological-physical coupling in the central equatorial Pacific during the onset of the 1997-98 El Niño. *Geophysical Research Letters*, **25**(19), 3543-3546.
- Chavez, F.P., P.G. Strutton, G.E. Friederich, R.A. Feely, G. Feldman, D. Foley and M.J. McPhaden, 2000: M.J. Biological and chemical response of the equatorial Pacific Ocean to the 1997-98 El Niño, *Science*, **286**, 2126-2131.
- Chavez, F.P., D. Wright, R. Herlien, M. Kelley, F. Shane and P.G. Strutton, 2000: A device for protecting moored spectroradiometers from bio-fouling. *Journal of Oceanic and Atmospheric Technology*, **17**, 215-219.
- Dugdale, R.C. and F.P. Wilkerson 1998: Silicate regulation of new production in the equatorial Pacific upwelling, *Nature*, **391**, 270-273.
- Feely, R.A., R. Wanninkhof, T. Takahashi and P. Tans 1999: Influence of El Niño on the equatorial Pacific contribution to atmospheric CO<sub>2</sub> accumulation. *Nature*, **398**, 597-601.
- Frouin, R., D.W. Ligner, and C. Gautier, 1989: A simple analytical formula to compute clear sky total and photosynthetically available solar irradiance at the ocean surface. *Journal of Geophysical Research*, **94**, 9731-9742.
- McClain C.R. and G.S. Fargion, 1999a: SIMBIOS Project 1998 Annual Report. *NASA Tech. Memo. 1999-208645*, Eds., NASA Goddard Space Flight Center, Goddard, Maryland, 105pp.
- McClain C.R. and G.S. Fargion, 1999b: SIMBIOS Project 1999 Annual Report. *NASA Tech. Memo. 1999-209486*, Eds., NASA Goddard Space Flight Center, Goddard, Maryland, 137pp.
- Morel, A. 1988: Optical modeling of the upper ocean in relation to its biogenous matter content (Case I waters). *Journal of Geophysical Research*, **93**, 10749-10768.
- Strutton, P.G. and Chavez, F.P. Radiant heating in the equatorial Pacific: Spatial and Temporal variability. *Deep-Sea Research I*, in revision.
- Ryan, J.P., P.S. Polito, P.G. Strutton and F.P. Chavez, Anomalous phytoplankton blooms in the equatorial Pacific. *Progress in Oceanography*, in revision.
- Strutton, P.G., J.P. Ryan and F.P. Chavez, 2001: Enhanced chlorophyll associated with tropical instability waves in the equatorial Pacific. *Geophysical Research Letters*, **28**(10), 2005-2008.
- Strutton, P.G. and F.P. Chavez, 2000: Primary productivity in the equatorial Pacific during the 1997-98 El Niño.

*Journal of Geophysical Research*, **105**(C11), 26,089-26,101. Tans, P.P., I. Y. Fung, T. Takahashi 1990: Observational constraints on the global atmospheric CO<sub>2</sub> budget, *Science*, **247**, 1431-1438.

Strutton, P.G., Chavez, F.P., Ryan, J.P. and Friederich, G.E., 2002: Merging data from ships, satellites, moorings and drifters to understand biological-physical coupling in the oceans. In preparation for 'Handbook of scaling methods in aquatic ecology: Measurement, analysis and simulation', CRC Press.

Takahashi, T, R.A. Feely, R.F. Weiss, R. Wanninkhof, D.W. Chipman, S.C. Sutherland and T.T. Takahashi 1997: Carbon dioxide and climate change. *Proceedings of the National Academy of Sciences*, **94**, 8314-8319.

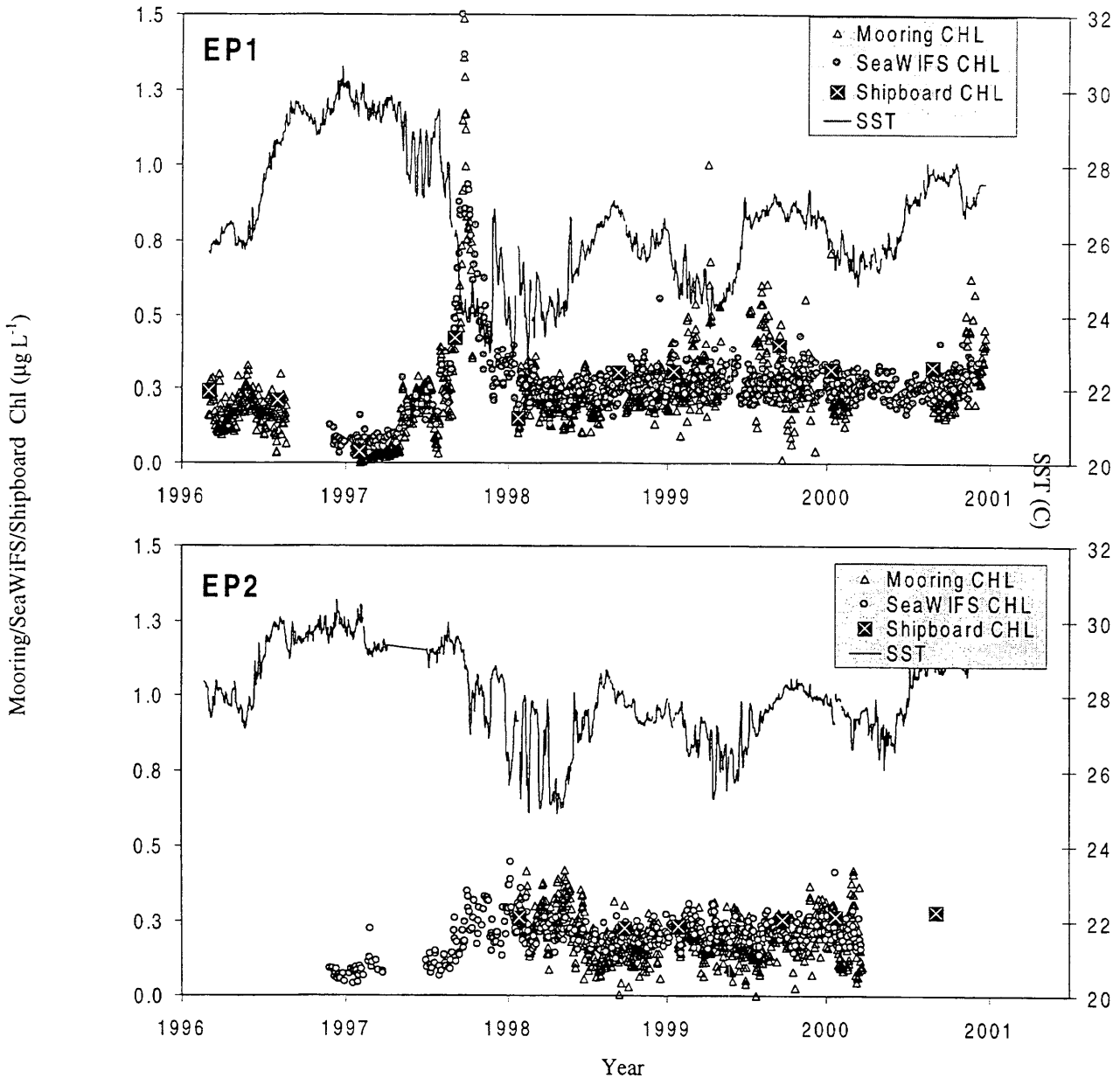


Figure 5.3: The time series of chlorophyll derived from the MBARI optical instruments on the TAO moorings at 0° 155°W (EP1) and 2°S 170°W (EP2). For comparison, SeaWiFS chlorophyll for the mooring location is also plotted (circles). The time series of SST indicates that the highest chlorophyll concentrations occurred during the retreat of the 1997-98 El Niño, in mid 1998 at EP1. SeaWiFS and mooring chlorophyll exhibit relatively good agreement over more than an order of magnitude of chlorophyll concentrations.

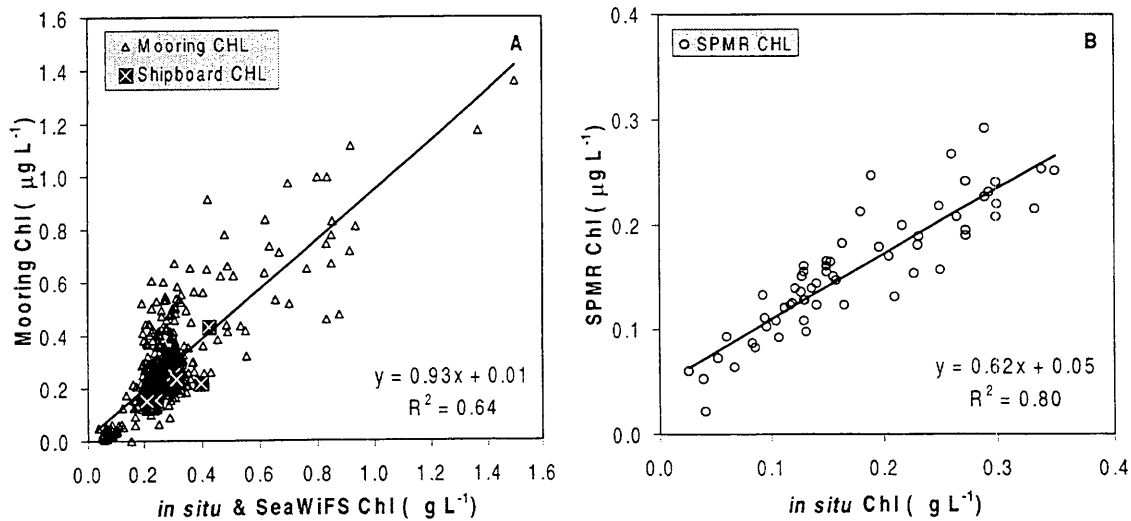


Figure 5.4: (A) Comparison of SeaWiFS and shipboard *in situ* chlorophyll with mooring-derived chlorophyll for the MBARI instruments at  $0^\circ$   $155^\circ\text{W}$  (EP1). Mooring-derived chlorophyll is calculated using algorithm by Morel, A. (1988). Regression analysis for SeaWiFS vs. Mooring Chl is also shown. (B) Comparison of chlorophyll from shipboard measurements with chlorophyll calculated from SPMR casts. SPMR chlorophyll is calculated using OC4V4 algorithm by O'Reilly, J.O. All data have been subject to quality control.

Table 5.1: Summary of cruises during which *in situ* data have been obtained by MBARI in support of SIMBIOS. All cruises were undertaken aboard the NOAA ship *Ka'imimoana*, with the exception of GasEx II cruise aboard the *Ronald H. Brown* (see: [www.pmel.noaa.gov/co2/gasex2](http://www.pmel.noaa.gov/co2/gasex2)). Meridional transects indicate the lines occupied by the ship. Along each line, CTD stations were performed approximately every degree of latitude from  $8^\circ\text{N}$  to  $8^\circ\text{S}$ , except for GasExII. Measurements consisted of extracted chlorophyll (Chl) plus nitrate, phosphate and silicate (Nutrients) at 8 depths between 0 and 200m. On selected cruises, primary production (PP) and new production (NP) measurements were also made using  $^{14}\text{C}$  and  $^{15}\text{N}$  incubation techniques, respectively. Daily optical profiles were obtained using the Satlantic SeaWiFS Profiling Multispectral Radiometer (SPMR) where indicated.

Cruise ID	Dates	Meridional transects	Measurements
GP6-00-KA	14-Oct-00 to 14-Nov-00	155W and 170W	Chl, NP, PP, Nutrients, SPMR
GP7-01-RB	16-Oct-00 to 22-Nov-00	95W and 110W	Chl, Nutrients
GP8-00-KA	16-Nov-00 to 14-Dec-00	165W and 180W	Chl, Nutrients
GP1-01-KA	14-Jan-01 to 15-Feb-01	140W and 125W	Chl, Nutrients
GasEx II	28-Jan-01 to 08-Mar-01	125W and 140W	Chl, NP, PP, Nutrients, SPMR
GP2-01-KA	28-Mar-01 to 05-May-01	95W and 110W	Chl, Nutrients
GP3-01-KA	29-May-01 to 29-Jun-01	155W and 170W	Chl, NP, PP, Nutrients, SPMR
GP4-01-KA	02-Jul-01 to 31-Jul-01	165E and 180	Chl, Nutrients
GP5-01-KA	13-Aug-01 to 03-Sep-01	125W and 140W	Chl, Nutrients
GP7-01-KA	28-Sep-01 to 25-Oct-01	155W and 170W	Chl, NP, PP, Nutrients, SPMR
GP8-01-KA	01-Nov-01 to Dec-01	165E and 180	Chl, Nutrients

*This research was supported by the  
SIMBIOS NASA contract # 00193*

## PEER REVIEWED PUBLICATIONS

- Chavez, F.P., Strutton, P.G., Friederich, G.E., Feely, R.A., Feldman, G.C., Foley, D.G. and McPhaden, M.J., 1999: Biological and chemical response of the equatorial Pacific Ocean to the 1997-98 El Niño. *Science*. **286**, 2126-2131.
- Chavez, F.P., Strutton, P. G. & McPhaden, M. J., 1998: Biological-physical coupling in the equatorial Pacific during the onset of the 1997-98 El Niño. *Geophysical Research Letters*., **25**(19), 3543-3546.
- Chavez, F.P., Wright, D., Herlien, R., Kelley, M., Shane, F. and Strutton, P.G., 2000: A device for protecting moored spectroradiometers from bio-fouling. *Journal of Oceanic and Atmospheric Technology*, **17**, 215-219.
- Schwarz, J.N., Gege, P., Kowalczyk, P., Kaczmarek, S., Carder, K.L., Muller-Karger, F., Varela, R., Chavez, F.P., Clark, D.K., Cota, G.F., Cunningham, A., McKee, D., Kishino, M., Mitchell, B.G., Phinney, D.A., Raine, R., Trees, C.C., Zaneveld, J.R.V., Pegau, S. Two models for Gelbstoff absorption. *Oceanologia*, in preparation..
- Strutton, P.G. and Chavez, F.P. Radiant heating in the equatorial Pacific: Spatial and Temporal variability. *Deep-Sea Research I*, in revision.
- Ryan, J.P., Polito, P.S., Strutton, P.G. and Chavez, F.P. Anomalous phytoplankton blooms in the equatorial Pacific. *Progress in Oceanography*, in revision.
- Strutton, P.G., Ryan, J.P. and Chavez, F.P. 2001: Enhanced chlorophyll associated with tropical instability waves in the equatorial Pacific. *Geophysical Research Letters*, **28**(10), 2005-2008.
- Strutton, P.G. and Chavez, F.P. 2000: Primary productivity in the equatorial Pacific during the 1997-98 El Niño. *Journal of Geophysical Research*, **105**(C11), 26,089-26,101.
- Cota, G.F., Hooker, S.B., McClain, C.R., Carder, K.L., Muller-Karger, F., Harding, L., Magnuson, A., Phinney, D., Moore, G.F., Aiken, J., Arrigo, K.R., Letelier, R.M. and Culver, M. SeaWiFS Postlaunch Calibration and Validation Analyses, Part 3, SeaWiFS Postlaunch Technical Report Series, Volume 11, NASA Tech. Memo. 2000-206892, S.B. Hooker and E.R. Firestone, Eds., NASA Goddard Space Flight Center, Greenbelt, Maryland, 2001. .

## PRESENTATIONS

- Chavez, F.P., Feldman, G.C., McPhaden, M.J., Foley, D.G. and Strutton, P.G., 1998: Remote Sensing of the Equatorial Pacific during 1997-98. AGU Fall Meeting, San Francisco, CA, December, Invited
- Friederich, G.E., Chavez, F.P., Strutton, P.G. and Walz, P., 1998: Bio-optical and Carbon Dioxide Time Series From Moorings in the Equatorial Pacific During 1997-1998. AGU Fall Meeting, San Francisco, CA.
- Friederich, G E Walz, P M Strutton, P G Burczynski, M G Chavez, F P Seasurface pCO<sub>2</sub> Time Series from Moorings in Equatorial and Coastal Upwelling Systems. AGU Ocean Sciences meeting, San Antonio, TX.
- Kuwahara, V.K., Strutton, P.G., Penta, B., Drake, E., and Chavez, F.P., 2001: Bio-optics from Moorings: Satellite Validation and Ecosystem Dynamics. AGU Fall Meeting, San Francisco, CA, December.
- Strutton, P.G., Merging data from ships, satellites and moorings to understand biological-physical coupling in the equatorial Pacific, Invited seminar, Oregon State University, November 2001.
- Strutton, P.G. and Chavez, F.P., Temporal and spatial variability of phytoplankton productivity during GasExII, Oral presentation, GasExII workshop, Seattle, October 2001.
- Strutton, P.G., Chavez, F.P., Drake, E., Kuwahara, V.K., Friederich, G. and Ryan, J., 2001: Merging Data from Ships, Satellites and Moorings to Understand Biological-Physical Coupling in the Equatorial Pacific. AGU Fall Meeting, San Francisco, CA, December.

## OTHER PUBLICATIONS

- O'Reilly, J. E., Maritorena, S., O'Brien, M.C., Siegel, D.A., Toole, D., Menzies, D., Smith, R.C., Mueller, J.L., Mitchell, B.G., Kahru, M., Chavez, F.P., Strutton, P.G.,

- Strutton, P.G., Chavez, F.P., Foley, D.G., Sclining, B.M. and McPhaden, M.J., 1999: Remote Sensing of Biological-Physical Coupling in the Equatorial Pacific. ASLO Ocean Sciences Meeting, Santa Fe, NM.
- Strutton, P.G., Chavez, F.P. and McPhaden, M.J., 1998: In situ measurements of primary productivity in the equatorial Pacific during the 1997-98 El Niño. AGU Fall Meeting, San Francisco, CA.
- Strutton, P.G., Chavez, F.P. and McPhaden, M.J., 1998: Primary productivity in the equatorial Pacific during the onset of the 1997-98 El Niño. AGU/ASLO Ocean Sciences Meeting, San Diego, CA.
- Strutton, P.G., Chavez, F.P. and McPhaden, M.J., 1998: Primary productivity in the equatorial Pacific during the onset of the 1997-98 El Niño. Pacific Climate Workshop, Catalina Island, CA.
- Strutton, P.G., Ryan, J.P., Polito, P. and Chavez, F.P., 2000: High Chlorophyll in the Equatorial Pacific During 1998 Associated With Tropical Instability Wave Fronts. AGU Ocean Sciences meeting, San Antonio, TX
- Strutton, P.G., Chavez, F.P. and McPhaden, M.J., 1998: Biological-physical coupling in the central equatorial Pacific during the 1997-98 El Niño, Ocean Optics XIV, Kailua-Kona, H

## Chapter 6

# Satellite Ocean-Color Validation Using Ships of Opportunity

Robert Frouin, David L. Cutchin

*Scripps Institution of Oceanography, University of California San Diego, La Jolla*

Pierre-Yves Deschamps

*Laboratoire d'Optique Atmosphérique, Université des Sciences et Technologie de Lille, France*

### 6.1 INTRODUCTION

Our investigation's objective is to continue and extend a ship-of-opportunity program (merchant ships, research vessels) developed during the last four years to collect concomitant normalized water-leaving radiance and aerosol optical thickness over the world's oceans. A global, long-term data set of these variables is needed to verify whether satellite retrievals of normalized water-leaving radiance are within acceptable error limits and, eventually, adjust atmospheric correction schemes. The volunteer ships are equipped with portable SIMBAD radiometers that measure both variables in typical spectral bands of satellite ocean color sensors.

The basic measurement program includes research cruises and merchant ship voyages mostly in the Pacific Ocean (SIO network); it complements the ships/routes operated by the University of Lille in the Atlantic and Indian Oceans (LOA network). The data collected, after proper quality control and processing, are delivered to the SIMBIOS project office (SeaBASS archive). They complement in situ data acquired by other satellite validation programs, including the mostly land-based AERONET aerosol-monitoring network.

The SIMBAD data collected by the SIO and LOA networks are intended to check the radiometric calibration of satellite sensors after launch and to evaluate satellite-derived ocean color variables (i.e., normalized water-leaving radiance, aerosol optical thickness, aerosol type). Analysis of the SIMBAD data is expected to provide information on the accuracy of satellite retrievals of water-leaving radiance, an understanding of the discrepancies between satellite and in situ data, and algorithms that reduce the discrepancies, contributing to more accurate and consistent global ocean color data sets.

### 6.2 RESEARCH ACTIVITIES

During the period from 01 November 2000 to 31 October 2001, SIMBAD measurements were made during 12 cruises of opportunity, including one merchant ship voyage. The cruises are listed below with name of cruise, SIMBAD instrument used, region of measurements, name of operator, and dates of measurements. The location of the measurements is displayed in Fig. 6.1. The data were collected mostly off the West Coast of the United States (CalCOFI cruises) and in the Sea of Japan (ACE-Asia experiment). 1540 complete data sets were produced, bringing to 4054 the total number of data sets available since October 1996 (i.e., in the SeaBASS archive). Excluding the three ongoing campaigns (IOFFE01, PERTH0102, and CalCOFI 0110NH –see Table 6.1), a total of 51 campaigns with SIMBAD measurements were realized during October 1996-October 2001.

Table 6.1: SIMBAD cruises during 11/1/2000 – 12/31/2001

CalCOFI 0101JD, Simbad03, Southern California Bight, David Starr Jordan, Antoine Poteau, 07 Jan 01 - 22 Jan 01
AMLR2001, Simbad06, Antarctica, R/V Yuzhmoregeologiya, John Wieland, 08 Feb 01 - 05 Mar 01
ACEASIA2001, Simbad03/07, Honolulu-Yokosuka, R/V Ron Brown, Robert Frouin, 26 Feb 01 - 20 Apr 01
IMECOCAL 0106/07, Simbad08, Ensenada-San Carlos, R/V Francisco de Ulloa, Elsa Alguirre, 26 Jun 01 - 16 July 01
CalCOFI 0107NH, Simbad03, Simbad07, Southern California Bight, R/V New Horizon, Antoine Poteau, 10 Jul 01 - 27 Jul 01
JUN01KN, Simbad06, Tropical Atlantic, R/V Knorr, Ajit Subramanian, 25 Jun 01 - 19 Aug 01
P380108, Simbad07, Honolulu-Valdez, M/V Chevron Mississippi, David Cutchin, 04 Aug 01 - 12 Aug 01
PERTH0102, Simbad08, offshore Perth, Australia, Mervyn Lynch, Sep 01 - Sept 02
IOFFE01, Simbad03, Simbad07, R/V Akademik Ioffe, Kiel-Recife-Ushuaia- Antarctica (and back), 05 Oct 01 - April 02
CalCOFI 0110NH, Simbad06, Southern California Bight, R/V New Horizon, Antoine Poteau, 25 Oct 01 - 11 Nov 01

To extend the SIMBAD measurement program, last year several collaborative efforts were initiated. First, CICESE, Mexico agreed to our participation in the regular, quarterly IMECOCAL cruises off Baja California. The advantage of the IMECOCAL cruises, compared with the CalCOFI cruises, is that they take place in a less cloudy region, providing more match-ups per cruise. Second, a cooperative agreement was signed between the Scripps Institution of Oceanography and the Shirshov Institute of Oceanology to collect ocean-color evaluation data during the yearly, 6-month R/V Akademik Ioffe cruises from Kaliningrad, Russia to Antarctica via Ushuaia, Argentina. The measurement program includes not only SIMBAD measurements, but also collection of water samples for pigment and absorption analysis. Third, SIMBAD measurements now are complementing an ongoing satellite calibration and evaluation program undertaken by Curtin University, with cruises every 6 weeks off Perth, Australia along a 40 km transect perpendicular to the coast.

Version 1.6 of the SIMBAD processing code was released, with creation of a special PC version of the code (there are differences in the way Unix and PC Fortran compilers behave) and creation of PC executable online. Code can be downloaded at <http://polaris/~simbad/Software.html>.

The calibration coefficients of the various SIMBAD instruments for sun and sea modes were analyzed statistically over the period October 1996-October 2001. The analysis revealed a significant loss of instrument sensitivity with time at 560 nm, especially for instrument No. 8 (a change of 1.5% in the sun-mode coefficient, equivalent to 0.2 in optical thickness, during the 4-year period). However, with a suitable temporal fit the variability is reduced. Examination of the history of calibration coefficients since October 1996 indicates that, due to uncertainty in the calibration coefficients, measurements of optical thickness are made with an accuracy of  $\pm 0.02$  and measurements of water-leaving radiance with a relative accuracy of  $\pm 3\%$  (Fig. 6.2).

### 6.3 RESEARCH RESULTS

A long-term, monthly climatology of near-surface phytoplankton pigment concentration was also built by integrating monthly data sets from various satellite sensors, namely CZCS, POLDER, and SeaWiFS. The grid used is an equal-angle, rectilinear grid of size 2048 lines and 4096 pixels, for the full global range. This is the standard SeaWiFS grid used for the L3 monthly products. Data periods were Nov 78 - Jun 86 for CZCS, Nov 96 - Jun 97 for the POLDER instrument, and Sep 97 - Nov 00 (at this time) for SeaWiFS. The processing basics are described below.

- The SeaWiFS pigment data were extracted from each of the 40 monthly global SeaWiFS files and then 12 averages were formed, one for each month of the year.

- The CZCS pigment data were extracted from each of the 90 monthly global CZCS files, and 12 averages were formed, as above.
- The POLDER pigment data was extracted from each of the 8 monthly global POLDER files, missing values were filled in (to a depth of 5 layers), and an interpolation made to the smaller SeaWiFS grid.
- The CZCS monthly averages were expanded out to the larger SeaWiFS grid, and then composite monthlies were formed by reconstituting the sums from the three data sets (since the number of pixels averaged were saved for each) and forming monthly super-averages.
- The monthly composites were read in, and the number of good time-series data samples per pixel was determined (including the use of the land and sea-ice masks). If at least 2 good samples were found for a given pixel, a linear time-interpolation was made for that pixel, and the estimated values were used to fill whatever missing values were present.
- A Delaunay triangulation of available nearest neighbors was finally applied to compute linear interpolates that replaced missing values in the grid.

Figure 6.3 displays the resulting pigment concentration field for January and July, and Figure 6.4 the number of points used in the averages. The missing data at high latitudes during winter are filled adequately. A comparison of the SeaWiFS and CZCS monthly data sets gives a correlation coefficient of 0.59, a bias of  $0.86 \text{ mgm}^{-3}$  (higher SeaWiFS values), and a root-mean-squared difference of  $0.13 \text{ mgm}^{-3}$ . The higher SeaWiFS values during Sep 97 - Nov 00 may be attributed to higher concentrations in the tropical Pacific after the 1997-1998 El Niño, although algorithm errors (e.g., due to atmospheric correction) are not excluded. In the next step OCTS and in situ pigment concentration data from the SeaBASS archive (period 1961-2000) will be integrated, after calibration of the various satellite data sets (taken separately) against the in-situ data. A new algorithm to estimate phytoplankton chlorophyll concentration from SeaWiFS top-of-atmosphere radiance was developed. The algorithm utilizes the change in local spatial contrast of the SeaWiFS radiance at 443 and 555 nm. Assuming that the atmosphere does not change over short distances (a few kilometers), the ratio of the spatial contrast in the blue and green is a monotonous function of the pigment concentration. The effect of a changing atmosphere over a few kilometers is taken into account, at least partly, by subtracting the 865 nm radiance from the blue and green radiance. Preliminary results show that the ratio of spatial contrasts in the blue and green is not noisy, and is strongly correlated to the corresponding chlorophyll concentration (as derived by the standard SeaWiFS project bio-optical algorithm) (Fig. 6.5). The advantage of the new algorithm is that no explicit atmospheric

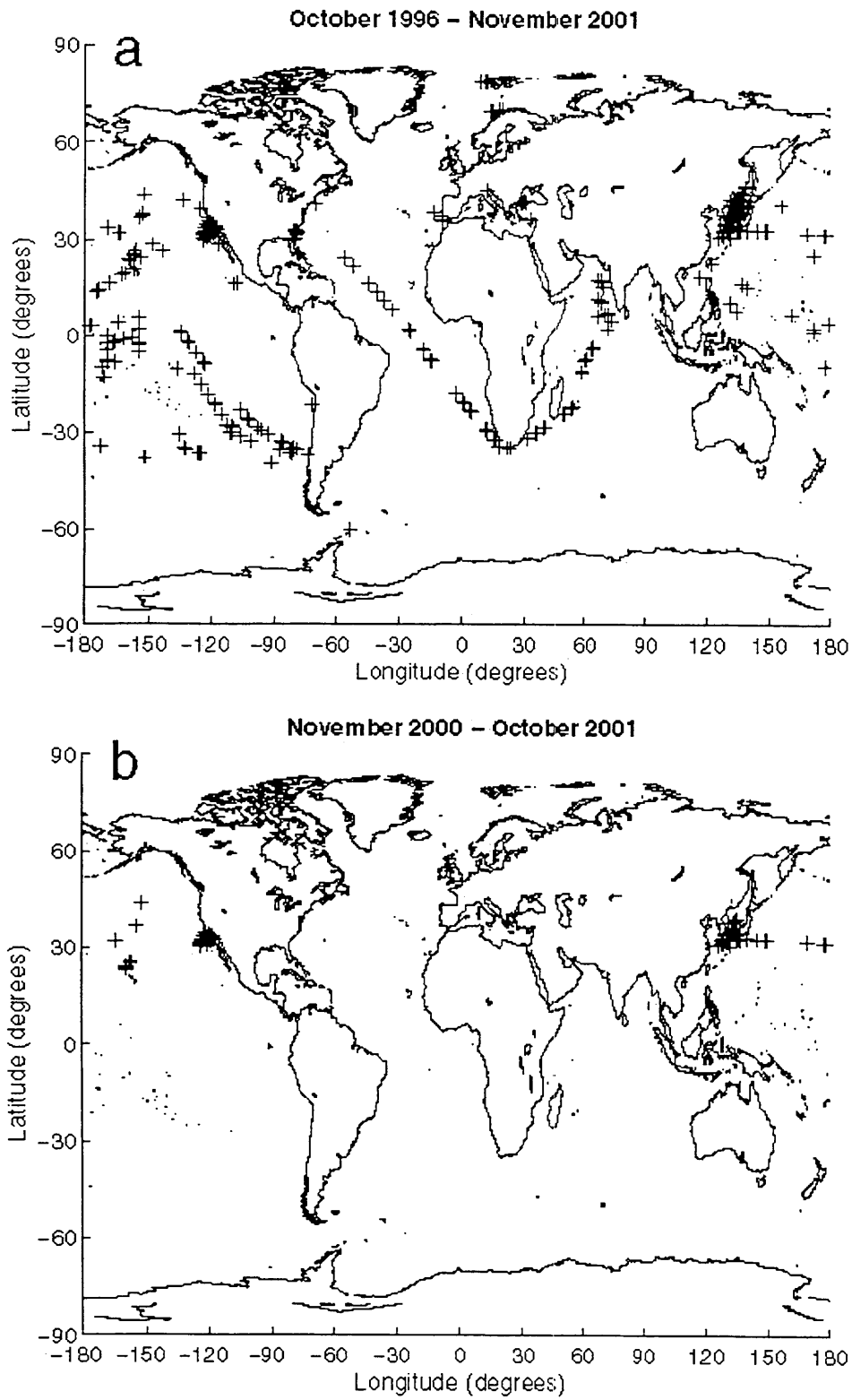


Figure 6.1: Location of the SIMBAD data sets

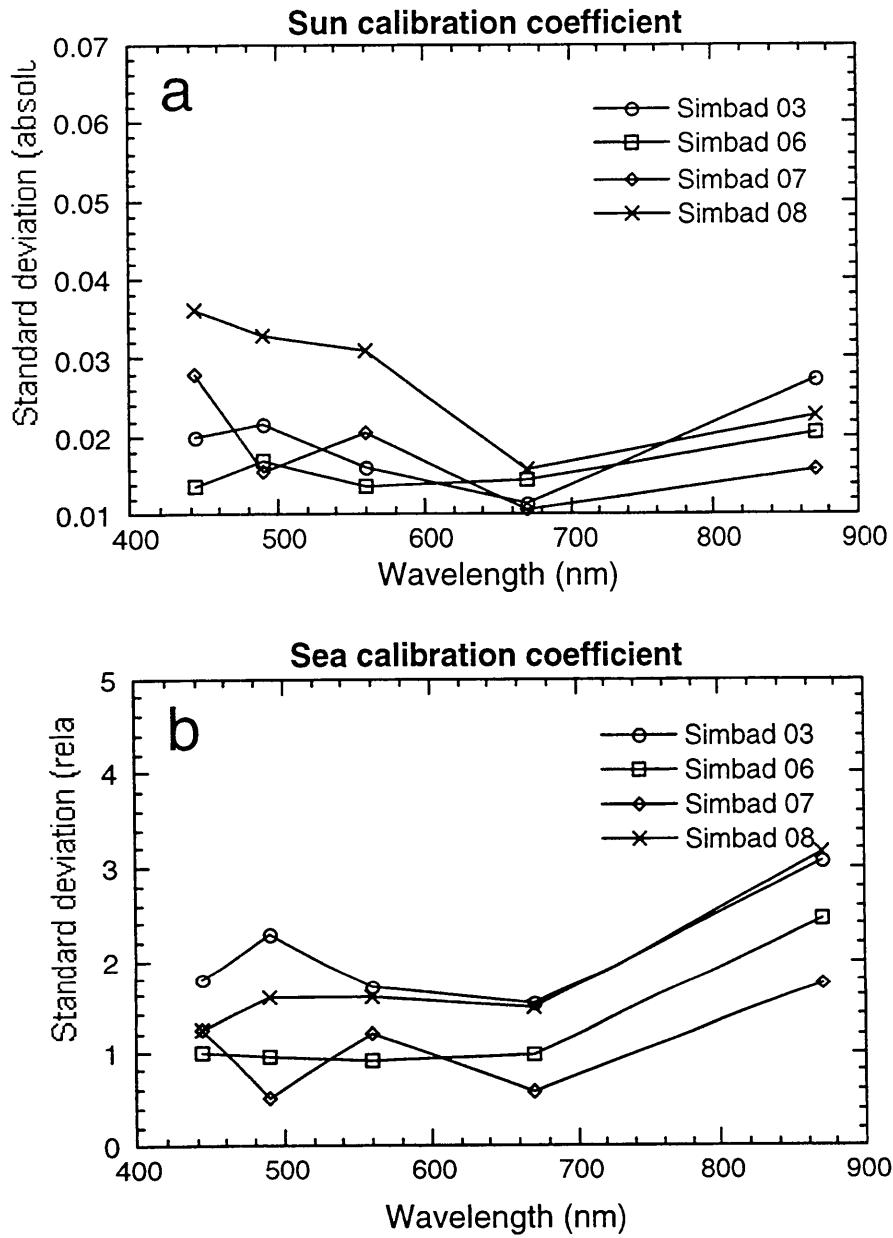


Figure 6.2: Standard deviation of sun and sea calibration coefficients for various Simbad instruments during the period October 1996-October 2001, trend removed (see text).

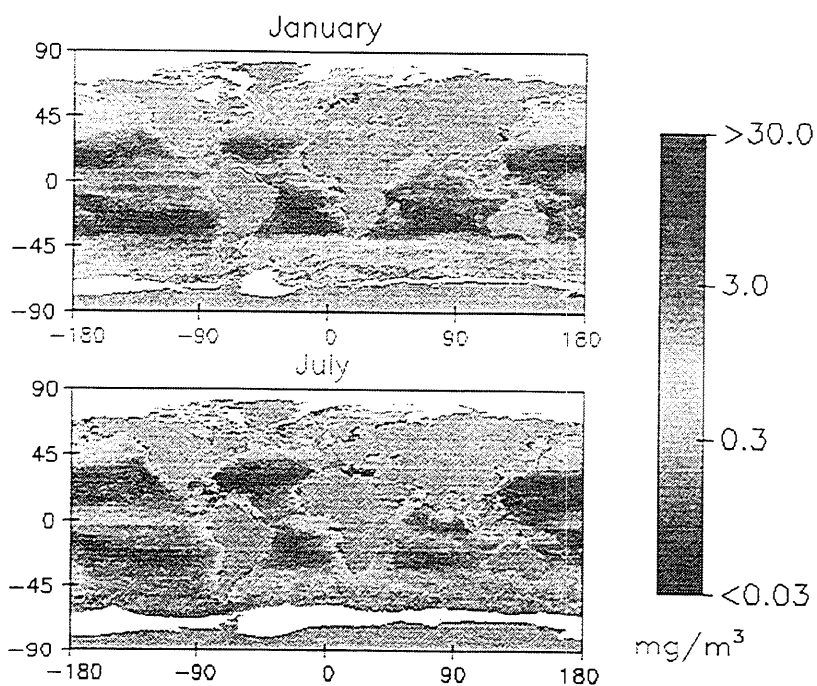


Figure 6.3: January and July distribution of near-surface phytoplankton pigment concentration in the world's oceans from CZCS, POLDER, and SeaWiFS data.

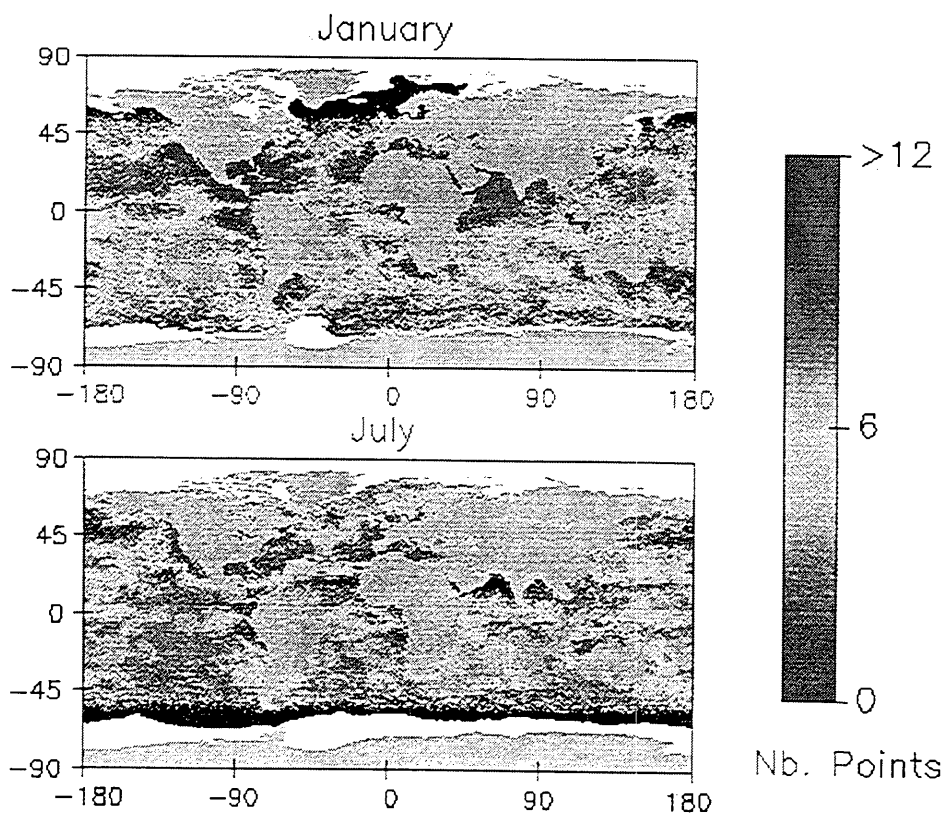


Figure 6.4: Number of observations used in the averages of Figure 6.3.

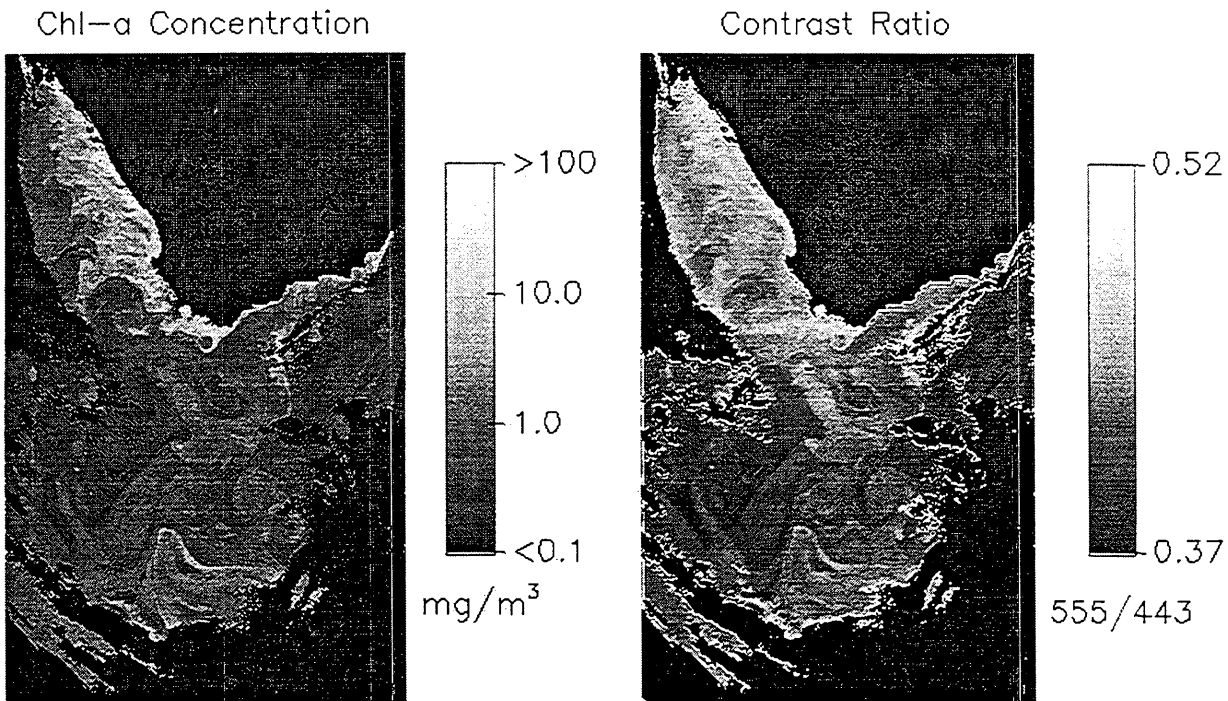


Figure 6.5: Imagery of chlorophyll concentration derived with the standard SeaWiFS algorithm (left) and corresponding imagery of the ratio of spatial contrast in SeaWiFS radiance at 555 nm and 443 nm (right). The data were acquired off the coast of South Africa on 14 February 1999. Note the strong correlation between the two types of images.

correction of the top-of-atmosphere radiance is required, but more tests are indeed necessary before concluding about the general applicability of the algorithm.

The ACE-Asia experiment provided a comprehensive calibration and validation data set covering a wide range of oceanic and atmospheric conditions, with detailed information on aerosol optical properties, type, and vertical distribution. Figure 6 displays a time series of SIMBAD measurements of aerosol optical thickness at 870 nm (Fig. 6a) and Angström coefficient (Fig. 6b). Aerosol optical thickness was quite low across the Pacific Ocean from Hawaii to Japan (Julian days 75 to 90), with values generally less than 0.2. Close to Japan, in the Korea Strait, the Sea of Japan, and the East China Sea (Julian days 91 to 107) aerosol conditions were more variable with several dust and pollution events. On Julian day 99 optical thickness was especially large ( $> 0.9$  at 870 nm) with a relatively small Angström coefficient (about 0.3) characteristic of large particles. At some locations during some days diurnal variability was pronounced. On Julian day 102 in the Korea Strait, for example, aerosol optical thickness decreased from about 0.45 to 0.25 at 870 nm during the period of a few hours, while Angström coefficient increased from 0.2 to 0.7. The higher Angström coefficient in the afternoon was associated

with smaller particles, which is consistent with the size distributions measured onboard the ship.

Figure 6.7 displays the corresponding time series of SIMBAD-derived marine reflectance (Fig. 6.7a) and reflectance ratio (Fig. 6.7b). Marine reflectance in the blue (443 nm and 490 nm) was high during the first part of the cruise (open ocean waters), until Julian day 90. Then it remained low yet variable (East coast of Japan, in the Korea Strait, the Sea of Japan, and the East China Sea). On Julian day 99 the ship was in the Japan Sea, and the lowest reflectance at 443 nm ( $< 0.005$ ) was measured. The reflectance ratios, 443/560 and 490/560, were low during Julian days 98-103 when the ship was in the Sea of Japan and in the Korea Strait, indicating high chlorophyll concentrations during those days.

A number of good days for evaluating SeaWiFS- and MODIS-derived ocean-color, with varied and contrasted conditions, were identified. They are listed below with their main characteristics.

07 April 01: Korea Strait, weak winds from the Northeast, calm sea, shallow boundary layer, aerosol optical thickness of about 0.2 at 870 nm.

- 08 April 01: Sea of Japan, weak wind from the Southwest, calm sea small particles, aerosol optical thickness of about 0.2 at 870 nm.
- 09 April 01: Sea of Japan, weak wind from the East, very calm sea, dust, aerosol optical thickness of 0.6-0.8 at 870 nm, high chlorophyll concentration.
- 12 April 01: Korea Strait, strong wind from the West, thick boundary layer, whitecaps, dust and pollution, changing aerosols, multiple aerosol layers, aerosol optical thickness of 0.3-0.4 at 870 nm.
- 13 April 01: Korean Strait, strong wind from the West, whitecaps, aerosols in the boundary layer, pollution, aerosol optical thickness of about 0.15, North-South transect toward Coast of Japan.
- 15 April 01: East China Sea, weak wind, calm sea, transect Fukua Island – Cheju Island, aerosol optical thickness at 870 nm increasing toward Cheju (0.07 to 0.16), but smaller particles.
- 19 April 01: Pacific Ocean, strong wind from the West, whitecaps, pollution, aerosol optical thickness of about 0.15 at 870 nm.

ACE-Asia (see above). Even though the number of match-ups is small, the data set is comprehensive, allowing a detailed and complete analysis of each case.

A long-term, monthly climatology of phytoplankton pigment concentration will be created by merging/integrating in situ data (SeaBASS archive) and satellite data (CZCS, OCTS, POLDER, and SeaWiFS). This climatology, which can easily be updated as new data become available, will serve as a reference in studies of inter-annual variability and will be useful in various investigations of climate and climate change.

The new algorithm to estimate chlorophyll concentration from space, based on spatial contrast of the satellite imagery, will be further investigated. The computation of the spatial contrast will be refined. Various contrast ratios will be examined and the relation between these ratios and pigment concentration, its sensitivity to phytoplankton type, will be established. The algorithm will be applied to imagery acquired in varied atmospheric and oceanic regimes and compared with standard algorithms.

Aerosol models for ocean color remote sensing will be revisited. A classification of aerosol models obtained from atmospheric optics measurements made by CIMEL radiometers (AERONET, SIMBIOS) will be made using Kohonen maps. These models will be compared with those used in current atmospheric correction schemes and used alternatively in the schemes. Kohonen mapping will also be used to classify top-of-atmosphere imagery into aerosol and water classes that will be labeled (e.g., type of aerosol, range of pigment concentration, type of water).

## 6.4 FUTURE WORK

During the second year of the project (01 November 2001-31 October 2002), collection of SIMBAD data will continue during the quarterly CalCOFI and ICOMECAL cruises. A more comprehensive measurement program onboard R/V Ioffe from Kiel to Antarctica and back will be organized, with eventually a leg from Miami to Kiel dedicated to the training of students. SIMBAD measurements will also be made during the regular transects off Perth, Australia. The focus, however, will be on the following specific tasks.

Five advanced SIMBAD radiometers (SIMBADAs) will be assembled to complement the four SIMBAD instruments of the SIO network. The advanced version is lighter and more compact, operates without cables, has improved electronics, reduced noise, a larger internal memory, better batteries with internal charger, easier display of the viewing angles, and measures in 11 spectral bands instead of 5, from 350 to 870 nm. The necessary software to process the SIMBADA data, including correction of residual polarization, will be developed.

The SeaWiFS- and MODIS-derived ocean-color will be evaluated using in situ data collected during selected days of

## ACKNOWLEDGMENTS

We wish to thank all the officers and scientists that have collected SIMBAD data, Antoine Poteau for processing SIMBAD data and maintaining the SIMBAD radiometers, John McPherson for programming support, and the SIMBIOS project scientists and staff for providing match-up data and for many helpful discussions (and more). This work is supported by the National Aeronautics and Space Administration under contract NAS5-00194, the Scripps Institution of Oceanography, the Centre National d'Etudes Spatiales, and the Centre National de la Recherche Scientifique.

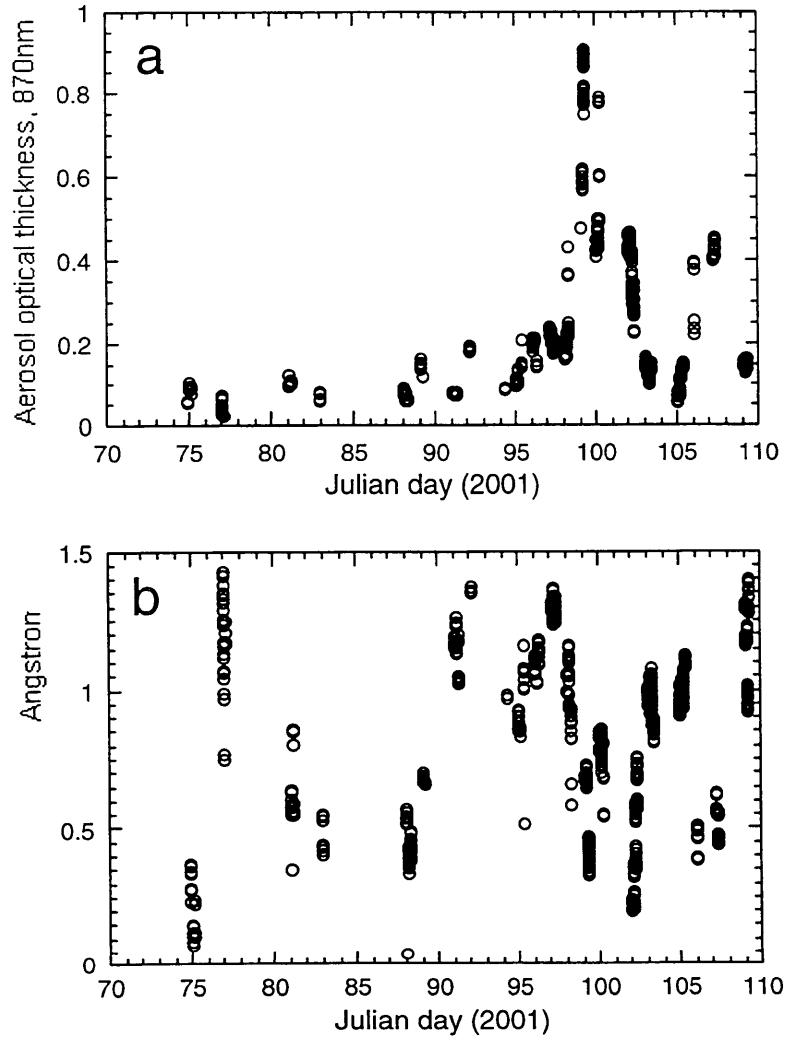


Figure 6.6: Time series of aerosol optical thickness at 870 nm (a) and Angström coefficient (b) during ACE-Asia.

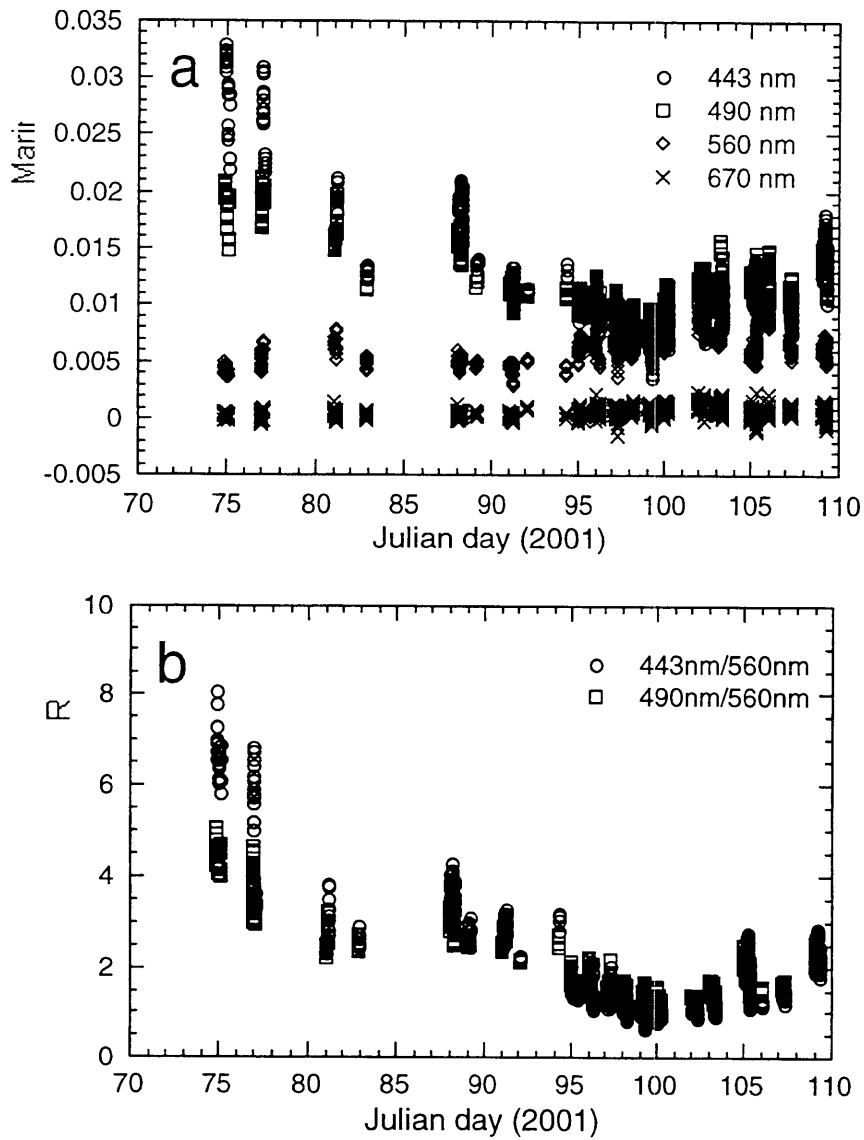


Figure 6.7: Time series of marine reflectance just above the surface (a) and reflectance ratio (b) during ACE-Asia.

*This research was supported by the  
SIMBIOS NASA contract # 00194*

## PEER REVIEWED PUBLICATIONS

- Nakamoto, S., S. Prasanna Kumar, J. M. Oberhuber, J. Ishizaka, K. Muneyama, and R. Frouin, 2001: Response of the equatorial Pacific of chlorophyll pigments in a mixed layer-isopycnal ocean general circulation model. *Geophys. Res. Lett.*, **28**, 2021-2024.
- Shell, K., R. Frouin, S. F. Iacobellis, and R. C. J. Somerville, 2001: Influence of Phytoplankton on Climate. Proc. of the 12th Symposium on Global Change and Climate Variations, January 2001, Albuquerque, New Mexico, 247-250, published by the American Meteorological Society.
- Behrenfeld, M. J., J. T. Randerson, C. R. McClain, G. C. Feldman, S. O. Los, C. J. Tucker, P. G. Falkowski, C. B. Field, R. Frouin, W. E. Esaias, D. K. Kolber, and N. H. Pollack 2001: Biospheric primary production during and ENSO transition. *Science*, **291**, 2594-2597.
- Frouin, R., B. Franz, and M. Wang, 2001: Algorithm to estimate PAR from SeaWiFS data. Version 1.2-Documentation. [http://orca.gsfc.nasa.gov/seawifs/par/doc/seawifs\\_par\\_wfigs.pdf](http://orca.gsfc.nasa.gov/seawifs/par/doc/seawifs_par_wfigs.pdf).
- Frouin, R., S. F. Iacobellis, and P.-Y. Deschamps, 2001: Influence of oceanic whitecaps on the global radiation budget. *Geophys. Res. Lett.*, **28**, 1523-1526.
- Holben, D. N., D. Tanré, A. Smirnov, T. F. Eck, I. Slutsker, N. Abuhassan, W. W. Newcomb, J. S. Schafer, B. Chatenet, F. Lavenue, Y. F. Kaufman, J. Vande Castle, A. Setzer, B. Markham, D. Clark, R. Frouin, R. Halthore, A. Karneli, N. T. O'Neill, C. Pietras, R. T. Pinker, K. Voss, and G. Zibordi, 2001: An emerging ground-based aerosol climatology: Aerosol optical depth from AERONET. *J. Geophys. Res.*, **106**, 12067-12097.
- Tratt, D. M., R. Frouin, and D. L. Westphal, 2001: The April 1998 Asian Dust event: A Southern California perspective. *J. Geophys. Res.*, **106**, 18371-18379.
- Nicolas, J.-M., P.-Y. Deschamps, and R. Frouin, 2001: Spectral reflectance of oceanic whitecaps in the visible and near-infrared: Aircraft measurements over open ocean. *Geophys. Res. Lett.*, in press.
- Husar, R. B., D. Tratt, D. Jaffe, S. Gasso, T. Gill, N. S. Laulinen, F. Fu, M. Reheis, Y. Chun, D. Westphal, B. N. Holben, G. Geymard, I. McKendry, N. Kuring, G. C. Feldman, C. R. McClain, R. Frouin, J. Merrill, D. Dubois, F. Vignola, T. Murayama, N. Sugimoto, S. Nickovic, W. E. Wilson, K. Sassen, B. A. Schichtel, and S. R. Falke, 2001: The Asian Dust event of April 1998. *J. Geophys. Res.*, in press.
- Voss, K. J., E. J. Welton, P. K. Quinn, R. Frouin, M. Miller, and R. M. Reynolds, 2001: Aerosol optical depth measurements during the Aerosols-99 experiment. *J. Geophys. Res.*, in press.
- Nakamoto, S., S. Prasanna Kumar, J. M. Oberhuber, H. Saito, K. Muneyama, and R. Frouin, 2001: Chlorophyll modulation in mixed layer dynamics in a mixed-layer isopycnal general circulation model. *Proc. Indian Acad. Sci.*, in press.
- Nakamoto, S., H. Saito, K. Muneyama, T. Sato, S. Prasanna Kumar, and R. Frouin, 2001. Ocean bio-geophysical modeling using mixed-layer-isopycnal general circulation model. *Recent Developments in Geophysics*, in press.
- Frouin, R., and S. F. Iacobellis, 2001: Influence of phytoplankton on the global radiation budget. *J. Geophys. Res.*, in revision.

## Chapter 7

# Merging Ocean Color Data From Multiple Missions

Watson W. Gregg

*NASA Goddard Space Flight Center, Greenbelt, Maryland*

### 7.1 INTRODUCTION

We propose to investigate, develop, and test algorithms for merging ocean color data from multiple missions. We seek general algorithms that are applicable to any retrieved Level-3 (derived geophysical products mapped to an Earth grid) ocean color data products, and that maximize the amount of information available in the combination of data from multiple missions. Most importantly, we will investigate merging methods that produce the most complete coverage in the smallest amount of time, nominally, global daily coverage. We will emphasize 4 primary methods: 1) averaging, 2) subjective analysis, 3) blending, and 4) statistical (optimal) interpolation. We will also assess the ability to produce fuller coverage in larger time increments, including 4-day, 8-day (weekly), monthly, and seasonal. Secondly, we will investigate the ability of the missions to produce coverage at different times of day, for diel variability and dynamical evaluations, and develop algorithms to produce this information, again on as full a spatial coverage as possible. We intend to develop methods that are not mission-specific, but take advantage of the unique characteristics of the missions as much as possible. However, given the peculiarities of sensor design and performance, and mission characteristics, we acknowledge that individual merging methods may be required to take full advantage of the unique characteristics of the missions as much as possible, and produce the highest quality data set.

### 7.2 RESEARCH ACTIVITIES

Work has focused on analysis, development, and testing of candidate merger algorithms. We began investigating four possible approaches for merging ocean color satellite data: (1) simple splicing/averaging, where data from two or more satellites are averaged where they coexist at grid points, and use of a single satellite in gaps where only one exists; (2) subjective analysis, where specific dependences and deficiencies are identified using knowledge about sensor environmental conditions and co-located observations are merged using different weighting functions for the sensors;

(3) the Conditional Relaxation Analysis Method (CRAM), where the best data are selected as interior boundary conditions into a merged set using Poisson's equation; and (4) optimal interpolation, where merging occurs by weighting individual sensor data to minimize spatial covariance function. The latter two algorithms were developed under separate funding. The algorithms have been characterized and implemented in software; their capabilities and limitations are known, as well as their ability to be modified. The application of algorithms and potential modifications depends on a characterization of the merged data sets.

Significant progress has been made on each of these techniques with the majority of analysis this year focusing on blending. The blended analysis has traditionally been applied to merging satellite and in situ data. Also known as the Conditional Relaxation Analysis Method (CRAM), this analysis assumes that in situ data are valid and uses these data directly in the final product. To blend multiple satellite ocean color data sets, one sensor's data would replace the role of the in situ data as the internal boundary condition (IBC). In January 2001, initial results of the application of blended analysis using SeaWiFS and early MODIS data were presented at the SIMBIOS Science Team Meeting in Greenbelt, Maryland. SeaWiFS chlorophyll data were used as the IBC. The radiometric calibration of the MODIS data was insufficient for scientific use but served the purpose of algorithm investigation. For this preliminary analysis, six weeks of daily Level-3 globally mapped MODIS and SeaWiFS data were obtained from the Goddard DAAC. Routines were written in IDL (Interactive Data Language) to extract the MODIS and SeaWiFS chlorophyll images from their native HDF (Hierarchical Data Format), to scale and orient the images properly, to retrieve the accompanying quality flags for MODIS, and to save the resulting images as FORTRAN binary. Global equal-area mapped MODIS data is available at 4-km, 36-km, and 1-degree; SeaWiFS standard mapped images are at 9-km resolution. Both are available daily, weekly, monthly and yearly. For testing, the blend code was modified to run at different spatial resolutions and several weeks of blended results were obtained using daily 36-km and 1-degree data. Running the blend code at a higher spatial resolution on a global data set is possible, but time consuming.

Generally, MODIS pixels extend further north and south into the upper latitudes than SeaWiFS. Because SeaWiFS is the IBC and is not present in this area, the blending in these regions is suspect. Therefore, the blend code was modified to identify the latitudinal extent of the input SeaWiFS data and to restrict blending in these high latitudes to avoid incorrect results. While blending significantly reduces sensor gaps, even more success can be achieved by pre-averaging data in time. Therefore, 2- and 4-day averages of 1-degree SeaWiFS and MODIS data were created and used as inputs into the blend analysis. Statistical analyses were undertaken to determine the relative contribution of SeaWiFS to the blended product. In addition, various techniques were tested to determine how well the blended analysis was working. For example, a simulated SeaWiFS image (a 4-day 1-degree data set with every other value set to 0.0 in checkerboard fashion) was blended with MODIS. Differences between withheld SeaWiFS pixels and blended pixels were then compared. Using averaged 4-day input MODIS and SeaWiFS data, a proof-of-concept comparison was made between blended output and results using another ocean color merging algorithm, averaging. These preliminary results suggested that the blending analysis can significantly enhance ocean color data sets, but that improvements in MODIS quality were necessary before the assessment of merging algorithms could reliably be determined in a quantitative fashion. Throughout the year, close contact was kept with MODIS personnel on data quality, production, and availability issues, as MODIS data quality drove the schedule. Finally, beginning in mid-August 2001, calibrated MODIS data were made available. According to MODIS personnel, the Ocean Version 3.2.x (a.k.a. Collection 3) data products show dramatic improvements over the prior Version 1 as this new version reflects improved science algorithms, image de-stripping, and band-band gain adjustments. Therefore, we have begun to order, download and reformat each of MODIS's three chlorophyll products: chlor\_MODIS, chlor\_a\_2, and chlor\_a\_3 along with their associated quality control files. Using the quality flag files for each product, data deemed to be bad, fair or questionable is omitted. As of this writing (10/15/01), 30 days of re-calibrated MODIS data have been obtained from the Goddard DAAC and reformatted. It should be noted that the DAAC's current interface for ordering MODIS data is cumbersome because each data product for each day must be specified. Ordering a range of days is not permitted. To determine which of the three MODIS chlorophyll products is most compatible with SeaWiFS, we researched each MODIS algorithm and performed our own statistical intercomparisons. Using daily SeaWiFS data regridded to 36-km from its original 9-km resolution and 'good' quality 36-km MODIS data, regional and global root mean squares (rms) revealed that the 'chlor\_a\_2' product best matches SeaWiFS chlorophyll at these spatial and temporal

resolutions (62% rms). This is not surprising as this product is analogous to the SeaWiFS retrieval algorithm. The 'chlor\_a\_3' algorithm (semi-analytic) had an rms difference of 105% and the 'chlor\_MODIS' was 154%. SeaWiFS data characterization is ongoing. An analysis to examine the relationship between the Level-3 Standard Mapped Images (SMI) and the binned data sets was undertaken to determine which data are best suited for blending. The binned values were formatted to be comparable with the SMI using IDL and FORTRAN programs. Statistics and histograms revealed that either data set would be useful for blending, and since the SMI product is already mapped, it will be used in future blending. An investigation was made to examine a possible source of reduced quality SeaWiFS data related to absorbing aerosols. If such reduced quality were identified using aerosol data then it could possibly be controlled for, thereby producing a higher quality merged ocean color data product. Therefore, several days of Total Ozone Mapping Spectrometer (TOMS) aerosol index data were downloaded and converted into FORTRAN binary images. Using IDL, scatterplots comparing daily SeaWiFS chlorophyll and TOMS Earth Probe aerosol index were prepared but showed no relationship. This suggests that the SeaWiFS aerosol masking algorithms are working properly by correctly identifying absorbing aerosols or that the TOMS index is inadequate for characterization. Several preliminary tasks (such as creating a new land-ocean mask, determining the optimum number of blend iterations, intercomparing the MODIS chlorophyll products, and updating statistical analysis code) were completed and now blending of daily re-calibrated MODIS (specifically, 'good' quality 'chlor\_a\_2') and SeaWiFS at 36km resolution has begun. Initial results suggest that modifications may be necessary to the algorithm based on incompatibilities of the data sets. A log transformation is under consideration.

### 7.3 FUTURE WORK

An invitation to join the International Ocean Colour Coordinating Group's (IOCCG) working group on data binning issues was accepted and a first draft of a section on data assimilation requirements for ocean color data products was completed. Attendance at a workshop in France in October was accepted, but had to be cancelled due to travel restrictions. An offer to contribute to the meeting otherwise has been tendered to the convener, David Antoine. The workshop is still on schedule for late October. While working with 36-km MODIS data in January 2001, a binning problem was discovered. We prepared statistics and histograms in IDL to illustrate the problem and contacted the MODIS team. As a result, the MODIS Level 3 Ocean 36-km and 1-degree data files were temporarily unavailable to the public until the problem was corrected.

## Chapter 8

# Bio-Optical and Remote Sensing Observations in Chesapeake Bay

Lawrence W. Harding Jr. and Andrea Magnuson

*University of Maryland Center for Environmental Science, Cambridge, Maryland*

### 8.1 INTRODUCTION

Bio-optical measurements in turbid near-shore waters are essential to recover chlorophyll concentrations (*chl-a*) from satellite remote sensing of ocean color because of the complex optical properties of these waters and the high variability of constituents that influence light absorption and reflectance. Radiance-ratio algorithms, such as OC4v.4 that is used in SeaWiFS standard processing for *chl-a*, are effective for oceanic Case 1 waters (Morel and Prieur, 1977; Gordon and Morel, 1983) where there is a co-varying relationship of remote-sensing reflectance ( $R_{RS}$ ) and *chl-a* (e.g. O'Reilly *et al.*, 1998, 2000). In contrast, freshwater inputs to Case 2 coastal waters are accompanied by high concentrations of suspended material and colored dissolved organic matter (CDOM) that may dominate absorption and vary independently of *chl-a*. Bio-optical algorithms for Case 2 waters must account for the absorption and scattering of multiple components of the water column. Coastal waters with high particle scattering pose additional problems with respect to atmospheric correction. SeaWiFS atmospheric correction procedures assume water-leaving radiances are negligible in the NIR, which can be an invalid assumption in Case 2 waters. (Siegel *et al.*, 2000). In such cases, part of the satellite signal that has its source in the water column is inappropriately attributed to the atmosphere.  $L_{WN}$  returned by standard SeaWiFS processing can be underestimated and sometimes negative, resulting in overestimates of *chl-a* when an empirical radiance ratio algorithm, such as OC4v.4, is used (Bailey *et al.*, 2000).

A significant part of our SIMBIOS effort has been to provide ship-based bio-optical measurements for Chesapeake Bay and adjacent coastal waters of the Mid-Atlantic Bight (MAB) to aid in algorithm development and validation of satellite-derived products for Case 2 waters. Chesapeake Bay is an important Case 2 validation site because of the extensive data set of pigment, bio-optical and related *in situ* measurements that is available from past and on-going research efforts. Since 1995, a series of three cruises per year (spring, summer and fall) has been conducted, providing a

time-series of bio-optical measurements with seasonal coverage. In collaboration with other research groups, we have continued this cruise series in 2001, and will continue through 2003. The bio-optical data set now consists of approximately 400 stations with measurements of both inherent (dissolved, pigmented particulate and non-pigmented particulate absorption spectra) and apparent (downwelling radiance/upwelling irradiance) optical profiles, over 600 stations with pigment analyses by high performance liquid chromatography (HPLC), and over 2,100 measurements of fluorometric *chl-a*. All of these data have been submitted to SeaBASS. We have used these data to validate SeaWiFS products for this area. Our own modeling efforts are focused on developing a bio-optical algorithm specific to this region.

### 8.2 RESEARCH ACTIVITIES

We participated on three cruises during 2001 (April, July and October) that covered the main stem of Chesapeake Bay. Sampling consisted of *in-situ* radiometric profiles and the collection of discrete samples for measuring absorption spectra, pigments by HPLC, and *chl-a* by fluorometry. Ten stations were visited on each cruise for bio-optical measurements. Discrete samples were collected from additional stations throughout the Bay for fluorometric *chl-a* analyses.

Spectral absorption coefficients (300-800 nm) of particulate material were measured by concentration on Whatman GF/F filters and analyzed on a dual beam spectrophotometer (Shimadzu UV-2401PC UV-VIS) before and after extraction with hot methanol for determination of absorption coefficients due to pigmented ( $a_{ph}$ ) and non-pigmented ( $a_t$ ) components. Seawater samples collected for analysis of the dissolved fraction were filtered through 0.2  $\mu$ m cellulose syringe filters. Absorbance of the filtrate was measured in 10 cm cuvettes on an HP8452A Diode Array spectrophotometer at wavelengths from 190 to 820 nm against a Milli-Q water blank for the determination the absorption coefficient due to CDOM ( $a_{CDOM}$ ).

*In-situ* bio-optical profiles were obtained with a MER-2040 (Biospherical Instruments, Inc.) underwater radiometer that measured downwelling irradiance ( $E_d$ ) and upwelling radiance ( $L_u$ ) at thirteen spectral bands. A MER-2041 mounted on the deck provided simultaneous measurements of surface downwelling irradiance. Radiometric profiles were processed according to accepted protocols (Fargion & Mueller, 2000). An instrument self-shading correction was applied to all measurements of surface upwelling radiance ( $L_u^0$ ) (Gordon & Ding, 1992, Zibordi & Ferrari, 1995, Fargion & Mueller, 2000). Discrete samples were collected for the analysis of photosynthetic pigments by HPLC and *chl-a* by fluorometry. In addition to our routine sampling, we arranged to conduct an inter-laboratory comparison of HPLC determinations of photosynthetic pigment concentrations with Dr. Trees' laboratory at CHORS. Samples were collected from three stations spanning the north-south axis of the Bay. At each station six samples were collected by filtration using a homogenous source. The filters were stored frozen using accepted protocols, and analyzed at the Horn Point Laboratory Analytical Services facility according to HPLC methods based on Van Heukelem and Thomas (2001). Replicates were shipped to Dr. Trees' laboratory for independent analyses. The samples were submitted to each laboratory using a coding by station not provided to the analyst to assure "blind" comparisons. Samples for the inter-laboratory comparison were collected on the July and October cruises of 2001, and will be collected on three cruises in 2002. Reporting of HPLC results will be made to the SIMBIOS program office by the PIs. The radiometric measurements made in Chesapeake Bay were expanded in 2001 with the purchase of three new above water and in-water instruments, including (1) Satlantic MicroPro (free-fall profiler); (2) Satlantic HyperTSRB (tethered surface buoy); and (3) ship-mounted Satlantic SeaWiFS Aircraft Simulator (SAS III) sensors (above water measurements). The main acquisition in support of SIMBIOS is the MicroPro profiler that has advantages over the MER due to the small diameter and ease of deployment. The instrument self shading correction using the MER can reach 50% in the upper Chesapeake Bay, and the smaller diameter of the MicroPro should lessen this problem. We have made nearly simultaneous measurements from the new instruments and the MER 2040/41 during the summer and fall cruises in 2001, and we will be continuing these comparative measurements in 2002 and 2003.

*In situ* data collected during the 1998-2000 sampling period were used for validation of SeaWiFS products for the same period. SeaWiFS Level 1a HRPT images of the Chesapeake Bay / MAB region from were processed to Level 2 using the Siegel NIR atmospheric correction option utilizing bands 7 and 8. Images were processed with all of the standard masks, including land, cloud, glint, stray light, and high light. To avoid pixels with large atmospheric paths, all pixels with

satellite zenith angles greater than  $56.0^\circ$  were masked. Direct comparisons were made between satellite and *in-situ* measurements of  $L_{WN}$ , *chl-a* and K<sub>d</sub>490. SeaWiFS  $L_{WN}$  were compared with *in-situ*  $L_{WN}$  calculated as:

$$L_{WN} = F_o (L_W / E_s) = F_o (R_{RS}) \quad (1)$$

where  $F_o$  is the extraterrestrial solar irradiance and  $L_W$  is an instrument self-shade corrected value. Valid match-ups between SeaWiFS observations and *in-situ* measurements of  $L_{WN}$  and K<sub>d</sub>490 were limited to a time window of  $\pm 3$  hours. *Chl-a* match-ups were considered valid if the satellite observation and *in-situ* sample collection occurred on the same day. Time series of *chl-a* from *in-situ*, aircraft, and SeaWiFS sources were compared to determine if SeaWiFS resolved spatial and temporal variability of *chl-a* present in the *in-situ* data. Additional measurements made during the 1995-2000 Chesapeake Bay cruises include a large dataset of primary productivity observations that will be submitted to SIMBIOS in the coming year. These data have been used in the development of a depth-integrated primary productivity model for Chesapeake Bay (Harding *et al.*, 2001). We are extending the database of observations used to develop the model to include aircraft and satellite ocean color estimates of *chl-a*. The increased spatial and temporal resolution of these remote sensing data sources is expected to improve the performance of the model.

## 8.3 RESEARCH RESULTS

### *Relationships between Inherent and Apparent Optical Properties*

Our data analysis has focused on the relationships between measured inherent and apparent optical properties in turbid Case 2 waters. Spectral absorption coefficients in this region indicated that the relative importance of CDOM, phytoplankton and detrital/tripton absorption to the total water column absorption ( $a_T$ ) varied along the salinity gradient (Fig. 1).  $a_{CDOM}$  exhibited a strong conservative relationship, while  $a_d$  decreased exponentially with salinity.  $a_{ph}$  exhibited no strong relationship with salinity except for the consistent appearance of a maximum at salinities of 10-15 psu. This maximum of  $a_{ph}$  may correspond to an alleviation of light-limitation along the main stem axis of the Bay as  $a_d$  decreased in a seaward direction. Detrital absorption dominated the total water column absorption in the upper Bay. In the mid- and lower Bay  $a_{ph}$  generally was greater than  $a_{CDOM}$  and  $a_d$ , although the differences in the relative importance of each fraction were usually small. Absorption coefficients in the MAB waters were an order of magnitude lower and were found to be CDOM-dominated, especially at the blue wavelengths.

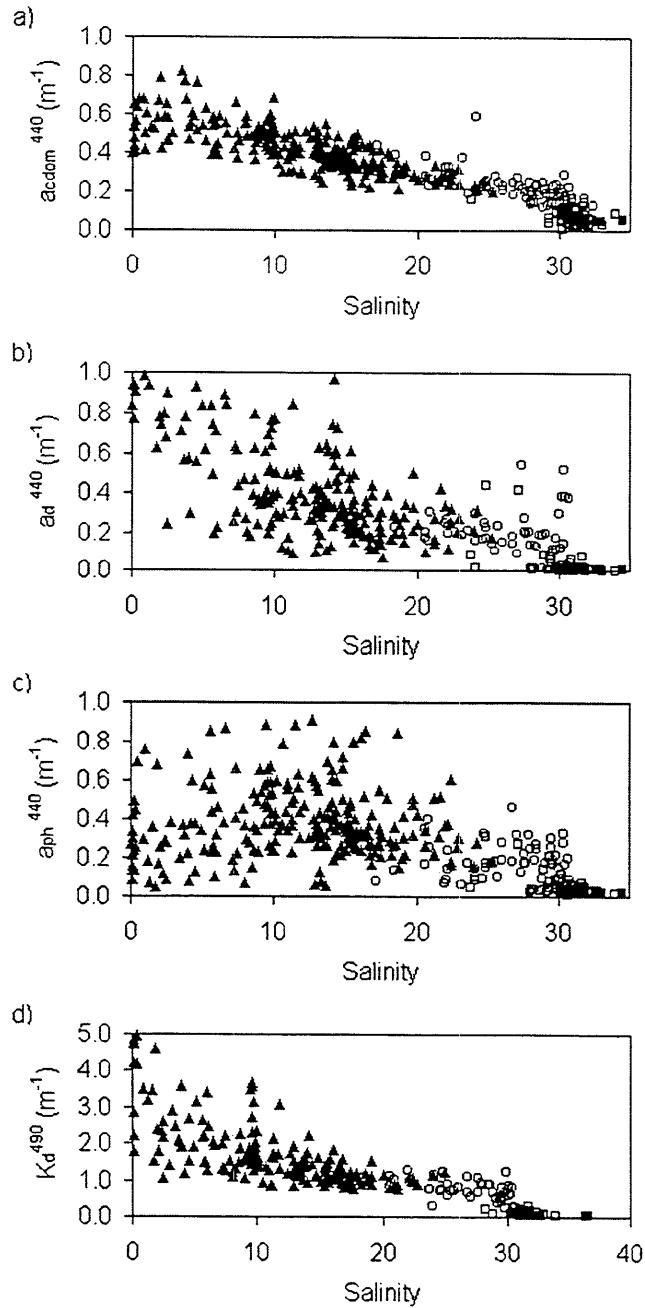


Figure 8.1: Distribution of absorption and attenuation coefficients with salinity in the Bay and offshore waters: (a)  $a_{CDOM}$  at 440 nm, (b)  $a_d$  at 440 nm, (c)  $a_{ph}$  at 440 nm, and d)  $K_d$  at 490 nm. Symbols indicate the following regions:  $\blacktriangle$  = Chesapeake Bay,  $\circ$  = Inshore,  $\square$  = Offshore.

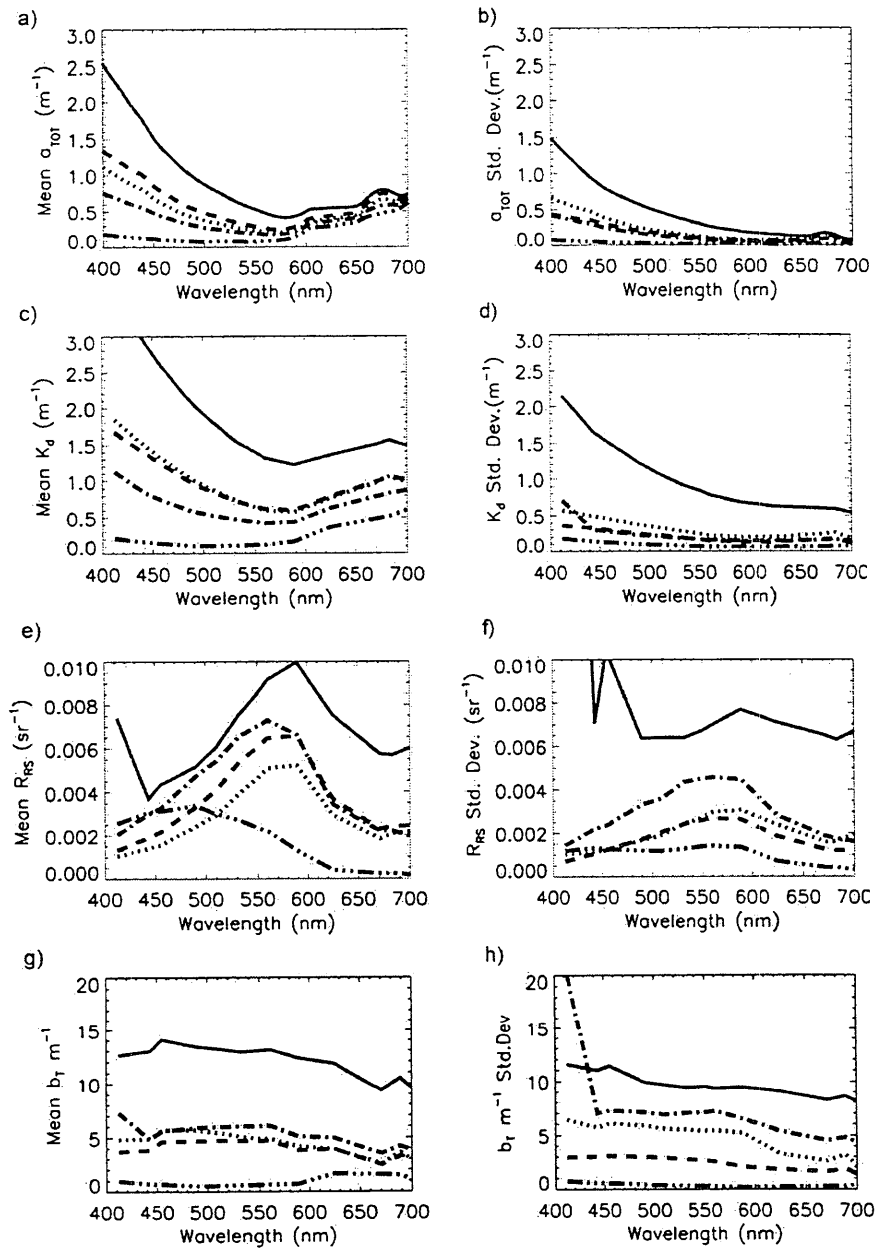


Figure 8.2: Spectral  $a_T$ ,  $K_d$ ,  $R_{RS}$  and  $b_T$  for regions within Chesapeake Bay and adjacent MAB waters: upper Chesapeake Bay (solid), mid-Chesapeake Bay (dotted), lower Chesapeake Bay (dash), inshore MAB (dash-dot), and offshore MAB (dash-dot-dot-dot). (a-b) mean and standard deviation of total absorption coefficients, (c-d) mean and standard deviation of diffuse attenuation coefficient, and (e-f) mean and standard deviation of  $b_T$  calculated from Equation 2. Mean values represent data collected on cruises in 1996-2000.

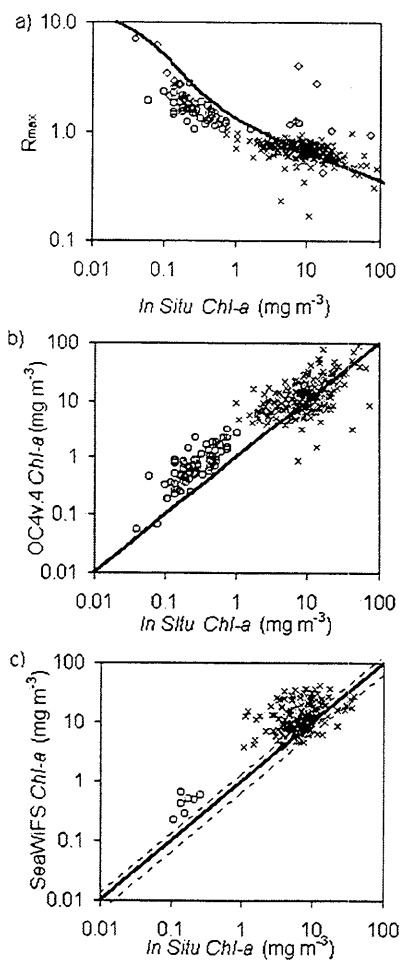


Figure 8.3: (a)  $R_{max}$  for the *in-situ* radiance data vs. *in situ chl-a*. Symbols indicate the maximum ratio used for each station:  $R_{RS443} / R_{RS555}$  ( $\diamond$ ),  $R_{RS490} / R_{RS555}$  ( $\circ$ ), and  $R_{RS510} / R_{RS555}$  ( $\times$ ). Solid line represents OC4v.4. (b) Comparison of OC4v.4 calculated from *in-situ* radiance data and the measured *chl-a* for each station for Chesapeake Bay/inshore MAB ( $\times$ ) and offshore MAB ( $\circ$ ). (c) Comparison of *in-situ* and SeaWiFS-derived *chl-a* for Chesapeake Bay/inshore MAB ( $\times$ ) and offshore MAB ( $\circ$ ). Solid line is the 1:1 line. Dashed lines indicate the SeaWiFS uncertainties goal for *chl-a* of  $\pm 35\%$ . Data from cruises in 1996 – 2000.

Regional trends in the magnitude and spectral shape of  $R_{RS}$  and  $K_d$  reflect the interplay of both absorption and scattering (Fig. 8.2).  $K_d$  decreased in magnitude and flattened out with distance down the Bay and offshore, similar to the pattern observed for  $a_T$ . Maxima in  $R_{RS}$  shifted from 589 nm in the Bay to 560 nm in the inshore MAB and 443 nm in the offshore MAB, reflecting the progressive decrease in  $a_T$  with distance offshore. However, the magnitude of  $R_{RS}$  did not decrease sequentially down the Bay. The highest  $R_{RS}$  values were found in the upper Bay.  $R_{RS}$  increased from relatively low values in the mid-Bay to higher values in the lower Bay and inshore waters. Scattering in the water column likely controls variability in the magnitude of  $R_{RS}$ . In order to obtain an estimate of particle scattering we used *in-situ* optical data as inputs to a model relating diffuse attenuation to absorption and scattering (Kirk, 1981, 1984, 1994). Based on Monte Carlo simulations Kirk (1994) derived:

$$\frac{K_d(z_m)}{a_T} \equiv \left[ 1 + 0.245 \frac{b_T}{a_T} \right]^{1/2} \quad (2)$$

for turbid waters where  $K_d(z_m)$  is the attenuation coefficient at the midpoint of the euphotic zone. The results for Chesapeake Bay indicated little variability of  $b_T$  with wavelength. Mean values of  $b_T$  were  $10 \text{ m}^{-1}$  in the upper Bay,  $5 \text{ m}^{-1}$  in the lower Bay and inshore waters, and an order of magnitude lower in the offshore waters (Fig. 8.2). A great deal of variability exists for each region, but the mean values are in agreement with a previous study in Chesapeake Bay (Gallegos *et al.*, 1990), and provide an indication of spatial variability in the relative importance of scattering in this region.

#### OC4v.4 Performance in Chesapeake Bay

*In-situ* radiance data from Chesapeake Bay / MAB were used as inputs to OC4v.4:

$$C = 10.0^{(0.366 - 3.067 R_{\max} + 1.930 R_{\max}^2 + 0.649 R_{\max}^3 - 1.532 R_{\max}^4)} \quad (3)$$

where  $R_{\max} = \log_{10}(R_{RS}^{443} > R_{RS}^{490} > R_{RS}^{510})$  selects the maximum of the three  $R_{RS}$  ratios (443/555, 490/555, and 510/555) (O'Reilly *et al.*, 2000). Comparisons of OC4v.4 – modeled *chl-a* with measured *chl-a* indicated a tendency for OC4v.4 to overestimate *chl-a* in the Bay (mean ratio =  $1.72 \pm 1.44$ ) (Fig. 8.3; Table 8.1). In the offshore waters dominated by CDOM there was a large bias in the OC4v.4-modeled *chl-a* (mean ratio  $2.72 \pm 1.43$ ). Standard deviations of the ratios indicate that under the best circumstances (*i.e.*, no uncertainty in the radiance observations) uncertainty of *chl-a* predicted from OC4v.4 was at least a factor of two.

#### SeaWiFS – In Situ Match-ups

Comparisons of *in-situ* and SeaWiFS  $L_{WN}$  showed a strong wavelength dependency (Table 8.2). SeaWiFS greatly underestimated  $L_{WN}$  at 412 and 443 nm, and the percentage of negative  $L_{WNS}$  was large. The number of negative values decreased significantly at 490 and 510 nm, and there were no match-up stations that had negative SeaWiFS values at 555 nm. All of the negative  $L_{WNS}$  occurred at Chesapeake Bay stations. In the MAB SeaWiFS  $L_{WNS}$  were within ten percent of *in-situ* values at 490, 510 and 555 nm, but significant errors remained at 412 and 443 nm. The mean ratio for  $K_d490$  also improved from 0.840 in the Bay to 0.965 in the MAB.

Errors in the satellite-derived  $L_{WNS}$  introduced additional errors to the SeaWiFS-derived *chl-a* values. The bands usually used in OC4v.4 are 510 nm in the Bay and 490 nm in the MAB. These bands exhibited biases in these waters of ~22% and ~7%, respectively (Table 8.2). Comparisons of OC4v.4 – modeled *chl-a* and SeaWiFS *chl-a* with *in situ* values showed that *chl-a* values estimated by SeaWiFS were even higher than those estimated from OC4v.4 alone (Table 8.1), reflecting the large bias in SeaWiFS  $L_{WN}$  at 510 nm. In the MAB where the bias in  $L_{WN}$  was relatively small, the OC4v.4 and SeaWiFS *chl-a* were similar. While the OC4v.4 algorithm avoids using wavebands with the greatest bias due to atmospheric correction problems, underestimates of  $L_{WN}$  by SeaWiFS still introduce additional bias to the estimates of *chl-a* in the Bay.

#### Spatial and Temporal Variability in *Chl-a* – SeaWiFS, Aircraft and Field Data

An extensive aircraft remote sensing program in Chesapeake Bay (<http://www.cbrsp.org>; Harding *et al.*, 1992, 1995) made it possible to compare spatial and temporal variability of surface *chl-a* from three independent data sources, aircraft, satellite, and ship. A time series of *in-situ*, aircraft and satellite *chl-a* from 1998 to 2000 showed that SeaWiFS captured seasonal and inter-annual variability of *chl-a* that was evident in the aircraft and ship data (Fig. 8.4). In 1998, *chl-a* from SeaWiFS showed a two to three-fold increase during the spring bloom period (February and March) in much of the mid- and lower Bay (Fig. 8.4). The timing and spatial extent of the bloom were consistent with the aircraft and ship data. By the April cruise, *chl-a* from satellite and ship returned to pre-bloom levels. This level of agreement between data sources was representative of the results for all three years of the time series.

A salient feature of the three-year time series was that SeaWiFS returned reasonable *chl-a* values for the lower Bay and for most of the mid-Bay, but just north of latitude 38.2°N. (between the Potomac and Patuxent R. mouths), SeaWiFS significantly overestimated *chl-a*. One explanation could be that high detrital absorption in the upper Bay result in high

scattering and non-negligible water leaving radiances in the NIR, leading to overestimates of *chl-a* in the upper Bay from errors in the atmospheric correction that produce underestimates of  $L_{WN}$  at key bands from SeaWiFS. South of latitude 38.2°N., SeaWiFS still had a tendency overestimate *chl-a* by about a factor of two. There were occasional images (~1-2 scenes each year) in which 3-4 fold increases of *chl-a* occurred for a single satellite image. The cause of these sporadic deviations is not known and should be investigated further. However, they are anomalies in the time series.

## 7.4 FUTURE WORK

Validation of SeaWiFS  $L_{WN}$ , K490 and *chl-a* revealed problems in atmospheric correction and in the performance of the bio-optical algorithm that were not unexpected for Case 2 waters. OC4v.4 - *chl-a* exhibited a bias to higher values due to absorption by CDOM and detrital components that was attributed to phytoplankton. High uncertainties resulted from variable contributions of phytoplankton, CDOM and detrital fractions to absorption and scattering in the water column. The increased bias of SeaWiFS *chl-a* estimates relative to OC4v.4-*chl-a* in Chesapeake Bay likely reflects a problem in atmospheric correction. Even with the use of the Siegel 7/8 iteration scheme, SeaWiFS  $L_{WN}$ s in Chesapeake Bay were still underestimated at 412, 443, 490 and 510 nm, causing OC4v.4 to return overestimates of *chl-a*. The atmospheric correction problem appeared to dominate in the upper Bay where overestimates of *chl-a* were large. In the mid- and lower Bay the bias can be attributed primarily to the performance of OC4v.4, and secondarily to underestimates of SeaWiFS  $L_{WN}$ s. The atmospheric correction problem was less significant in the offshore waters where  $L_{WN}$  returned by SeaWiFS were in closer agreement with *in situ* values. Despite the bias in *chl-a*, we found that SeaWiFS did resolve relative changes in *chl-a* in lower and mid-Chesapeake Bay on time scales of days to weeks, provided the changes in *chl-a* were greater than the uncertainty in the SeaWiFS *chl-a* estimate.

Further improvement in satellite-derived *chl-a* for this region requires a bio-optical algorithm that includes terms describing the absorption and scattering of all components. Analysis of existing bio-optical data will continue in an effort to appropriately parameterize a semi-analytical algorithm for this region. Absorption has been well characterized in this system. Scattering is obviously important to the ocean color signal of these waters. Refinement of a region-specific bio-optical model would clearly benefit from direct measurements of scattering, as well as studies of particle size distributions and composition. Efforts will be made to obtain these measurements in the coming year.

## REFERENCES

- Bailey, S.W., C.R. McClain, P.J. Werdell and B.D. Schieber, 2000: Normalized water-leaving radiance and *chl-a* a match-up analyses. In: McClain, C.R. R.A. Barnes, R.E. Eplee, Jr., B.A. Franz, N.C. Hsu, F.S. Patt, C.M. Pietras, W.D. Robinson, B.D. Schieber, G. M. Schmidt, M. Wang, S.W. Bailey, P.J. Werdell: SeaWiFS Postlaunch Calibration and Validation Analyses, Part 2. NASA Tech. Memo. 2000-206892, Vol. 10, S.B. Hooker and E.R. Firestone, Eds., NASA Goddard Space Flight Center, Greenbelt, Maryland, 12-29.
- Fargion, G.S. and J.L. Mueller, 2000: Ocean Optics Protocols for Satellite Ocean Color Sensor Validation, Revision 2, NASA Tech. Memo. 2000-209966, S.B. Hooker and E.R. Firestone, Eds., NASA Goddard Space Flight Center, Greenbelt, Maryland, 184 p.
- Gallegos, C.L., D.L. Correll, and J.W. Pierce, 1990: Modeling spectral diffuse attenuation, absorption, and scattering coefficients in a turbid estuary. *Limnol. Oceanogr.*, **35**, 1486-1502.
- Gordon, H.R. and A. Morel, 1983: Remote assessment of ocean color for interpretation of satellite visible imagery, a review, in R.T. Barber, N.K. Mooers, M.J. Bowman and B. Zeitzschel, Eds., Lecture Notes on Coastal and Estuarine Studies, Springer-Verlag, New York, 114 pp.
- Gordon, H.R. and K. Ding, 1992: Self-shading of in-water optical instruments. *Limnol. Oceanogr.*, **37**, 491-500.
- Harding, L.W., Jr., E.C. Itsweire and W.E. Esaias, 1992: Determination of phytoplankton *chl-a* in the Chesapeake Bay with aircraft remote sensing. *Rem. Sens. Environ.*, **40**, 79-100.
- Harding, L.W., Jr., E.C. Itsweire and W.E. Esaias, 1995: Algorithm development for recovering *chl-a* in the Chesapeake Bay using aircraft remote sensing, 1989-1991. *Photogramm. Eng. Rem. Sens.*, **61**, 177-185.
- Kirk, J.T.O., 1981: Monte Carlo study of the nature of the underwater light field in, and the relationships between optical properties of, turbid yellow waters. *Aust. J. Mar. Freshwaters Res.* **32**, 517-532.
- Kirk, J.T.O., 1984: Dependence of relationship between inherent and apparent optical properties of water on solar altitude. *Limnol. Oceanogr.*, **29**(2), 350-356.

- Kirk, J.T.O., 1994: Characteristics of the light field in highly turbid waters: A Monte Carlo study, *Limnol. Oceanogr.*, **39**(3), 702-706.
- Morel, A. and L. Prieur, 1977: Analysis of variations in ocean color. *Limnol. Oceanogr.*, **22**, 709-722.
- O'Reilly, J.E., S. Maritorena, B.G. Mitchell, D.A. Siegel, K.L. Carder, S.A. Garver, M. Kahru, and C. McClain, 1998: Ocean color algorithms for SeaWiFS, *J. Geophys. Res.*, **103**(C11), 24,937-24,953.
- O'Reilly, J.E. et al., 2000: SeaWiFS Postlaunch Calibration and Validation Analyses, Part 3. NASA Tech. Memo. 2000-206892, Vol. 11, S.B. Hooker and E.R. Firestone, Eds., NASA Goddard Space Flight Center, Greenbelt, Maryland, 49 p.
- Siegel, D.A., M. Wang, S. Maritorena and W. Robinson, 2000: Atmospheric correction of satellite ocean color imagery: the black pixel assumption. *Appl. Opt.*, **39**, 3,582-3,591.
- Van Heukelem, L and C.S. Thomas, 2001: Computer-assisted high-performance liquid chromatography method development with applications to the isolation and analysis of phytoplankton pigments. *J. Chromatogr. A*, **920**, 31-49.
- Zibordi, G. and G.M. Ferrari, 1995: Instrument self-shading in underwater optical measurements: experimental data. *Appl. Opt.*, **34**, 2750-2754.

*This research was supported by  
SIMBIOS NASA contract # 00195*

## PEER REVIEWED PUBLICATIONS

- Harding, L.W., Jr., W.D. Miller, R.N. Swift and C.W. Wright. 2001: Aircraft remote sensing, in J.S. Steele, S. Thorpe, and K. Turekian, Eds., *Encyclopedia of Ocean Sciences*, Academic Press, London, 113-122.
- Harding, L.W., Jr., M.E. Mallonee, M.E., and E.S. Perry, 2001: Toward a predictive understanding of primary production in a temperate, partially stratified estuary. *Est. Coast. Shelf Sci.* (in press).
- Magnuson, A., L.W. Harding, Jr., and M.E. Mallonee, 2001: Bio-optical and remote sensing observations in Chesapeake Bay (in prep.).

## PRESENTATIONS

- Magnuson, A., L.W. Harding, Jr., and M.E. Mallonee, 2001: Satellite and aircraft remote sensing in Chesapeake Bay. Poster presented to the SIMBIOS Science Team Meeting at Goddard Space Flight Center, Greenbelt, Maryland, January 2001.
- Harding, L.W., Jr., 2001: Aircraft remote sensing of ocean color in Chesapeake Bay to estimate chlorophyll and primary productivity. Presentation to EPA Environmental Monitoring and Assessment (EMAP) Conference, Pensacola Beach, Florida, 23-27 April 2001.
- Magnuson, A., L.W. Harding, Jr., and M.E. Mallonee, 2001: Chesapeake Bay as seen by SeaWiFS. Presented to the SeaWiFS Science Team Meeting, San Diego, California, May 2001.

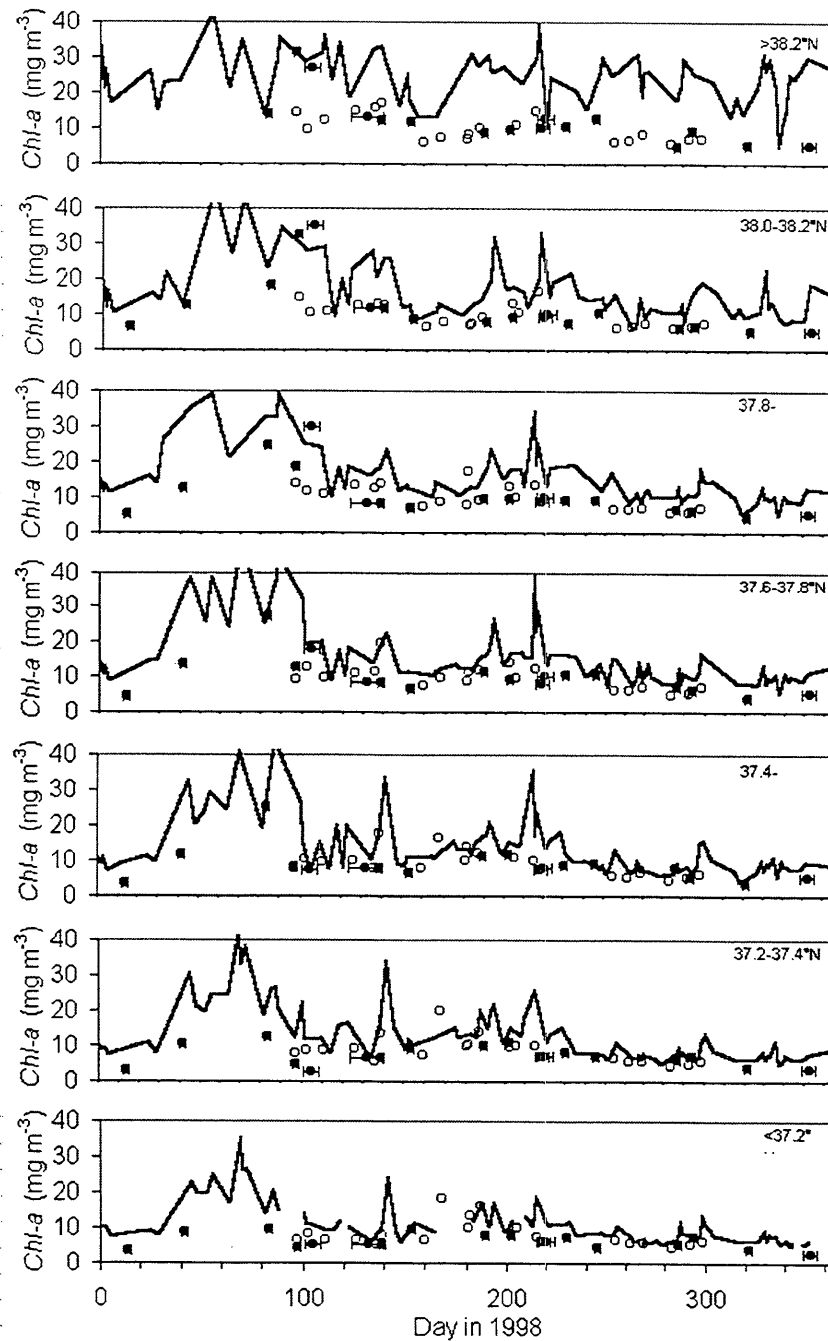


Figure 8.4: Time series of regional mean chl-a observations from cruises, aircraft and SeaWiFS imagery in 1998. Regional mean values were calculated from surface chl-a maps interpolated from in-situ station data (filled  $\circ$ ) and aircraft transects ( $\circ$ ), and SeaWiFS imagery (thick line). In-situ data symbols include error bars indicating the length of the cruise. An average of all data north of  $38.2^{\circ}\text{N}$  is provided in the upper panel. Average values for  $0.2^{\circ}$  latitude bands are provided in all remaining panels.

Table 8.1: Comparison of the mean ratio of *chl-a* calculated from OC4v.4, using *in situ* radiance measurements, and *in situ chl-a*, with the mean ratio of same day match-ups of SeaWiFS-derived and *in situ chl-a*.

Region	<u>OC4v.4<sup>a</sup></u> <i>In Situ</i>	<u>SeaWiFS<sup>b</sup></u> <i>In Situ</i>
	Mean ( $\pm$ sd))	Mean ( $\pm$ sd)
Chesapeake Bay/ Inshore MAB	1.77 ( $\pm$ 1.44) n = 260	2.10 ( $\pm$ 1.69) n = 235
Offshore MAB	2.72 ( $\pm$ 1.43) n = 64	2.69 ( $\pm$ 0.97) n = 7
Overall	1.95 ( $\pm$ 1.36) n = 324	2.12 ( $\pm$ 1.66) n = 242

<sup>a</sup> Ratio of OC4v.4 *chl-a* calculated using *in-situ* radiances and *in situ chl-a*. All *in-situ* data obtained on cruises in 1996-2000.

<sup>b</sup> Match-ups of SeaWiFS 3x3 pixel mean and *in-situ chl-a* during 1998-2000.

Table 8.2. Statistics for match-ups between *in situ* and SeaWiFS observations (3x3 pixel mean) of  $L_{WN}$ ,  $K_d^{490}$  and *chl-a* for Chesapeake Bay and MAB waters. Match-ups of  $L_{WN}$  and  $K_d^{490}$  were limited to *in situ* observations made within  $\pm 3$  hours of the satellite pass. Chlorophyll match-ups consisted of satellite and *in situ* observations on the same day. The differences in the number of  $L_{WN}$  match-ups at each waveband reflect the omission of match-ups with negative  $L_{WN}$  at lower wavebands. SeaBASS values included for comparison.

Region	Parameter	Mean Ratio	Standard Deviation	Coefficient of Variance	Number of Match-Ups	Range of <i>In Situ</i> Values
Chesapeake Bay/ Inshore MAB						
	$L_{WN}^{412}$	0.240	0.044	0.185	3	0.014-0.707
	$L_{WN}^{443}$	0.598	0.251	0.419	4	0.011-0.988
	$L_{WN}^{490}$	0.790	0.173	0.219	7	0.032-1.45
	$L_{WN}^{510}$	0.782	0.331	0.423	8	0.053-1.63
	$L_{WN}^{555}$	0.962	0.273	0.284	9	0.223-2.01
	$K_d^{490}$	0.840	0.474	0.565	8	0.578-2.436
	<i>Chl a</i>	2.100	1.69	0.805	235	1.1-38.2
Offshore MAB						
	$L_{WN}^{412}$	0.378	0.249	0.658	7	0.141-2.145
	$L_{WN}^{443}$	0.776	0.327	0.422	7	0.243-1.916
	$L_{WN}^{490}$	0.928	0.249	0.269	7	0.407-1.464
	$L_{WN}^{510}$	0.983	0.224	0.228	7	0.394-1.589
	$L_{WN}^{555}$	0.957	0.235	0.246	7	0.266-1.838
	$K_d^{490}$	0.965	0.379	0.393	7	0.028-4.68
	<i>Chl a</i>	2.69	0.97	0.361	7	.11-.27
SeaBASS <sup>1</sup>						
	$L_{WN}^{412}$	0.856	0.222	0.259	119	0.330-3.238
	$L_{WN}^{443}$	0.957	0.246	0.256	141	0.219-2.709
	$L_{WN}^{490}$	0.973	0.206	0.211	153	0.252-1.695
	$L_{WN}^{510}$	1.075	0.236	0.219	136	0.215-0.127
	$L_{WN}^{555}$	1.106	0.279	0.252	149	0.127-0.538
	$K_d^{490}$	1.225	0.287	0.222	125	0.018-0.340
	<i>Chl a</i>	1.061	0.498	0.434	76	0.062-4.650

<sup>1</sup>Bailey et al. (2000)

## Chapter 9

# Refinement of Protocols for Measuring the Apparent Optical Properties of Seawater

Stanford B. Hooker

*NASA/GSFC/SeaWiFS Project, Greenbelt, Maryland*

Giuseppe Zibordi and Jean-François Berthon

*JRC/IES/Inland and Marine Waters, Ispra, Italy*

André Morel and David Antoine

*CNRS/UPMC/Laboratoire d'Océanographie de Villefranche, Villefranche-sur-Mer, France*

## 9.1 INTRODUCTION

Ocean color satellite missions, like the Sea-viewing Wide Field-of-view Sensor (SeaWiFS) or the Moderate Resolution Imaging Spectroradiometer (MODIS) projects, are tasked with acquiring a global ocean color data set, validating and monitoring the accuracy and quality of the data, processing the radiometric data into geophysical units using a set of atmospheric and bio-optical algorithms, and distributing the final products to the scientific community. The long-standing objective of the SeaWiFS Project, for example, is to produce water-leaving radiances to within 5% absolute (Hooker and Esaias 1993). The accurate determination of upper ocean apparent optical properties (AOPs) is essential for the vicarious calibration of ocean color data and the validation of the derived data products, because the sea-truth measurements are the reference data to which the satellite are compared (Hooker and McClain 2000). The uncertainties associated with *in situ* AOP measurements have various sources, such as, the deployment and measurement protocols used in the field, the absolute calibration of the radiometers, the environmental conditions encountered during data collection, the conversion of the light signals to geophysical units in a data processing scheme, and the stability of the radiometers in the harsh environment they are subjected to during transport and use.

In recent years, progress has been made in estimating the magnitude of some of these uncertainties and in defining procedures for minimizing them. For the SeaWiFS Project, the first step was to convene a workshop to draft the SeaWiFS Ocean Optics Protocols. The protocols adhere to the Joint Global Ocean Flux Study (JGOFS) sampling procedures (Joint Global Ocean Flux Study 1991) and define the standards for

optical measurements to be used in SeaWiFS radiometric validation and algorithm development (Mueller and Austin 1992). The protocols are periodically updated as deficiencies are identified and outstanding issues are resolved (Mueller and Austin 1995, and Mueller 2000). The follow-on inquiries into controlling uncertainties investigated a variety of topics. The SeaWiFS Intercalibration Round-Robin Experiment (SIRREX) activity demonstrated that the uncertainties in the traceability between the spectral irradiance of calibration lamps were approximately 1.0%, and the intercomparisons of sphere radiance was approximately 1.5% in absolute spectral radiance and 0.3% in stability (Mueller et al. 1996). The first SeaWiFS Data Analysis Round Robin (DARR-94) showed differences in commonly used data processing methods were about 3–4% of the aggregate mean estimate (Siegel et al. 1995). Hooker and Aiken (1998) made estimates of radiometer stability using the SeaWiFS Quality Monitor (SQM), a portable and stable light source, and showed the stability of radiometers in the field during a 36-day deployment was on average to within 1.0% (although some channels occasionally performed much worse). More recently, Hooker and Maritorena (2000) quantified differences in the in-water methods and techniques employed for making radiometric measurements and demonstrated a total uncertainty in the measurement of in-water AOPs at approximately the 3% level.

## 9.2 RESULTS

### *Open Ocean*

The SeaWiFS Field Team has combined the collection of ground-truth observations with specific experiments to

investigate the sources of uncertainties in AOP measurements. Many of the experiments and data collection opportunities took place during several Atlantic Meridional Transect (AMT) cruises on board the Royal Research Ship *James Clark Ross* (JCR) between England and the Falkland Islands (Aiken et al. 2000). The majority of the AMT data set was from Case-1 conditions and took place from September 1995 to June 1999.

Water-leaving radiances can be derived by extrapolating in-water measurements taken close to the sea surface or they can be obtained directly from above-water measurements. More recently, additional experiments and data collection activities have been executed to extend the AMT predominantly in-water data set to other open ocean areas and above-water methods. These include a) the *Productivité des Systèmes Océaniques Pélagiques* (PROSOPE) cruise, which took place between 4 September and 4 October 1999; b) a cruise into the Mid-Atlantic Bight, which took place between 24 April and 3 May 2000, and c) two cruises into Exuma Sound, which took place between 24 February and 1 March 2000, as well as, 22 February and 1 March 2001.

Although it has not been as extensively validated as the in-water approach, above-water methods for vicarious calibration remain nevertheless attractive, because a) the data can presumably be collected more rapidly and from a ship underway, and b) the frequently turbid and strongly absorbing waters in shallow Case-2 environments impose severe limitations on in-water measurements, particularly because of the instrument self-shading effect.

Above- and in-water measurements of  $L_w(\lambda)$  can be related to one another using the pointing geometry of the sensors, the sun geometry, the (surface) interface transmission, and the so-called  $Q$ -factor. The  $Q$ -factor relates the upward radiance field below the surface with that exiting the surface, the angular bidirectional dependency of these fields, and the transformation of radiance or irradiance into reflectance (Morel and Gentili 1996). In-water measurements of the  $Q$ -factor with nadir-pointing instruments (the usual case) are denoted  $Q_n(\lambda)$  and are calculated as the ratio of the upward irradiance to the upwelling radiance,  $Q_n(\lambda) = E_u(\lambda)/L_u(\lambda)$ .

The data from the most recent cruises agreed well with the AMT data set in terms of the accuracy of the in-water AOP measurements and the uncertainties in inverting the optical data into chlorophyll *a* concentration using a standard ocean color algorithm, but they also confirmed two inconsistencies in the AMT data set. The first inconsistency was the amplitude and spectral dependence of  $Q_n(\lambda)$  did not agree with theoretical studies. To more completely investigate this result, special so-called  $Q$ -factor experiments were conducted during the PROSOPE and Mid-Atlantic Bight cruises. In these experiments, sequential casts were made during clear-sky conditions in homogeneous, Case-1 waters during an extensive part of the afternoon (i.e., during a

significant change in the solar zenith angle,  $\theta$ ). Figure 9.1 shows the distribution of  $Q_n(\lambda)$  as a function of  $\theta$ . Although the general shape of increasing  $Q_n(\lambda)$  with increasing solar zenith angle is in agreement with theory, the amplitudes are incorrect, and more important, the wavelength dependence is inverted:  $Q_n(\lambda)$  decreases with increasing  $\lambda$ , whereas theory predicts it should increase.

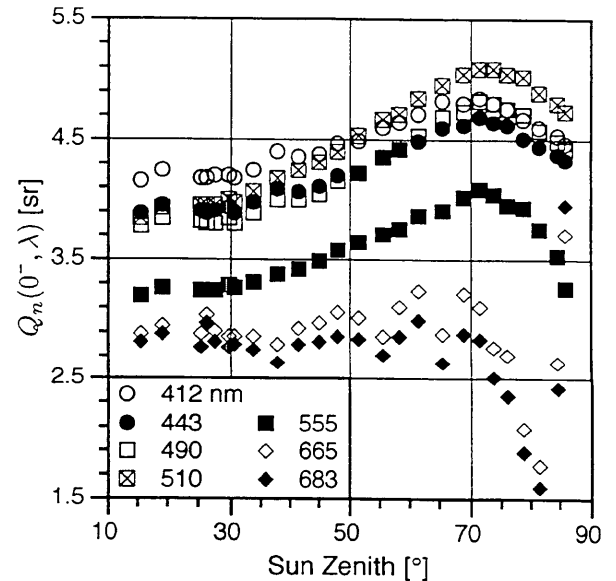


Figure 9.1: The distribution of  $Q_n(\lambda)$  as a function of the solar zenith angle.

The second inconsistency was the above-water  $L_w(\lambda)$  values collected from a large research vessel disagreed with the in-water values, which were collected simultaneously, by as much as 13–27%. All the field instruments were intercalibrated, and the in-water instruments were floated far away from the ship before any data were recorded, so the most likely explanation for the disagreement was platform contamination in the above-water data.

This possibility was analyzed by devising a diagnostic parameter,  $r(865)$ , based on the principles involved in the formulation of two above-water methods: Morel (1980) and the SeaWiFS Ocean Optics Protocols (Mueller and Austin 1995), hereafter referred to as M80 and S95, respectively. When using an above-water method, the total radiance measured above the sea surface,  $L_T(\lambda)$ , includes the wanted information,  $L_w(\lambda)$ , plus a contamination term,  $\Delta L$ , originating from light reflected by the sea surface and into the sensor:

$$L_T(\lambda) = L_w(\lambda) + \Delta L, \quad (1)$$

where the pointing requirements have been omitted.

The processing of above-water data consists of removing the contamination term,  $\Delta L$  in (1), which adds to the marine signal and originates from reflections at the air–sea interface. The sky radiance,  $L_r(\lambda)$ , reflected off the wave-roughened surface into the detector is *a priori* at the origin of the  $\Delta L$  signal. Reflected radiation from the sampling platform is, however, another source of contamination. Even if only the sky reflection is considered, its contribution to  $L_T(\lambda)$  is always important. For Case-1 waters, in the near-infrared domain (e.g., at 780 and 865 nm) where the sea is essentially black, this contribution amounts to 100%, and decreases toward short wavelengths where the diffuse ocean reflectance departs from zero. In Case-2 waters, particularly when the sediment load is high, the water reflectance may deviate from zero in the near infrared and contribute to the  $\Delta L$  signal.

The M80 glint correction method is based on the existence of a black target in the near-infrared region at a reference wavelength,  $\lambda_r$ . The above-water radiance measured at  $\lambda_r$  is entirely due to surface reflection, and this estimate is extended over the whole spectrum by using the spectral dependence of the incident sky radiance measured in the direction appropriate for reflection from the sea surface. Estimated glint is subtracted from the total signal to recover  $L_w(\lambda)$ . The S95 method makes use of the same set of measurements, but they are used differently. The glint is removed through a constant interface reflectance factor,  $\rho$  which is applied to all the spectral sky radiances; in general,  $\rho$  depends on the capillary wave slopes, and, thus, on wind speed (Austin 1974 and Mobley 1999).

A comparison of the output of the M80 and S95 correction methods allows the detection of any ship contamination in the  $L_T(\lambda)$  signal in Case-1 waters. This is because the M80 method is sensitive to, and, thus, is able to identify a ship perturbation, whereas the S95 method, based on a theoretical value of the reflectance factor, will just ignore it. The presence of a ship perturbation can be detected with the ratio

$$r(865) = \frac{L_T(865) / L_r(865)}{\rho} \quad (2)$$

where the numerator comes from M80 and the denominator from S95. Under normal circumstances, i.e., in the absence of a ship perturbation,  $r(865) = 1$ , within the accepted variance (and provided that  $\rho$  is given a correct value). Any other reflected radiation added to the sky-reflected radiation will lead to  $r(865) > 1$ , and the departure from unity is an estimate of this effect. Figure 9.2 presents the  $r(865)$  values for the PROSOPE cruise plotted as a function of the pointing angle of the above-water radiometers with respect to the side of the ship,  $\alpha$ .

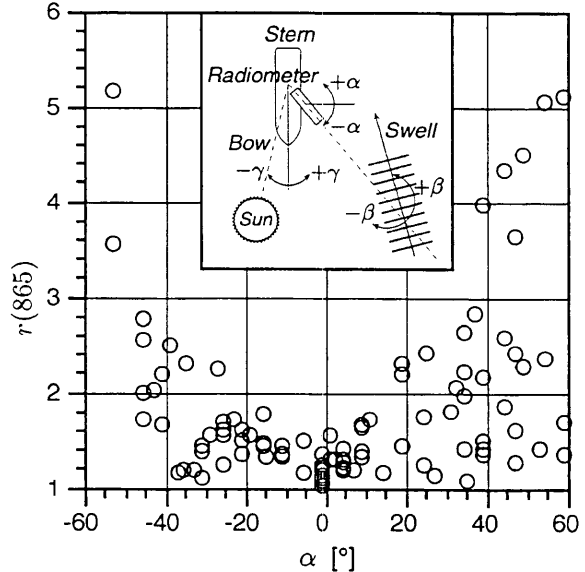


Figure 9.2: The distribution of  $r(865)$  as a function of  $\alpha$  (negative  $\alpha$  values are towards the bow and positive  $\alpha$  values towards the stern). Out of the total data set of 128 casts, 19 were in overcast conditions and 109 were in clear-sky conditions; overcast data are not shown as separate symbols, because they fall within a narrow range (slightly larger than 1) and all at  $\alpha = 0$ , so they would obscure the clear-sky results. The inset panel shows the pointing angle of the above-water radiometers with respect to the ambient swell ( $\beta$ ), and the angle of the sun with respect to the bow ( $\gamma$ ).

Although the PROSOPE data set was composed of 137 simultaneous above- and in-water casts, 9 were excluded because of unanticipated cloud interference, ship movement during the cast, etc. The remaining 128 casts provide a good distribution of data with respect to  $\alpha$ , and show that when the instrument is pointed perpendicular to the side of the ship ( $\alpha = 0$ ), the  $r(865)$  values are a little larger than 1, which suggests a reduced contamination by the ship. As the radiometers are pointed more and more towards the bow or stern, that is when the distance from the ship to the surface spot decreases,  $r(865)$  dramatically increases, reaching values as high as 4–5 when  $\alpha \pm 60^\circ$ . These large ratios indicate the radiation reflected by the surface and seen by the sensor is largely dominated by that originating from the superstructure.

These high values, however, are not observed in a systematic manner. For example, when  $\alpha = 40^\circ$  or  $60^\circ$ ,  $r(865)$  values span the interval 1–5, which deserves another kind of analysis, involving  $\gamma$ , i.e., the angle between the center line of the ship and the position of the sun (Fig. 2 inset panel). According to the sign of  $\gamma$  the port side of the ship (where the

above-water radiometers were installed) is, or is not, illuminated by the sun, which makes a difference in the intensity (and spectral composition) of the light reflected from the superstructure.

An analysis of  $r(865)$  as a function of  $\gamma$  shows the contamination effects of the ship are reduced when the side from which the sensor is operated is in shadow, so that the superstructure is only illuminated by the sky radiation (or by uniform clouds); the contamination increases when the port side is sunlit, or if the bridge is sunlit (when  $\gamma$  is small). The geometrical aspect of the contamination is not surprising; more surprising is the importance of the effect and its complexity related to the shape of the superstructure. As with many ships, elements of the forward superstructure on the research vessel used during PROSOPE sloped to the sides of the vessel, which provided reflection opportunities under a variety of sun geometries with respect to the bow.

Although not as significant as the sun geometry, the effects of surface gravity waves on the above-water measurements were quantifiable: a) measurements along the wave troughs were a significant local minimum, which means they were radiometrically darker than the wave crests at all wavelengths; b) the darkening effect was the largest at 412 and 555 nm; and c) at 510–555 nm, a converse trend (i.e., a brightening) seemed to occur.

#### Coastal Ocean

The PROSOPE above-water data were collected with instruments fixed to the pointing assembly. Although the instruments could be pointed to arbitrary angles in the vertical and horizontal planes, they were sufficiently massive that they could not be safely operated at very high points on a ship's superstructure, particularly in high sea states. In anticipation of working on smaller boats in coastal waters, a very small system that could be gimballed and, thus, would not be as negatively influenced by ship motion was developed. This required the SeaWiFS Field Team to fund the development of a new class of optical sensors, which are significantly smaller and lighter than those currently available. These new sensors are manufactured by Satlantic, Inc. (Halifax, Canada) and are referred to as the OCR-500 series of instruments.

The new above-water instrument is called the micro Surface Acquisition System (microSAS) and is pictured in Fig. 9.3. The above-water radiometers are mounted on movable plates contained within a gimbal. The plates can be set to an arbitrary vertical (nadir or zenith) angle with respect to the horizontal plane between 0–50° (most data are currently collected at 40°). In addition, the entire sensor assembly can be rotated to arbitrary azimuthal viewing angles to within 0.5°. A sun compass at the top of the assembly allows for easy pointing of the instrument to  $\pm 90^\circ$  (in 15° increments) with respect to the solar plane. The ballast for the gimbal contains a

compass with built-in tilt and roll sensors. The latter ensures confirmation of the vertical orientation of the sensors during data acquisition, and permits fine tuning (ballasting and tensioning) of the gimbal structure in any sea state.

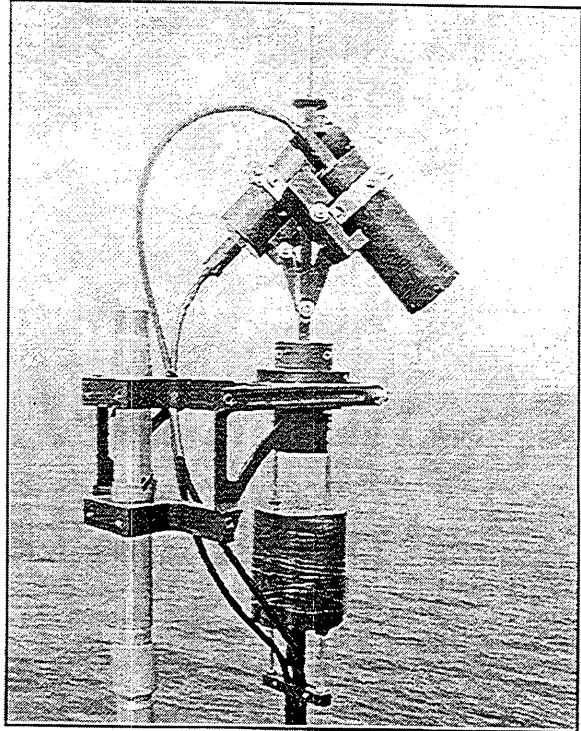


Figure 9.3: The microSAS instrument composed of the upward-pointing  $L_1$  sensor and the downward-pointing  $L_2$  sensor. The ballast, containing the compass with tilt and roll sensors, is the large black cylinder below the gimbal plane.

The Italian Coastal Atmosphere and Sea Time-Series (CoASTS) project is a cooperative activity between the European Joint Research Centre (JRC) and the Italian National Research Council (CNR). As part of the field campaigns, which started in October 1995 and continues to-date, atmospheric and marine measurements are periodically performed at the *Acqua Alta* Oceanographic Tower (AAOT). The tower is located in the northern Adriatic Sea approximately 15 km southeast of the city of Venice in approximately 17 m of water (Zibordi et al. 1999).

The SeaWiFS Photometer Revision for Incident Surface Measurements (SeaPRISM) was conceived by the SeaWiFS Field Team, and developed by the JRC and CIMEL Electronique (Paris, France). SeaPRISM is based on a CE-318 sun photometer, which is an automatic system that measures the direct sun irradiance plus the sky radiance in the sun and almucantar planes (Hooker et al. 2000). The revision to the CE-318 that makes the instrument useful for ocean color

activities is a capability for measuring the sea surface using the M80 and S95 methods. What makes this instrument particularly powerful is it can operate autonomously, so a sampling site can be continuously monitored in between field campaigns that completely characterize the bio-optical conditions of the site.

A prototype SeaPRISM was successfully deployed for a one-year period at the AAOT which was compared to simultaneous deployments of an in-water system (Zibordi et al. 2002). The SeaPRISM measurements showed a slope in the least-squares linear regression fit equal to 1.05 with a determination coefficient of 0.99. More specifically, the intercomparisons exhibited average unbiased percentage difference (UPD)<sup>1</sup> values of 6.9, 7.2, and 23.0% at 440, 500, and 670 nm, respectively; the intercomparison of the water-leaving radiance ratios,  $L_w(440)/L_w(500)$ , exhibited a UPD of 5.3%.

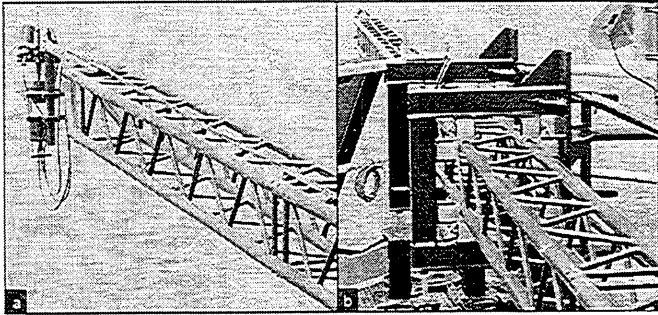


Figure 9.4: The extensible deployment system used at the AAOT showing a) the box frame fully extended with the microSAS instruments mounted at the end, and b) the support system. The box frame is made up of tubular sections commonly used in the construction of aerial towers. The small cross section of the frame, and the fact that it is painted black, ensured a minimum perturbation by the frame on the surface of the water.

The success of the prototype SeaPRISM system has led to a plan to deploy a small number of production SeaPRISM units at a variety of offshore oil and gas platforms in the Adriatic Sea south of the AAOT. The towers are in different water depths and typical water regimes than the AAOT, so the small network will provide an unprecedented description of the coastal ocean and atmosphere with autonomous instruments. The above-water results achieved with the open ocean analyses (Fig. 9.2), however, suggest an analysis of

platform perturbations on the above-water measurements is needed.

In preparation for a tower perturbation experiment, the JRC developed an extensible deployment system for a lightweight above-water system (Fig. 9.4). The extensible system was composed of a tubular box frame that was connected together with prefabricated sections. The box frame was approximately 25 m long and could be extended 11 m away from the tower and still remain rigid (at a 10 m extension, the frame sagged approximately 1°). The microSAS instrument was mounted at the end of the frame, and was positioned with respect to the sun before the frame was extended the desired distance away from the tower. The gimbal ensured the sensors achieved a horizontal reference (to within  $\pm 0.5^\circ$ ) after the frame was positioned. The frame was moved in and out by hand, guided by rollers mounted within a series of square supports.

The basic experimental plan was to make a series of above-water measurements in 1 m increments with respect to the tower (usually 10 incremental measurements were made), all the while observing the pointing requirements with respect to the solar plane ( $90^\circ$  with respect to the sun). The latter ensured that a variety of viewing distances with respect to the tower base were collected. The experiment took place from 18–29 June 2001 during predominantly clear skies. A total of 42 experiments were conducted composed of 435 individual above-water casts (3 min measurement sequences).

The space series of sequential measurements will be compared to the farthest viewing point to see if there is an increasing perturbation in the above-water data as the measurements are made closer and closer to the tower base. The above-water data will also be compared to a variety of in-water measurements (including discrete water filtration samples, inherent optical properties, AOPs, etc.) taken at the same time; these data will also be used to determine the homogeneity of the water during each experiment.

#### Laboratory Measurements

If a total 5% uncertainty level is to be maintained for a vicarious calibration exercise (remote plus *in situ* instrumentation), approximately half of the uncertainty budget, i.e., 2.5%, is available for the ground-truth component (actually if quadrature sums are used, the ground-truth component is closer to 3.5%). This means individual contributions of uncertainty must be at approximately the 1% level, which is a state-of-the-art objective. In the investigation of laboratory sources of uncertainty, two uncertainty thresholds were considered: 2.5% as a hoped for minimum (because it represents almost all of the ground-truth uncertainty budget), and 1.0% as a needed goal (because it

<sup>1</sup> The UPD between  $N$  realizations of two data products  $F^A$  and

$$F^B \text{ is computed as } \frac{200}{N} \sum_{i=1}^N \frac{|F^A(\lambda) - F^B(\lambda)|}{F^A(\lambda) + F^B(\lambda)}.$$

permits some expansion in the other components of the total uncertainty budget).

The poor agreement between *in situ* and theoretical values of  $Q_n(\lambda)$  (Fig. 9.2) suggests there could be a problem with the in-water data. The accuracy of an AOP determination is a function of the quality of the observational measurement, the data acquisition methodology, and the data processing method employed. The former includes the accuracy of the optical calibration and the radiometric stability of the instruments while they are being used in the field. The data acquisition programs have been rigorously reviewed and tested (including comparisons with commercial software) and show no evidence of data corruption. The stability of the radiometers has been repeatedly measured and intercompared in the field—with the exception of early instruments constructed with so-called “soft filters” (Hooker and Aiken 1998), they are stable to within 1% and intercompare during simultaneous casts to within 2% (Hooker and Morel 2001). This leaves only optical calibration and data processing as potential problems. To investigate the possible importance of data processing methods on the final data products, a round-robin intercomparison was organized (Hooker et al. 2001a). Three processors from three different groups were intercompared: the JRC (J), Satlantic (S), and the SeaWiFS Project or GSFC (G). The focus of the round-robin study was the estimation of a variety of commonly used data products derived from two different classes of in-water optical instruments. Eleven parameters important to bio-optical analyses were intercompared. The parameters were calculated for a data set covering a large range of total chlorophyll *a* concentration (0.08–2.43 mg m<sup>-3</sup>). All three processors were intercompared using 40 optical profiles; the JRC and GSFC processors were further intercompared using an additional 10 casts (the larger data set increased the amount of data in very clear waters, thereby extending the lowest total chlorophyll *a* concentration to 0.027 mg m<sup>-3</sup>). The data were also separated according to the oceanic environment, deep ocean (DO) or shallow coastal (SC), and according to the instrument type, free-fall (FF) profiler or winch and crane (WC) system. The instruments used with these data included the SeaWiFS Optical Profiling System (SeaOPS), the Low-Cost NASA Environmental Sampling System (LoCNESS), the Wire-Stabilized Profiling Environmental Radiometer (WiSPER), and a variant of the miniature NASA Environmental Sampling System (miniNESS). SeaOPS and WiSPER are deployed using a winch and crane, whereas, LoCNESS and miniNESS are floated away from the sampling platform and deployed by hand. The deep ocean data were all from Case-1 conditions, and the shallow coastal data were from Case-2 conditions or from water near the threshold between Case-1 and Case-2 in terms of the Loisel and Morel (1998) classification scheme.

In this study, no one data processing system was assumed to be more correct than another, so the UPD was used for intercomparisons. In terms of overall spectral averages, many

of the JRC and GSFC (JG) results intercompared to within 2.5%, but none of the Satlantic results intercompared with the other processors (JS and GS) at this level. Band-ratio averages, however, frequently intercompared to within 2.5% for all processor combinations, even when the overall spectral averages did not. If the JRC and GSFC processor options were made more similar (same extrapolation intervals, data filtering, etc.), the two processors usually intercompared to within 1%. An example of this for the upwelled radiance at null depth,  $L_u(0^-)$ , and the diffuse attenuation coefficient,  $K_d$ , is shown in Fig. 5. These variables were selected, because they are very important to the calibration and validation process:  $L_u(0^-)$  is used directly in calculating  $L_w(\lambda)$ , and  $K_d$  (Fig. 9.5b) is the most common variable to describe the attenuation of light in the upper layers of the water column.

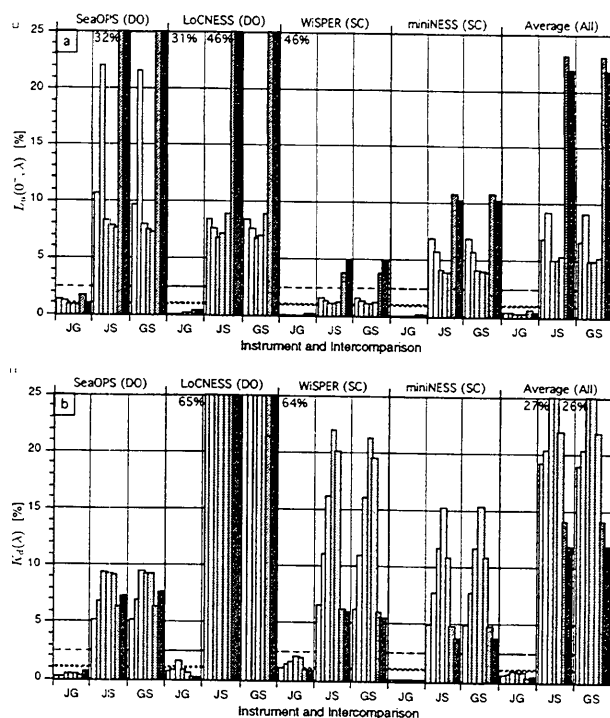


Figure 9.5: The average processing uncertainties for the JG, JS, and GS intercomparisons of a)  $L_u(0^-)$ , and b)  $K_d$ . The dashed line sets the 2.5% intercomparison objective and the dotted line the 1.0% objective. Uncertainties above 25% are shown clipped at the 25% level, and the maximum uncertainty achieved is given at the top of the panel to the side of the clipped bars. The individual wavelengths are shown as the sequential bars with varying intensities of gray (going from left to right, blue is light gray and red is dark gray). The instrument (and deployment location) codes are given along the top of the subpanels. The overall average of all the data (40 casts) is given in the right-most three intercomparisons.

The  $L_u(0^-)$  results (Fig. 9.5a) show the lowest uncertainties with the Satlantic processor are for the shallow coastal data, and in all cases, the largest uncertainties are for the red wavelengths—none of the Satlantic uncertainties are below 1.0%, although, the blue-green WiSPER wavelengths are within 2.5%. Better agreement in the shallow coastal (predominantly Case-2) data rather than the deep ocean (Case-1) data are unexpected, but it has a simple explanation: the shallow water depth constrains the options for selecting the extrapolation interval.

The JG uncertainties are always below 2.5%, and mostly below 1.0% except for the blue and red SeaOPS data. The  $K_d$  uncertainties (Fig. 9.5b) show much higher overall uncertainties with respect to the Satlantic processor, particularly for the LoCNESS data set where every wavelength has an uncertainty above 25%. None of the Satlantic uncertainties are below 2.5%, whereas all of the JG uncertainties are, and most of the JG uncertainties are to within 1.0% (the primary exception are the WiSPER data). These results suggest a database constructed with processed data from a wide source of contributors will have substantially higher uncertainties than a database constructed with raw data which is processed with a single processor, although band ratios regularly provide reduced uncertainties with respect to individual spectral uncertainties.

To minimize observational uncertainties, the SeaWiFS Project has sponsored a variety of multidisciplinary workshops to outline the observations and sampling protocols required for bio-optical algorithm development (Mueller and Austin 1992 and 1995). One of the consequences of the workshops was the establishment of the series of aforementioned SIRREX activities to demonstrate and advance the state of the art for calibrating the instruments used in field activities. Although prior SIRREX activities significantly reduced the uncertainties in optical calibrations, some important sources of uncertainty were not quantified. One of the most important of these, from the vantage of the calibration equation, was the immersion factor.<sup>2</sup>

For commercial radiometers, the raw data are converted to physical units based on a formulation given by the manufacturer. For Satlantic sensors, the  $i$ th sample for a radiometer at center wavelength  $\lambda$ , are converted to physical units according to the following equation:

$$C(\lambda, t_i) = C_c(\lambda) I_f(\lambda) [V(\lambda, t_i) - \bar{D}(\lambda)] \quad (3)$$

where  $C(\lambda, t_i)$  is the calibrated value ( $C$  is replaced by  $E_d(z)$ ,  $E_u(z)$ ,  $L_u(z)$ , or  $E_d(0^+)$  depending on the sensor type),  $C_c(\lambda)$  is the calibration coefficient,  $I_f(\lambda)$  is the immersion factor,  $V(\lambda, t_i)$  is the raw voltage (in digital counts) measured by the instrument at time  $t_i$  (which also sets the depth,  $z$ ), and  $\bar{D}(\lambda)$  is the average dark value (in digital counts) measured during a special “dark cast” with the caps on the radiometer.

The immersion factor is a first-order term in the sense that the uncertainty in this term is represented at the same level as the calibration coefficient, so the final uncertainty of the calibrated data are heavily dependent on the uncertainty in the immersion factor. For irradiance sensors, the immersion factor is determined experimentally. A suggested and acceptable procedure is as follows (Mueller and Austin 1995):

- The instrument is placed in a tank of water with all surfaces painted black.
- The sensor is leveled with the irradiance collector plate facing upward.
- A tungsten-halogen lamp with a small filament, powered by a stable power supply, is placed at some distance above the water surface.
- An initial reading is taken with the water level below the collector, i.e., with the collector in the air and dry.
- The depth of the water is increased in steps and readings are recorded for all wavelengths from each carefully measured depth.

Note that in most cases, water is removed from the tank with a pump, and data are usually recorded in between pumping intervals.

The amount of energy arriving at the collector varies with the water depth and is a function of several factors: a) the attenuation at the air–water interface, which varies with wavelength, b) the attenuation over the water pathlength, which is a function of depth and wavelength; and c) the change in solid angle of the light leaving the source and arriving at the collector, caused by the light rays changing direction at the air–water interface, which varies with wavelength and water depth. When all of these effects are properly accounted for, the immersion factor can be computed.

The SIRREX-8 activity is taking place during the last three months of 2001 and is concerned with the round-robin determination of immersion factors for nine Satlantic radiometers at three different calibration facilities (Hooker and Zibordi 2002a). A picture of the tank used at the first facility, the Center for Hydro-Optics and Remote Sensing (CHORS), from 28 September to 9 October 2001 is shown in Fig. 9.6. The other two facilities will be the JRC and Satlantic. All of the data will be processed by the JRC to ensure there are no

<sup>2</sup> The immersion factor is the coefficient accounting for the change in sensor responsivity when the in-air calibration is applied to in-water measurements ( $I_f = 1$  for above-water sensors).

extra uncertainties as a result of differences in data processing methods.

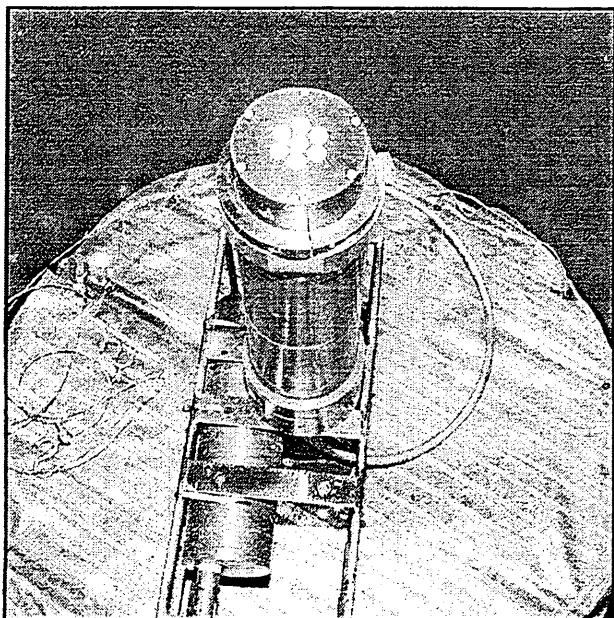


Fig. 9.6: The water tank used at the CHORS calibration facility for measuring immersion factors. The radiometer is set inside a large tube atop an aluminum grate that is covered in a fine mesh. The mesh helps dissipate the turbulence caused by the addition or removal of water.

A preliminary comparison of the immersion coefficients for a sensor used during the first phase of SIRREX-8 at CHORS is shown in Fig. 9.7 (Zibordi and Hooker 2002). For the CHORS work, one radiometer, an  $E_u$  sensor (S/N 130), was selected as a baseline instrument and was subjected to a variety of experiments and trials. The data shown in Fig. 9.7 are for three of the trials when the amount of particles in the tank was kept very low (clean water conditions ensure the surface reflectance is in keeping with the Fresnel reflectance assumption).

The CHORS data show excellent agreement between trials and good agreement with respect to the average value from the three days of data. The latter is an important point, because the *a priori* expectation is that the immersion coefficients should be spectrally uniform (within experimental, manufacturing, and age-dependent limits). The CHORS data shows this is basically the case, except in the blue where the values at 412 nm are depressed and the values at 443 nm are elevated. The Satlantic values show a much greater spectral dependence with maximal values in the blue, decreasing through the green, and then minimal in the red. The differences between the Satlantic and CHORS data are significantly large, i.e., they are much larger than the 2% uncertainty demonstrated for Satlantic irradiance calibrations

during SIRREX-7 (Hooker et al. 2001b). The immersion coefficients can be presented as percentages, so the maximum differences in the blue, green, and red are approximately 19, 8, and 6%, respectively, for these initial results.

Most manufacturers, Satlantic included, do not characterize the immersion coefficients for each instrument they produce, because of the time (and thus, cost) involved in the extra laboratory work. The standard technique, as described above, can require as much as—or even more than—2 h to complete one realization. Assuming three trials are an acceptable minimum for characterization work, this means almost one day of laboratory time would have to be added to the cost of each instrument. Consequently, instrument manufacturers rely on characterizing a class of diffuser designs and then assigning the immersion factors to all instruments manufactured within the class.

The SIRREX-7 preliminary results suggest the class characterization approach is questionable and a considerable amount of effort is needed to recharacterize the instruments being used in calibration and validation activities. In an effort to lower the cost involved, one of the objectives of SIRREX-7 was to test new procedures that can be executed in less time than the standard method (approximately one-sixth the time), or executed with lower cost components (Hooker and Zibordi 2002b).

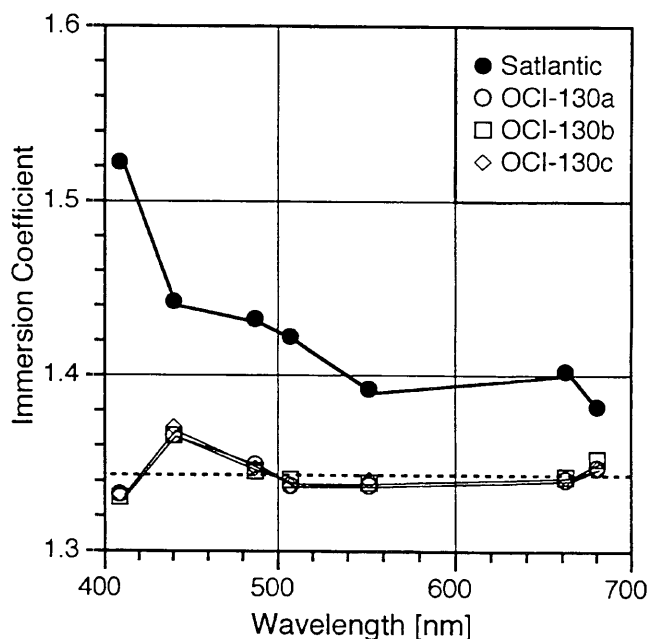


Figure 9.7: The immersion coefficients supplied by Satlantic (filled circles) and as determined with the JRC data processor from the CHORS data during SIRREX-8 for  $E_u$  sensor S/N 130 for three days of measurements (open circles). The dashed line is the average from the three CHORS measurements.

## 9.4 FUTURE WORK

The planned activities (and nominal schedule) for the second year (FY02) are as follows:

- Complete the laboratory trials and the publications associated with the immersion coefficient study;
- Analyze and document the importance of tower perturbations on above-water measurements from an offshore structure;
- Estimate the uncertainties in Labsphere plaque calibration factors (they do not provide a directional-directional calibration that is the same as the way the plaques are used in radiometric calibrations);
- Validate the second-generation microNESS profiler (which will now have the capability of measuring  $E_u$ ) and the second-generation microSAS above-water instrument (February–March 2002);
- Ascertain why the theoretical and *in situ*  $Q$ -factors do not agree;
- Reprocess the SeaWiFS Field Team data set with corrected immersion coefficients (a new data processor is in the final stages of testing); and
- Continue field campaigns for ocean color calibration and validation including a Medium Resolution Imaging Spectrometer (MERIS) cruise within 120 days of the start of operations (April–May 2002), initialization of the SeaPRISM network (June 2002), and site characterization experiments for the *Bouée pour l'acquisition de Séries Optiques à Long Terme*<sup>3</sup> (BOUSSOLE) Program (August 2001).

For the  $Q$ -factor work, the new GSFC optical data processor is being modified to explore particular aspects of instrument problems with respect to calculating the  $Q$ -factor from *in situ* data.

## REFERENCES

- Aiken, J., N.W. Rees, S. Hooker, P. Holligan, A. Bale, D. Robins, G. Moore, R. Harris, and D. Pilgrim, 2000: The Atlantic Meridional Transect: overview and synthesis of data. *Prog. Oceanogr.*, **45**, 257–312.
- Austin, R.W., 1974: "The Remote Sensing of Spectral Radiance from Below the Ocean Surface." In: *Optical Aspects of Oceanography*, N.G. Jerlov and E.S. Nielsen, Eds., Academic Press, London, 317–344.
- Firestone, E.R., and S.B. Hooker, 2001: SeaWiFS Postlaunch Technical Report Series Cumulative Index: Volumes 1–11. *NASA Tech. Memo. 2001–206892, Vol. 12*, S.B. Hooker and E.R. Firestone, Eds., NASA Goddard Space Flight Center, Greenbelt, Maryland, 24 pp.
- Hooker, S.B., and W.E. Esaias, 1993: An overview of the SeaWiFS project. *Eos, Trans., Amer. Geophys. Union*, **74**, 241–246.
- , —, and L.A. Rexrode, 1993: Proceedings of the First SeaWiFS Science Team Meeting. *NASA Tech. Memo. 104566, Vol. 8*, S.B. Hooker and E.R. Firestone, Eds., NASA Goddard Space Flight Center, Greenbelt, Maryland, 61 pp.
- , C.R. McClain, J.K. Firestone, T.L. Westphal, E-n. Yeh, and Y. Ge, 1994: The SeaWiFS Bio-Optical Archive and Storage System (SeaBASS), Part 1. *NASA Tech. Memo. 104566, Vol. 20*, S.B. Hooker and E.R. Firestone, Eds., NASA Goddard Space Flight Center, Greenbelt, Maryland, 40 pp.
- , and J. Aiken, 1998: Calibration evaluation and radiometric testing of field radiometers with the SeaWiFS Quality Monitor (SQM). *J. Atmos. Ocean. Tech.*, **15**, 995–1,007.
- , and S. Maritorena, 2000: An evaluation of oceanographic radiometers and deployment methodologies. *J. Atmos. Ocean. Tech.*, **17**, 811–830.
- , and C.R. McClain, 2000: The Calibration and Validation of SeaWiFS Data. *Prog. Oceanogr.*, **45**, 427–465.
- , G. Zibordi, J-F. Berthon, S.W. Bailey, and C.M. Pietras, 2000: The SeaWiFS Photometer Revision for Incident Surface Measurement (SeaPRISM) Field Commissioning. *NASA Tech. Memo. 2000–206892, Vol. 13*, S.B. Hooker and E.R. Firestone, Eds., NASA Goddard Space Flight Center, Greenbelt, Maryland, 24 pp.
- , and A. Morel, 2001: Platform and environmental effects on above- and in-water determinations of water-leaving radiances. *J. Atmos. Ocean. Tech.*, (submitted).
- , S. Maritorena, G. Zibordi, and S. McLean, 2001a: Results of the Second SeaWiFS Data Analysis Round-Robin, March 2000 (DARR-00). *NASA Tech. Memo. 2001–206892, Vol. 15*, S.B. Hooker and E.R. Firestone, Eds., NASA Goddard Space Flight Center, Greenbelt, Maryland, 71 pp.

<sup>3</sup> Buoy for the acquisition of a long-term optical series.

- , S. McLean, J. Sherman, M. Small, G. Zibordi, and J. Brown, 2001b: The Seventh SeaWiFS Intercalibration Round-Robin Experiment (SIRREX-7), March 1999. *NASA Tech. Memo. 2001-206892, Vol. 17*, S.B. Hooker and E.R. Firestone, Eds., NASA Goddard Space Flight Center, Greenbelt, Maryland, (in press).
- , and G. Zibordi, 2002a: The Eighth SeaWiFS Intercalibration Round-Robin Experiment (SIRREX-8), September–December 2001. *NASA Tech. Memo. 2002-206892, Vol. 19*, S.B. Hooker and E.R. Firestone, Eds., NASA Goddard Space Flight Center, Greenbelt, Maryland, (in prep.).
- , and —, 2002b: New methods for determining the immersion coefficient of marine radiometers. *Limnol. Oceanogr.*, (in prep.).
- Joint Global Ocean Flux Study, 1991: JGOFS Core Measurements Protocols. *JGOFS Report No. 6*, Scientific Committee on Oceanic Research, 40 pp.
- Loisel, H., and A. Morel, 1998: Light scattering and chlorophyll concentration in case 1 waters: A reexamination. *Limnol. Oceanogr.*, **43**, 847–858.
- Mobley, C.D., 1999: Estimation of the remote-sensing reflectance from above-surface measurements. *Appl. Opt.*, **38**, 7,442–7,455.
- Morel, A., 1980: In-water and remote measurements of ocean color. *Bound.-Layer Meteorol.*, **18**, 177–201.
- , and B. Gentili, 1996: Diffuse reflectance of oceanic waters, III. Implication of bidirectionality for the remote sensing problem. *Appl. Opt.*, **35**, 4,850–4,862.
- Mueller, J.L., 2000: “Overview of measurement and data analysis protocols” and “In-water radiometric profile measurements and data analysis protocols.” In: Fargion, G.S., and J.L. Mueller, Ocean Optics Protocols for Satellite Ocean Color Sensor Validation, Revision 2. *NASA Tech. Memo. 2000-209966*, NASA Goddard Space Flight Center, Greenbelt, Maryland, 87–97.
- , and —, 1992: Ocean Optics Protocols for SeaWiFS Validation. *NASA Tech. Memo. 104566, Vol. 5*, S.B. Hooker and E.R. Firestone, Eds., NASA Goddard Space Flight Center, Greenbelt, Maryland, 43 pp.
- , and —, 1995: Ocean Optics Protocols for SeaWiFS Validation, Revision 1. *NASA Tech. Memo. 104566, Vol. 25*, S.B. Hooker, E.R. Firestone, and J.G. Acker, Eds., NASA Goddard Space Flight Center, Greenbelt, Maryland, 66 pp.
- , B.C. Johnson, C.L. Cromer, S.B. Hooker, J.T. McLean, and S.F. Biggar, 1996: The Third SeaWiFS Intercalibration Round-Robin Experiment, SIRREX-3, September 1994. *NASA Tech. Memo. 104566, Vol. 34*, S.B. Hooker, E.R. Firestone, and J.G. Acker, Eds., NASA Goddard Space Flight Center, Greenbelt, Maryland, 78 pp.
- Siegel, D.A., M.C. O’Brien, J.C. Sorensen, D.A. Konhoff, E.A. Brody, J.L. Mueller, C.O. Davis, W.J. Rhea, and S.B. Hooker, 1995: Results of the SeaWiFS Data Analysis Round-Robin (DARR-94), July 1994. *NASA Tech. Memo. 104566, Vol. 26*, S.B. Hooker and E.R. Firestone, Eds., NASA Goddard Space Flight Center, Greenbelt, Maryland, 58 pp.
- Zibordi, G., J.P. Doyle, and S.B. Hooker, 1999: Offshore tower shading effects on in-water optical measurements. *J. Atmos. Ocean. Tech.*, **16**, 1,767–1,779.
- , S.B. Hooker, J-F. Berthon, and D. D’Alimonte, 2002: Autonomous above-water radiance measurements from an offshore platform: A field assessment experiment. *J. Atmos. Ocean. Tech.*, (in press).
- , and —, 2002: An evaluation of immersion coefficients for Atlantic marine radiometers. *J. Atmos. Ocean. Tech.*, (in prep.).

## Chapter 10

# Optimization Of Ocean Color Algorithms: Application To Satellite And In Situ Data Merging.

Stéphane Maritorena and David A. Siegel

*Institute for Computational Earth System Science, UCSB, Santa Barbara, CA 93106-3060, USA*

André Morel

*Laboratoire de Physique et Chimie Marines, Villefranche Sur Mer, France*

### 10.1 INTRODUCTION

The objective of our program is to develop and validate a procedure for ocean color data merging which is one of the major goals of the SIMBIOS project. While ocean color data merging is generally intended to operate using NASA's Level-3 global gridded products (IOCCG, 1999), our merging procedure uses a semi-analytical ocean color model and takes place at the normalized water-leaving radiance level (Level-2). There are several benefits to such an approach: it is consistent in terms of the algorithm used to generate data products (along with their associated uncertainties), it generates not only Chl but also additional inherent optical properties (IOP), it can handle data sources with similar or different bands and, uncertainties in the data sources can be accounted for in the merging procedure. The core of the procedure is based on the semi-analytical ocean color model described by Garver and Siegel (1987) and updated by Maritorena et al. (2001), thereafter referred to as the GSM01 model. The procedure has been tested successfully with in situ data (Siegel & Maritorena, 2001). Although the model has been optimized for global scale applications it is still tentative because the data set used for its optimization was not fully suited for that purpose and because the formulation of several sub-components of the model can be improved. To overcome the first of these limitations we are developing a comprehensive ocean color data set that contains all the inherent and apparent optical properties required for ocean color semi-analytical algorithm development and testing. Once the data set will be completed, it will be used to develop the final version of the merging algorithm. In addition, a new optimization of the model parameters (i.e. the coefficients used in the model sub-components) is foreseen to relax some simplifying assumptions used in the current model. The use of the merging

procedure with satellite data will also require a BRDF correction scheme to take the different viewing and illumination geometry of the data sources into account. Global and regional optimized parameterizations will be compared and ways to reconcile the two approaches will be investigated.

### 10.2 RESEARCH ACTIVITIES

Most of the work since the beginning of the SIMBIOS contract has been devoted to the development of the IOP/AOP data set. The original list of required parameters and information is listed in Table 10.1. Most of the data included in the present data set come from the NASA SIMBIOS SeaBASS archive although some data sets or subsets were directly provided to us. We have collected all available wavelengths for each of the variables listed in table to ensure analyses can be conducted with any individuals or combinations of bands. The current status of the data set is presented on Table 10.2 as well as the number of wavelengths available for each variable. Note that a "NA" in Table 10.2 does not necessarily mean that the data does not exist, it may indicate that they are not yet incorporated in the data set. Several quality control (QC) procedures have been developed, including :

- Test for negative values (except the default "missing" value).
- Comparison of  $K_d$  values with  $K_d$  for pure seawater (lower limit)
- Comparison of  $K_d$  values with  $K_d$  modeled as in Morel & Maritorena, (2001)
- Comparison of  $R_{rs}$  data [=  $L_u(0+)/E_d(0+) = L_w/E_s$ ] with the SeaBAM data.
- Comparison of  $R_{rs}$  data with  $R_{rs}$  modeled as in Morel & Maritorena, (2001)

- Comparison of  $E_d(0^-)$  and  $E_s (=E_d(0^+))$
- Comparison of  $E_d(0^+)$  with the mean solar extraterrestrial irradiance (upper limit)
- Comparison of  $a_p$  and  $a_{ph}$  data with the Morel and Maritorena, (2001) model (when Chl is available)
- Check value of  $a_{ph}^*(675)$
- Computation of the slope,  $S$ , of  $a_g(\lambda)$  and  $a_d(\lambda)$ .
- Comparison of  $b_b$  data to various  $b_b$  models (Kopelevich, 1983, Gordon et al., 1988, Morel and Maritorena, 2001 when Chl is available or Carder et al., 1999 when  $R_{rs}$  is available).

*Calculate exponent of particulate backscattering ( $n$ )*

Several analyses have been conducted on the data. In particular, the component absorption has been studied using the data collected in the AOP/IOP data set and this studies demonstrates that the absorption of the soluble fraction of seawater is a major contributor to the absorption budget over most of the Chl range of oceanic waters. These data were also used to validate the  $a_{cdm}$  retrievals of the GSM01 model derived from SeaWiFS data (Fig. 9.1, Siegel et al., 2001).

As mentioned earlier, we are in the process of improving the GSM01 model. The main feature we are working on is a parameterization that allows the model to work with data sources having any kind of bands ensuring a full compatibility of the model whatever the satellite being used in the merging process. The alternative parameterizations for particulate backscattering ( $b_{bp}$ ) are also being tested.

Since we plan on first testing the merging procedure using SeaWiFS and MODIS data, we have downloaded some MODIS Level-2 data from the GES DAAC in order for us to get more familiar with the data. This work is underway.

### 10.3 FUTURE WORK

We will continue to develop and QC the AOP/IOP data set. The first tests of satellite data merging using our procedure will take place during the second year of our SIMBIOS contract. We plan on merging SeaWiFS and MODIS data for a few case-studies sites were in situ data are generally available (e.g. BBOP, CalCOFI, Plumes and Blooms or any other "SIMBIOS Diagnostic site"). Beside the data merging itself, one key aspect of these initial tests will be to configure properly the weighting of the data sources based on their associated uncertainties (see Siegel and Maritona, 2001). We will implement new parameterizations in the GSM01 model and optimize its parameters using the AOP/IOP data set and simulated annealing (Maritorena et al., 2001).

### REFERENCES

- Carder K.L., F.R. Chen, Z.P. Lee, S.K. Hawes and D. Kamykowski. 1999: Semianalytic Moderate-Resolution Imaging Spectrometer algorithms for chlorophyll a and absorption with bio-optical domains based on nitrate-depletion temperatures. *J. Geophys. Res.*, **104**: (C3) 5403-5421.
- Garver, S.A., and D.A. Siegel, 1997: Inherent optical property inversion of ocean color spectra and its biogeochemical interpretation: I. Time series from the Sargasso Sea. *J. Geophys. Res.*, 102, 18,607-18,625.
- Gordon, H.R., O.B. Brown, R.H. Evans, J.W. Brown, R.C. Smith, K.S. Baker, and D.K. Clark. 1988: A semi-analytic radiance model of ocean color. *J. Geophys. Res.*, **93**, 10,909-10,924.
- Kopelevitch, O.V. 1983: Small-parameter model of optical properties of sea water, Chapter 8 in *Ocean Optics*, vol 1: *Physical Ocean Optics*, A.S. Monin (Ed.), Nauka Pub., Moscow.
- Maritorena S., D.A. Siegel and A. Peterson. 2001: Optimization of a Semi-Analytical Ocean Color Model for Global Scale Applications. In revision for *Applied Optics*.
- Morel A. and S. Maritorena. 2001: Bio-optical properties of oceanic waters : a reappraisal. *J. Geophys. Res.*, **106**(C4) : 7163-7180.
- Siegel, D.A. and S. Maritorena, 2001: Spectral Data assimilation for merging satellite Ocean Color imagery. SIMBIOS Project 2000 Annual Report. NASA TM-2001-209976. G. Fargion & C. R. McClain Eds, NASA Goddard Space Flight Center, Greenbelt, Maryland, pp 117-123.
- Siegel, D.A., S. Maritorena, N.B. Nelson, D.A. Hansell and M. Lorenzi-Kayser. 2001: Global Distribution and Dynamics of Colored Dissolved and Detrital Organic Materials. In Press *Journal of Geophysical Research*.

*This research was supported by  
the SIMBIOS NASA contract #00196*

## PEER REVIVED PUBLICATIONS

Maritorena S., D.A. Siegel & A. Peterson. 2001: Optimization of a Semi-Analytical Ocean Color Model for Global Scale Applications. In revision for *Applied Optics*.

Siegel, D.A., S. Maritorena, N.B. Nelson, D.A. Hansell & M. Lorenzi-Kayser. 2001: Global Distribution and Dynamics of Colored Dissolved and Detrital Organic Materials. In Press *Journal of Geophysical Research*.

Morel A. and S. Maritorena. 2001: Bio-optical properties of oceanic waters : a reappraisal. *J. Geophys. Res.*, **106**(C4) : 7163-7180.

## PRESENTATIONS

O'Reilly J. and S. Maritorena 2001: A Review of Bio-Optical Chlorophyll Algorithms and Future Challenges. Presentation Fall AGU Meeting, San Francisco, Dec. 2001.

Maritorena S, D.A. Siegel 2001: Dominance of Colored Dissolved Organic Material in Determining Light Availability in the Sea. Poster Fall AGU Meeting, San Francisco, Dec. 2001.

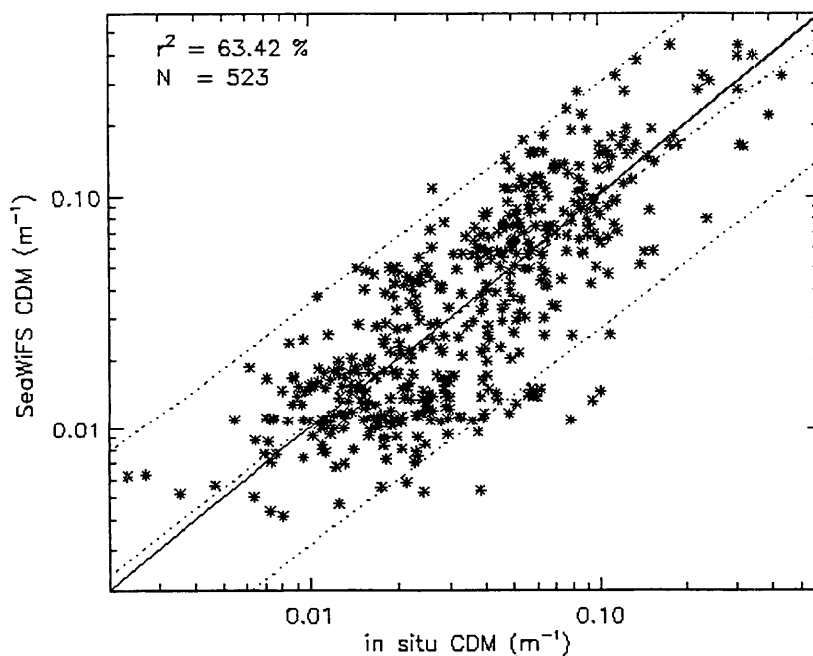


Figure 10.1: Comparison of near-simultaneous SeaWiFS and *in situ* CDM observations from around the world ( $N = 523$ ). The  $r^2$  value for the log-transformed CDM estimates is 63.42% and the fit power-law relation is  $CDM_{\text{WiFS}} = 0.775 * (CDM_{\text{field}})^{0.935}$  (the middle dotted line). The outer dotted lines represent 95% confidence interval for the fit. (From Siegel et al., 2001).

Table 10.1: Required observations for the AOP-IOP data set

Data type	Description	Notation
AOP	Spectral upwelled radiance below the surface	$L_u(\lambda, 0^-)$
	Spectral upwelled irradiance below the surface	$E_u(\lambda, 0^-)$
	Spectral incident irradiance at the surface	$E_d(\lambda, 0^+)$
	Spectral diffuse attenuation coefficient	$K_d(\lambda)$
IOP	Spectral total absorption coefficient	$a(\lambda)$
	Spectral absorption coefficient of phytoplankton	$a_{ph}(\lambda)$
	Spectral absorption coefficient of detrital particulate	$a_d(\lambda)$
	Spectral absorption coefficient of dissolved organic matter	$a_y(\lambda)$
	Spectral backscattering coefficient of particulate	$b_{bp}(\lambda)$
Pigment data	Spectral beam attenuation coefficient	$c(\lambda)$
	HPLC pigments	
	Fluorometric [Chl a]	
	Biliproteins	
Metadata	Date of collection of the data	
	Time of collection of the data	
	Latitude and longitude	
	Description of sea state	
	Description of sky state	
	Instrument identification	
	Calibration information	
	Cruise identification	
	Station identification	

Table 10.2: Present status of the AOP/IOP data set (extract). The first number in each cell indicates the number of stations for which data are available. The numbers in parentheses indicate the number of available wavelengths.

Experiment	Chl	$K_d$	$L_w$	$E_s$	$b_b$	$a_d$	$a_g$	$a_{ph}$
Indoex	35	35 (12)	35 (6)	35 (12)	na	35 (250)	na	na
Ace-Asia	50	50 (18)	50 (18)	50 (18)	na	50 (225)	50 (200)	50 (225)
BBOP	142	142 (12)	142 (12)	142 (6)	na	86 (250)	86 (200)	86 (250)
CALCOFI	176	160 (12)	160 (12)	97 (12)	na	273 (225)	273 (150)	273 (225)
ECOFRONT	16	na	28 (6)	28 (6)	na	16 (200)	16 (148)	16 (195)
EcoHAB	180	80 (1)	80 (6)	80 (6)	na	180 (200)	180 (150)	180 (200)
Globec Biomapper	26	na	na	na	na	26 (250)	26 (250)	26 (250)
GOCAL	na	na	54 (7)	52 (5)	41 (6)	na	na	na
Gulf of Maine	148	na	55 (7)	55 (7)	na	148 (200)	148 (209)	148 (150)
JGOFS	68	68 (12)	68 (12)	68 (12)	na	68 (225)	68 (225)	68 (225)
Ocean Research Consortium	25	na	25 (6)	25 (5)	25 (3)	21 (470)	21 (470)	21 (470)
Plumes and Blooms	370	304 (7)	304 (9)	304 (12)	91 (7)	338 (225)	338 (225)	338 (225)
Sea of Japan	36	36 (12)	36 (12)	36 (12)	36 (6)	na	na	na
Scotia Prince Ferry	4442	na	2191 (6)	4009 (6)	4433 (4)	na	na	na
Tongue of the Ocean	96	na	82 (6)	82 (6)	16 (6)	96 (200)	96 (225)	96 (200)
Total	5810	875	2466	5063	4642	1337	1302	1302

## Chapter 11

# Aerosol Optical Properties over the Oceans: A Summary of the FRSR Database, Calibration Protocol and Measurement Uncertainties

Mark A. Miller, R.M Reynolds, and M.J. Bartholomew

*The Brookhaven National Laboratory, Earth Systems Science Division, New York*

### 11.1 INTRODUCTION

The aerosol scattering component of the total radiance measured at the detectors of ocean color satellites is determined with atmospheric correction algorithms. These algorithms are based on aerosol optical thickness measurements made in two channels that lie in the near-infrared portion of the electromagnetic spectrum. The aerosol properties in the near-infrared region are used because there is no significant contribution to the satellite-measured radiance from the underlying ocean surface in that spectral region. In the visible wavelength bands, the spectrum of radiation scattered from the turbid atmosphere is convolved with the spectrum of radiation scattered from the surface layers of the ocean. The radiance contribution made by aerosols in the visible bands is determined from the near-infrared measurements through the use of aerosol models and radiation transfer codes. Selection of appropriate aerosol models from the near-infrared measurements is a fundamental issue.

There are several challenges with respect to the development, improvement, and evaluation of satellite ocean-color atmospheric correction algorithms. A common thread among these challenges is the lack of over-ocean aerosol data. Until recently, one of the most important limitations has been the lack of techniques and instruments to make aerosol measurements at sea. There has been steady progress in this area over the past five years, and there are several new and promising devices and techniques for data collection. The development of new instruments and the collection of more aerosol data from over the world's oceans have brought the realization that aerosol measurements that can be directly compared with aerosol measurements from ocean color satellite measurements are difficult to obtain. There are two problems that limit these types of comparisons: the cloudiness of the atmosphere over the world's oceans and the limitations of the techniques and instruments used to collect aerosol data from ships. To address the latter, we have developed a new type of shipboard sun photometer.

There are two primary types of sun photometer used to measure the aerosol optical depth: narrow field-of-view radiometers aimed at the solar disk and rotating shadow-band radiometers. Shadow-band radiometers are wide-field-of-

view radiometers that employ an occulting apparatus to add directional capabilities. Just as narrow-field-of-view radiometers must be accurately aimed, a serious drawback for measurements on ships at sea, conventional shadow-band radiometers also require exact orientation. Fast-Rotating Shadow-band Radiometers (FRSRs) are a hybrid form of the original shadow-band radiometer design, but do not have a rigid requirement for orientation. Thus, it is possible to use a slightly modified version of the land-based FRSR on ships. As compared to land-based FRSRs, shipboard FRSRs require much faster rotation of the occulting arm, faster-response silicon detectors, higher data sampling rates, and more sophisticated data analysis.

As part of our NASA SIMBIOS contract and with additional support from the Department of Energy's (DOE) Atmospheric Radiation Measurement (ARM) Program, we developed and deployed a new instrument during the past two years: the shipboard Fast-Rotating Shadow-band Radiometer (FRSR; Reynolds et al., 1999). This instrument makes continuous, semi-automated shipboard measurements of the direct-normal, diffuse, and global irradiance in seven channels (415 nm, 500 nm, ~610 nm, ~660 nm, ~862 nm, 936 nm, and broadband) and does not require a mechanically stabilized platform, thereby making it cost effective and reliable. The FRSR can operate continuously for months on a ship and can be monitored by someone with minimal training. The FRSR is part of a Portable Radiation Package (PRP), which also contains broadband solar and IR Eppley radiometers. The PRP has been deployed extensively during the past two years, traversing parts of all three oceans, and has demonstrated stable calibration. It has moved from proof-of-concept to a nearly operational instrument.

The shipboard FRSR measures spectral global and diffuse irradiance with 2-minute resolution. These data are combined with information about the pitch, roll, and heading of the ship to calculate the 2-minute spectral direct-normal irradiance. From these data, the aerosol optical thickness can be computed during clear periods using the Langley regression technique, or continuously if high quality extraterrestrial calibration coefficients are known. In addition, the diffuse irradiance measured by the FRSR can be used to evaluate

fractional cloudiness, thereby providing a means to test cloud-filtering algorithms used in satellite ocean color retrievals.

Our strategy for collecting relevant aerosol data from over the oceans has evolved over the past four years. As a benchmark of our progress, we (our group at the Brookhaven National Laboratory) believe that we have increased the number of shipboard aerosol measurements over the world's oceans by several orders of magnitude. In this report, we summarize our progress in expanding the data base of over ocean optical measurements during the past year. We also discuss our data processing strategy, especially our uncertainty analyses, and comment on plans for the future.

### *Evaluating Ocean Color Atmospheric Correction Algorithms*

An aerosol correction algorithm was developed by Gordon (1978), applied to the problem of phytoplankton pigment retrieval by Gordon and Clark (1981), and used in the Coastal Zone Color Scanner by Gordon et al. (1980). Mathematically, the atmospheric correction parameters,  $\varepsilon(\lambda_i, \lambda_j)$ , for the Gordon scheme are given by

$$\varepsilon(\lambda_i, \lambda_j) = \frac{\omega_a(\lambda_i)\tau_a(\lambda_i)p_a(\theta, \theta_0, \lambda_i)}{\omega_a(\lambda_j)\tau_a(\lambda_j)p_a(\theta, \theta_0, \lambda_j)}, \quad (1)$$

where  $\omega_a(\lambda_i)$  is the aerosol single scattering albedo,  $\tau_a(\lambda)$  is the aerosol optical thickness, and  $p(\theta, \theta_0, \lambda_i)$  is the aerosol scattering phase function. The Gordon technique is to model  $\varepsilon(\lambda_i, \lambda_j)$  using a power-law relationship defined as

$$\varepsilon(\lambda_i, \lambda_j) = \left( \frac{\lambda_i}{\lambda_j} \right)^{-n}. \quad (2)$$

The coefficient  $n$  is determined for two wavelengths in the near infrared and used to select an aerosol model. From this model, radiation transfer codes are used to estimate the satellite radiance contribution of the aerosol in the visible wavelengths (Gordon and Wang, 1994).

Evaluation of this atmospheric correction scheme therefore involves collection of shipboard data from which the characteristics of  $\varepsilon(\lambda_i, \lambda_j)$  may be determined for a wide variety of aerosol conditions. The majority of the variance associated with  $\varepsilon(\lambda_i, \lambda_j)$  is the result of variance in  $\tau_{\lambda_a}$ , so measurements of  $\tau_{\lambda_a}$  provide a surrogate for explicit measurements of  $\varepsilon(\lambda_i, \lambda_j)$ .

## 11.2 REASERCH RESULTS

There are currently nine PRPs with their resident FRSRs; a tenth PRP is under construction. As shown in Table 10.1, four of the ten instruments are permanently deployed on vessels that traverse various parts of the world's oceans: National Oceanic and Atmospheric Administration's (NOAA), NOAA's Ronald Brown, Japan Marine Science Center's R/V Mirai, and Royal Caribbean Cruise Line's Explorer of the Seas. Four of the five remaining units are deployed on ships of opportunity, three in support of University of Miami projects. They are deployed on medium to large ships making lengthy voyages or on ships traveling to a unique part of the world's oceans. Data are collected continuously from the instrument using a laptop computer, recorded on CD or disk, and shipped to BNL for analysis. Table 10.2 shows a catalogue of the data that currently reside in the database. The initial releases of most of these data have been submitted to SEABASS.

### *Calibration Of The Frsr*

Calibration of the FRSRs is done at regular intervals (six months to one year) at a high elevation location using the Langley Method. In the past, the traditional location for these calibrations has been Mauna Loa. Due to the costs associated with Mauna Loa deployments, last spring we attempted a calibration of our radiometers at the astronomical observatory on Mt. Lemmon in Arizona. The Mt. Lemmon site is at considerable elevation (3 km) and is located in the dry desert southwest. Analyses of the Mt. Lemmon calibration data show that it is a worthy site for calibration in the late spring after most of the snow on the mountain has melted. Summer may be a less optimal time for calibration at Mt. Lemmon due to the increasing frequency of convection above the peaks. Analyses also show that the morning Langley plots should be used, as upslope wind conditions in the afternoon tend to transport aerosols from the boundary layer into the atmosphere above the radiometer site on Mt. Lemmon. In summary, Mt. Lemmon appears to be a cost-effective solution for the calibration of radiometers for the SIMBIOS program.

Another important finding during the past year involves the capability to perform spot Langley calibrations on the ships on clear days. The section that follows details work to quantify the uncertainties associated with measurements of  $\tau_{a\lambda}$  and  $\alpha$  made with the FRSR on ships. These calculations demonstrate the difficulty associated with Langley calibrations at sea. The crux of the problem is that the uncertainties associated with the measurement of direct-normal irradiance on a ship increase as the solar zenith angle increases. The Langley calibration technique is strongly dependent on the measurements made at high zenith angles, so calibration of marine FRSRs must be made on land because shipboard

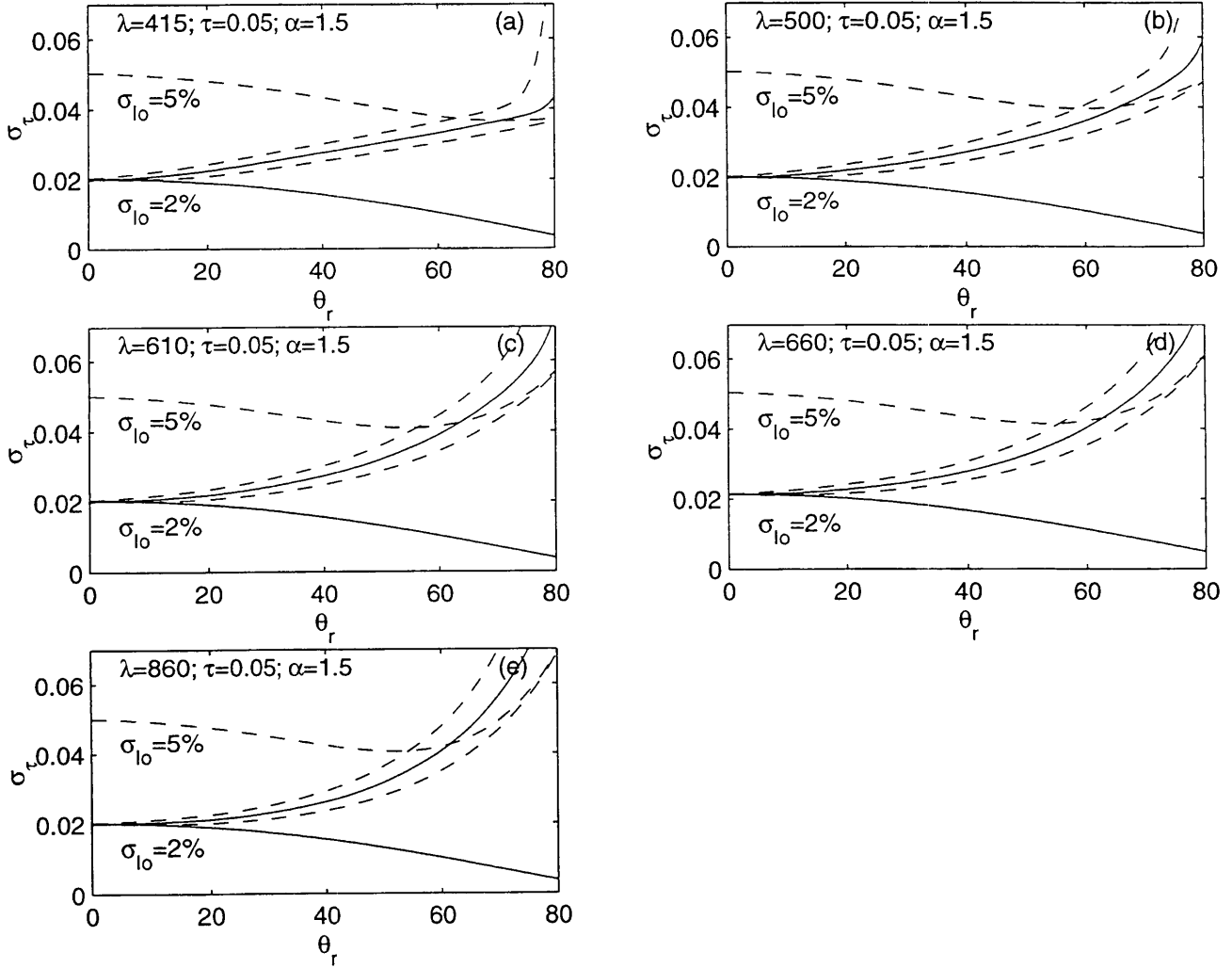


Figure 11.1: Plots of the uncertainty in the measurement of  $\tau_{\lambda_a}, \sigma_{\tau_{\lambda_a}}$ , versus the solar zenith angle,  $\theta_r$ , for a clean maritime air mass with large sea-salt particles ( $\tau_{\lambda_a} = 0.05$ ,  $\alpha = 0$ ) at (a) 415 nm, (b) 500 nm, (c) 610 nm, (d) 660 nm, and (e) 860 nm. The worst case scenario for the relationship between the solar azimuth and ship azimuth combined with the best case for calibration of the extra-terrestrial irradiance (2% uncertainty) is shown for a  $\pm 5^\circ$  envelope of ship pitch angles (the solid line within the envelope is zero degrees). The best case scenario is indicated with the solid line that moves from 0.02 to progressively lower values as the solar zenith angle increases. The dashed line above shows the approximate displacement of the family of curves if the calibration uncertainty is increased to 5%.

Table 11.1: Current Deployments

Unit	Ship or Location	Status	Location
P01	Akademic Ioffe	Ship of Opportunity	Atlantic transect and Antarctic
P02	Ka'imimoana	Permanent	Tropical Western Pacific
P03	Ewing	Ship of Opportunity	Piraeus to Freemantle
P04	BNL	Ship of Opportunity	BNL Radiation Platform
P05	Explorer of the Seas	Permanent	Caribbean
P06	JAMSTEC	Preparing for Island Deploy	Tropical Western Pacific
P07	Mirai	Permanent	North Pacific to Tropics
P08	BNL	Transfer Standard	BNL Radiation Platform
P09	Ron Brown	Permanent	Variable
P10	Under Construction	Ship-of-opportunity	To be determined

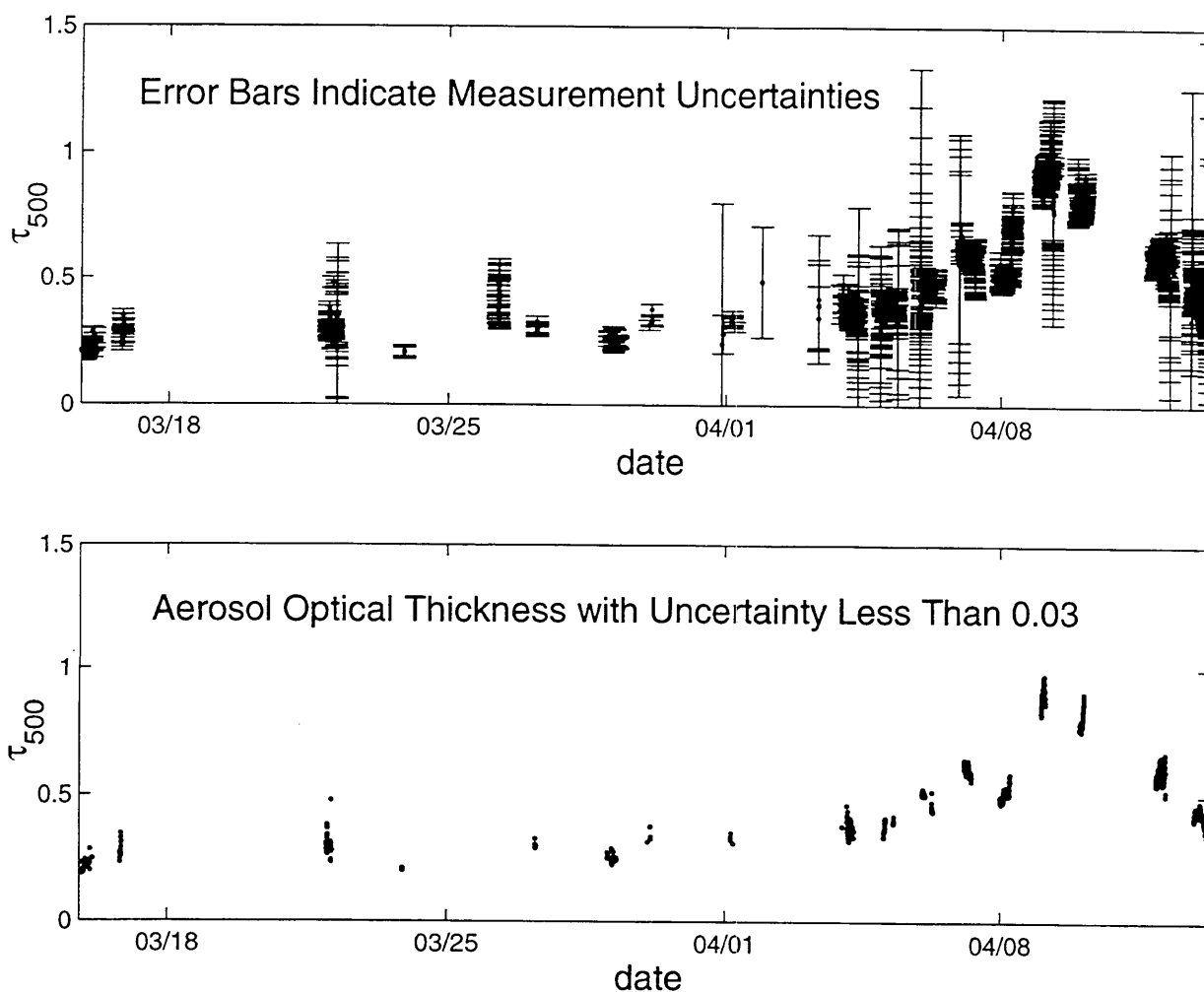


Figure 11.2: (a) Plots of  $\tau_{\lambda_a}$  at 500 nm for the ACE-ASIA Experiment, along with the calculated uncertainty of each individual measurement as a consequence of ship motion. (b) plots of  $\tau_{\lambda_a}$  at 500 nm for which the uncertainty in the measurement of  $\tau_{\lambda_a}$  is 0.03 or less.

calibrations contain too much inherent uncertainty due to platform motion.

We have amassed a data record that is long enough for us to address calibration drift in the FRSR head. There are two methods that can be used to quantify this drift. The most obvious method is to compare the values of extra-terrestrial irradiance between two Langley calibrations, which are typically performed a few months apart. This method will reveal drift, but gives no information about the temporal variability of the drift between the two calibrations. A method that we are currently developing relies on comparison of the broadband irradiance measured by the FRSR with the broadband irradiance measured with the independent Eppley PSP, which is part of the portable radiation package. This

technique has the advantage of providing a time history of the drift, since the calibration of the Eppley PSP is more stable. We have used this technique to examine calibration drift on the FRSR and found that it does not always decay in a steady manner during deployments. The calibration of the FRSR on some of our units tends to change incrementally, while little or no drift is observed in other units.

We theorize that the calibration drift we are observing is caused by degradation of the material used in the head diffuser assembly. Using the PSP, we can correct for this drift, but we are likely to institute a routine swap of the diffusers in our units on a periodic basis.

### FRSR Data Analysis

We have continued to aggressively pursue a method to quantify the uncertainties associated with our measurements. During the past year, we have successfully completed this task and are currently applying it to our database. The foundation of our method is a calculation of the variance,  $\sigma^2$ , associated with the measurement techniques. The variance equations for  $\tau_a(\lambda)$  and  $\alpha$  (the Angstrom exponent), are given by

$$\sigma_{\tau_\lambda}^2 = \left(\frac{1}{m}\right)^2 \left[ \left(\frac{\sigma_{I_{\lambda 0}}}{I_{\lambda 0}}\right)^2 + \left(\frac{\sigma_{I_{\lambda N}}}{I_{\lambda N}}\right)^2 + \sigma_{\tau_{\lambda R}} + \sigma_{\tau_{\lambda O}} \right] \quad (3)$$

$$\sigma_\alpha^2 = \left\{ \ln\left(\frac{\lambda_1}{\lambda_2}\right) \right\}^{-2} \left[ \left(\frac{\sigma_{\tau_{\lambda 1}}}{\tau_{\lambda 1}}\right)^2 + \left(\frac{\sigma_{\tau_{\lambda 2}}}{\tau_{\lambda 2}}\right)^2 \right]^{1/2}, \quad (4)$$

where  $m$  is the air mass and  $I_\lambda$  is the direct-normal irradiance. The subscripts 0 and  $N$  indicate the extra-terrestrial value and the measured value, respectively, and the subscripts 1 and 2 indicate the two wavelengths used in the calculation of the Angstrom exponent. The subscripts  $R$  and  $O$  denote the Rayleigh and Ozone contributions. These variance equations provide a means to evaluate  $\sigma^2$  for each individual measurement, thereby permitting a running assessment of the quality of the aerosol measurements. The variance equations also permit the data to be filtered according to the uncertainty in  $\tau_a(\lambda)$ ,  $\alpha$ , or both variables.

The challenge in using (3) and (4) is the definition of  $\sigma_{I_{\lambda 0}}^2$  and  $\sigma_{I_{\lambda N}}^2$ , the variances in the extra-terrestrial irradiance and the direct-normal irradiance. The former can be evaluated by comparing Langley calibration derived values of  $I_{\lambda 0}$  with those measured by a combination of satellite and model calculations (see Thullier et al., 1988). These comparisons generally indicate that our absolute calibrations are within 2% of the accepted values. The term  $\sigma_{I_{\lambda N}}^2$  is more challenging. Expansion of this term reveals that it is dependent on the uncertainty in the orientation of the radiometer with respect to the sun. To demonstrate and quantify this uncertainty, we have developed a full model of the functional dependence of  $\sigma_{I_{\lambda N}}^2$  on radiometer orientation, which is in turn a function of the wave conditions and sun angle. Results from this model (Figure 11.1) show that the uncertainty in a measurement of  $\tau_{a\lambda}$  is dependent on the orientation of the radiometer with respect to the sun. The uncertainty in  $\tau_{a\lambda}$ ,  $\sigma_\tau$ , can be less than 0.02 for all solar

zenith angles if the relative solar azimuth angle is orthogonal to the pitch and/or roll plane of the ship. If the pitch and/or roll is in the same plane as the relative solar azimuth angle,  $\sigma_\tau$  rapidly degrades and can exceed 0.04 at large relative solar zenith angles. Of critical importance, however, is radiometer calibration,  $\sigma_{I_{\lambda 0}}^2$ , as is the case with land-based units.

The uncertainty in each individual measurement of  $I_{\lambda N}$ , and hence  $\tau_{a\lambda}$  and  $\alpha$ , can be computed by specifying the pitch, roll, heading, latitude, longitude, and time using the model we have developed. This enables filtering schemes to be devised on the basis of uncertainty. An example of the use of this technique is shown in Figure 11.2 using data collected on the R/V Ron Brown from the ACE-ASIA experiment. As the figure shows,  $\sigma_\tau < 0.03$  for 66% of the cloud-free measurements taken during the experiment.

## 11.3 CONCLUSION

We believe that we have essentially perfected the marine shadow-band technique and have learned how to track any calibration drift that may occur. The size of the FRSR database continues to grow rapidly and we have developed a configuration control system to document all aspects of the data. Each radiometer has a calibration document that is always kept current and changes to calibrations are noted. Our new technique to track calibration drift using the on-board Eppley PSP is showing great promise. Furthermore, our understanding of instrument uncertainties has become mature. Thus, we are approaching a method-of-operation worthy of the designation "marine shadow-band network".

We are finally in a position to evaluate  $\tau_{a\lambda}$  used in atmospheric correction models with the data we have collected from the FRSR. We have an extensive database of aerosol optical properties from over the world's oceans and have developed the method for quantifying the uncertainties associated with the measurements. Two manuscripts describing the FRSR database are in preparation and a third describing satellite match-ups is planned. We anticipate that all three manuscripts will be submitted within the next year. The bottom line is that we believe we have a robust, repeatable, and reliable technique for evaluating satellite data.

It is now time to begin thinking about additional radiometric characteristics of the marine atmosphere. We need to quantify the effects of widely scattered clouds on the optical thickness observed by the satellite. Indeed, it may be time to alter our thinking such that we begin speaking in terms of optical thickness, rather than aerosol optical thickness. In cirrus or widely scattered cumulus conditions, it may be possible to accurately characterize the underlying ocean. If we work toward improving our understanding of the cloud and

aerosol system, as opposed to looking for completely clear conditions, the capabilities of ocean color satellites may be enhanced. Toward that end, we need to be looking past the direct-normal irradiance measurements of the FRSR as the principal tool for satellite evaluation. We need to begin to analyze and understand the direct-normal irradiance as it is the key to achieving a better understanding of the cloud and aerosol system that is present in the marine atmosphere.

## REFERENCES

- Gordon, H.R. 1978: Removal of atmospheric effects from satellite imagery of the oceans. *Applied Optics*, **17**, 1631-1636.
- Gordon, H.R., D.K. Clark, J.L. Mueller, and W.A. Hovis 1980: Phytoplankton pigments derived from the Nimbus-7 CZCS: initial comparisons with surface measurements. *Science*, **210**, 63-66.
- Gordon, H.R., and D.K. Clark 1981: Clear water radiances for atmospheric correction of coastal zone color scanner imagery, *Applied Optics*, **20**, 4175-4180.
- Gordon, H.R. and M.Wang 1994: Retrieval of water-leaving radiance and aerosol optical thickness over the oceans with SeaWiFS: a preliminary algorithm. *Applied Optics*, **33**, 443-452.
- Reynolds, M.R., M.A. Miller, and M.J. Bartholomew, 1999: A fast-rotating, spectral shadowband radiometer for marine applications, *J. Atmos. Ocean. Tech.*, **18**, 200-214.
- Thuiller, G., M. Herse, P.C. Simon, D. Labs, H. Mandel, and D. Gillotay, 1998: Observations of the solar spectral irradiance from 200 nm to 870 nm during the ATLAS 1 and ATLAS 2 missions by the SOLSPEC spectrometer, *Metrologia*, **35**, 689-695.

Table 11.2: FRSR deployments

<b>Cruise</b>	<b>Ship</b>	<b>Location</b>	<b>Status</b>	<b>Duration</b>
Aero99	Ron Brown	Atlantic Oceans	SEABASS	1 month
Ant00	Polarbird	Antarctic	Radiation-no FRSR	1.5 months
Ex0127-138	Exp. Seas	Caribbean	SEABASS	2.5 months
Ex0139-140	Exp. Seas	Caribbean	Data just received	2 weeks
Indo99	Ron Brown	Indian Ocean	SEABASS	1 month
Ka0008	Ka'imimoan	Tropical Western Pacific	SEABASS	1 month
Ka0009	Ka'imimoan	Tropical Western Pacific	SEABASS	1 month
Ka0101	Ka'imimoan	Tropical Western Pacific	Not processed	5-days
Ka0102	Ka'imimoan	Hawaii to Southern California	SEABASS	1 month
Ka0104	Ka'imimoan	Southern California to Hawaii	SEABASS	10 days
Ka0105	Ka'imimoan	Hawaii to Tropical Pacific	SEABASS	1 month
Ka0106	Ka'imimoan	Tropical Pacific	SEABASS	1 month
Ka0107	Ka'imimoan	Tropical Western Pacific	SEABASS	1 month
Kn01	Knorr	Tropical Atlantic	SEABASS	2 months
Mel99	Melville	Gulf of California	SEABASS	20 days
Mr00k3	Mirai	Sea of Japan to North Pacific	SEABASS	2 months
Mr00k4	Mirai	Japan to Tropical Western Pacific	SEABASS	1 month
Mr00k5	Mirai	Japan to Western Pacific	SEABASS	1 month
Mr00k6	Mirai	Tropical Western Pacific	In processing	1 month
Mr00k7	Mirai	Japan to Eastern Indian Ocean	In processing-no FRSR	1 month
Mr00k7a	Mirai	Japan to Tropical Western Pacific	In processing-no FRSR	1 month
Mr00k8	Mirai	Tropical Western Pacific	In processing	1 month
Mr01k1	Mirai	Tropical Western Pacific to Japan	In processing	1 month
Mr01k2	Mirai	Sea of Japan	In processing	1 months
Mr01k3	Mirai	Sea of Japan to North Pacific	In processing	1.5 months
Mr01k4	Mirai	North Pacific to Sea of Japan	Data just received	1 month
N99mr	Mirai	Tropical Western Pacific	SEABASS	1 month
N99rb	Ron Brown	Tropical Western Pacific	SEABASS	1 month
N99na	Nauru	Tropical Western Pacific	SEABASS	1 month
Pstar00	Polar Star	Australia to California	SEABASS	2 months
Rb0009	Ron Brown	Southern California to Tropics	SEABASS	1 month
Rb0100	Ron Brown	South Carolina to South Florida	Radiation-no FRSR	1 month
Rb0101	Ron Brown	Equatorial Pacific	SEABASS-2 FRSRs	1 month
Rb0102	Ron Brown	Mid-Pacific to Japan	SEABASS-2 FRSRs	1 month

## Chapter 12

# Bio-Optical Measurement and Modeling of the California Current and Southern Oceans

B. Greg Mitchell

*Scripps Institution of Oceanography, University of California San Diego, La Jolla, California*

### 12.1 INTRODUCTION

This SIMBIOS project contract has supported in situ ocean optical observations in the California Current, and the north Pacific, Southern and Indian Oceans. Our principal goals are to validate standard or experimental ocean color products through detailed bio-optical and biogeochemical measurements, and to combine ocean optical observations with modeling to contribute to satellite vicarious radiometric calibration and algorithm development.

In collaboration with major oceanographic ship-based observation programs (CalCOFI, JGOFS, AMLR, INDOEX, and ACE Asia) our SIMBIOS effort has resulted in data from diverse bio-optical provinces. For these global deployments we generate a methodologically consistent data set encompassing a wide-range of oceanic conditions. We have initiated several collaborations with scientists in East Asian countries to study the complex Case 2 waters of their marginal seas. Global data collected in recent years have been integrated with our on-going CalCOFI time-series. The combined database we have assembled now comprises more than 800 stations and includes observations for the clearest oligotrophic waters, highly eutrophic blooms, red-tides and coastal case 2 conditions. The data has been used to validate water-leaving radiance estimated with SeaWiFS as well as bio-optical algorithms for chlorophyll pigments. The comprehensive data is utilized for development of standard and experimental algorithms.

### 12.2 RESEARCH ACTIVITIES

We continue to participate on CalCOFI cruises to the California Current System (CCS) for which we have an 8-year time-series. This region experiences a large dynamic range of coastal and open ocean trophic structure and has experienced strong interannual forcing associated with the El Niño – La Niña cycle from 1997-2000 (Kahru and Mitchell, 2000; Kahru and Mitchell, 2001a). CalCOFI data provides an excellent

reference for evaluating our other global data sets (O'Reilly et al. 1998).

During the third year of our contract, we participated in 3 CalCOFI cruises, one cruise in collaboration with NOAA AMLR to the Southern Ocean, and the ACE Asia cruise to the northwest Pacific on NOAA R/V Ronald Brown. The global distribution of our present data set is shown in Figure 12.1. On most cruises, an integrated underwater profiling system was used to collect optical data and to characterize the water column. The system included an underwater radiometer (Biospherical Instruments MER-2040 or MER-2048) measuring depth, downwelling spectral irradiance ( $E_d$ ) and upwelling radiance ( $L_u$ ) in 13 spectral bands. A MER-2041 deck-mounted reference radiometer (Biospherical Instruments) provided simultaneous measurements of above-surface downwelling irradiance. Details of the profiling procedures, characterization and calibration of the radiometers, data processing and quality control are described in Mitchell and Kahru (1998). The underwater radiometer was also interfaced with 25 cm transmissometers (SeaTech or WetLabs), a fluorometer, and SeaBird conductivity and temperature probes. When available, additional instrumentation integrated onto the profiling package included AC9 absorption and attenuation meters (WetLabs Inc.), and a Hydrosat-6 backscattering meter (HobiLabs). For the AMLR and ACE Asia cruises in 2001 we deployed our new Biospherical Instruments PRR 800 free fall radiometer that included 19 channels of surface irradiance 312- 865 nm and three geometries of underwater radiometry ( $L_u$ ,  $E_u$ ,  $E_d$ ) from 312-700 nm. We have shown that measuring these three radiometric geometries with our MER 2048 allowed us to retrieve backscatter and absorption coefficients (Stramska et al., 2000).

At in situ optical stations discrete water samples were collected from a CTD-Rosette immediately before or after each profile for additional optical and biogeochemical analyses. Pigment concentrations were determined fluorometrically and with HPLC. All HPLC samples acquired

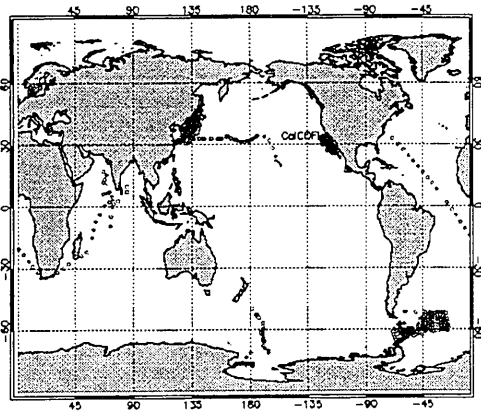


Figure 12.1: Global distribution of bio-optical stations accomplished in the past 5 years by the Scripps Photobiology Group (SPG). All stations include spectral reflectance and fluorometric chlorophyll. Most include particle and soluble absorption and HPLC pigments. For some CalCOFI and all international cruises since 1997 we have deployed Hydrosat backscatter and AC9 absorption and attenuation meters to better understand the variables that govern remote sensing reflectance.

in the past year have been submitted to San Diego State University for analysis under a separate SIMBIOS contract. Spectral absorption coefficients (300-800 nm) of particulate material were estimated by scanning particles concentrated onto Whatman GF/F filters (Mitchell 1990) in a dual-beam spectrophotometer (Varian Cary 1). Absorption of soluble material was measured in 10 cm cuvettes after filtering seawater samples through 0.2  $\mu\text{m}$  pore size polycarbonate filters. Absorption methods are described in more detail in Mitchell et al. (2001a). For some cruises we collected measurements of other optical and phytoplankton properties including photosynthesis, particulate organic matter (carbon and nitrogen), phycoerythrin pigment, and size distribution using flow cytometry and a Coulter Multisizer.

## 12.3 RESEARCH RESULTS

Our normalized water leaving radiances ( $L_{\text{WN}}$ ) at SeaWiFS bands for global data, except Southern Ocean, are plotted against surface chl-a in Figure 12.2A. Data collected during these cruises represents approximately 25% of the data used for development of the SeaWiFS OC4v4 algorithm (O'Reilly et al., 2000). Kahru and Mitchell (1999; 2001a) have shown that the chl-a retrieved by satellite in the CalCOFI region is in good agreement with our ship data when computed with our regional algorithm or NASA's OC4v4. Southern Ocean results for in situ observations during JGOFS

(1997-1998) and AMLR (2000-2001) indicate a strong deviation from NASA's OC4v4 algorithm relationship for chl-a in the range 0.1-2.0  $\text{mg m}^{-3}$  (Figure 12.2B). This region has been shown to have bio-optical algorithms that are different than low latitude regions such as CalCOFI (Mitchell and Holm-Hansen, 1991; Mitchell, 1992; Arrigo et al., 1998; Dierssen and Smith, 2000). We have developed a new Southern Ocean chl-a algorithm based on an OC4-type fit to the Southern Ocean data set (Figure 12.2B; Mitchell et al., 2001b). These results underscore the need for more data to serve as a basis for regional algorithms to improve estimates of chl-a from ocean color remote sensing. A global ocean color data processing scheme needs to be specified that can transition from low latitude to high latitude without arbitrary discontinuities. More data and advanced models are required to resolve issues regarding Southern Ocean bio-optical algorithms and to understand the causes of observed differentiation. For a better understanding, it is essential to determine not only reflectance and chlorophyll, but also inherent optical properties including absorption and backscattering as reported by Reynolds et al. (2001). Generally, there are few observations in the Southern Ocean, and even fewer with detailed observations including inherent optical properties. During our AMLR cruise in January 2002 we will deploy our Hydrosat backscatter meter and collect water samples for measurement of particle and soluble absorption, HPLC pigments and particle size distribution to extend our understanding of Southern Ocean algorithm issues.

Processing SeaWiFS data with SeaDAS v4.1 still results in significant underestimates of  $L_{\text{WN}}$  at 412 and 443 for some of our case 1 water match ups with high resolution HRPT data. Figure 12.3 shows spectral  $L_{\text{WN}}$  for two ACE Asia stations, both in Case 1 water types with moderate chl-a concentrations (0.3 – 0.5  $\text{mg chl-a m}^{-3}$ ). The offshore station between Hawaii and Japan had reasonable retrieval of spectral  $L_{\text{WN}}$  (Figure 12.3A) but the Kuroshio intrusion station between Japan and Korea did not (Figure 12.3B). We believe this difference is caused by errors in the aerosol models in the atmospheric correction for SeaWiFS for atmospheres that have significant terrestrial or anthropogenic aerosols. Continued research on atmospheric aerosols is required to improve the accuracy of  $L_{\text{WN}}$  if we are to be able to apply multi-wavelength bio-optical retrieval algorithms that require accurate estimates of  $L_{\text{WN}}$  at 412 and 443 (e.g. Garver and Siegel, 1997; Carder et al., 1999). Collaborations with aerosols chemists and atmospheric optics experts will be expanded in the next year using ACE Asia and INDOEX data sets.

With colleagues in Korea, China, Japan and Hong Kong we have assembled a large regional data set from the East China Sea, South China Sea and coastal waters of Eastern

Asia. Figure 12.4 shows reflectance ratios for SeaWiFS bands plotted against chl-a for CalCOFI and Asian data sets. Where the Asian data deviate, it is usually toward a lower ratio compared to CalCOFI. One dramatic difference between the East Asian data and our CalCOFI data set is the very high variance in the relationship between particle absorption and chl-a (Figure 12.5). Soluble absorption in the region also tends to be higher than for CalCOFI (data not shown). The reflectance trends for Asian data (Figure 12.4) are consistent with higher absorption that is likely due both to detrital and soluble absorption. This recently merged data set is being used to evaluate Case 2 algorithms in collaboration with our Asian colleagues (Kahru et al., 2001b).

## 12.4 FUTURE WORK

We will continue our approach of acquiring detailed data sets at the global scale for ocean color satellite validation and algorithm development. CalCOFI will continue as our core field program and we plan to complete one detailed CalCOFI cruise per year and 3 that have a minimal set of chl-a and reflectance data. We are advising the CalCOFI program on concepts for a permanent optics program to be integrated into their routine CTD profiling. A close cooperation has been initiated with the IMEMECOCAL program off Baja California that is coordinated by scientists from CICESE in Ensenada, Mexico. Data from their cruises starting in 1997 will be available to us in 2002. The Southern Ocean and East Asian marginal seas will continue to be a high priority since it is evident that standard algorithms for chl-a do not perform well in these regions. In January, 2002 we will participate in the NOAA AMLR cruise to the Southern Ocean. During 2002 we will organize a SIMBIOS workshop to address polar algorithm issues. Modeling efforts will continue to improve our understanding of regional bio-optical properties and their relationship to biogeochemical parameters (e.g. Stramska et al., 2000; Reynolds et al, 2001; Loisel et al., 2001). The models and data will contribute to development of advanced algorithms and parameterizations for semi-analytical inversion models for the retrieval of inherent optical properties and biogeochemical properties besides chl-a.

## REFERENCES

- Arrigo, K.R., D.H. Robinson, D.L. Worthen, B. Schieber and M.P. Lizotte 1998: Bio-optical properties of the southwestern Ross Sea. *Journal of Geophysical Research*. **103**(C10): 21,683-21,695.
- Carder, K.L., F.R. Chen, Z.P. Lee and S.K. Hawes 1999: Semianalytic moderate-resolution imaging spectrometer algorithms for chlorophyll a and absorption with bio-optical domains based on nitrate-depletion temperatures. *Journal of Geophysical Research*. **104**(C3): 5,403-5,421.
- Dierssen, H.M. and Smith, R.C. 2000: Bio-optical properties and remote sensing ocean color algorithms for Antarctic Peninsula waters, *Journal of Geophysical Research*, **105**(C11): 26301-26312.
- Garver, S.A. and D.A. Siegel 1997: Inherent Optical Property Inversion of Ocean Color Spectra and its Biogeochemical Interpretation: 1. Time series from the Sargasso Sea. *Journal of Geophysical Research*, **102**(C8): 18,607-18,625.
- Kahru, M. and B.G. Mitchell 1999: Empirical chlorophyll algorithm and preliminary SeaWiFS validation for the California Current. *International Journal of Remote Sensing*. **20**(17): 3,423-3,430.
- Kahru, M. and B.G. Mitchell 2000: Influence of the 1997-98 El Niño on the surface chlorophyll in the California Current. *Geophysical Research Letters*. **27**(18): 2,937-2,940.
- Kahru, M. and B.G. Mitchell 2001a: Seasonal and non-seasonal variability of satellite-derived chlorophyll and colored dissolved organic matter concentration in the California Current. *Journal of Geophysical Research*. **106**(C2): 2517-2529.
- Kahru, M., B. G. Mitchell, J. Wieland, J. C. Chen, N. W. Man, and Y. S. Suh 2001b: Validation of Ocean Color Algorithms in East Asian Marginal Seas. American Geophysical Union Conference. San Francisco. 10-14 December, 2001.
- Loisel, H. and D. Stramski 2000: Estimation of the inherent optical properties of natural waters from the irradiance attenuation coefficient and reflectance in the presence of Raman scattering. *Applied Optics*. **39**(18): 3,001-3,011.
- Mitchell, B.G. 1990: Algorithms for determining the absorption coefficient of aquatic particulates using the quantitative filter technique (QFT). In: Spinrad, R., ed., *Ocean Optics X*, Bellingham, Washington, SPIE, 137-148.

- Mitchell, B.G. 1992: Predictive bio-optical relationships for polar oceans and marginal ice zones. *Journal of Marine Systems*. **3**: 91-105.
- Mitchell, B.G. and M. Kahru 1998: Algorithms for SeaWiFS standard products developed with the CalCOFI bio-optical data set. *Cal. Coop. Ocean. Fish. Invest. R.* **39**: 133-147.
- Mitchell, B.G. and O. Holm-Hansen, 1991: Bio-optical properties of Antarctic Peninsula waters: Differentiation from temperate ocean models. *Deep-Sea Research I*. **38**(8/9): 1,009-1,028.
- Mitchell B. G. , M. Kahru, J. Wieland and M. Stramska 2001a: Determination of spectral absorption coefficients of particles, dissolved material and phytoplankton for discrete water samples. In: NASA, Ocean Optics Protocols for Satellite Ocean Color Sensor Validation.
- Mitchell, B. G., M. Kahru, R. Reynolds, J. Wieland, D. Stramski, C. Hewes, O. Holm-Hansen 2001b: Evaluation of Chlorophyll-a Ocean Color Algorithms for the Southern Ocean. American Geophysical Union. San Francisco. 10-14 December, 2001.
- O'Reilly, J.E., S. Maritorena, B.G. Mitchell, D.A. Siegel, K.L. Carder, S.A. Garver, M. Kahru and C. McClain 1998: Ocean color chlorophyll algorithms for SeaWiFS. *Journal of Geophysical Research*. **103**(C11): 24,937-24,953.
- O'Reilly, J.E., S. Maritorena, D.A. Siegel, M.C. O'Brien, D.A. Toole, B.G. Mitchell, M. Kahru, et al. 2000: Ocean color chlorophyll a algorithms for SeaWiFS, OC2 and OC4: Version 4. In: NASA, SeaWiFS Postlaunch Calibration and Validation Analyses.
- Reynolds, R.A., D. Stramski and B.G. Mitchell 2001: A chlorophyll-dependent semianalytical reflectance model from derived from field measurements of absorption and back scattering coefficients within the Southern Ocean. *Journal of Geophysical Research*. **106**(C4): 7125-7138.
- Siegel, D.A., M. Wang, S. Maritorena and W. Robinson 2000: Atmospheric correction of satellite ocean color imagery: The black pixel assumption. *Appl. Opt.* **39**(21): 3,582-3,591.
- Stramska, M., D. Stramski, B.G. Mitchell and C.D. Mobley 2000: Estimation of the absorption and backscattering coefficients from in-water radiometric measurements. *Limnology and Oceanography*. **45**(3): 628-641.

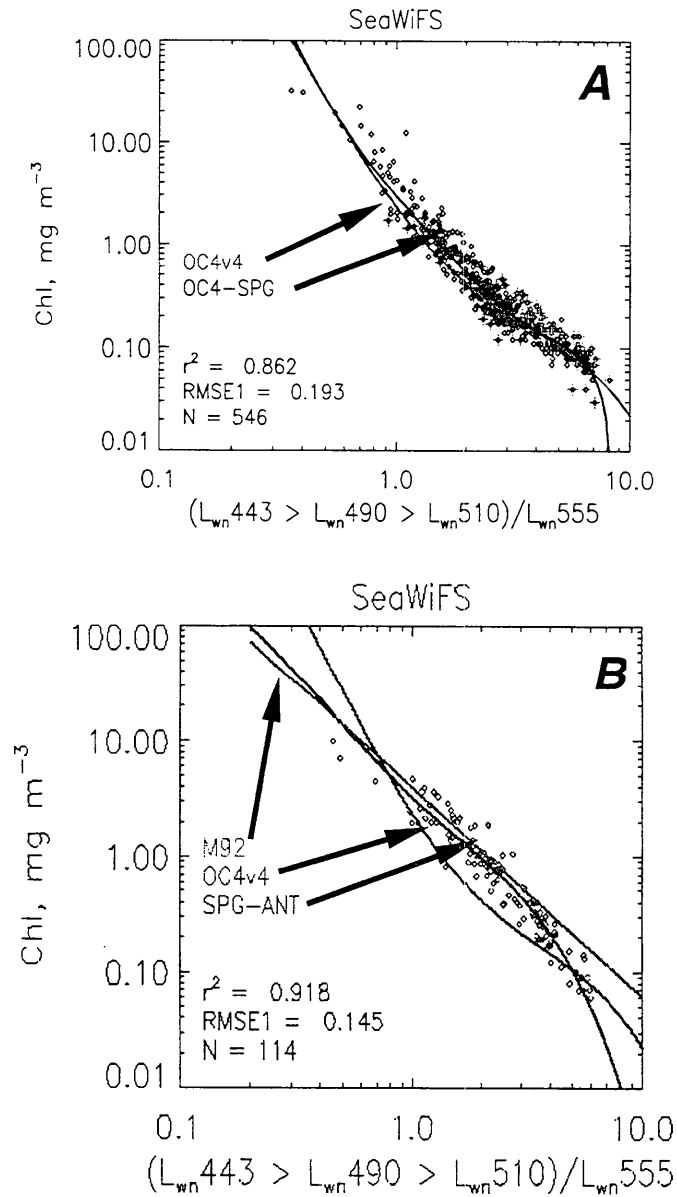


Figure 12.2: A. Maximum band ratio algorithms for the SPG Case 1 global data set excluding our Southern Ocean JGOFS and AMLR data. These data comprise approximately 25% of NASA's SeaWiFS chl-a algorithm data set used by O'Reilly et al. (2000). The lines are fits for NASA's SeaWiFS OC4v4 and our OC4-type fit to the SPG data set. Minor differences between OC4v4 and OC4-SPG fit to our data are evident for chl-a between 0.3 – 3.0 mg m<sup>-3</sup>. B. Spectral reflectance band ratios plotted against chl-a for our Southern Ocean data set. The curved line through the data is our SPG-ANT relationship for the Southern Ocean and the curved line that does not fit the data is NASA's standard OC4v4 relationship. The linear line is the Mitchell (1992) Antarctic fit.

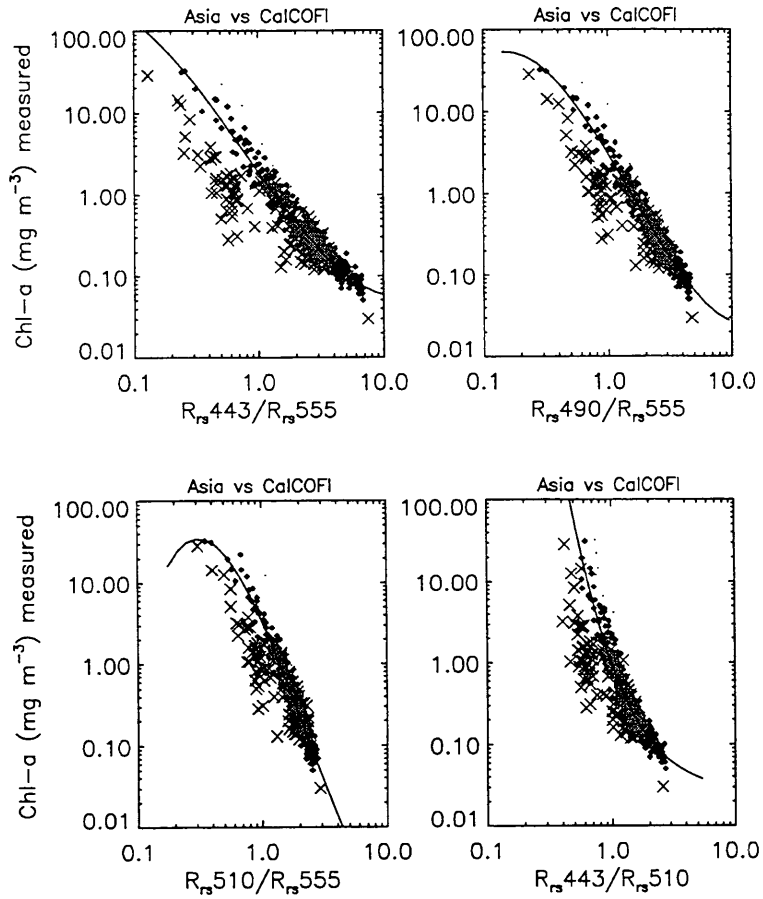


Figure 12.3: Scatter plots of ocean spectral reflectance ratios for various SeaWiFS bands plotted against chl-a for our CalCOFI ( $\circ$ ) and East Asian region (X) data sets. CalCOFI data have a coherent relationship, but some of the East Asian waters diverge due to complexity of Case 2 water constituents including detrital absorption, CDOM and mineral particles.

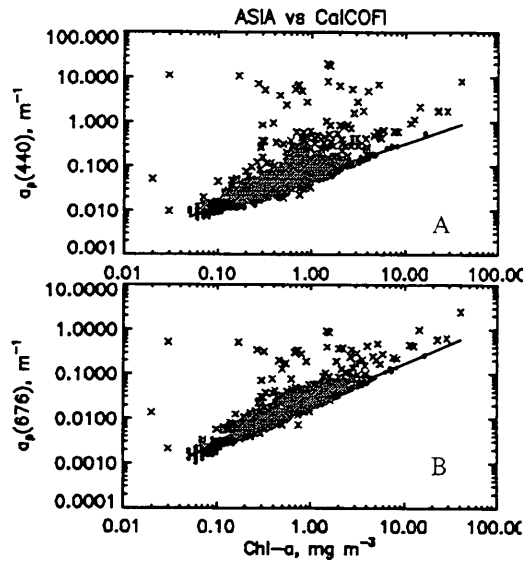


Figure 12.4: Spectral absorption by ocean particles plotted against chl-a for CalCOFI ( $\bullet$ ) and our East Asian data set ( $\times$ ). A. 440 nm; B. 676 nm. The line is a power fit to our CalCOFI data. Some of the Asian data is consistent with CalCOFI, but many near-coastal or shelf stations exhibit much higher absorption per unit chl-a than CalCOFI due to detrital pigments. This strong blue absorption will make retrieval of chl-a from passive reflectance in the blue very difficult in these waters since the dominant absorption will be from detritus and soluble material rather than chl-a and associated photosynthetic pigments.

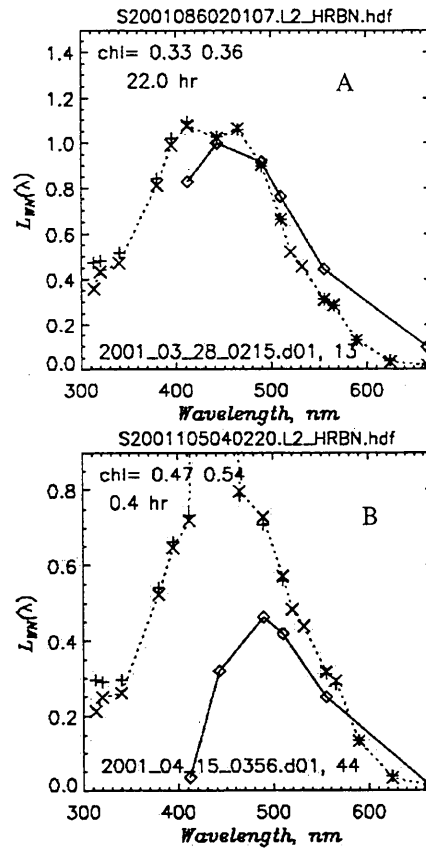


Figure 12.5: Lwn matchups between ACE Asia in situ radiometry (x) and SeaWiFS (◇) in the open north Pacific (A) and in the Kuroshio intrusion between Japan and Korea (B). Both had similar chl-a concentrations and were Case 1 waters. The large discrepancy in the east Asian region is attributed to errors in the aerosol models for SeaWiFS atmospheric corrections.

## Chapter 13

# Variability in Ocean Color Associated with Phytoplankton and Terrigenous Matter: Time Series Measurements and Algorithm Development at the FRONT Site on the New England Continental Shelf.

John R. Morrison and Heidi M. Sosik

*Woods Hole Oceanographic Institution, Woods Hole, Massachusetts*

### 13.1 INTRODUCTION

Fronts in the coastal ocean describe areas of strong horizontal gradients in both physical and biological properties associated with tidal mixing and freshwater estuarine output (e.g. Simpson, 1981 and O'Donnell, 1993). Related gradients in optically important constituents mean that fronts can be observed from space as changes in ocean color as well as sea surface temperature (e.g., Dupouy et al., 1986). This research program is designed to determine which processes and optically important constituents must be considered to explain ocean color variations associated with coastal fronts on the New England continental shelf, in particular the National Ocean Partnership Program (NOPP) Front Resolving Observational Network With Telemetry (FRONT) site. This site is located at the mouth of Long Island sound and was selected after the analysis of 12 years of AVHRR data showed the region to be an area of strong frontal activity (Ullman and Cornillon, 1999). FRONT consists of a network of modem nodes that link bottom mounted Acoustic Doppler Current Profilers (ADCPs) and profiling arrays. At the center of the network is the Autonomous Vertically Profiling Plankton Observatory (AVPPO) (Gallager et al. 1998, Thwaites et al. 1998). The AVPPO consists of buoyant sampling vehicle and a trawl-resistant bottom-mounted enclosure, which holds a winch, the vehicle (when not sampling), batteries, and controller. Three sampling systems are present on the vehicle, a video plankton recorder, a CTD with accessory sensors, and a suite of bio-optical sensors including Satlantic OCI-200 and OCR-200 spectral radiometers and a WetLabs ac-9 dual path absorption and attenuation meter. At preprogrammed times the vehicle is released, floats to the surface, and is then winched back into the enclosure with power and data connection maintained through the winch cable. Communication to shore is possible through a bottom cable and nearby surface telemetry buoy, equipped with a mobile

modem, giving the capability for near-real time data transmission and interactive sampling control.

### 13.2 RESEARCH ACTIVITIES

#### *AVPPO deployments*

During the first year of the contract the bio-optical sensors were successfully integrated with the rest of the systems on the AVPPO with extensive tests both on shore and in the test well on the Woods Hole Oceanographic Institution (WHOI) dock. Two deployments were made prior to October 1, 2001, with another scheduled for October 4, 2001.

The AVPPO was initially deployed during cruise CT001206 on December 8, 2000, from the R/V Connecticut at the FRONT site (40.9922 °N, -79.7332 °W) in 32 m of water. The unit functioned successfully sending back both environmental and bio-optical data after each profile. The telemetry buoy was equipped with a surface reference radiometer (Satlantic, OCI-200 sensor with Stor-Dat data logger) and single-wavelength combined absorption and optical backscattering sensor (HOBILabs,  $a-\beta_{\text{eta}}$ ). An ADCP was mounted on the AVPPO bottom enclosure. During the deployment cruise a number of radiometer casts using a Satlantic SeaWiFS Profiling Multichannel Radiometer (SPMR) were made with accompanying CTD and rosette water sample profiles. Discrete water samples were collected for determination of the concentrations of pigments (both HPLC and fluoremetric assays), suspended particulate matter (SPM), and nutrients, as well as particulate and colored dissolved organic matter (CDOM) absorption. At midday on Tuesday December 12, communications with the mooring were lost during a scheduled activity period. Meteorological conditions at the time were severe with winds in excess of 60 miles per hour. Communications were regained at the next scheduled activity, six hours later, but showed that the

controller, on the bottom-mounted enclosure, was unable to talk to all instruments on the buoyant vehicle. This continued to be the case with all subsequent activity periods. On December 19, the next available weather window and after another bad storm, the mooring was recovered during cruise CT001219. The buoyant profiler was absent with the cable severed. All other components of the system were intact. The profiler was discovered partially buried on a beach on Block Island on January 1, 2001. Some damage was apparent upon inspection of the instruments after their return to WHOI, including some scratches on the radiometer heads. All instruments were subsequently returned to the manufacturers for repair and calibration. During this deployment 47 profiles were made.

The second deployment was during cruise CT010912 on September 13, 2001 from the R/V Connecticut at a site in Massachusetts Bay (42.2423 °N, -70.5571 °W) in 44 m of water. Discrete water samples were collected from a CTD rosette for pigment and IOP measurements. The AVPPO was recovered at the end of the cruise on September 20, 2001. During this deployment 81 profiles were made.

#### *Additional Cruises*

Bio-optical data was also collected from an additional cruise, EN355 (May 31, 2001 to June 13, 2001). 11 optical stations were performed which included included; SPMR casts, CTD casts with discrete water samples for pigment and inherent optical property (IOP) measurements, absorption and attenuation profiles with ac-9's, and backscatter and absorption measurements with an  $\alpha$ -beta.

### 13.3 RESEARCH RESULTS

From the initial four day AVPPO deployment, at the FRONT site, hydrographic data from the mooring showed the regular occurrence of colder, less saline water at semi-diurnal timescales, Figure 13.1A-B. This was also apparent in the bio-optical data, from both the fluorometer, Figure 13.1C, and the IOPs from the ac-9 on the AVPPO, Figure 13.1D-F, which showed that the colder less saline water had the greatest attenuation and absorption. Decomposition of the spectral absorption measured by the ac-9, achieved by assigning characteristic shapes to algal and non-algal fractions and minimizing the sum of square deviations between predicted and observed spectra, suggested that the majority of the variability in the optical signal was due to changes in the non-algal component, Figure 13.1G-H. The non-algal slope, S, was also retrieved using the decomposition and was within the range of previously observations (mean=0.0120 nm<sup>-1</sup>, std=2.5×10<sup>-4</sup>, N=1274). The ADCP mounted on the AVPPO bottom enclosure indicated that the colder, less saline water

was associated with a southeasterly flow, Figure 2. Both a semi-diurnal and diurnal component were seen in the current measurements indicated by the greater magnitudes of the southerly flows around the middle of the days. Fourier transformation of the sea surface elevation showed the presence of M2, S2, O1, and K1 tidal harmonics.

The remote sensing reflectance from the AVPPO, an Apparent Optical Property (AOP) obtained from measurements using OC-200 radiometer heads, showed two distinct shapes most clearly seen by the ratio of 550 to 510 nm, Figure 13.3A. On all days, higher ratios were associated with colder, less saline waters and lower ratios with warmer more saline waters, Figure 13.3B. Most of the variability in the ratio appeared to be associated with variations in the non-algal component from decomposition of spectral absorption measurements, Figure 13.3C. There appeared to be little relationship with algal absorption estimates from the decomposition, Figure 13.3D.

Initial results from the Massachusetts Bay deployment again showed changes in bio-optical properties on tidal timescales, Figure 13.4. Semi-diurnal events appeared to rapidly move surface waters to depths of 35 m.

### 13.4 CONCLUSIONS

Results from the first two deployments of the AVPPO have shown the potential for a profiling mooring to study the variability associated with the complex dynamics of coastal environments including fronts. During the observation period at the FRONT site the change in hydrographic and bio-optical properties can be explained by the influx of hydrographically and optically different water from Long Island Sound on tidal timescales. The rapid change in properties is indicative of a coastal ocean front. The contiguous measurement of both IOPs and AOPs in differing water masses over short periods of time will be useful in future algorithm development and validation. The deployments also highlighted some of the difficulties of operating complex oceanographic equipment in coastal environments.

### REFERENCES

- Dupouy, C., J.P. Rebert, and D. Toure, 1986: Nimbus-7 coastal zone color scanner pictures of phytoplankton growth on an upwelling front in Senegal. In: *Marine Interfaces Ecohydrodynamics*, J.C.J. Nihoul (Ed.), Elsevier Science Pub., 617-664.
- Gallager, S. M., F. T. Thwaites, C. S. Davis, A. M. Bradley and A. Girard. 1998: Time series measurements in the coastal ocean: The Autonomous Vertically Profiling Plankton Observatory (AVPPO), *Sea Technology*.

- O'Donnell, J., 1993: Surface Fronts in Estuaries: A Review. *Estuaries*, **16**, 12-39.
- Simpson, J. H., 1981: The shelf-sea fronts: implications of their existence and behaviour. *Phil. Trans. R. Soc. Lon. A*, **302**, 531-546.
- Thwaites F. T., S. M. Gallager, C. S. Davis, A. M. Bradley, A. Girard and W. Paul. 1998: A winch and cable for the autonomous vertically profiling plankton observatory, *Proc. Oceans*, **98**.
- Ullman, D.S., and P.C. Cornillon, 1999: Satellite-derived sea surface temperature fronts on the continental shelf off the northeast U.S. coast. *J. Geophys. Res.*, **104**, 23459-23478.

*This research was supported by  
SIMBIOS NASA contract #00198*

## **PRESENTATIONS**

Morrison, J.R., Sosik, H.M., Codiga, D.L., Gallager, S.M., and Fargion, G.S., 2001: Time Series Measurements and

Algorithm Development at the FRONT Site on the New England Continental Shelf, *EOS. Trans. AGU*, 82(47), Fall Meet. Suppl., Abstract # OS52A-0525 , 2001

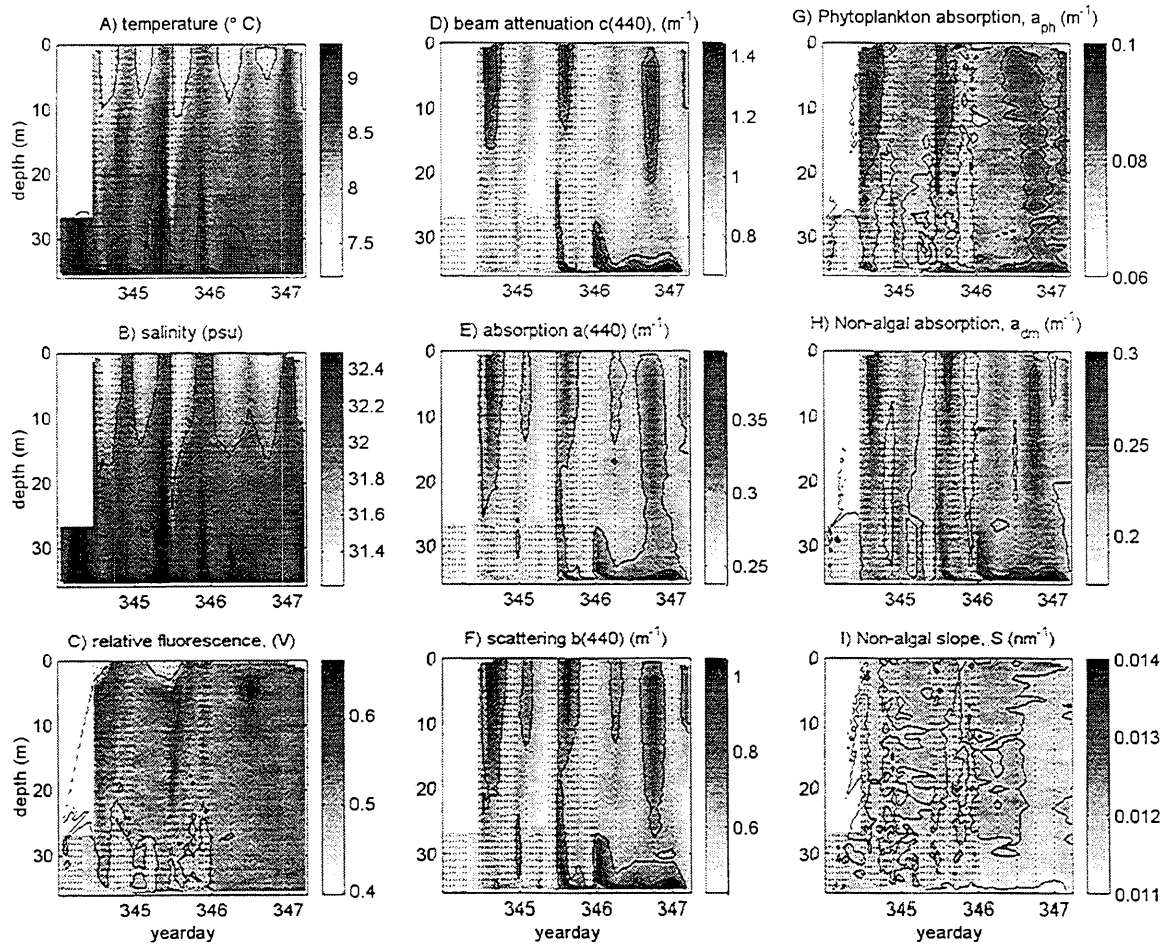


Figure 13.1: Interpolated hydrographic and bio-optical data from the first deployment of the AVPPO at the FRONT site. A and B show the semi-diurnal influx of colder, less saline waters at the surface, and C, the fluorometer output. The IOPs from the ac-9, D to F, also show semi-diurnal variation. Decomposition of the spectral absorption measured by the ac-9 suggested that the majority of the variability in the optical signal was due to changes in the non-algal component, G and H (absorption values are at 440 nm). The non-algal slope was also retrieved, I. Black dots indicate measurement positions used for the interpolations.

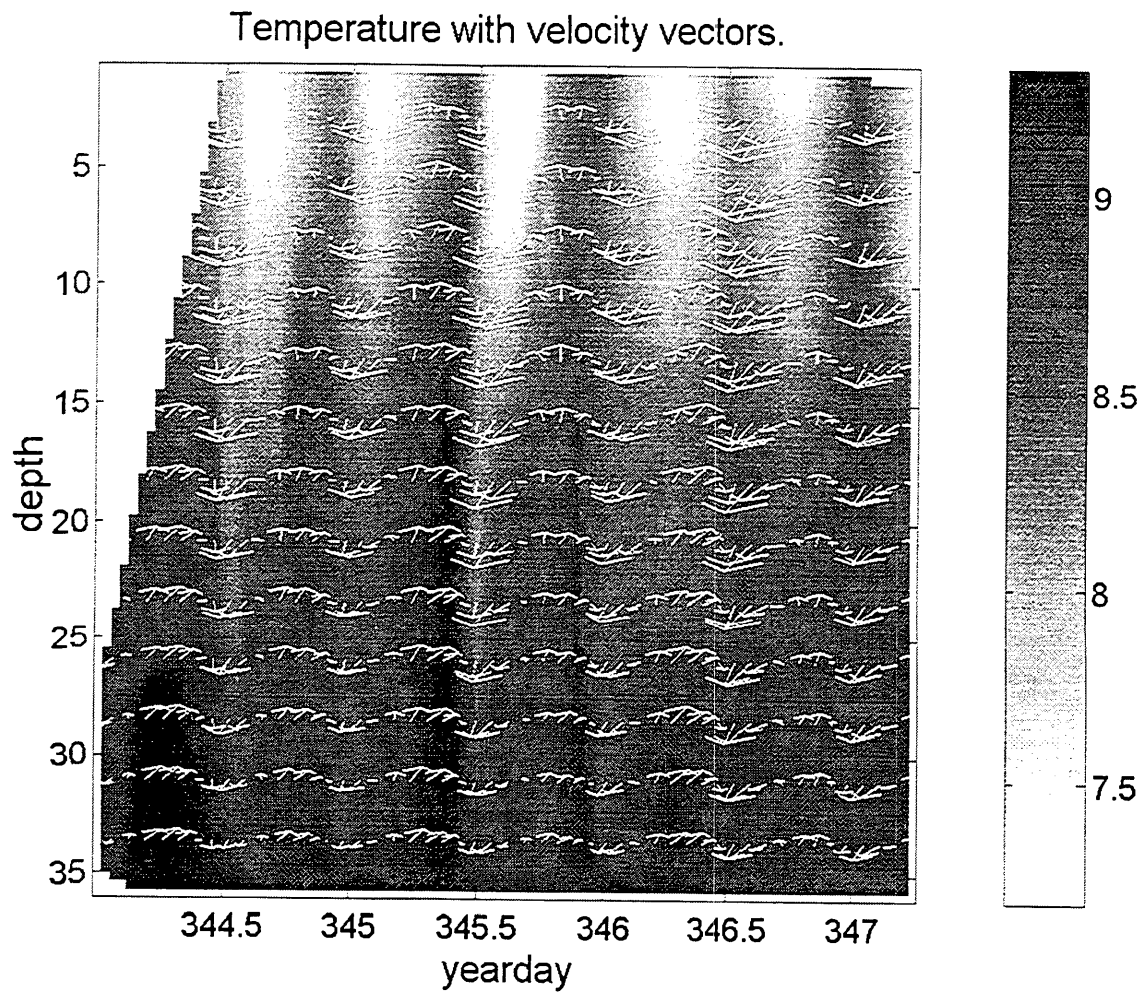


Figure 13.2: Current vectors (white arrows), measured using the ADCP mounted on the AVPPO bottom enclosure, superimposed upon interpolated temperature data indicated that the colder less saline water was associated with a southeasterly flow.

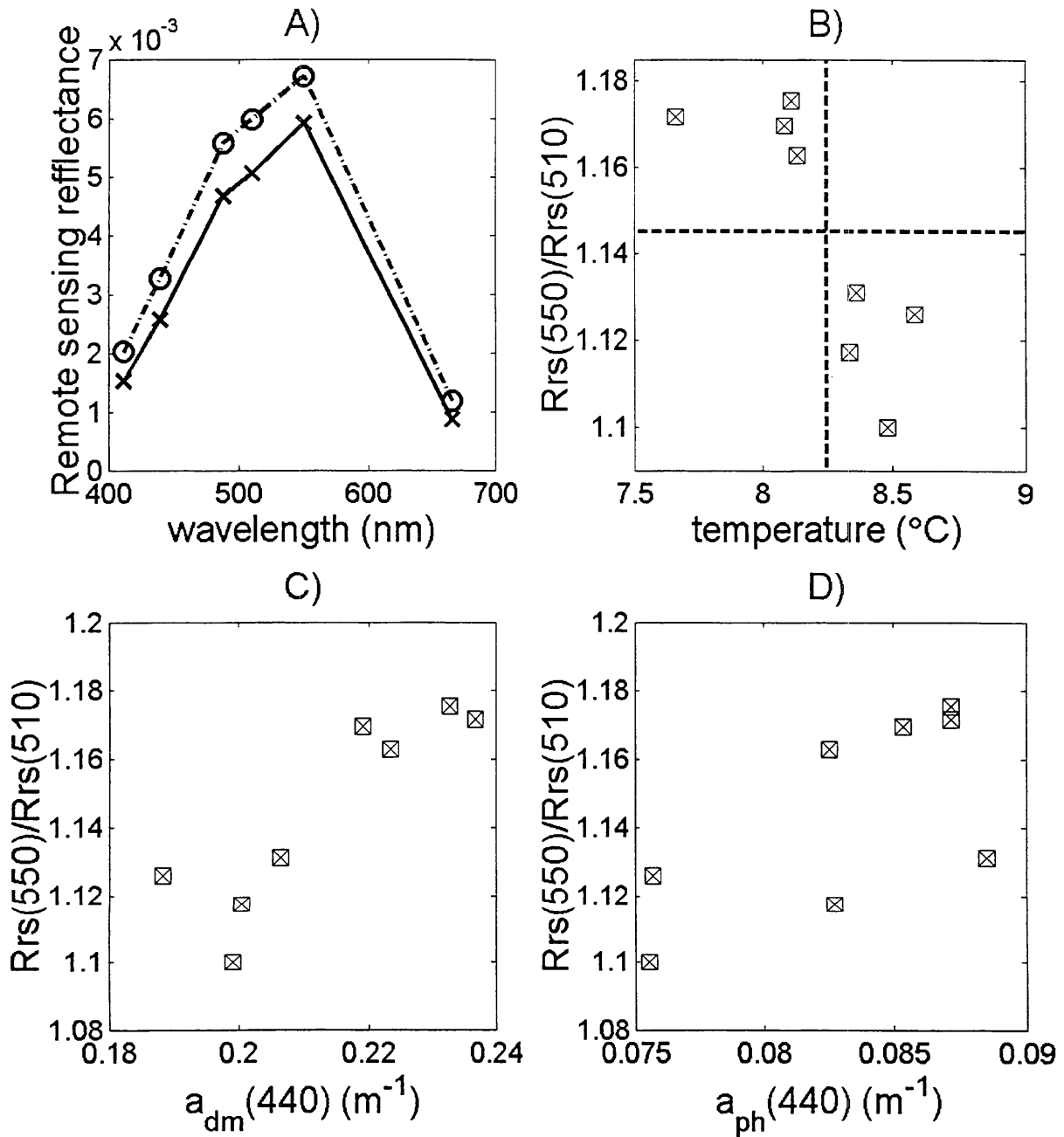


Figure 13.3: The remote sensing reflectance from the AVPPO showed two distinct shapes associated with 'cold', x with solid line, and 'warm' waters, o with dot-dashed line, A. On all days, higher ratios of the ratio of remote sensing reflectances at 550 to 510 nm were associated with colder less saline waters and lower ratios with warmer more saline waters, B. The relationships of the 550 to 510 ratio with the non-algal,  $a_{dm}$ , C, and phytoplankton,  $a_{ph}$ , absorptions.

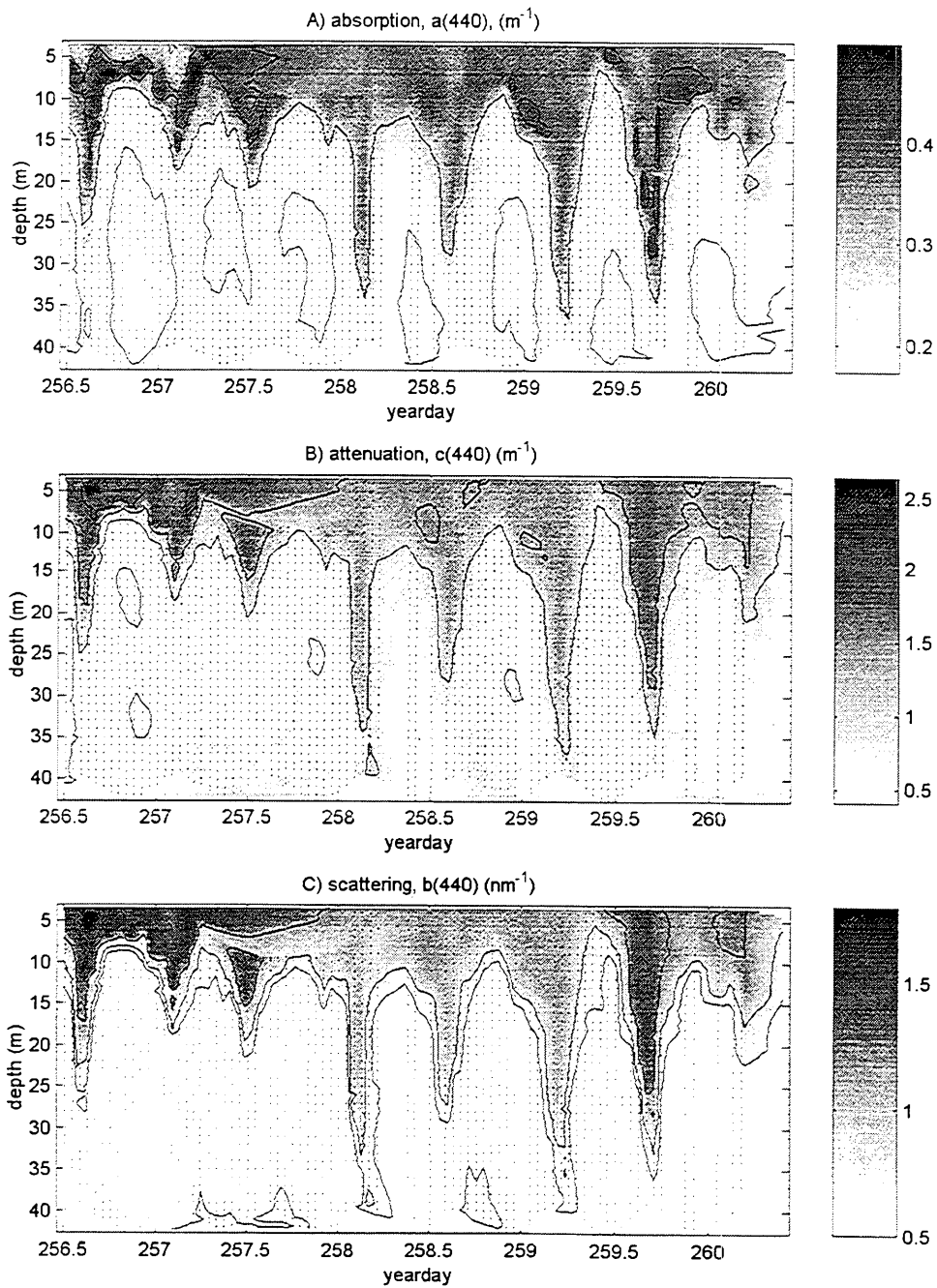


Figure 13.4: Interpolated Inherent Optical Properties from the AVPPO ac-9 from the Massachusetts Bay deployment show a semi-diurnal movement to depth of surface waters, A to C. Black dots indicate measurements positions used for the interpolations.

## Chapter 14

# Ocean Optics Protocols and SIMBIOS Protocol Intercomparison Round Robin Experiments (SPIRREX).

James L. Mueller

*Center for Hydro-Optics and Remote Sensing, San Diego State University, California*

### 14.1 INTRODUCTION

The objective of research under this contract is the maintenance and annual revision of the document "Ocean Optics Protocols for Satellite Ocean Color Validation (e.g. Fargion and Mueller 2000).

### 14.2 RESEARCH ACTIVITIES

The research activities under the first year of this contract were devoted to the preparation of "Ocean Optics Protocols for Satellite Ocean Color Validation, Revision 3" (Mueller et al. 2002), building on Revision 2 (Fargion and Mueller 2000). The important updates, additions and revisions in the Revision 3 document are summarized in the next section.

### 14.3 RESEARCH RESULTS

Revision 3 to the ocean optics protocol document (Mueller et al. 2002) comprises several significant changes compared to Revision 2 (Fargion and Mueller 2000). The most obvious of these are 3 new chapters, and the resulting renumbering of the other chapters to reflect the new insertions in the document. The new chapters are:

Chapter 2, "Fundamental Definitions, Relationships and Conventions", introduces the radiometric quantities, inherent optical properties, fundamental concepts and terminology underlying the *in situ* measurement and analysis protocols discussed throughout the document. The chapter also discusses the scales adopted in these protocols for such quantities as extraterrestrial solar irradiance, and the absorption and scattering coefficients of pure water.

Chapter 11, "MOBY, A Radiometric Buoy for Performance Monitoring and Vicarious Calibration of Satellite Ocean Color Sensors: Measurement and Data Analysis Protocols", by Clark et al, was added to document the specific measurement and data analysis protocols used in the operation of this critical radiometric observatory. The MOBY normalized water-leaving radiance time series has provided

the principal, common basis for vicarious calibration of satellite ocean color sensors. The material in Chapter 11 is provided background information essential for investigators combining MOBY and satellite sensor data for validation studies.

Chapter 13, "Normalized Water-Leaving Radiance and Remote Sensing Reflectance: Bidirectional Reflectance and Other Factors", by Morel and Mueller, explains the physics underlying the bidirectionality of the ocean's reflectance and water-leaving radiance. An outline is then presented describing the general methods for accounting for and removing bidirectional effects from exact normalized water-leaving radiance, together with a simplified method of its determination for Case 1 waters using lookup tables that are available on-line over the INTERNET. The information in this chapter is critical, because the only form of water-leaving radiance that allows a valid match-up comparison between satellite and *in situ* determinations is exact normalized water-leaving radiance.

Several of the renumbered chapters carried over from Revision 2 were significantly revised, while others were modified only slightly. The overviews of instrument characteristics and associated characterization methods (Chapter 4) and field measurements and data analysis (Chapter 9) were revised to reflect the changed content of the more detailed chapters in those two parts of the document. Chapter 15, was revised to provide more focused protocols for spectrophotometric determinations of absorption by particles and dissolved materials in seawater samples, citing the workshop results presented in the Revision 2 version where needed. The chapters describing methods for HPLC measurements of phytoplankton pigments (Chapter 16) and fluorometric chlorophyll a (Chapter 17) were updated and revised. The procedures for calibrating and characterizing radiometers (Chapter 6) were modified to clarify the procedural details. Methods for calibrating and using, sun photometers and sky radiance instruments (Chapters 7 and 14) were also revised, but will require further updates in Revision 4. The remaining chapters were also edited for consistency, but the substance of these chapters remains intact.

## 14.4 FUTURE WORK

Some of the deficiencies and corrective steps that will be taken in Revision 4, scheduled for completion in 2002, include: Protocols for instrument calibration and methods of measurement and analysis for inherent optical properties (IOP), which are currently summarized briefly in Chapters 4 and 9, will be addressed in a new chapter in Revision 4.

Another new chapter will be added to Revision 4 describing protocols for radiometric and bio-optical measurements from moored and drifting buoys. These methods will differ in many respects from the specialized MOBY vicarious calibration observatory (Chapter 11 of Revision 3), because of the different objectives and deployment circumstances associated with these types of buoys.

Protocols for radiometric measurements from aircraft, although mentioned in the Revision 3 protocols, are not provided in any detail. A new chapter on this topic will be included in Revision 4.

Existing chapters will also be revised. Chapter 6, for example, will be revisited and updated to develop a strategy for moving the SIMBIOS community to calibrations based on the NIST 2000 detector based scale of spectral irradiance, and the consequences and importance of NIST Spectral Irradiance

and Radiance responsivity Calibrations with Uniform Sources (SIRCUS) facility. Other examples of planned revisions include the expansion of Chapter 2 to include atmospheric radiometric quantities and processes relevant to ocean color, and additions to Chapter 10 to address extrapolation of in-water profiles of upwelled radiance to the sea surface.

## ACKNOWLEDGEMENTS

This research was supported under SIMBIOS NASA Contract Number 00199.

## REFERENCES

- Fargion, G.S. and J.L. Mueller, 2000: Ocean Optics Protocols for Satellite Ocean Color Sensor Validation, Revision 2, NASA TM 2001-209955, NASA Goddard Space Flight Center, Greenbelt, Maryland, 184 pp.
- Mueller, J.L., et al., 2002: Ocean Optics Protocols for Satellite Ocean Color Sensor Validation, Revision 3, NASA TM 2002-TBD, Mueller, J.L. and G. Fargion (Eds.), NASA Goddard Space Flight Center, Greenbelt, Maryland, (In Press).

## Chapter 15

# Bermuda Bio Optics Project

Norm Nelson

*Institute for Computational Earth Science, UCSB, Santa Barbara, California*

### 15.1 INTRODUCTION

The Bermuda BioOptics Project (BBOP) is a collaborative effort between the Institute for Computational Earth System Science (ICESS) at the University of California at Santa Barbara (UCSB) and the Bermuda Biological Station for Research (BBSR). This research program is designed to characterize light availability and utilization in the Sargasso Sea, and to provide an optical link by which biogeochemical observations may be used to evaluate bio-optical models for pigment concentration, primary production, and sinking particle fluxes from satellite-based ocean color sensors. The BBOP time-series was initiated in 1992, and is carried out in conjunction with the U.S. JGOFS Bermuda Atlantic Time-series Study (BATS) at the Bermuda Biological Station for Research. The BATS program itself has been observing biogeochemical processes (primary productivity, particle flux and elemental cycles) in the mesotrophic waters of the Sargasso Sea since 1988. Closely affiliated with BBOP and BATS is a separate NASA-funded study of the spatial variability of biogeochemical processes in the Sargasso Sea using high-resolution AVHRR and SeaWiFS data collected at Bermuda (N. Nelson, P.I.). The collaboration between BATS and BBOP measurements has resulted in a unique data set that addresses not only the SIMBIOS goals but also the broader issues of important factors controlling the carbon cycle.

### 15.2 RESEARCH ACTIVITIES

BBOP personnel participate on all BATS cruises, which are conducted monthly with additional cruises during the spring bloom period, January through May. Table 15.1 contains a list of data products relevant to SIMBIOS. The BBOP project collects continuous profiles of apparent optical properties (AOPs) in the upper 200m and deployments are planned to optimize match-ups with the BATS primary production incubations and with SeaWiFS overpasses. In 1999, a free-falling Atlantic profiling radiometer system (SPMR/SMSR s/n 028) became our primary profiling

instrument. The primary optical measurements are downwelling vector irradiance and upwelling radiance,  $E_d(z,t,\lambda)$  and  $L_u(z,t,\lambda)$ , respectively. Derived products include remote sensing reflectance ( $R_{rs}(z,\lambda)$ ) and down- and upwelled attenuation coefficients ( $K_d(z,\lambda)$ ,  $K_u(z,\lambda)$ ). The sampling package also includes a second mast-mounted radiometer with wavebands matching those on the underwater instrument for measuring incident downwelling vector irradiance,  $E_d(0^+,t,\lambda)$ . This system was upgraded to 11 channels in 2000, and both instruments are calibrated three times annually at UCSB. The profiler also includes a WetStar fluorometer and Ocean Sensors CTD sensors. Its cable was recently replaced after three years of service.

Bottle samples for fluorometric chlorophyll-*a* and inherent optical properties (IOPs) are also collected. Chlorophyll-*a* is collected once or twice daily during each cruise. Discrete samples for determining the absorption spectra of particulates,  $a_{ph}(z,\lambda)$  and  $a_d(z,\lambda)$ , and CDOM ( $a_g(z,\lambda)$ ) are collected according to Nelson *et al* (1998). Particulate absorption spectra are determined using the quantitative filter technique (Mitchell, 1990) and CDOM absorption according to Nelson *et al* (1998). Hyperspectral observations of above water  $R_{rs}^+(\lambda)$  are collected using the Analytical Spectral Devices FieldSpec spectrometer (ASD, Boulder CO). This instrument has begun experiencing problems during the past year, most likely due to exposure to corrosive salt spray at sea.

### 15.3 RESEARCH RESULTS

Careful attention to instrument behavior and calibration is crucial to assuring high quality time-series data. We have continued our efforts to determine the long-term calibration behavior of our SPMR systems (sn028, owned by BBSR and sn039, owned by BBOP) using several lamps traceable to our

own NIST standard. Our past experience with radiometric calibrations has shown that calibration coefficients used in the field should be averages of many calibrations using several different lamps (O'Brien *et al.*, in press). We now have more than 2 years of calibration data for SPMR-028 (one year in its current configuration), and can begin to assess the long-term variability of some of its channels. Figure 15.1 shows the normalized calibration coefficients for several channels on one irradiance head (SPMR system sn028, irradiance head 058), including calibrations at both UCSB and Satlantic. Calibration coefficients for most channels are within 3%, and many are within 1%, even when comparing calibrations at different laboratories. Not shown are two of the UV channels (325 and 340nm), which often differ from the norm by as much as 25%. Both irradiance and radiance heads have had these two sensors replaced at least once since 1999. Since lamp output is quite low in the UV, calibration results in this range are extremely difficult to replicate, and it is not always clear whether differences between individual calibrations are due to sensor degradation or simply to lamp variability. The growing lack of sensitivity in the UV channels may also be due to degradation of the cosine collector material (S. McLean, pers. comm.). In addition, there has been some variability in the behavior of our NIST standard, which must be resolved before long-term averages can be computed (D. Menzies, pers. comm.). Hence, all of our SPMR data submitted to date have been processed using a single recent calibration rather than an average, and will be updated when we can more accurately describe the behavior of both the sensors and lamps, especially in the UV. In March of 2001, the effects of immersion on both our SPMR irradiance sensors were measured at CHORS. We found significant differences between the measured and factory-supplied immersion coefficients, and between the immersion responses of the two instruments. As expected, the values provided by the factory agreed well with CHORS measurements in the red and green parts of the spectrum, (within ~5%). In the blue and UV portions, the two differed by as much as 20%. At wavelengths less than 380nm, the two instruments showed large differences between their responses, and only fair reproducibility (data not shown). After application of the new immersion coefficients,  $R_{rs}0$  values measured with SPMR-028 agreed fairly well with those from with MER-8733, for which immersion coefficients were measured in 1998 (Figure 15.2). The peak in the reflectance spectrum at 380 (Fig. 15.2b) and the unexpected difference between the SPMR 028 and 039 spectra indicate that our immersion coefficients may still be in error in the UV, and that these measurements may need to be repeated.

We are continuing to examine the relationships between retrieved chlorophyll *a* from SeaWiFS imagery and *in situ* factors controlling optical properties, particularly chlorophyll *a* and CDOM. One interesting result of this time series is that

SeaWiFS consistently overestimated *in situ* chlorophyll *a* during the summer months of 1998 and 2000, but agreed well in 1999 (Fig. 15.3a). An *in situ* explanation for this phenomenon could be that unusually high CDOM concentrations were present at the surface in 1998 and 2000, leading to lower blue reflectance values. However, radiometric data (Fig. 15.3b-d) indicates that the algorithm is actually responding to overly high green reflectances, which suggests that the atmospheric correction is at least partially responsible. The mid-latitude Sargasso Sea is subject to large inputs of Saharan dust during the summer, and our current working hypothesis is that inter-annual variability non-standard aerosol spectra due to dust are responsible for the varying skill of the SeaWiFS chlorophyll retrieval.

Another focus of our work this year has been the dynamics of chromophoric dissolved organic matter (CDOM), which influences ocean color by way of its influence on absorption of blue and ultraviolet light, and is an important intermediate in climate-relevant photochemical reactions. Using global data from SeaWiFS, we have evaluated, for the first time, the global time/space distribution of colored dissolved organic materials or CDOM (Siegel *et al.*, in press). With these new data, we have shown that open ocean CDOM distributions are not created from run-off of terrestrial materials, but by local oceanic processes. Working with other SIMBIOS researchers and their data sets, we also have shown that CDOM makes the dominant contribution to blue light absorption in the global ocean indicating that the problem of the contribution of CDOM to ocean color is greater than had been expected (Siegel *et al.* in prep).

We have continued our field and laboratory work on the (biological) sources and (physical) sinks of CDOM in the Sargasso Sea, with additional NSF support. Ship time from these investigations has allowed us to make a section of in-water optical properties and CDOM from the BATS site south to 25N (Fig. 15.4); these additional data will be contributed to SeaBASS. Our research in this area also includes developing a method for retrieving quantum yield spectra for photochemical reactions from field measurements of irradiance spectra, absorption coefficient spectra of CDOM, and *in situ* photochemical production rates. This new capability will enable us to branch out to study a large number of global biogeochemical problems including the light-induced cycling of carbon monoxide and dimethyl sulfide (both important tropospheric trace gases).

## REFERENCES

- Mitchell, B.G., 1990: Algorithms for determining the absorption coefficient for aquatic particles using the

quantitative filter technique. *Ocean Optics X*, Siegel, D.A., S. Maritorena, N. B. Nelson, D.A. Hansell and M. Lorenzi-Kayser, (In press): Global ocean distribution of colored dissolved and detrital materials. *Journal of Geophysical Research*.

O'Brien, M.C., D.W. Menzies, D.A. Siegel, and R.C. Smith, (In Press): Long-Term Calibration History of Several Marine Environmental Radiometers (MERs). NASA Tech. Memo, SeaWiFS Postlaunch Calibration and Validation Analyses, Part 3, Chap. 4.

D.A. Siegel, S. Maritorena, B.G. Mitchell, N.B. Nelson, H.M. Sosik, J.R. Morrison, K.L. Carder, M. Kahru, J. Wieland, B. Langston. (In prep) Dominance of Colored Dissolved Organic Material in Determining Light Availability in the Sea. for *Limnol. & Oceanogr.*

Nelson, N.B., D.A. Siegel, and A.F. Michaels, 1998: Seasonal dynamics of colored dissolved material in the Sargasso Sea, *Deep Sea Research I*, **45**, 931-957.

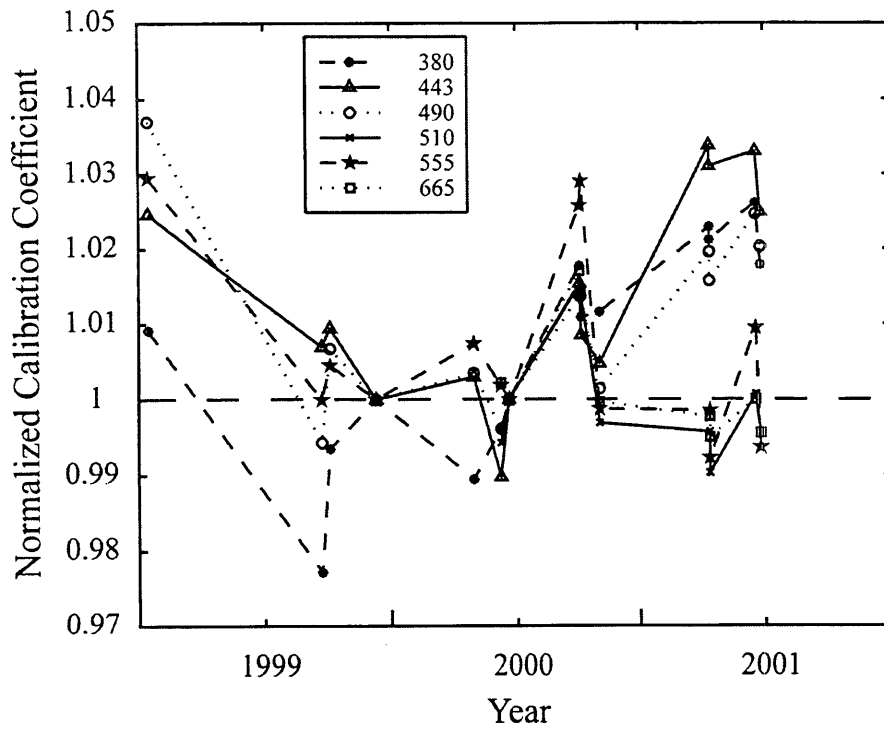


Figure 15.1: Calibration history for SPMR system sn028, Irradiance head sn058, low gain.

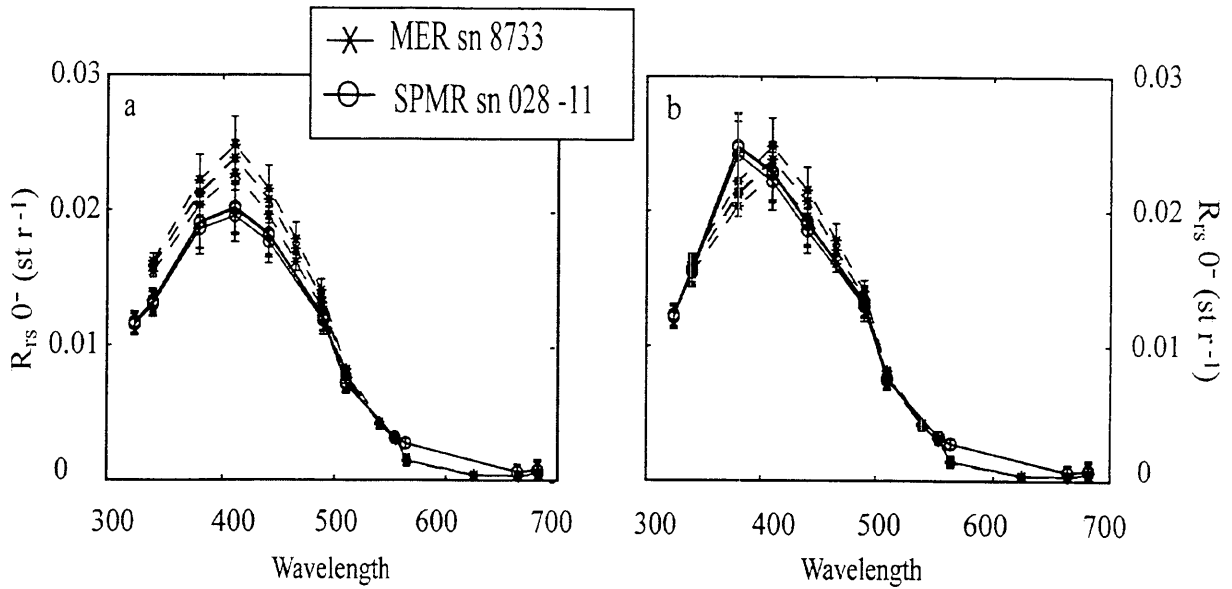


Figure 15.2: Comparison of average remote sensing reflectance ( $L_w/E_d$ ) in the top 20m from the BBOP Biospherical MER-2040 s/n 8733 (x), and the BBSR Atlantic SPMR s/n 028 (o), during July 2000. a) Using factory-supplied immersion coefficients for SPMR s/n 028, b) using immersion coefficients for SPMR s/n 028 measured at CHORS, March 2001.

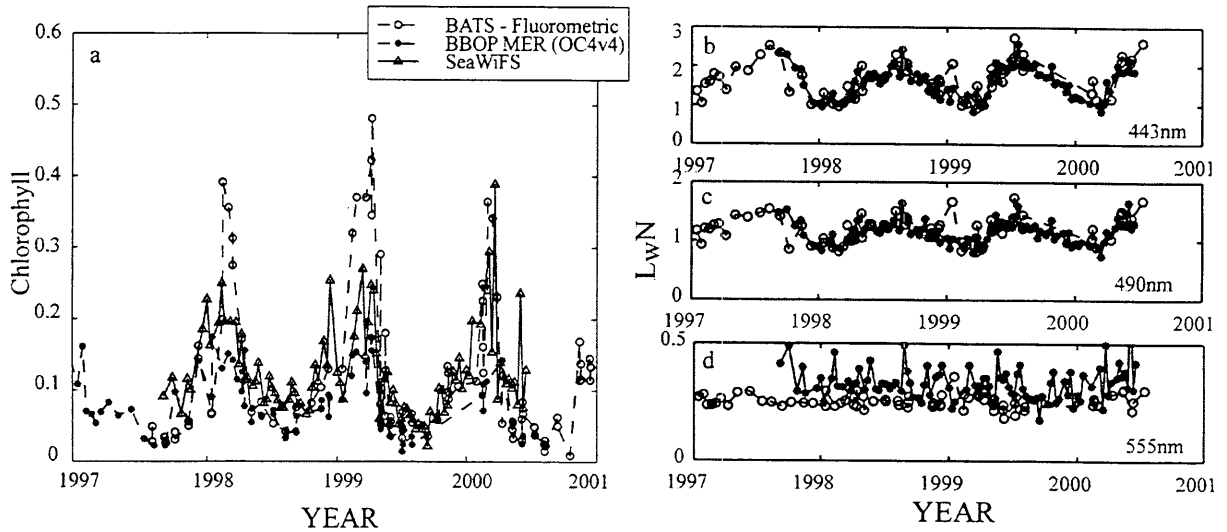


Figure 15.3: a) bottle fluorometric Chlorophyll-a samples compared to field radiometric data converted to Chlorophyll using OC4v4 and SeaWiFS Chlorophyll-a (8-day averages). b-d) time series of  $L_wN$  at 443, 490 and 555nm measured by BBOP and SeaWiFS.

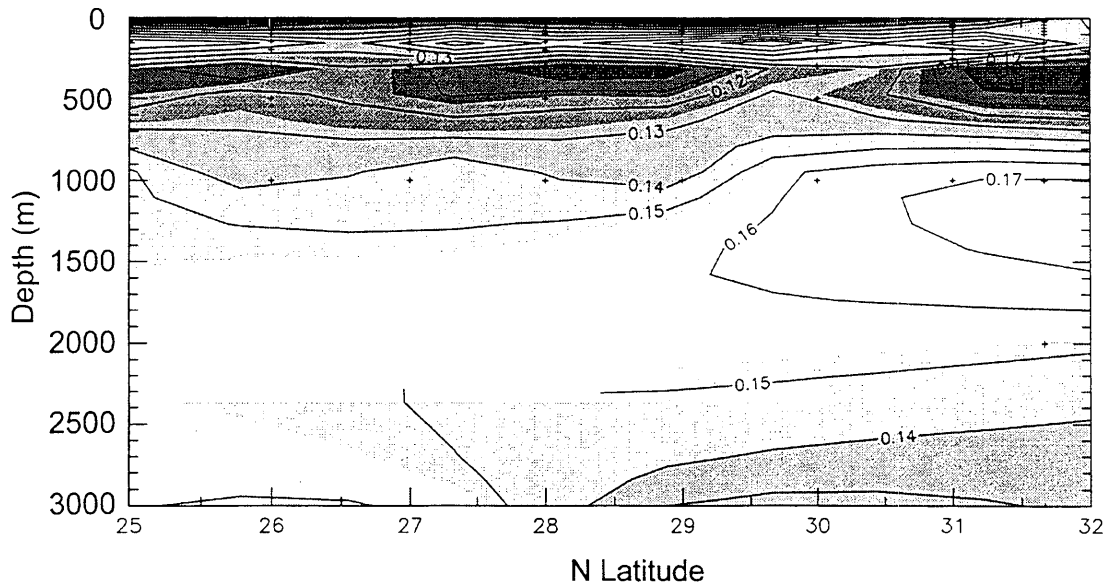


Figure 15.4:  $a_g$  (325nm),  $m^{-1}$  Section along the 64°40'W line from the BATS site (31°40'N) to 25°N, August 2001. This plot shows the surface minimum and subsurface maximum of CDOM demonstrated by Nelson et al. (1998) extending across the whole Sargasso Sea system. Also apparent are a gyre-wide minimum present in the subtropical mode water (250-500m).

TABLE 15.1: A PARTIAL LIST OF MEASUREMENTS MADE BY BBOP & BATS

BBOP Direct Measurements and Primary Derived Products :

$E_d(z,\lambda)$	Downwelling vector irradiance (325, 340, 380, 412, 443, 488, 510, 555, 565, 665 & 683 nm)
$E_d(0^+, \lambda)$	Incident irradiance (325, 340, 380, 412, 443, 488, 510, 555, 565, 665 & 683 nm)
$L_u(z,\lambda)$	Upwelling radiance (325, 340, 380, 412, 443, 488, 510, 555, 565, 665 & 683 nm)
chl-fl(z)	Chlorophyll fluorescence with a WetStar fluorometer
T(z) & S(z)	Temperature and conductivity with Ocean Sensors probes (calibrations by Satlantic)
$a_{tp}(\lambda)$	Particulate absorption spectrum by QFT
$a_d(\lambda)$	Detrital particle absorption spectrum by MeOH extraction
$a_{ys}(\lambda)$	Colored dissolved absorption spectrum
chl-a(z)	Discrete chlorophyll <i>a</i> determinations via Turner fluorometry
$L_{wN}(\lambda)$	Normalized water leaving radiance (325, 340, 380, 412, 443, 488, 510, 555, 565, 665 & 683 nm)
$R_{RS}(0^-, \lambda)$	In-water remote sensing reflectance (325, 340, 380, 412, 443, 488, 510, 555, 565, 665 & 683 nm)
$K_d(z,\lambda)$	Attenuation coefficient for $E_d(z,\lambda)$ (325, 340, 380, 412, 443, 488, 510, 555, 565, 665 & 683 nm)
$K_l(z,\lambda)$	Attenuation coefficient for $L_u(z,\lambda)$ (325, 340, 380, 412, 443, 488, 510, 555, 565, 665 & 683 nm)
$R_{RS}(0^+, \lambda)$	Above-water remote sensing reflectance (350 to 1050 nm)
$a_{ph}(\lambda)$	Phytoplankton absorption spectrum (= $a_p(\lambda) - a_{det}(\lambda)$ )
<PAR(z)>	Daily mean photosynthetically available radiation at depths of the <i>in situ</i> $C^{14}$ incubations

U.S. JGOFS BATS (NSF) and Related Biogeochemistry Sampling Programs

Primary Production ( <i>in situ</i> $^{14}C$ incubation)	Sinking flux (sediment trap array)
Phytoplankton pigments (fluorometric & HPLC)	Nutrients ( $NO_3+NO_2$ , $SiO_4$ , $PO_4$ )
$CO_2$ system (alkalinity, $TCO_2$ and $pCO_2$ )	Continuous atmosphere & surface $pCO_2$
Dissolved oxygen (continuous & discrete)	Zooplankton biomass & grazing
POC & PON (POP infrequently)	DOC & DON (DOP infrequently)
Full water column, WOCE-standard CTD profile	Bacterial abundance and rates
Phytoplankton abundance by flow cytometry	Coccolithophore abundance
Validation spatial cruises (5 days, 4cruises/year)	Deep ocean sediment sinking rates

*This research was supported by  
the SIMBIOS NASA contract # 00200*

## PEER REVIEWED PUBLICATIONS

- Behrenfeld, M.J., E. Marañón, D.A. Siegel and S.B. Hooker, 2001: Modeling oceanic primary production: Photoacclimation and nutrient effects on light-saturated photosynthesis. In press *Marine Ecology Progress Series*.
- Dickey, T., S. Zedler, D. Frye, H. Jannasch, D. Manov, D. Sigurdson, J. D. McNeil, L. Dobeck, X. Yu, T. Gilboy, C. Bravo, S. C. Doney, D.A. Siegel and N. Nelson, 2001: Physical and biogeochemical variability from hours to years at the Bermuda Testbed Mooring: June 1994 - March 1998. *Deep Sea Research, II*, **48**, 2105-2140.
- Mitchell, B.G. and others including N. Nelson 2000: Determination of spectral absorption coefficients of particles, dissolved material, and phytoplankton for discrete water samples. In: *Ocean Optics Protocols for Satellite Ocean Color Sensor Validation, Revision 2*, eds. G.S. Fargion and J.L. Mueller, NASA TM2000209966.
- Nelson, N.B. and D.A. Siegel. (In Press): Chomophoric DOM in the Open Ocean: Biogeochemistry of Marine Dissolved Organic Matter, Edit by D. A. Hansell and C. A. Carlson.
- Nelson, N.B., N.R. Bates, D.A. Siegel, and A.F. Michaels, 2001: Spatial variability of the CO<sub>2</sub> sink in the Sargasso Sea. *Deep-Sea Research, Part II*. **48**, 1801-1821.
- O'Brien, M.C., D.W. Menzies, D.A. Siegel, and R.C. Smith, (In Press): Long-Term Calibration History of Several Marine Environmental Radiometers (MERs). NASA Tech. Memo, SeaWiFS Postlaunch Calibration and Validation Analyses, Part 3, Chap. 4.
- Siegel, D.A. 2001: Oceanography - The Rossby rototiller. *Nature*, **409**, 576-577.
- Siegel, D.A., S. Maritorena, N. B. Nelson, D.A. Hansell and M. Lorenzi-Kayser, (In press): Global ocean distribution of colored dissolved and detrital materials. *Journal of Geophysical Research*.
- Siegel, D.A., D.M. Karl and A.F. Michaels 2001: Interpretations of biogeochemical processes from the U.S. JGOFS Bermuda and Hawaii time series sites. *Deep-Sea Research, Part II*. **48**, 1403-1404.
- Siegel, D.A., N.B. Nelson, M.C. O'Brien, T.K. Westberry, J.R. Morrison, A.F. Michaels, E.A. Caporelli, J.C. Sorensen, S.A., Garver, E.A. Brody, J. Ubante and M.A. Hammer, 2001: The Bermuda BioOptics Project: Bio-optical modeling of primary production from space-sensible variables. *Deep Sea Research, II*, **48**, 1865-1896.
- Siegel, D.A., M. Wang, S. Maritorena and W. Robinson. 2000: Atmospheric correction of satellite ocean color imagery: the black pixel assumption. *Applied Optics*, **39**, 3582-2591.
- Sorensen, J.C., and D.A. Siegel 2001: Variability of the effective quantum yield for carbon assimilation in the Sargasso Sea. *Deep-Sea Research, Part II*. **48**, 2005-2035.
- Toole, D.A., and D.A. Siegel, (In press): Modes and mechanisms of ocean color variability in the Santa Barbara Channel. *Journal of Geophysical Research*.

## SUBMITTED

- Maritorena, S., D.A. Siegel and A.R. Peterson: Optimal tuning of a semi-analytical model for global applications. Submitted to *Applied Optics*.
- Westberry, T.K., and D.A. Siegel: Natural fluorescence variability in the Sargasso Sea. Submitted to *Deep-Sea Research, Part I*.

## PRESENTATIONS

- Armstrong, R.A., and D.A. Siegel, 2001: A large cachement area for sediment traps is not incompatible with sharply defined patterns of benthic deposition. Oral presentation made at the 2001 ASLO Aquatic Sciences Meeting in Albuquerque, NM, February 2001.
- Najjar, R., O. Zafiriou, G. Cutter, R. Kieber, and N. Nelson 2001: A model of diurnal and seasonal variations of carbon monoxide, carbonyl sulfide, and hydrogen peroxide in Sargasso Sea surface waters. ASLO Aquatic Sciences Meeting in Albuquerque, NM, February 2001

- Nelson, N.B. and A.J. Scott 2001: Light energy availability for photochemistry in the Sargasso Sea on seconds to seasons time scales. ASLO Aquatic Sciences Meeting in Albuquerque, NM, February 2001.
- Siegel, D.A., 2000: Gelbstoff, Gilvin and Chromophoric Dissolved Organic Material: Distribution, Dynamics and Implications. Presented at the Department of Marine Chemistry and Geochemistry, Woods Hole Oceanographic Institution. Woods Hole, MA., Oct. 17, 2000.
- Siegel, D.A., 2001: Global distribution and dynamics of chromophoric dissolved organic matter: Implications for marine photochemistry. Invited presentation made at the 2001 ASLO Aquatic Sciences Meeting in Albuquerque, NM, February 2001.
- Siegel, D.A., 2001: Gelbstoff, Gilvin and Chromophoric Dissolved Organic Material: Distribution, Dynamics and Implications or Love That Dirty Water!! Presented to the Biological Sciences Department, University of Southern California. Los Angeles, CA., Apr. 11, 2001.
- Siegel, D.A., 2001: Distribution and Dynamics of Chromophoric Dissolved Organic Material: Implications for Marine Photochemistry. Presented at the NASA Ocean Color Science Team Workshop. San Diego, CA., May 24, 2001.
- Siegel, D.A., 2001: Satellite views of the North Atlantic Spring Bloom. Presented at the U.S. JGOFS Synthesis and Modeling Program Workshop. Woods Hole, MA., July 18, 2001.
- Toole, D.A., D.A. Siegel and J.W. Dacey, 2001: Modeling of upper ocean biogenic sulfur cycling in the Sargasso Sea. Poster presented at the 2001 ASLO Aquatic Sciences Meeting in Albuquerque, NM, February 2001.
- Westberry, T.K., and D.A. Siegel, 2001: Phytoplankton natural fluorescence in the Sargasso Sea: Prediction of primary production rates or an index for eddy induced nutrient fluxes. Oral presentation made at the 2001 ASLO Aquatic Sciences Meeting in Albuquerque, NM, February 2001.

## Chapter 16

# Plumes and Blooms: Modeling the Case II Waters of the Santa Barbara Channel

D.A. Siegel, S. Maritorena and N.B. Nelson

*Institute for Computational Earth System Science, University of California, Santa Barbara, California*

### 16.1 INTRODUCTION

The goal of the Plumes and Blooms (PnB) project is to develop, validate and apply to imagery state-of-the-art ocean color algorithms for quantifying sediment *plumes* and phytoplankton *blooms* for the Case II environment of the Santa Barbara Channel. We conduct monthly to twice-monthly transect observations across the Santa Barbara Channel to develop an algorithm development and product validation data set. The PnB field program started in the summer of 1996. At each of the 7 PnB stations, a complete verification bio-geo-optical data set is collected. Included are redundant measures of apparent optical properties (remote sensing reflectance and diffuse attenuation spectra), as well as *in situ* profiles of spectral absorption, beam attenuation and backscattering coefficients. Water samples are analyzed for component *in vivo* absorption spectra, fluorometric chlorophyll, phytoplankton pigment (by the SDSU CHORS laboratory), inorganic nutrient and biogenic and lithogenic silica concentrations (Table 16.1). We are also in the process of developing quality assurance procedures for optical data sets to assess complimentary optical property determinations. Our goal is to use the PnB field data set to objectively tune semi-analytical models of ocean color for this site and apply them using available satellite imagery (SeaWiFS and MODIS). In support of this goal, we have also been addressing SeaWiFS ocean color and AVHRR SST imagery (Otero et al., 2001). We also are using the PnB data set to address time/space variability of water masses in the Santa Barbara Channel and its relationship to the 1997/1998 El Niño and have been active in various outreach activities (see below).

### 16.2 RESEARCH ACTIVITIES

The big issue we have had to overcome was the loss of the *R/V Ballena* in November 2000. The *Ballena* capsized and was lost after when a rogue wave broke over her wheelhouse

in shallow water north of Pt. Conception. No one was hurt and it was not during a PnB cruise. We have continued the PnB field program now leasing time on a small boat, *The Spirit*. Our partnership with the Channel Islands National Marine Sanctuary (CINMS) provides sea time on the *Ballena* as a match where we provide them a research focus. The loss of *Ballena* has resulted in a large uncosted expense for the PnB project and huge hassles for the PnB staff to overcome. Many of our operations have had to be cutback due to the limited capability of the *Spirit*. For example, we could not use our SeaBird 911+ CTD/rosette system and had to hang bottles on wire rope. This results in reduced CTD data quality and more work at sea. We have been assured by CINMS that a replacement vessel will be in place by the summer of 2002. Funds for a new research vessel are in place and we have had extensive input in this process. Issues with the *Ballena* aside, the PnB project has had a very successful field year. We have conducted 16 one-day cruises since November 2000 and have completed nearly 100 stations. Nearly 200 discrete samples have been collected and HPLC samples have been sent to SDSU for analysis. All data have been submitted successfully to the SeaBASS system once they have been analyzed. We have also incorporated the PnB data set in the global AOP/IOP data set being compiled by Maritorena on his SIMBIOS project and have provided it to Jay O'Reilly for his algorithm work. The PnB project has also participated in two cruises on the *R/V Pt. Sur* in support of the Santa Barbara Channel Long Term Ecological Research (LTER) study ([sbc.lternet.edu/](http://sbc.lternet.edu/)). We expect this collaboration to continue through the lifespan of the PnB program. We have continued our acquisition and analysis of satellite ocean color (SeaWiFS) and thermal imagery (AVHRR) from the UCSB HRPT ground station (HUSC). The UCSB ground station is supported by SIMBIOS, NSF and NOAA/NESDIS. Of particular interest are the match-ups between the PnB field sampling and the satellite data ([www.icess.ucsb.edu/~moterero/ASLO\\_2001\\_Poster.html](http://www.icess.ucsb.edu/~moterero/ASLO_2001_Poster.html)).

Many comparisons between SeaWiFS and field estimates are quite good especially when assessing time/space patterns.

However, direct comparisons of several properties are disappointing and a significant underestimate of the SeaWiFS estimated  $L_{wN}(412)$  values remains. That said, the time/space patterns are consistent between satellite and field data sets (see below). The PnB project has an extensive education and outreach component. We are active in local K-12 education and have provided content for an online "Plumes and Blooms Curriculum" assembled by the CINMS education coordinator (see [www.cinms.nos.noaa.gov/pcw2/](http://www.cinms.nos.noaa.gov/pcw2/)). This curriculum is designed for 4<sup>th</sup> through 8<sup>th</sup> graders in the Santa Barbara and Ventura Counties. We have also participated with last summer's Sustainable Sea Expedition program in the Santa Barbara Channel and will with the upcoming Jason and Project Oceanography visits. Our outreach component has also made several presentations at several public meetings dealing with issues as diverse as watershed processes and coastal pollution to the California space industry.

### 16.3 RESEARCH RESULTS

Academic research has gone along two major fronts; 1) the analysis of field and satellite data to assess the sources of ocean color variability (Toole and Siegel, 2001; Otero et al., 2001) and the assessment of the time/space variability in the Santa Barbara Channel (Siegel et al. 2001; Shipe et al. 2001; Mertes and Warrick, 2001). Of particular interest is our work assessing the sources and modes of ocean color variability within the Santa Barbara Channel from the six-year PnB observational record (Siegel et al. 2001; Toole and Siegel, 2001). The characterization of the substances, processes, and mechanisms that regulate coastal ocean color variability is crucial for the application of ocean color imagery to the management of marine resources. Using an empirical orthogonal function analysis, we find that nearly two-thirds of the observed variability in remote sensing reflectance is contained in a backscattering mode. Phytoplankton absorption makes a much smaller contribution to the observed variance in the water-leaving radiance spectrum. Hence, particulate backscattering associated with suspended sediment concentrations is the dominant driver of ocean color variability for this environment. However, sediment plumes appear to play a much smaller role on biological processes. An empirical partitioning of physical, biological and chemical oceanographic parameters suggests that physical oceanographic processes (i.e., upwelling and horizontal advection) have the dominant role in determining phytoplankton pigment biomass for this region. Similar partitioning is found spatially using satellite ocean color imagery from the SeaWiFS mission. We expect to have

several manuscripts (in addition to Toole and Siegel, 2001) on the spatial/temporal partitioning between Plumes and Blooms submitted over the next year.

### 16.4 FUTURE WORK

PnB has had a good year, especially considering the loss of the *Ballena*. We plan to continue our field program as we have in past years. From an analysis perspective, we plan to focus on the evaluation of the inherent optical property determinations made and their relationship with the determinations of water-leaving radiance. We will also tune a semi-analytical ocean color model using PnB data with the goal of assessing differences in ocean color model tunings on local and global scales. There are also several data quality issues that we want to work out. These include a re-estimation of the path length amplification factor used in the processing of particulate absorption spectra and a convergence of methods between the LTER and PnB projects. Satellite data analyses are falling far behind our progress in the field program. The major reason is that the so-called "negative water leaving radiance problem" has not been satisfactorily corrected in the version 3 processing of SeaWiFS imagery (see Otero et al. 2001 on line poster). We will continue to work with Goddard staff to help find solutions in the next reprocessing.

### REFERENCES

- Mertes, L.A.K., and J.A. Warrick, 2001. Measuring flood output from 110 coastal watersheds in California with field measurements and SeaWiFS. *Geology*, **29**, 659-662.
- Siegel, D.A., and others, 2001: Time-series assessment of sediment plumes and phytoplankton blooms in the Santa Barbara Channel, California. EOS Trans., AGU, 82(47) Fall Meet. Suppl., Abstract 0S51E-06.
- Shipe, R.F., U. Passow, M.A. Brzezinski, D.A. Siegel and A.L. Alldredge, 2001: Effects of the 1997-98 El Nino on seasonal variations in suspended and sinking particles in the Santa Barbara Basin. In press *Progress in Oceanography*.
- Toole, D.A., and D.A. Siegel, 2001: Modes and mechanisms of ocean color variability in the Santa Barbara Channel. In press *Journal of Geophysical Research*.

TABLE 16.1: PLUMES AND BLOOMS MEASUREMENTS AND DATA PRODUCTS

Direct Measurements:	
$E_d(z,\lambda)$	Downwelling vector irradiance (325, 340, 380, 412, 443, 490, 510, 555, 565, 665 & 683 nm)
$E_d(0^+, \lambda)$	Incident irradiance (325, 340, 380, 412, 443, 490, 510, 555, 565, 665, 683 & 350-1050 nm)
$L_u(z,\lambda)$	Upwelling radiance (325, 340, 380, 412, 443, 490, 510, 555, 565, 665 & 683 nm)
$a(z,\lambda)$	<i>In situ</i> absorption spectrum using WetLabs AC-9 (410,440,490,520,565,650,676 & 715 nm)
$c(z,\lambda)$	<i>In situ</i> beam attenuation spectrum (same as above)
$b_b(z,\lambda)$	<i>In situ</i> backscattering spectrum - HOBI Hydroscat (442,470,510,532, 590 & 671 nm)
T(z) & S(z)	SeaBird temperature and conductivity probes
$a_p(z_0,\lambda)$	<i>In vivo</i> particulate absorption spectrum by Mitchell (1990)
$a_{det}(z_0,\lambda)$	<i>In vivo</i> detrital particle absorption spectrum by MeOH extraction
$a_g(z_0,\lambda)$	<i>In vivo</i> colored dissolved absorption spectrum
chl-a( $z_0$ )	Discrete chlorophyll <i>a</i> determinations by Turner fluorometry
pigs( $z_0$ )	Discrete phytoplankton pigment sample to be run by HPLC (SDSU CHORS analysis)
nuts( $z_0$ )	Discrete inorganic nutrient concentrations (NO <sub>3</sub> , SiO <sub>4</sub> , PO <sub>4</sub> , NO <sub>2</sub> )
PSi( $z_0$ )	Discrete particulate biogenic & lithogenic silica concentrations
$L_{sat}(x,y,\lambda)$	SeaWiFS and AVHRR imagery from the HUSC ground station
Primary Derived Products:	
$R_{rs}(0^-, \lambda)$	In-water remote sensing reflectance from profiling radiometry (see above)
$L_{wN}(\lambda)$	Normalized water leaving radiance calculated from $R_{RS}(0^+, \lambda)$ and $R_{RS}(0^-, \lambda)$
$a_{ph}(z_0, \lambda)$	<i>In vivo</i> phytoplankton absorption spectrum (= $a_p(z_0, \lambda) - a_{det}(z_0, \lambda)$ )
$K_d(z, \lambda)$	Attenuation coefficient for $E_d(z, \lambda)$ from profiling radiometry (also $K_L(z, \lambda)$ )
$b(z, \lambda)$	<i>In situ</i> total scattering spectrum (= $c(z, \lambda) - a(z, \lambda)$ )
Chl(x,y), etc.	Processed SeaWiFS and AVHRR imagery

*This research was supported by  
the SIMBIOS NASA contract #00201*

## PEER REVIEWED PUBLICATIONS

- Mertes, L.A.K., and J.A. Warrick, 2001: Measuring flood output from 110 coastal watersheds in California with field measurements and SeaWiFS, *Geology*, **29**, 659-662.
- Nelson, N.B., and D.A. Siegel, 2001: Chromophoric DOM in the Open Ocean. In press in: *Biogeochemistry of Marine Dissolved Organic Matter*, D.A. Hansell and C.A. Carlson, eds. Academic Press.
- Shipe, R.F., U. Passow, M.A. Brzezinski, D.A. Siegel and A.L. Alldredge, 2001: Effects of the 1997-98 El Nino on seasonal variations in suspended and sinking particles in the Santa Barbara Basin, In press *Progress in Oceanography*.
- Siegel, D.A., M. Wang, S. Maritorena and W. Robinson, 2000: Atmospheric correction of satellite ocean color imagery: The black pixel assumption. *Applied Optics*, **39**, 3582-2591.
- Siegel, D.A., S. Maritorena, N. B. Nelson, D.A. Hansell and M. Lorenzi-Kayser, 2001: Global ocean distribution of colored dissolved and detrital materials, In press *Journal of Geophysical Research*.
- Toole, D.A., and D.A. Siegel, 2001: Modes and mechanisms of ocean color variability in the Santa Barbara Channel, In press *Journal of Geophysical Research*.
- Toole, D.A., D.A. Siegel, D.W. Menzies, M.J. Neumann and R.C. Smith, 2000: Remote sensing reflectance determinations in coastal environments: impact of

instrumental characteristics and environmental variability. *Applied Optics*, **39**, 456-469.

### Submitted

Maritorena, S., D.A. Siegel and A.R. Peterson, 2001: Optimal tuning of a semi-analytical model for global applications. In review in *Applied Optics*.

Siegel, D.A., and others, 2001: Time-series assessment of sediment plumes and phytoplankton blooms in the Santa Barbara Channel, California. Submitted to *Continental-Shelf Research*.

Siegel, D.A., 2001: Dispersion and the Design of Marine Protected Areas. Seminar presented at the Institute for Computational Earth System Science, University of California at Santa Barbara, May 2, 2001.

Siegel, D.A., 2001: Education and Research at the University of California or Satellite Views of Plumes and Blooms of the Santa Barbara Channel. Presented at the Space Coast Summit 2001 sponsored by the California Space Authority, Santa Maria, CA, August 6, 2001.

## PRESENTATIONS

Otero, M.P., D.A. Siegel, and E.A. Fields, 2001: Satellite view of plumes and blooms in the Santa Barbara Channel; Validation and description. Poster presented at the 2001 ASLO Aquatic Sciences Meeting in Albuquerque, NM, February 2001.

## Chapter 17

# Algorithms for Processing and Analysis of Ocean Color Satellite Data for Coastal Case 2 Waters

Richard P. Stumpf

*NOAA National Ocean Service, Silver Spring, Maryland*

Robert A. Arnone and Richard W. Gould, Jr.

*Naval Research Laboratory (NRL), Stennis Space Center, Mississippi*

Varis Ransibrahmanakul

*Technology Planning and Management Corporation, Silver Spring, Maryland*

Patricia A. Tester

*NOAA National Ocean Service, Beaufort, North Carolina*

### 17.1 INTRODUCTION

The development of several new ocean color sensors has significantly enhanced our ability to understand processes in the open ocean. Applicability of the sensors to the coastal zone will require additional improvements to the standard global algorithms for both the atmospheric correction and the bio-optical models. With the short temporal scales and fine spatial scales of coastal processes, applying and inter-comparing multiple sensors will assure their use in improving our understanding of a range of processes and events including algal bloom development, river plumes, and resuspension events. SeaWiFS imagery has shown problems when applied to the coastal zone-in particular underestimating the water reflectance in the blue bands (412-490 nm). Two major factors linked to atmospheric correction produce this effect: (1) scattering from inorganic particles that produces water-leaving radiance in the near-infrared, where all radiance is presumed to come from the atmosphere and (2) absorbing aerosols associated with the land that cannot be incorporated into atmospheric corrections based on near-infrared (NIR) bands. Iterative techniques, which draw on coupling the atmospheric and oceanic models, offer a solution to these problems, but these require valid ocean bio-optical models for Case 2 waters that are robust in a coupled atmosphere-ocean model. Our objective is to develop and improve the functionality and utility of SeaWiFS and other ocean color

satellite in Case 2 water. We are collecting data sets of bio-optical properties in turbid, Case 2 waters. These data sets will provide the basis for testing and evaluating *in situ* and atmospheric correction algorithms for the coastal waters. In coastal waters with a high sediment load or high concentrations of colored dissolved organic matter (CDOM), standard processing algorithms typically fail (negative or erroneous retrievals of water-leaving radiance) due to invalid assumptions related to the atmospheric correction. Our efforts will focus on describing the reflectance properties at near-infrared (NIR) and blue wavelengths in coastal waters, and how we can utilize these properties to improve the atmospheric correction. We will modify and develop new coastal bio-optical algorithms, and we will validate the algorithms and atmospheric corrections and compare the new results with current ocean color algorithms. Finally, we will process MODIS imagery with the new coastal algorithms and compare the results with SeaWiFS imagery.

### 17.2 RESEARCH ACTIVITIES

We have made substantial progress in four areas this year, starting in April 2001: 1) cruise and data collection, 2) improved algorithms, 3) evaluation data sets and matchups, and 4) MODIS software processing. We collected *in situ* bio-optical data on nine cruises see Table 17.1.

Table 17.1 Cruises

Experiment	Cruise	Date	# Stations Each Cruise
Cojet 3 –Northern Gulf of Mexico	Mopex	16-May-01	36
Cojet 3–Northern Gulf of Mexico	Ocolor1	16-May-01	22
Cojet 3–Northern Gulf of Mexico	Lgssur	16-May-01	31
Leo2001- East Coast –New jersey	R/V NorthStar	7/31- 8/02	25
11Sep01_ Biloxi- Northern Gulf of Mexico	Ocolor2	11-Sep	8
ECOHAB- West Florida Shelf	ECOHAB	9/25/00-9/29/00	25
NC-04/01- North Carolina	Pamlico	4/10/01-4/11/01	23
NC 07/01 North Carolina	Pamlico	7/24/01 – 7/26/01	16
NC 10/01 North Carolina	Pamlico	10/16/01 – 10/18/01	11
Ferry 8/01	Pamlico	5/01	4
Offshore 8/01	NC Shelf	8/1/01	2
Offshore 10/01	NC Shelf	10/19/01	3
<b>TOTALS</b>	12		<b>206</b>

Measurements in the Northern Gulf of Mexico include absorption coefficient, beam attenuation coefficient, scattering coefficient (ac9), remote sensing reflectance (above water method), aerosol optical thickness (Microtops), and HPLC pigments. A substantial number of these stations were collected during minimum cloud cover and matched up with SeaWiFS and MODIS passes. Measurements in North Carolina waters include water samples, water profile measurements (YSI), and remote sensing reflectance. The water samples were collected to determine chlorophyll, CDOM, filtered pad absorption, HPLC, total suspended solids (TSS), and nutrients. The April experiment in North Carolina co-occurred with overflights conducted by NASA-Wallops using airborne oceanic lidar (AOL), the Atlantic SAS, and two hyperspectral systems. We are assembling a satellite/in situ matchup database and we will be presenting SeaWiFS algorithm validation results at the San Francisco AGU Fall meeting in December 2001. The HPLC filters have been provided to CHORS and we are waiting for them to complete the processing, at which point we will submit the pigment results to SIMBIOS. We are in the process of submitting all the station data to SIMBIOS. Since this is our initial effort in data submission to SIMBIOS, we are learning the format requirements. The data collected to date will be submitted by November, 2001.

## 17.3 RESEARCH RESULTS

We have analyzed and quality-checked all the station data collected to date and we have developed a coupled ocean/atmosphere algorithm to improve SeaWiFS radiance retrievals in coastal waters.

### *Calibration (NOAA)*

The current calibration of SeaWiFS involves two steps: correction for temporal changes using lunar observations and periodic vicarious calibration of the radiance based on comparison with the Marine Optical Buoy (MOBY) sites. The later has potential uncertainty of 0.5 % in the top-of-atmosphere (TOA) radiance calibration (Barnes et al. 2000), partly because each band is calibrated independently. In coastal areas, the calibration of the 412 nm band is of particular concern owing to the need to correct for absorbing aerosols in the atmosphere and the need to monitor and compensate for colored dissolved organic matter (CDOM) in the water. Calibration errors of 0.5-1% between bands in the blue (412 nm, 443 nm, 490 nm) can introduce significant errors in the retrieved water reflectances (5-10% in case 1 water, and 20-100% in case 2 water).

Examination of the spectral shape in the blue shows fundamental differences between that observed in the field and that observed from SeaWiFS. We identified spectral shape characteristics from the statistical patterns seen in the field data. By adjusting the calibration of 412 nm, we found that we could match the statistical distribution of spectral slopes in SeaWiFS imagery to the field data (Figure 17.1).

The Kolmogorov-Smirnov test (e.g., Siegel 1956) was used to determine the statistical similarities between the distributions of field and satellite data at different calibrations. The results are presented in Figure 17.1, where 0 and 1 indicate the two distributions are alike and very much different, respectively. Our analysis suggests the optimum calibration at 412 nm should be 1% higher than the current. The analysis gives the same results for different atmospheric corrections in both Case 1 and Case 2 waters (although Case 2 waters provide a sharper separation), showing robustness, and does not use or require simultaneous field data. For validation, we computed the overall bias of 159 pairs of satellite and same-day measured remote sensing reflectance in US coastal waters for the existing calibration (thin line, Figure 17.2) and the new calibration (bold line, Figure 17.2). The new 412 calibration reduced most of the relative bias at 412 nm.

The analysis gives the same results for different atmospheric corrections in both case 1 and case 2 waters (although case 2 waters provide a sharper separation), showing robustness, and does not use or require simultaneous field data. For validation, the overall bias of 159 pairs of satellite and same-day measured remote sensing reflectance in US coastal waters was examined for the existing calibration and the new calibration (Figure 17.2). The new 412 calibration reduced most of the relative bias at 412 nm

#### *Validation of Atmospheric Correction and Chlorophyll Algorithms for Processing SeaWiFS data (NOAA)*

We have developed an evaluation protocol to evaluate the performance of the available atmospheric corrections (including the NOAA/NRL developmental atmospheric correction) and chlorophyll algorithms. To date, we have used 159 same-day field-satellite pairs of remote sensing reflectance spectra to determine the best atmospheric correction applicable to the entire US coastline. The five atmospheric corrections considered were developed by Gordon & Wang (1994), Siegel et al. (2000), Gould et al. (1998), Ruddick et al. (2000), and NOAA/NRL (Stumpf et al., in prep). We did not include the atmospheric correction developed by Hu et al. (2000) because it requires manual interaction and is not appropriate for automated processing.

Similarly, we have 124 same-day field-satellite pairs of chlorophyll to determine the most appropriate regional chlorophyll algorithms. The chlorophyll algorithms

considered were OC2V2 (O'Reilly), OC4V4 (O'Reilly et al. 1998), USF-analytical (Carder et al. 1999), CALP6 (Kahru and Mitchell 1999), and NOAA-coastal (Stumpf et al., 2000). The field measurements were obtained from NASA SIMBIOS database and NOAA collaborators (Nan Walker- LSU, Dana Woodruff-Battelle Marine Sciences Laboratory, Linda Traykovski-Woods Hole). In both the evaluations of atmospheric correction and chlorophyll algorithms, the selection procedure was designed to determine an algorithm that works best over a range of water types and compensates for distribution biases.

Preliminary results are encouraging to the developing algorithms. The results indicate a NOAA atmospheric correction estimated the best overall accurate remote sensing reflectance (Stumpf et al. in prep). The best chlorophyll algorithms vary by regions: NOAA-coastal algorithm for US Gulf of Mexico and Southeast, and central Gulf of Maine; NASA OC2V2, for California water (Ransibrahmanakul, in prep).

In addition to comparing the performances of the existing algorithms, the work to develop better chlorophyll algorithm is ongoing. In Pamlico Sound and Atchafalaya Bay, the NASA OC2V2 or OC4 appear to perform better than NOAA-coastal algorithm. We will be examining the factors influencing this, high CDOM may play a factor.

#### *New Algorithms (NRL)*

We modified the MS12 NASA SeaDAS code to include the NIR atmospheric correction method. We are testing and evaluating algorithms from coastal waters through a parallel software development with NASA SeaDAS software team. We have extracted the MS12 from SeaDAS so that it can be operated in stand-alone mode, and we have incorporated it into the NRL Automated Processing System (APS). Outputs from APS are directly compatible with SeaDAS except we have added routines to handle the new NRL products (presently a total of 65 products). The APS HDF-formatted products can be directly incorporated into SeaDAS, to employ all the functionality of the display and data manipulation routines. In addition, we can easily apply the changes in calibration that we routinely receive from the SeaDAS program. APS can produce "identical results" as the NASA standard processing and it can produce additional products that we use for comparison and research. We receive all NASA changes to SeaDAS MS12 and we incorporate these modifications into APS, so that we are consistent with standard NASA processing. APS has undergone several stages of development and upgrades continue. We have a beta 2.5 version that tests new algorithms and can handle MODIS processing (discussed later.)

Algorithm modifications in APS v2.5 fall into two broad categories: 1) changes to the atmospheric correction, and 2)

changes to the in-water bio-optical algorithms. Changes to the atmospheric correction include ability to drive a coupled atmosphere/ocean optical property model (we call this the NIR correction). This algorithm uses the NIR changes to estimate the water leaving radiance at 765 and 865 prior to the standard (Gordon and Wang) atmospheric correction approach. These modifications are applied to all coastal waters where problems with over-correction occur. The second category includes changes to bio-optical algorithms to estimate the total spectral absorption coefficient ( $a$ ), absorption due to phytoplankton ( $a_p$ ), absorption due to detritus and CDOM ( $a_{dg}$ ), and the backscattering coefficient. We included semi-analytical MODIS algorithms from Carder et al. (1999) and semi-analytical algorithms of Arnone et al. (2001). There are relationships between inherent optical properties (IOPs) and remote sensing reflectance, chlorophyll, and CDOM that are used in both these categories of algorithm development (1 and 2). In order to ensure that the same relationships are used throughout the software, we have assembled the bio-optical equations into isolated software modules that are called repeatedly during different stages of the processing. The algorithms that are used in processing select from these bio-optical modules. This permits self-consistent evaluations of the relationships and provides an easy method to test new relationships.

We developed improved SeaWiFS coastal ocean color algorithms to derived inherent optical properties, based on relationships between absorption, scattering and remote sensing reflectance. The linear remote sensing reflectance to scattering: absorption ratio ( $bb/a$ ) is the basis for open ocean algorithms where absorption (predominantly from chlorophyll) is greater than backscattering. In coastal waters, where backscattering from sediment can dominate absorption, the relationships of  $bb/(a+bb)$  and a non-linear and spectral dependence occurs between the reflectance and the backscatter: absorption ratio.

These nonlinear influences (Haltrin, 2001) affect not only the in water optical algorithms, but they are also coupled with the atmospheric correction in coastal waters. The removal of water leaving radiance in the near-IR (765 and 865 nm) is especially necessary in coastal waters. The non-linear relationship is used in estimating the water leaving radiance in the near-IR through an iterative pixel-by-pixel process using the 670 nm water leaving radiance.

We used SeaWiFS imagery and insitu measurements to evaluate the effects the non-linear relationships have on coastal algorithms where backscattering dominates the absorption. We compare these new products with the more standard NASA products and we highlight areas where regional differences are greatest (bays, estuaries).

## 17.4 CONCLUSION

### *Evaluation of algorithms / bio-optical algorithms (NOAA/NRL)*

We are evaluating and validating the algorithms and retrieved optical properties using in situ coastal bio-optical measurements collected from 1997- present (lifespan of SeaWiFS). This effort is designed to develop an architecture for 1) handling multiple cruises and satellite/*in situ* data matchups, and 2) to provide guidance on algorithm development, testing, and validation. Our focus has been mostly on coastal values, however there are data from offshore waters included as well (such as the Japan/East Sea).

Between the two groups, NOAA and NRL, we have an extensive data set. We are in the process of merging the information for examination of remote sensing reflectance and chlorophyll. NRL has a data set from over 18 cruises, representing 76 separate cruise days, with a total of approximately 150 stations with chlorophyll data, and a total of 330 stations with remote sensing reflectance measurements. Note that these are total station numbers; the actual number of matchups will be slightly lower after removal of contaminated SeaWiFS pixels (due to clouds, swath edge). NOAA has approximately 100 same-day match-ups of remote sensing reflectance and chlorophyll from the southeast and Gulf of Mexico. We assembled a database of in situ optical properties to evaluate SeaWiFS-derived properties collected from 1997 to present in a variety of coastal regions (Mississippi Bight, Mississippi River, West Florida Shelf, Loop Current, North Carolina, New Jersey). The data cover a broad range of absorption ( $0.4 - 15 \text{ m}^{-1}$ ) and scattering ( $0.1 - 27 \text{ m}^{-1}$ ) coefficients and remote sensing reflectance.

Optical properties derived from SeaWiFS were evaluated for 18 cruises in coastal and open ocean waters in the Gulf of Mexico, US East Coast, and the Japan/ East Sea. The inherent optical properties (absorption and scattering) were derived from SeaWiFS processing using a NIR correction with a coupled ocean- atmosphere algorithm. Coastal optical properties are more complex and differ greatly from chlorophyll - dominated open-ocean waters. The coupled algorithms improved results and extend SeaWiFS optical properties well into bays and estuaries where high sediments and CDOM absorption dominate the optical signature.

The *in situ* data were used to estimate the error associated with in-water optical algorithms based on remote sensing reflectance. We then estimated the error associated with satellite optical products for a variety of different optical regimes (CDOM rich, sediment rich, and chlorophyll rich). As a whole, we noted higher error associated with coastal waters than open ocean.

With the high CDOM patterns found in the region, we are examining the impact of CDOM on the determination of chlorophyll, as well as on the atmospheric correction.

#### *Sensor inter-comparison: MODIS & SeaWiFS (NRL)*

We are developing and implementing similar processing algorithms for MODIS that we are using for SeaWiFS. This enables us to evaluate and compare products and algorithms between two sensors. We have implemented MODIS software obtained from the University of Miami into APS 2.5; this is the "standard" processing that is being used by the MODIS – Oceans Science team (Gordon atmospheric correction). To date, we have:

- Obtained MODIS source code for modcolor subroutine from Miami (RATFOR source).
- Modified modcolor for input into APS (NRL-HDF) v2.5 which is a C file with 2 entry points in main loop of Miami Code (anly8dbl.rat).
- Developed make files based on GNU automaker/autoconf for modcolor.
- Compiled MODIS code on Linux and SGI – Required Portland Groups f90 compiler (Linux).
- Applied APS imgmap program for warping /registration based on PC-SeaPAC.
- Compared the MODIS products from DACC with products we are producing in APS.
- Developed procedures to automatically match input file with correct ancillary data.
- Developed procedures to automatically place regional images into data bases on web server.
- Processed ~40 MODIS scenes and corresponding SeaWiFS scenes and produced bio-optical products.
- Produced HDF MODIS files currently viewed under SeaDAS (NRL) for 12 products which include Rrs (l), k532, chlmod, chl\_carder, adg400\_card, aph\_card, chloc3, chl0c4, albedo865, tau865, l2flags, glint, foam, sst

We have identified several issues that require further work:

- Access to ancillary fields - requires met/ozone AND Reynolds OI/ SST . The met/ozone are coming from DAAC (SeaWiFS) and the Reynolds data come from NOAA. The processing requires real-time data and will not work with the climatology files (unlike anly8db1 for SeaWiFS). We are planning to use the SeaDAS Code for processing the met/ozone data directly.
- Limits on the file size (5-minute scene) and non partitioning of file size (lines vs. samples).
- Problems with in-water algorithms - are they real and systematic ?

- Issues with level 0 to level 1 - conversion is time dependent and a product of the MCST group.

We have shown our current MODIS results to Wayne Esaias in August 2001. Bio-optical products from SeaWiFS and MODIS (Terra) were compared from coastal and open ocean waters in the Gulf of Mexico and the US East Coast. Near coincident overpasses of these satellites (within 1 hour) were processed with similar methods to determine the inherent optical properties (absorption and scattering), diffuse attenuation coefficient (k) and the chlorophyll concentration. The similar spectral and spatial resolution and repeat cycles of these sensors enable us to assess temporal variability in coastal processes. We evaluate the satellite bio-optical products using coincident shipboard measurements and we assess the variability and regional dependence of the algorithms. Processing of MODIS and SeaWiFS imagery was performed on modified University of Miami (modcol) software on a LINUX operating system. We compared the "standard" processing code for these satellites with NIR atmospheric correction methods and determined the differences in optical properties within the coastal zone. The MODIS predicted coastal bio-optics were elevated relative to the SeaWiFS and shipboard values and were linked to the NIR correction. We noted largest differences in the high sediment estuarine regions and river discharge regions and smaller differences offshore (Figure 17.3). Because of the importance of atmospheric correction in bio-optical estimates, we examined the effects due to differences in the aerosol models and optical depths that were used by the two satellites (Figure 16.4).

## 17.5 FUTURE WORK

We anticipate the following cruises:

Nov 2001	– Northern Gulf of Mexico
March 2002	– Northern Gulf of Mexico
May 2002	– Northern Gulf of Mexico
Feb, April, 2002	– North Carolina
July, Oct. 2002	– North Carolina

In addition, we will be continuing development on the several fronts: bio-optical algorithms for chlorophyll, algal bloom, CDOM, and scattering; atmospheric correction and calibration required for coastal areas; and implementation with MODIS.

## REFERENCES

Barnes, R.A., R.E. Eplee Jr., W.D. Robinson, G.M., Schmidt, F.S. Patt, S.W. Bailey, M. Wang, and C.R McClain, 2000: The calibration of SeaWiFS on orbit, Earth Observing

- Systems V, William L. Barnes (eds.), Proceedings of *SPIE* Vol. **4135**, 281-293.
- Carder, K.L., F.R. Chen, Z.P. Lee, S.K. Hawes, D. Kamykowski, 1999: Semianalytical moderate resolution imaging spectrometer algorithms for chlorophyll a and absorption with bio-optical domains based on nitrate-depletion temperatures, *Journal of Geophysical Research*, **104**, 5403-5421.
- Fu, G., K.S. Baith, and C.R. McClain, 1998: SEADAS: the SeaWiFS Data Analysis System, Proceedings of the 4th Pacific Ocean Remote Sensing Conference, Qingdao, China, July 28-31.
- Gordon, H.R., and M. Wang, 1994: Retrieval of water leaving radiance and aerosol optical thickness over the oceans with SeaWiFS: a preliminary algorithm, *Applied Optics*, **33**, 443-452.
- Gould, R.W., Jr., R.A. Arnone, M. Sydor, 1998: Testing a new remote sensing algorithm to estimate absorption and scattering in CASE 2 waters, SPIE Ocean Optics XII, Hawaii, Nov, 1998.
- Hu, Chuanmin, K.L. Carder, F.E. Muller-Karger, 2000: Atmospheric correction of SeaWiFS imagery over turbid coastal waters: a practical method, *Remote Sensing of Environment*, **74**, 195-206.
- Kahru, K., and G.B. Mitchell, 1999: Empirical chlorophyll algorithm and preliminary SeaWiFS validation for the California current, *International Journal of Remote Sensing*, **20**, 34323-3429.
- O'Reilly, J.E., S. Maritorena, G.B. Mitchell, D.A. Siegel, K.L. Carder, S.A. Garver, M. Kahru, and C. McClain, 1998: Ocean color chlorophyll algorithms for SeaWiFS, *Journal of Geophysical Research*, **103**, 24937-24953.
- Ruddick, K., F. Ovidio, and M. Rijkeboer, 2000: Atmospheric correction of SeaWiFS imagery for turbid coastal and inland waters, *Applied Optics*, **39**, 897-912.
- Siegel, D., M. Wang, S. Maritorena, and W. Robinson 2000: Atmospheric correction of satellite ocean color imagery: the black pixel assumption, *Applied Optics*, **39**, 3582-3591.
- Sigel, S., 1956: *Nonparametric statistics for the behavioral sciences*. McGraw-Hill Book Company, New York.
- Stumpf, R.P. Arnone, R.A. R.W. Gould, P. Martinolich, V. Ransibrahmanakul, P.A. Tester, R.G. Steward, A. Subramaniam, M. Culver, J.R. Pennock, 2000: SeaWiFS ocean color data for US Southeast coastal waters. Sixth International Conference on Remote Sensing for Marine and Coastal Environments. Charleston SC. Veridian ERIM Intl. Ann Arbor MI, USA, p. 25-27.

*This research was supported by  
the SIMBIOS NASA interagency agreement # S-44796-X*

## PEER REVIEWED PUBLICATIONS

- Arnone, R.A. and R.W. Gould, 2001: Mapping Coastal Processes with Optical Signatures, *Backscatter*, **12**, 17-24.
- Gould, R.W., Jr., R.A. Arnone, and M. Sydor, 2001: Absorption, scattering, and particle size relationships in coastal waters: Testing a new reflectance algorithm, *Journal of Coastal Research*, **17**, 328-341.
- Gould, R.W., Jr., and R.A. Arnone: Temporal and spatial variability of satellite sea surface temperature and ocean color. *International Journal of Remote Sensing*, submitted.

Haltrin, V.I., Semi-empirical approach to the radiative transfer of light in open and coastal sea waters, *Applied Optics*, submitted.

## PRESENTATIONS

- Arnone, R.A., R.W. Gould, Jr., C.O. Chan, and S.D. Ladner, 2000: Uncoupling CDOM, scattering and chlorophyll properties in coastal waters using SeaWiFS ocean color. Abstract Published to Oceans from Space 2000, Venice, Italy, 9-13 October, 2000.
- Arnone, R.A., R.W. Gould, Jr., A.D. Weidemann, S.C. Gallegos, and V.I. Haltrin, 2000: Using SeaWiFS ocean

color absorption, backscattering properties to discriminate coastal waters. Abstract published Ocean Optics XV, Monaco, 16-20 October, 2000.

Gould, R.W., Jr., R.A. Arnone, and C.O. Chan, 2000: Temporal and spatial variability of satellite sea surface temperature and ocean color. Oceans from Space 2000, Venice, Italy, 9-13 October, 2000.

Gould, R.W. Jr., R.A. Arnone, C.M. Lee, and B.H. Jones, 2000: Characterizing surface and subsurface thermal and bio-optical fields in the Japan/East Sea during a spring bloom: Shipboard measurements and satellite imagery. Proceedings, Ocean Optics XV, Monaco, 16-20 October, 2000.

Gould, R.W., Jr., T.R. Keen, R.A. Arnone, R.H. Stavn, A.-R. Diercks, 2001: Bio-Optical variability in a barrier-island coastal environment: Coupling remote sensing imagery, shipboard measurements, and modeling results. Ocean

Odyssey 2001 Meeting, Joint meeting of IAPSO and IABO, Mar del Plata, Argentina, 21-28 October, 2001.

Ransibrahmanakul, V., R.P. Stumpf, A. Robertson, K. Casey, and K. Buja, 2001: Temporal patterns in chlorophyll and temperature around the coastal US, from September 1997 through 2001. 16<sup>th</sup> Biennial Conference of the Estuarine Research Federation, St. Pete Beach, FL, November 4-8, 2001.

Stumpf, R.P. and M.E. Culver: Forecasting harmful algal blooms in the Gulf of Mexico, 2001: 16<sup>th</sup> Biennial Conference of the Estuarine Research Federation, St. Pete Beach, FL, November 4-8, 2001.

Tester, P, S. Varnam, R. Swift, R.P. Stumpf, D. Eslinger, M. Culver, M. Black, 2001: Hurricane Floyd: NOAA, NASA and new remote sensing technologies. 16<sup>th</sup> Biennial Conference of the Estuarine Research Federation, St. Pete Beach, FL, November 4-8, 2001.

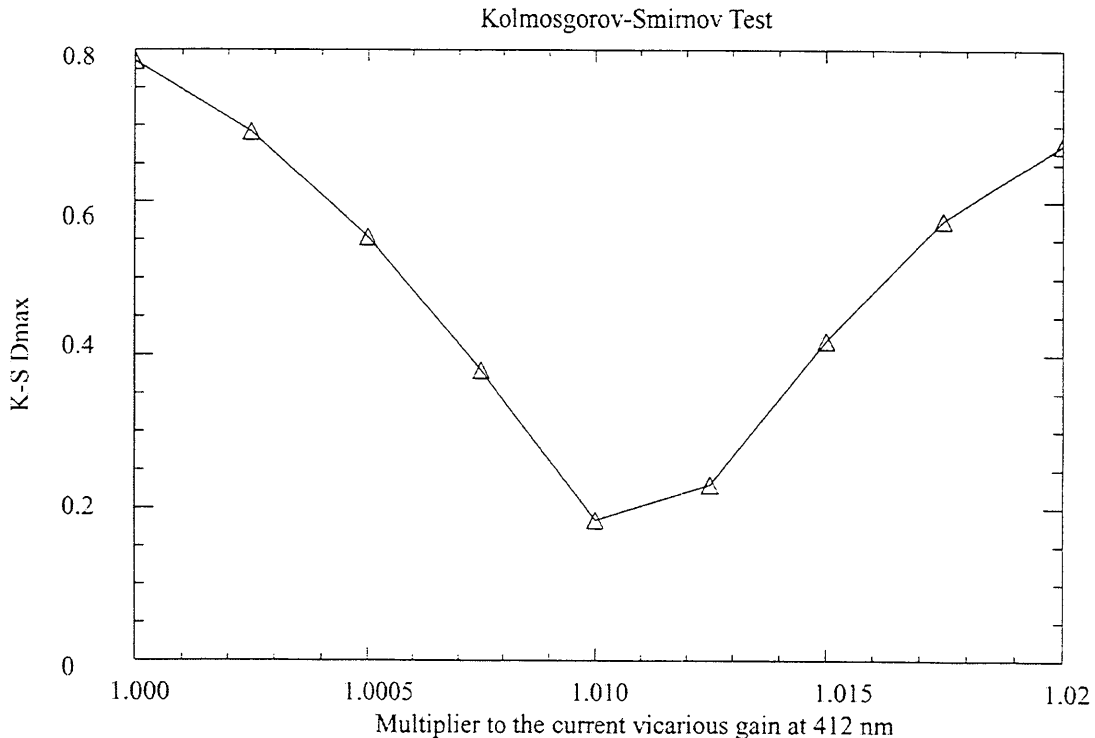


Figure 17.1: By adjusting calibration of 412 nm, we found that we could match the statistical distribution of spectral slopes in SeaWiFS imagery to the field data. The horizontal axis is the different multipliers to the current calibration of 412 nm (e.g. 1.00 means 1.00 x current calibration; and 1.01 = 1.01 x current calibration, etc). The Kolmogorov –Smirnov test (Siegel 1956) was used to compare the difference between the accumulative histograms of field and satellite data; a K-S Dmax of 0 indicates the two histograms are identical and 1 indicates the two histograms are significantly different.

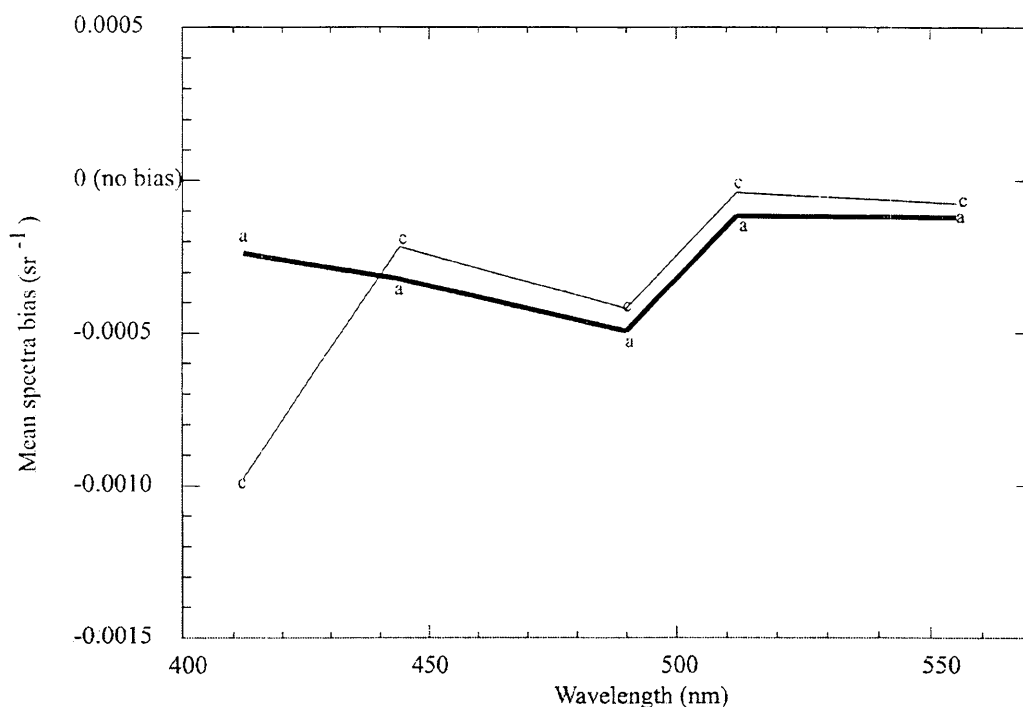


Figure 17.2: For validation, the overall bias of 159 pairs of satellite and same-day measured remote sensing reflectance in US coastal waters was examined for the existing calibration (thin) and the new calibration (bold). The new 412 calibration reduced most of the relative bias at 412 nm.

SeaWiFS 07/31/01 1753 GMT

MODIS 07/31/01 1623 GMT

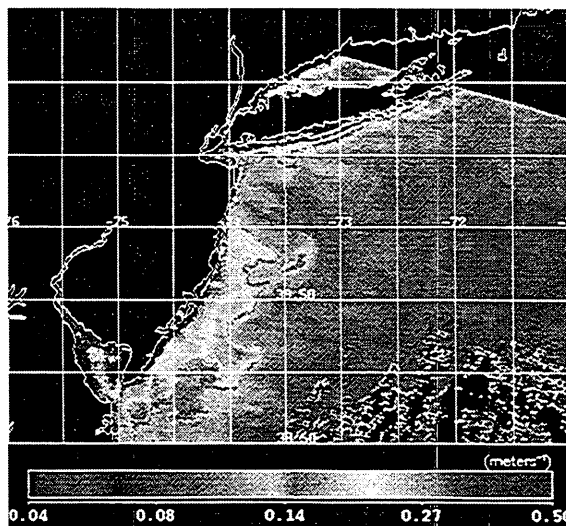
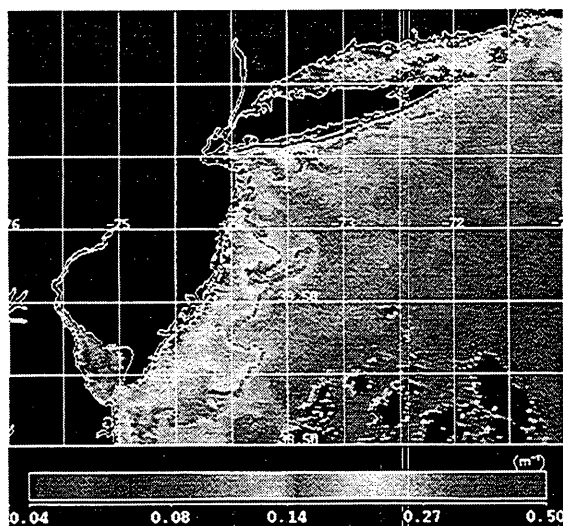


Figure 17.3: Bio-optical products from SeaWiFS and MODIS (Terra) were compared from coastal and open ocean waters in the Gulf of Mexico and the US East Coast (Diffuse Attenuation Coefficient at 532 ( $k_{532}$ )). The largest differences occur in the high sediment estuarine regions and river discharge regions and smaller differences offshore.

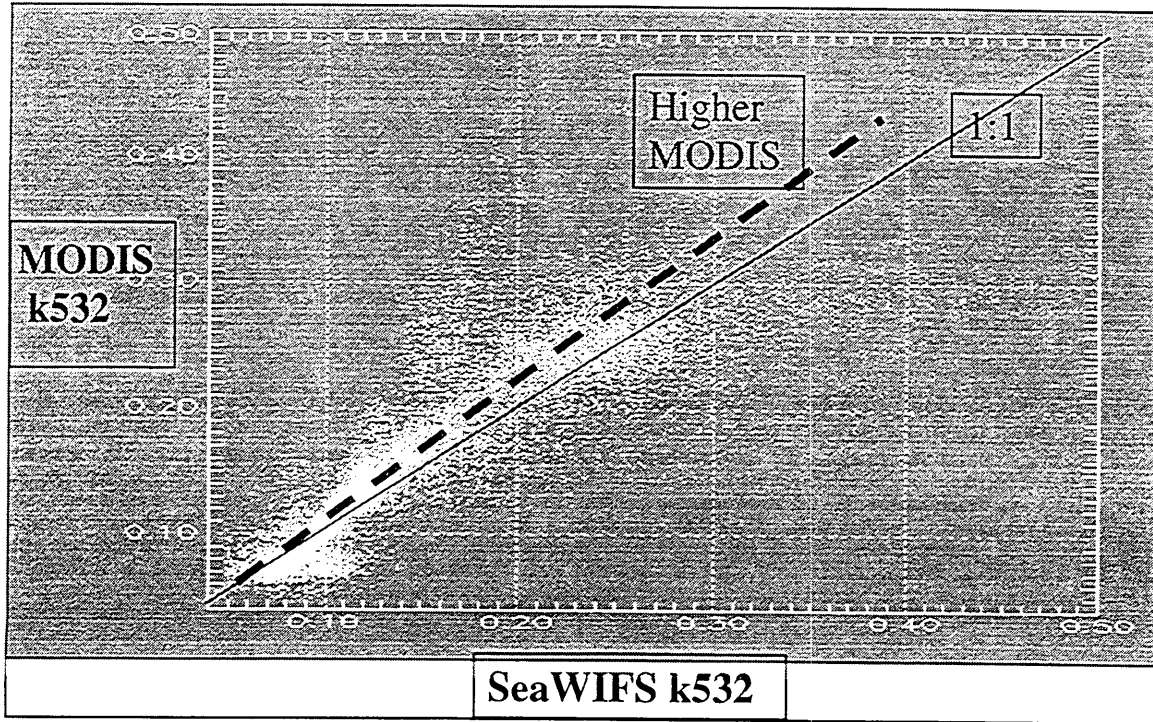


Figure 17.4: Examination of the effects due to differences in the aerosol models and optical depths that were used by the two satellites.

## Chapter 18

# Factors Affecting, and Impact of, Diazotrophic Microorganisms in the Western Equatorial Atlantic

Ajit Subramaniam

*University of Maryland, College Park, Maryland*

### 18.1 INTRODUCTION

The tropical Atlantic Ocean is a narrow basin surrounded by the largest and second largest river drainage systems in the world. It is characterized by substantial upwelling of subthermocline water rich in nutrients along its east coasts and the equator. Nutrients inputs from the riverine discharges and upwelling is further enhanced by the near chronic addition of Iron through dust blown from the Sahara and sub-Saharan Africa. The biological responses to these various forcings are clearly visible in ocean color satellite imagery as enhanced chlorophyll. However, there are few sea truth measurements that allow us to distinguish between real biological response and false positives due to the presence of dissolved organic matter transported by the rivers or the failure of atmospheric correction algorithms due to the presence of dust in the atmosphere.

Dove-tailing with two National Science Foundation funded studies – “Factors Affecting, and Impact of, Diazotrophic Microorganisms in the Western Equatorial Atlantic” and “Oceanic N<sub>2</sub> Fixation and Global Climate” – we are conducting field studies in the Atlantic and Pacific Oceans. The main objectives of our SIMBIOS funded project are to 1) validate ocean color satellite products using field measurements made under dusty skies and in the Amazon River plume, and 2) develop a semi-analytical *Trichodesmium* product. In this report, we present our activities in 2001.

### 18.2 RESEARCH ACTIVITIES AND RESULTS

We undertook two field surveys in the tropical and subtropical Atlantic Ocean – JAN01SJ in January/February 2001 and JUN01KN in June/August 2001. The JAN01SJ deployment lasted 47 days when 51 stations were occupied. Bio-optical profiles using a spectroradiometer, an AC9, a Hydrosat-6 and a CTD were made at 25 stations. Water samples taken for measuring particulate absorption, dissolved

absorption, fluorometric chlorophyll and HPLC pigments at six depths at these 25 stations. The JUN01KN deployment lasted 55 days and 55 stations were occupied. Bio-optical profiles using a spectroradiometer, an AC-9 and a CTD were taken at 43 stations. The Bio-optical measurements are described in detail below. A SIMBAD and a microtops sunphotometer were used on clear days on both cruises (12 microtops and 9 SIMBAD measurements in the JAN01SJ cruise and 18 microtops and 12 SIMBAD measurements on the JUN01KN cruise). A Brookhaven National Laboratory Shadowband radiometer was deployed on the JUN01KN cruise and about 50 days of data was collected.

The Atlantic SPMR free-falling spectroradiometer (13 channels at 340, 3880, 412, 443, 490, 510, 520, 555, 565, 620, 665, 670, 683 nm) was fished at least 20m away from the side of the ship and the matched surface reference sensor was floated 20m away from the ship. The slope and intercept of a linear regression to the natural log of the radiance data from the top 10m measured by the profiler was used to calculate the upwelling diffuse attenuation coefficient ( $K_d\lambda$ ), and the upwelling radiance at the surface.  $K_d\lambda$  from the profiler is also used to extrapolate the upwelling radiance from the surface reference from 0.75 cm to through the surface. The above surface downwelling irradiance measured by the surface reference is used to calculate two estimates of remote sensing reflectance and normalized water leaving radiance using the two estimate of water leaving radiance ( $L_w$ ). A SIMBAD was used on clear days to make above water radiance measurements following the SIMBIOS protocols Frouin (2000). After one dark scan, the SIMBAD is pointed directly at the sun for 3 scans. The instrument is then pointed at the water 45° from nadir and 135° from the sun's azimuth for 3 more scans, followed by 3 scans of the sun and one dark scan. The water-leaving radiance data from the three methods will be compared to each other and to the satellite-derived products.

Total absorption and attenuation profiles were made using an AC9 and following the protocols detailed by Twardowski *et al.* (1999). The AC9 was mounted in an optics cage along

with a Hydrosat (in the JAN01SJ cruise alone) and a Seabird CTD equipped with a Wetstar fluorometer. The optics cage was lowered at a rate of about 5m/minute in the water column to about 70m and then brought up, thus provide downcast and upcast profiles of total spectral absorption and attenuation at 9 wavelengths, spectral backscattering at 6 wavelengths, temperature, conductivity, and chlorophyll fluorescence.

Water was collected from six depths for phycoerythrin, fluorometric chlorophyll *a* (Trees *et al.* 2000), and HPLC pigment analysis and for particulate and dissolved absorption. The particulate and dissolved fractions of absorption were measured spectrophotometrically following Mitchell *et al.* (2000). Between 0.5 and 3L (depending on water type) of seawater was filtered through a GF/F filter and the absorption spectrum of the filter was measured for total particulate absorption using a Shimadzu UVPC2401 spectrophotometer. After measuring total absorption due to particulates, the filter was soaked in methanol (to remove polar soluble pigments) the absorption due to detritus was measured. Absorption due to the dissolved fraction was measured using a 10-cm path length cuvette filled with 0.2  $\mu$ m filtered seawater.

We have compiled a database of all the spectroradiometric remote sensing reflectance measurements made during cruises in the last three years (APR98RR, NOV99EW, JAN01SJ) where *Trichodesmium* counts was greater than about 1000 trichomes/L. We are working with Dr. Siegel and others at UC Santa Barbara to develop a semi-analytical model for detection of *Trichodesmium*. We have processed all the SeaWiFS imagery that corresponds to the field deployments (Figure 18.1) and are in the process of matching the field measurements to the satellite derived products.

### 18.3 FUTURE WORK

While much of the data described above has been processed, quality controlled and submitted to SeaBASS, due to the extremely long field deployments this year, we are still processing some data. We will complete match ups with both SeaWiFS and MODIS derived products. We plan to

participate in one short (~3 week) deployment in the tropical Atlantic Ocean, four short (~4 days each) deployments in Massachusetts Bay and one longer (45 days) deployment in the Pacific Ocean in 2002. We also hope to make significant progress in improving the *Trichodesmium* product.

### REFERENCES

- Frouin, R., B. Holben, M. Miller, C. Pietras, E. Ainsworth, J. Porter and K. Voss, 2000: Sun photometer and sky radiance measurements and data analysis protocols. *Ocean Optics Protocols for Satellite Ocean Color Sensor Validation, Revision 2*. G. S. F. a. J. L. Mueller. Greenbelt, MD, NASA GSFC. 2000-209966: 108-124.
- Mitchell, G. B., A. Bricaud, K. Carder, J. Cleveland, G. Ferrari, R. Gould, M. Kahru, M. Kishino, H. Maske, T. Moisan, L. Moore, N. Nelson, D. Phinney, R. Reynolds, H. Sosik, D. Stramski, S. Tassan, C. C. Trees, A. Weidemann, J. Wieland and A. Vodacek, 2000: Determination of spectral absorption coefficients of particles, dissolved material, and phytoplankton for discrete water samples. *Ocean Optics Protocols for Satellite Ocean Color Sensor Validation, Revision 2*. G. S. Fargion and J. L. Mueller. Greenbelt, MD, NASA GSFC. 2000-209966: 125-153.
- Trees, C. C., R. Bidigare, D. M. Karl and L. V. Heukelem, 2000: Fluorometric chlorophyll *a*: Sampling, laboratory methods, and data analysis protocols. *Ocean Optics Protocols for Satellite Ocean Color Sensor Validation, Revision 2*. G. S. Fargion and J. L. Mueller. Greenbelt, MD, NASA GSFC. 2000-209966: 162-169.
- Twardowski, M. S., J. M. Sullivan, et al., 1999: Microscale quantification of the absorption by dissolved and particulate material in coastal waters with an AC-9. *Journal of Atmos. Oceanic Tech* **16**: 691-707.

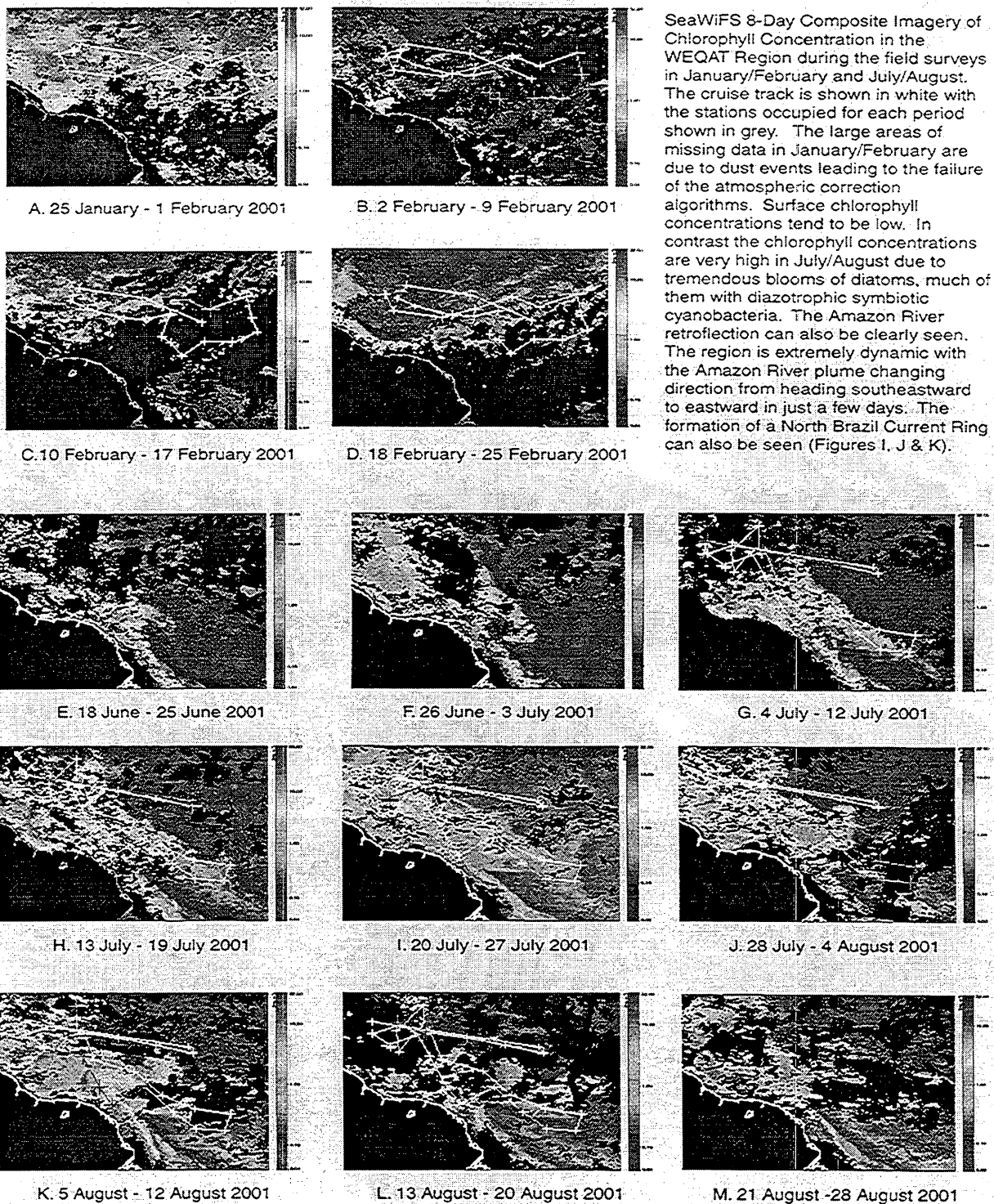


Figure 18.1: SeaWiFS 8-day composite imagery of chlorophyll concentration

*This research was supported by  
the SIMBIOS NASA contract #00192*

**PEER REVIEWED PUBLICATIONS**

Subramaniam, A., C. W. Brown, R. R. Hood, E. J. Carpenter, and D. G. Capone, 2001: Detecting *Trichodesmium* Blooms in SeaWiFS Imagery. *Deep-Sea Research Part II* Vol. 49/1-3 Pp 107-121.

Hood, R. R., A. Subramaniam, L.R. May, E.J. Carpenter, D.G. Capone, 2001: Remote Estimation of Nitrogen Fixation by *Trichodesmium*. *Deep-Sea Research Part II* Vol. 49/1-3 Pp 123-147.

Sañudo-Wilhelmy, S.A., Kustka, A.B., Gobler, C.J., Hutchins, D.A., Yang, M, Lwiza, K., Burns, J., Capone, D.G., Raven, J.A. and Carpenter, E.J., 2001: Phosphorus limitation of nitrogen fixation by *Trichodesmium* in the central Atlantic Ocean. *Nature* 411: 66-69.

Capone, D.G., 2001: Marine N<sub>2</sub> fixation: What's the fuss? *Current Opinions in Microbiology* 4: 341-348.

Michaels, A.F., D.M. Karl and D.G. Capone, in press: Element stoichiometry, new production and nitrogen fixation. *Oceanography*.

Karl, D.M., A. Michaels, B. Bergman, D.G. Capone, E.J. Carpenter, R. Letelier, F. Lipschultz, H. Paerl, D. Sigman and L. Stal, in press: Dinitrogen fixation in the world's oceans. *Biogeochemistry*.

**PRESENTATIONS**

Subramaniam, A., 2001: The PIRANA Paradigm. BioScience Day, University of Maryland. November 2001.

Carpenter *et al.*, 2001: Potential Influences of Riverine and Aeolian inputs on Nitrogen Fixation in the Atlantic. Biocomplexity Awardee Conference, National Science Foundation, Washington DC, October 2001.

Capone, D.G., 2001: Nitrogen fixation in the world's oceans. PICES meeting, Victoria, October 2001.

## Chapter 19

# HPLC Pigment Measurements For Algorithm Development and Validation in Support of the SIMBIOS Science Team

Chuck Trees and Jason Perl

*Center for Hydro-Optics and Remote Sensing, San Diego State University, California*

### 19.1 INTRODUCTION

Remotely sensed ocean color is determined by the absorption and scattering properties of dissolved organic material and suspended particulates. In most oceanic and many coastal areas, phytoplankton, with their associated suite of pigments, dominate the optical signal viewed by satellite sensors. These pigments have distinct spectral signatures, and therefore changes in the pigment-algal assemblage result in spectral shifts in absorption and reflectance. Therefore, accurate measurements of phytoplankton pigments are essential in understanding global carbon cycles in the ocean by minimizing satellite retrieval uncertainties when mapping these properties at regional to global scales.

The focus of this program is to characterize phytoplankton pigments in the water column during NASA's Sensor Intercomparison and Merger for Biological and Interdisciplinary Oceanic Studies (SIMBIOS) Project. This research is to provide high performance liquid chromatography (HPLC) pigment analysis on samples collected by the SIMBIOS Science Team for bio-optical algorithm validation and development. This effort will provide the SIMBIOS Project with an internally consistent pigment database of the highest quality to evaluate ocean color products.

### 19.2 RESEARCH ACTIVITIES

In November 2000, we received the new Thermo Quest Corporation's HPLC system, which was purchased by NASA, and included quaternary gradient pump (Model 4000), membrane degasser (Model SCM 1000E-010), autosampler with cooling and sample preparation options (Model AS3000-026), fluorometer (Model FL3000-140), photodiode array absorption detector (Model UV6000LP), Dell computer (Model GX110), DeskJet color printer *a*, allomer and epimer chlorophyll *a*, monovinyl chlorophyll *a* and divinyl chlorophyll *a*). Figure 19.1

(Model 600C), and HPLC software upgrades. In Jan 2001, a Thermo-Quest technician came to CHORS and setup the HPLC system, as well as installing the new software. Also during this period, we interviewed several applicants for the position of HPLC Analyst. We hired Mr. Jason Perl, who had worked for Dr. Ralf Goericke, SIO, for 3.5 years analyzing pigment samples by HPLC methods. Mr. Perl started work at CHORS on the 7th of Mar 2001 and has proved to be a valueable asset to the SIMBIOS Project. During the beginning of this year, the PI participated in the SIMBIOS Science Team Meeting and presented a review of pigment protocols to the various PI's collecting samples which included sampling, labeling, storage, and shipping.

During the first year of this contract, we started receiving pigment samples from other SIMBIOS PI's during the last week of April 2001. Because of the delay in receiving these samples, we were only able to process 1,362 pigment samples. The number of samples, analysis period and delivery date to the PI are shown in Table 1. In order to process these pigment samples, numerous pigment calibrations were performed. Nineteen pigment standards were purchased from DHI Water and Environment in Denmark which included the following; chlorophyll *c*2, chlorophyll *c*3, peridinin, 19' butanoyloxyfucoxanthin, fucoxanthin, 19' hexanoyloxyfucoxanthin, neoxanthin, prasinoxanthin, violaxanthin, diadinoxanthin, antheraxanthin, alloxanthin, diatoxanthin, lutein, zeaxanthin, crocoxanthin, echinenone, alpha-carotene, and beta-carotene. These standards were used to calibrate the absorption and fluorescence detectors. In addition, chlorophyll *a* and *b* standards were purchased at the same time from Sigma Chemical Company. The number of pigment calibrations, coefficient mean, standard deviation and coefficient of variation are summarized in Table 2. The chromatograms were analyzed and QC/QA protocols were followed. One such QC/QA method is to plot fluorometrically determined chlorophylls versus total HPLC chlorophyll *a* (chlorophyllide shows this plot indicating that the fluorometric method for estimating chlorophylls overestimates total chlorophyll *a*

by some 20%. This HPLC measured pigment data was compared to previously measured samples from a variety of research cruises over the last 15 years. Figure 19.2 shows this plot, indicating that these pigment data bases are not statistically different from each other.

Two intercalibration efforts on a small number of samples were performed between two other pigment laboratories. Duplicate samples were collected during cruises and/or deployments and then shipped to CHORS for analysis. This exercise showed that there was excellent agreement when photosynthetic and photoprotective carotenoids were compared. Large uncertainties were found when comparing monovinyl and divinyl chlorophyll *a* concentrations for one laboratory. For the other laboratory comparison differences were found for both chlorophylls *a* and *b*. We have been investigating these

differences and will follow this up with additional pigment intercalibration efforts.

### 19.3 FUTURE WORK

We processed all of the 1,362 pigment samples sent to CHORS during the first year of support. Comparisons between several laboratories on samples analyzed by the fluorometric method were in excellent agreement (within a few percent), where as, the HPLC inter-laboratory comparison had larger uncertainties. There were a few instrument malfunctions, but this not adversely effect HPLC pigment sample processing. Laboratory intercalibration efforts will continue so as to provide to the project an internally consistent pigment database.

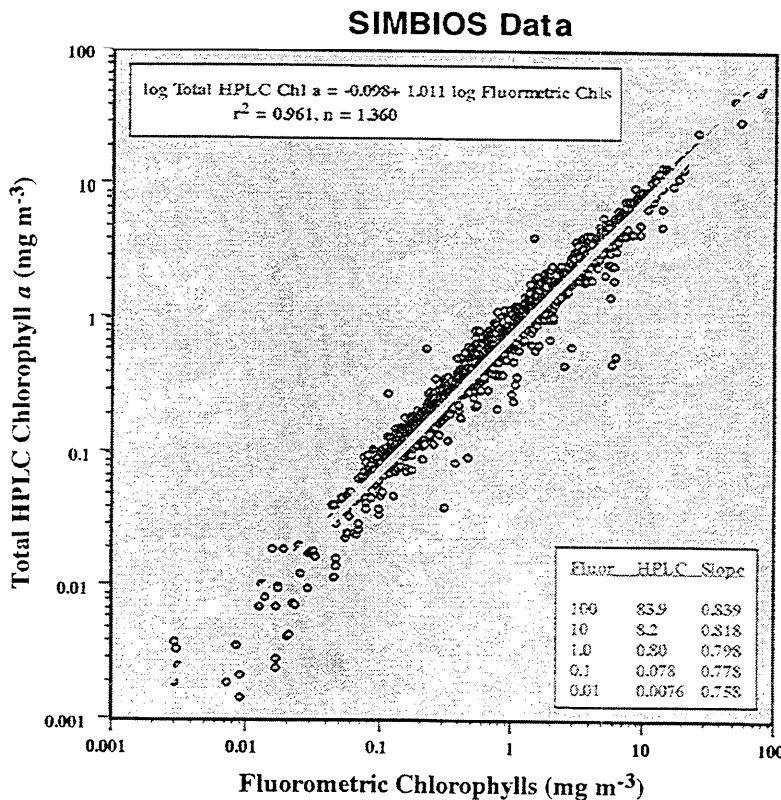


Figure 19.1: Regression model showing fluorometrically determined Chlorophyll *a* versus total Chlorophyll *a*

determined by HPLC.

## SIMBIOS and Others Data

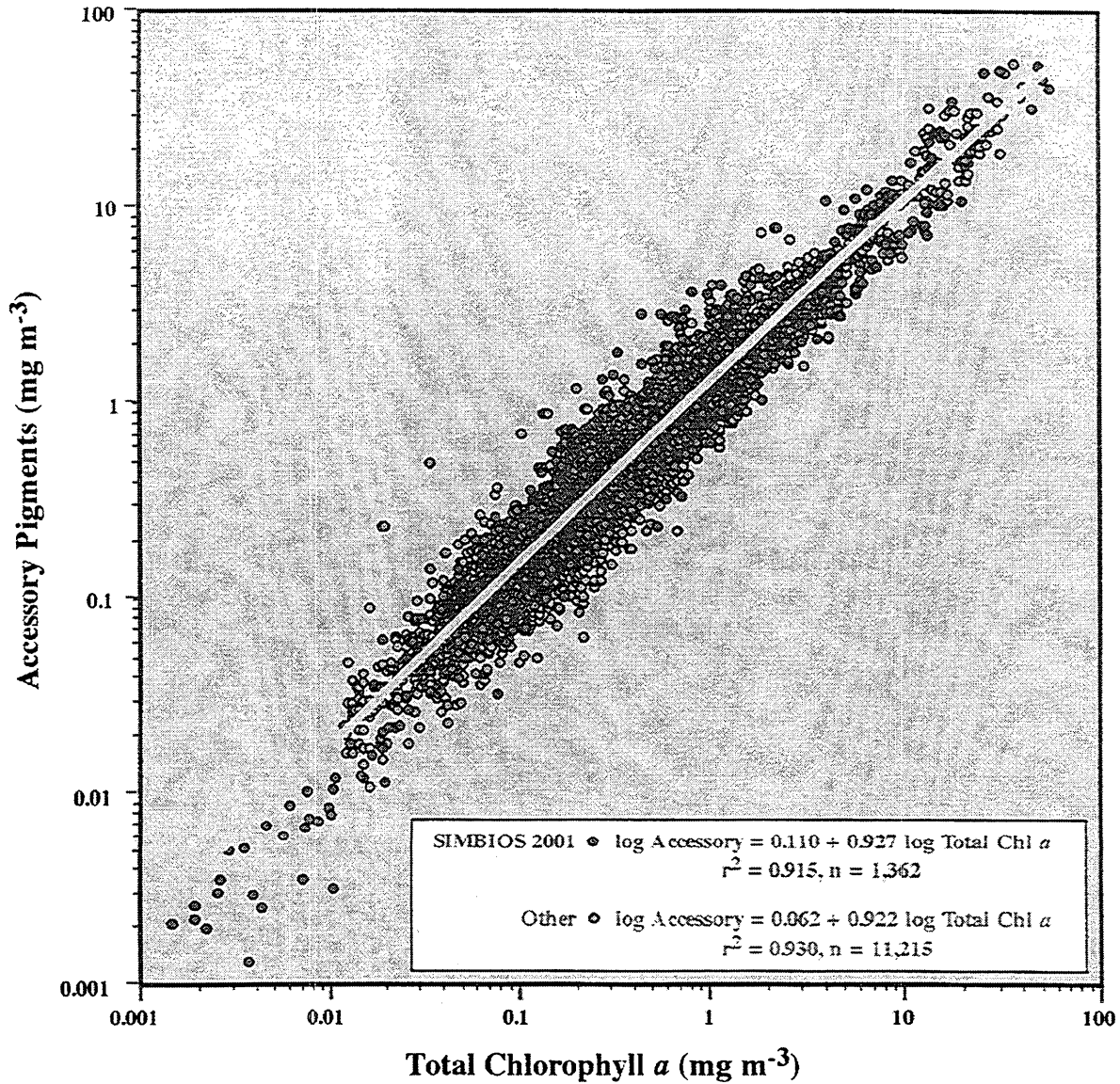


Figure 19.2: Regression model predicting accessory pigments versus total chlorophyll *a*, both determined by HPLC. The graph includes SIMBIOS data, as well as data collected from the global HPLC pigment data base.

Table 19.1: 2001 SIMBIOS-CHORS HPLC Status Log

R=received, RHPLC = run HPLC, CC/QC=concentration calculations and QC/QA, D=delivered								
PI	2001 Apr	2001 May	2001 Jun	2001 Jul	2001 Aug	2001 Sep	2001 Oct	2001 Nov
R. Stumpf	R	RHPLC	CC/QC			D	14	(33)
A. Subramaniam	R	RHPLC	CC/QC			D	149	(200)
D. Siegel		R	RHPLC	CC/QC		D	285	(299)
B. Arnone			R	RHPLC	CC/QC			D 107
					R, RHPLC, CC/QC			D 23
						R, RHPLC, CC/QC		D (45)
				R, RHPLC, CC/QC				R (50)
								D 209
G. Mitchell					R, RHPLC, CC/QC			D 144
F. Chavez					R, RHPLC, CC/QC			D 358 (91)
R. Morrison					R, RHPLC, CC/QC			D 44
Y. Dandonneau					R, RHPLC, CC/QC			D 21
L. Harding								R (18)
MOBY								

TABLE 19.2: During the last six months we performed up to five different HPLC pigment calibrations for a variety of phytoplankton pigments. The table below is a summary of these calibrations by pigment compound for the entire year (2001).

<b>Pigment Compound</b>	<b>Number of Calibrations</b>	<b>Mean</b>	<b>Standard Deviation</b>	<b>Coefficient of Variation</b>
Chlorophyll <i>a</i>	8	5.7270E-04	2.7750E-05	5
Chlorophyll <i>b</i>	8	4.3070E-04	2.5130E-05	6
Chlorophyll <i>c</i>	3	1.1490E-04	2.5800E-05	22
Peridinin	2	3.4820E-04	6.0570E-05	17
19'Butanoyloxyfucoxanthin	4	2.5310E-04	2.0270E-05	8
Fucoxanthin	4	2.5400E-04	1.1100E-05	4
19'Hexanoyloxyfucoxanthin	4	2.5720E-04	2.7290E-05	11
Diadinoxanthin	3	1.7170E-04	1.4860E-05	9
Diatoxanthin	4	1.6800E-04	1.7340E-05	10
Lutein	3	1.8090E-04	2.8020E-05	16

## Chapter 20

# Assessment, Validation, and Refinement of the Atmospheric Correction Algorithm for the Ocean Color Sensors

Menghua Wang

*University of Maryland, Baltimore County, Baltimore, Maryland*

### 20.1 INTRODUCTION

The primary focus of this proposed research is for the *atmospheric correction algorithms evaluation and development and satellite sensor calibration and characterization*. It is well known that the atmospheric correction, which removes more than 90% of sensor-measured signals contributed from atmosphere in the visible, is the key procedure in the ocean color remote sensing (Gordon and Wang, 1994). The accuracy and effectiveness of the atmospheric correction directly affect the remotely retrieved ocean bio-optical products. On the other hand, for ocean color remote sensing, in order to obtain the required accuracy in the derived water-leaving signals from satellite measurements, an on-orbit vicarious calibration of the whole system, i.e., sensor and algorithms, is necessary. In addition, it is important to address issues of (i) cross-calibration of two or more sensors and (ii) in-orbit vicarious calibration of the sensor-atmosphere system. The goal of these researches is to develop methods for meaningful comparison and possible merging of data products from multiple ocean color missions. With support and collaboration from the SIMBIOS project office, much efforts have been on studying and comparing the ocean color data derived from the Japanese Ocean Color and Temperature Scanner (OCTS) and the French Polarization and Directionality of the Earth's Reflectances (POLDER). OCTS and POLDER were both on board Japan's Sun-synchronous Advanced Earth Observing Satellite (ADEOS) from August 1996 to June 1997, collecting about 10 months of global ocean color data.

This provides a unique opportunity for developing methods and strategies for the merging of ocean color data from multiple ocean color sensors. In this report, I will very briefly discuss other research activities, but mainly focus on describe collective efforts (with SIMBIOS project office) in the OCTS and POLDER comparison study.

### 20.2 RESEARCH ACTIVITIES

- (a) Studies have been carried out to understand various effects on the performance of the SeaWiFS atmospheric correction algorithm for the ocean color and atmospheric aerosols: (i) the solar and viewing geometry effects, in particular, for cases of the large solar and viewing zenith angles; (ii) the Earth curvature effects, i.e., the spherical-shell atmosphere (SSA) vs. the plane-parallel atmosphere (PPA) (Ding and Gordon, 1994); (iii) effects of the sun glint contaminations on the derived SeaWiFS ocean and atmospheric products (Wang and Bailey, 2001); (iv) the effects of ocean surface wind speed on the SeaWiFS derived aerosol optical thickness; and (v) the effects of polarization in the aerosol lookup tables on the SeaWiFS derived ocean color and atmosphere products. These research works (except item (iii)) are still on going. Some preliminary results, however, show importance and necessary to account for some of these effects.
- (b) I have been working on activities for the International Ocean-Color Coordinating Group (IOCCG) atmospheric correction working group. The main objective of the working group is to quantify the performance of the various existing atmospheric correction algorithms used for the various ocean color missions. Therefore, the derived ocean color products from various ocean color missions can be meaningfully compared and possibly merged. As the atmospheric correction is a key procedure in the ocean color remote sensing, we want to answer question such as how can derived ocean color products from one sensor be best compared with those from others. We want to quantify the differences among the performance of the atmospheric correction algorithms. The core working group members are from OCTS/GLI (Japan), SeaWiFS (US), MODIS (US), POLDER (France), and MERIS (Europe). I am currently serving as the working group leader.
- (c) In collaboration with A. Isaacman, B. Franz, and C. McClain and the SIMBIOS project office, we have studied and compared the ocean color data derived the

OCTS and POLDER. The Japanese OCTS and French POLDER were both flown on the Japanese Sun-synchronous Advanced Earth Observing Satellite (ADEOS) from August 1996 to June 1997, collecting about 10 months of global ocean color data. ADEOS was on a polar orbit at an altitude of 800 km with local crossing time (descending node) at around 10:40 AM. This was the first time in history that two ocean color sensors were on board the same platform and viewed the global ocean with the same temporal and similar global spatial coverages. Therefore, it provides an ideal case for studying and comparing ocean color data derived from two different sensors, hence allowing development of a strategy for ocean color data merger from multiple ocean color sensors. In a recent study, Wang and Franz (2000) show that, using a vicarious inter-calibration approach between the MOS and the SeaWiFS (SeaWiFS ocean color data were used as "truth"), the ocean optical property data derived from two sensors can be meaningfully compared. The bias differences are significantly reduced between the two products. In that study (Wang and Franz, 2000), measurements from the two sensors had a temporal difference of about 90 minutes. In this study, we compare the ocean color data derived from OCTS and POLDER measurements using consistent data processing algorithms for both sensors and vicarious calibrations based on a common in situ data set from the Marine Optical Bouy (MOBY) (Clark et al., 1997) in the waters off Hawaii. Therefore, differences in the derived ocean color products from OCTS and POLDER are primarily associated with differences in instrument characteristics. A paper by Wang et al. (2002) was submitted to Applied Optics.

- (d) With requests from SIMBIOS project office, I have been helping and actively participating some on going SIMBIOS works/activities and other activities: (i) During Dr. Yongseung Kim's visit from Korea in Feb. 2001, I participated many discussions in helping for outline a strategy of the calibration and data processing for the Korea Ocean Scanning Multi-spectral Imager (OSMI). I have prepared and provided the necessary tables and data to process the OSMI data using the MSL12 and worked on some OSMI related issues; (ii) In collaboration with other SIMBIOS PIs and scientists, I have participated the CZCS data reanalysis effort for the data merging activity; (iii) I have been continuing some of the Germany Modular Optoelectronic Scanner (MOS) related works; and (iv) I have been actively participating the NASA-NASDA effort in processing the OCTS global data using the SIMBIOS MSL12 software.

## 20.3 RESEARCH RESULTS

Some results are briefly reported in here due to the length limitation for the document and also due to preliminary nature for some of on going works.

### *The Effects of the Wind on the SeaWiFS Aerosol Optical Thickness*

Various in situ matchup studies show that the SeaWiFS derived aerosol optical thickness at 865 nm is usually slightly overestimated comparing with the in situ observations. A study has been underway to evaluate the effects of ocean surface wind speed on the SeaWiFS derived aerosol optical thickness. Preliminary results show that, ignoring the surface wind speed in generating the aerosol lookup table, the derived aerosol optical thickness is usually overestimated by 10-20% for the global average wind speed (7.5 m/s). This could possibly explain why the SeaWiFS aerosol optical thickness is slight overestimated. Therefore, the overestimation of the SeaWiFS aerosol optical thickness is probably not from calibration of the SeaWiFS band 8. This work is continuing.

### *The Earth curvature Effects on the Rayleigh Radiance Computations*

The Earth curvature effects on the performance of the SeaWiFS atmospheric correction algorithm was studied by Ding and Gordon (1994) for a limited sensor viewing geometries. With some help from H. R. Gordon, some sensitivity studies have been conducted for a more complete solar and viewing geometries for the Earth's curvature effects on the Rayleigh radiance computations for the SeaWiFS wavelengths. Figure 20.1 provides example of the ratio values of the Rayleigh radiance computed using the spherical-shell-atmosphere (SSA) and the plane-parallel-atmosphere (PPA) for the various solar and viewing geometries and for the SeaWiFS 8 spectral bands. Note that the current SeaWiFS Rayleigh tables were computed using the PPA model. Figs. 1(a)-1(d) are ratio of the Rayleigh radiance values (SSA/PPA) for the solar zenith angles from 0°-80°, and for sensor zenith angles of 40°, 60°, 70°, and 80°, respectively. The relative azimuthal angle of 90° was used in the simulations. As expected, for the small solar and/or sensor zenith angles, the Earth curvature effects are negligible (ratios are nearly to 1), while for the very large angles there are some large radiance differences for the radiance computed using the PPA and SSA models. This work is still on going.

### The Solar and Viewing Geometry Effects

Simulations have been carried out for understanding of the solar and viewing geometry effects, in particular, for cases of the large solar and viewing zenith angles, on the performance of the SeaWiFS atmospheric corrections. Results show that, for maritime aerosols, the SeaWiFS atmospheric correction algorithm performed well for the solar and sensor zenith angles ranging from 0°-80°. However, there are some geometry dependences of results on the performance of the SeaWiFS atmospheric correction algorithm, more so on the relative azimuthal angle than the solar and sensor zenith angles. This work is continuing.

### Selected Results from OCTS/POLDER Comparisons

A series of measurements from OCTS and POLDER over the Sargasso Sea were collected for comparison. The satellite observations were obtained from a co-located 3°×3° box over the Sargasso Sea (latitude of 23.5°N to 26.5°N and longitude of 70°W to 73°W). Over the Sargasso Sea, OCTS data were all collected through the ground station at Wallops, Virginia. Therefore, OCTS data were processed from Level-0 to Level-1B using the SIMBIOS code, and then to Level-2 using MSL12. Figure 20.2 compares the histogram (%) of the retrieved normalized water-leaving radiance,  $[L_w(\lambda)]_N$ , between OCTS and POLDER over the Sargasso Sea. Over the Sargasso Sea, OCTS and POLDER data were acquired on November 20 and December 19 of 1996, and January 26, February 17, March 11, and April 14 of 1997 (there were data from each month for six months). Figs. 20.2(a)-2(f) are comparison results for the Sargasso Sea for data acquired from November 20, 1996 to April 14, 1997, respectively. The OCTS and POLDER  $[L_w(\lambda)]_N$  at 490 and 565 nm usually compare quite well, with small variations between the two measurements, while the POLDER  $[L_w(\lambda)]_N$  at 443 nm shows significant variations compared with the OCTS results (sometimes high and sometimes low). The shape of the histogram distributions from OCTS and POLDER, however, are generally similar. It was found that with our approach in processing OCTS and POLDER data, there are no obvious bias differences in the derived  $[L_w(\lambda)]_N$  between the two sensors, whereas the noise differences are difficult to correct since they depend mainly on the sensor characteristics.

## 20.4 FUTURE WORK

Research works will be continued to evaluate the various effects as discussed in this report on the performance of the

atmospheric correction and aerosol retrieval algorithms. It is planned to study and understand aerosol model effects and possibly to include other aerosol models, e.g., large particle size sea-salt aerosols (Porter and Clarke, 1997) and dust aerosol models (Longtin et al., 1988) for the dust study. It will also be continued in studying and development of the vicarious calibration and inter-calibration techniques from the in situ and/or various ocean color sensors measurements. This work will be certainly helpful to development of data merging techniques from multiple ocean color missions.

## REFERENCES

- Clark, D.K., H.R. Gordon, K.J. Voss, Y. Ge, W. Broenkow, and C. Trees 1997: Validation of atmospheric correction over the ocean, *J. Geophys. Res.*, **102**: 17,209-17,217.
- Ding, K., and H.R. Gordon 1994: Atmospheric correction of ocean-color sensors: effects of the Earth's curvature, *Appl. Opt.*, **33**: 7096-7106.
- Gordon, H.R., and M. Wang 1994: Retrieval of water-leaving radiance and aerosol optical thickness over the oceans with SeaWiFS: A preliminary algorithm, *Appl. Opt.*, **33**: 443-452.
- Longtin, D.R., E.P. Shettle, J.R. Hummel, and J.D. Pryce 1988: A Wind Dependent Desert Aerosol Model: Radiative Properties, AFGL-TR-88-0112, U.S. Air Force Geophysics Laboratory, Hanscom Air Force Base, Mass.
- Porter, J.N., and A.D. Clarke 1997: Aerosol size distribution models based on in situ measurements, *J. of Geophys. Res.*, **102**: 6035-6045.
- Wang, M., and S. Bailey 2001: Correction of the sun glint contamination on the SeaWiFS ocean and atmosphere products, *Appl. Opt.*, **40**: 4790-4798.
- Wang, M., and B.A. Franz 2000: Comparing the ocean color measurements between MOS and SeaWiFS: A vicarious intercalibration approach for MOS, *IEEE Trans. Geosci. Remote Sens.*, **38**: 184-197.
- Wang, M., A. Isaacman, B.A. Franz, and C.R. McClain 2002: Ocean color optical property data derived from OCTS and POLDER: A comparison study, *Appl. Opt.* (Accepted).

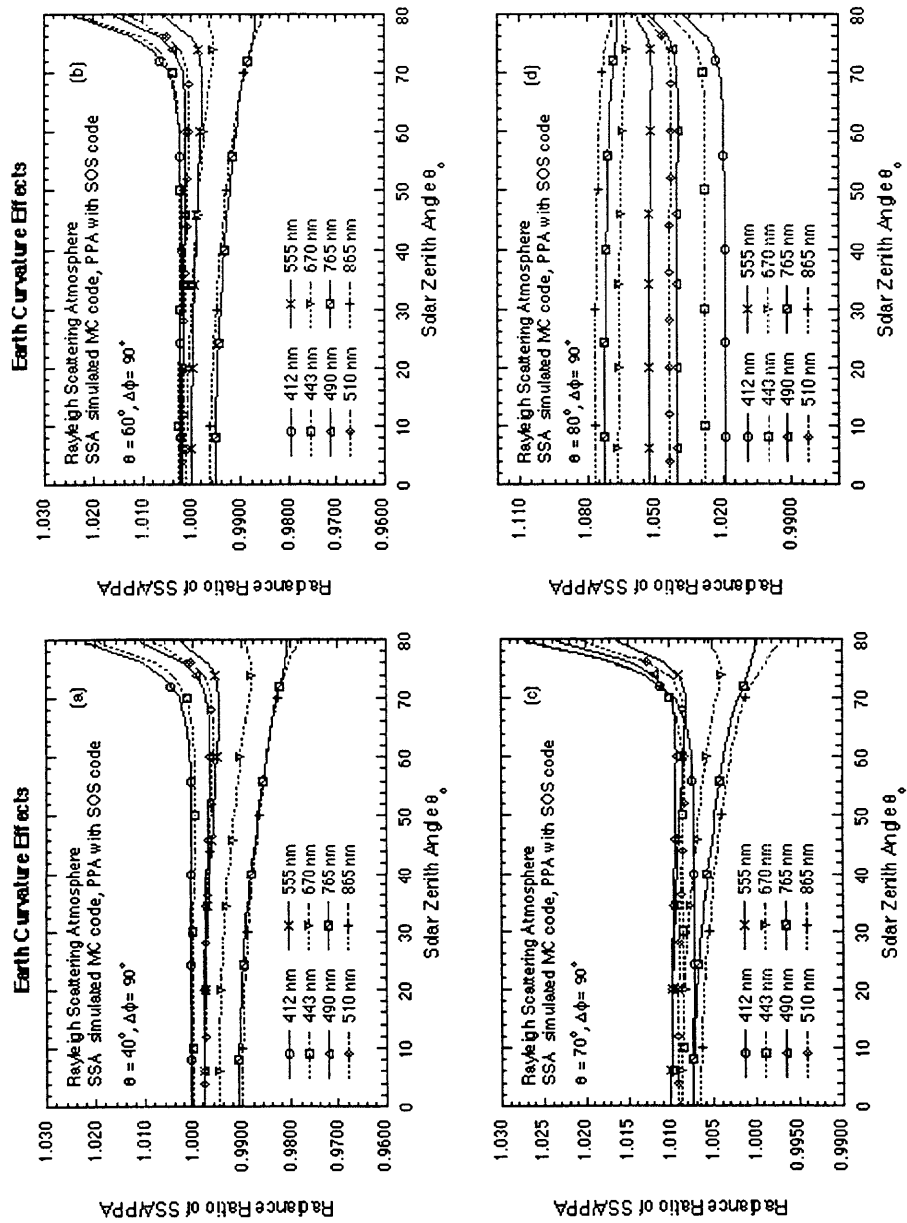


Figure 20.1: The ratio values of the Rayleigh radiance computed using the spherical-shell-atmosphere (SSA) and the plane-parallel-atmosphere (PPA) for the SeaWiFS 8 spectral bands and for the solar zenith angles from 0°-80° and sensor zenith angles of (a) 40°, (b) 60°, (c) 70°, and (d) 80°. The relative azimuthal angle of 90° was used.

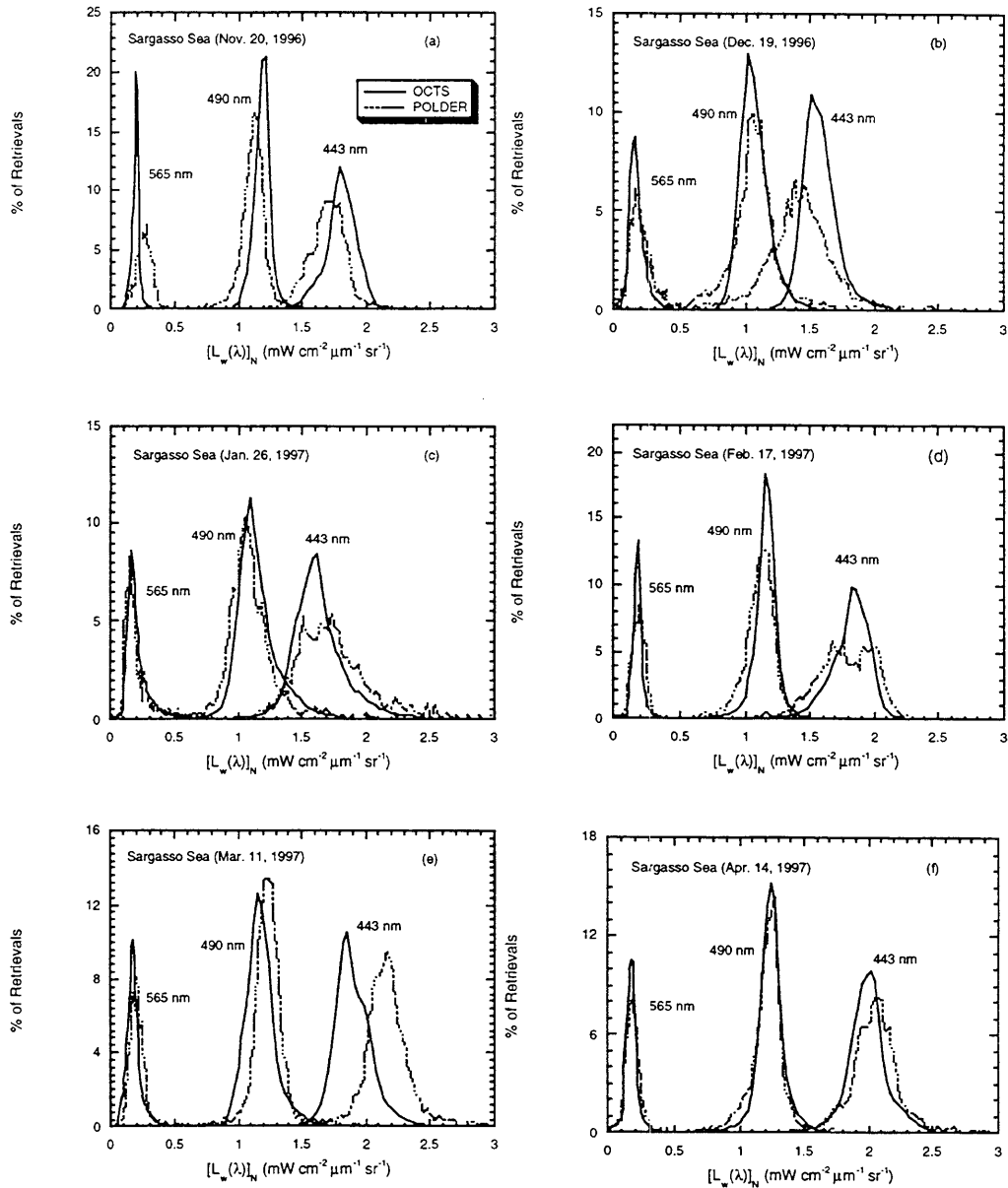


Figure 20.2: The histogram (%) of the OCTS-retrieved normalized water-leaving radiances at wavelengths 443, 490, and 565 nm compared with those from POLDER measurements over the Sargasso Sea for (a)-(f) from Nov. 20, 1996 to Apr. 14, 1997.

*This Research was supported by  
the NASA SIMBIOS Grant # NAS5-00203*

**PEER REVIEWED PUBLICATIONS**

Wang, M., B.A. Franz, R.A. Barnes, and C.R. McClain, 2001: Effects of spectral bandpass on SeaWiFS-retrieved near-surface optical properties of the ocean, *Appl. Opt.*, **39**, 343-348.

Wang, M. and S. W. Bailey, 2001: Correction of the Sun Glint Contamination on the SeaWiFS Ocean and Atmosphere Products, *Appl. Opt.*, **40**, 4790-4798.

**Accepted**

Chou, M. D., P. K. Chan, and M. Wang, Aerosol radiative forcing derived from SeaWiFS-retrieved aerosol optical properties, *J. Atmos. Sci.* (In press).

Eplee, R. E., Jr., W. D. Robinson, S. W. Bailey, D. K. Clark, P. J. Werdell, M. Wang, R. A. Barnes, and C.R. McClain The Calibration of SeaWiFS, Part 2: Vicarious Techniques, *Appl. Opt.* (In press).

Wang, M., A. Isaacman, B.A. Franz, and C.R. McClain Ocean Color Optical Property Data Derived from OCTS and POLDER: A Comparison Study, *Appl. Opt.* (Accepted).

Wang, M., The Rayleigh Lookup Tables for the SeaWiFS Data Processing: Accounting for the Effects of Ocean Surface Roughness, *Int. J. Remote Sens.* (Accepted).

**Submitted**

Gregg, W. W., M. E. Conkright, J. E. O'Reilly, F. S. Patt, M. Wang, J. Yoder, and N. Casey-McCabe, The NOAA-NASA CZCS reanalysis effort, *Appl. Opt.* (Submitted).

**PRESENTATIONS**

Wang, M. and S. W. Bailey, 2000: Correction of the sun glint contamination, presented at *the 5th Pacific Ocean Remote Sensing Conference*, Goa, India.

Wang, M., 2001: The IOCCG atmospheric correction working group status report, presented at *The Sixth IOCCG Committee Meeting*, La Jolla, California.

Wang, M., 2001: Retrieval of the aerosol optical properties from the SeaWiFS measurements, presented at *The AeroCenter Seminar Series*, NASA/GSFC, Greenbelt, Maryland.

Wang, M., 2001: Retrieval of ocean near-surface optical and microphysical properties from spaceborn sensors: Principles, Techniques, and Applications, Invited series of lectures presented at the National Satellite Ocean Application Service, Beijing, China.

Wang, M., 2001: Ocean color remote sensing, presented at the National Satellite Meteorology Research Institute, Beijing, China.

Wang, M., 2001: The current status of the atmospheric correction algorithms and vicarious calibration techniques for the ocean color remote sensing, Invited seminar presented at the Second Institute of Oceanography, Hangzhou, China.

## Chapter 21

# Measurements of the Vertical Structure of Aerosols and Clouds Over the Ocean Using Micro-pulse LIDAR Systems

Ellsworth J. Welton

*Goddard Earth Sciences and Technology Center, University of Maryland Baltimore County, Greenbelt, Maryland*

James D. Spinhirne

*NASA Goddard Space Flight Center, Greenbelt, Maryland*

James R. Campbell

*Science Systems and Applications, Inc., Lanham, Maryland*

Timothy A. Berkoff

*Goddard Earth Sciences and Technology Center, University of Maryland Baltimore County, Greenbelt, Maryland*

David Bates

*Physics Department, University of Miami, Coral Gables, Florida*

## 21.1 INTRODUCTION

The determination of the vertical distribution of aerosols and clouds over the ocean is needed for accurate retrievals of ocean color from satellites observations. The presence of absorbing aerosol layers, especially at altitudes above the boundary layer, has been shown to influence the calculation of ocean color [Gordon *et al.*, 1997a]. Also, satellite data must be correctly screened for the presence of clouds, particularly cirrus, in order to measure ocean color [Gordon *et al.*, 1997b].

One instrument capable of providing this information is a lidar, which uses pulses of laser light to profile the vertical distribution of aerosol and cloud layers in the atmosphere. However, lidar systems prior to the 1990s were large, expensive, and not eye-safe which made them unsuitable for cruise deployments. During the 1990s the first small, autonomous, and eye-safe lidar system became available: the micro-pulse lidar, or MPL [Spinhirne *et al.*, 1995]. The MPL is a compact and eye-safe lidar system capable of determining the range of aerosols and clouds by firing a short pulse of laser light (523 nm) and measuring the time-of-flight from pulse transmission to reception of a returned signal. The returned signal is a function of time, converted into range using the speed of light, and is proportional to the amount of light backscattered by atmospheric molecules (Rayleigh scattering), aerosols, and clouds. The MPL achieves ANSI eye-safe

standards by sending laser pulses at low energy ( $\mu\text{J}$ ) and expanding the beam to 20.32 cm in diameter. A fast pulse-repetition-frequency (2500 Hz) is used to achieve a good signal-to-noise, despite the low output energy. The MPL has a small field-of-view ( $\sim 100 \mu\text{rad}$ ) and signals received with the instrument do not contain multiple scattering effects. The MPL has been used successfully at a number of long-term sites and also in several field experiments around the world [Welton *et al.*, 2000; Peppler *et al.*, 2000; Voss *et al.*, 2001; Welton *et al.*, 2001a].

In 1999, members of the Micro-pulse Lidar group at GSFC submitted a proposal to organize a worldwide network of MPL systems to provide long-term measurements of the vertical distribution of clouds and aerosols at sites around the world. The original proposal also included support for a limited number of field experiments each year. In the summer of 2000, NASA EOS agreed to fund the proposal, and the MPL-Net project [Welton *et al.*, 2001b] was started. The CERES validation group at NASA LaRC contributed four MPL systems to MPL-Net, supplementing the existing stock of instruments. Finally, in the fall of 2000 the NASA SIMBIOS program agreed to fund another proposal to conduct lidar measurements from research vessels at sea using the SIMBIOS MPL system. This effort provides the SIMBIOS

project with continuous observations of aerosol and cloud vertical distributions during up to two cruises per year.

## 21.2 RESEARCH ACTIVITIES

### *ACE-Asia Cruise*

The third Aerosol Characterization Experiment (ACE) was conducted in Asia during March and April 2001. The experiment, referred to as ACE-Asia, utilized inland and island ground stations, aircraft, and ship platforms to study dust and pollution aerosols over Asia and the surrounding region. The Asian derived aerosols are important to satellite based ocean color measurements because the dust and pollution plumes transport far over the North Pacific Ocean. Dust absorbs sunlight in the visible wavelengths, and its vertical distribution over the ocean can affect the retrieval of ocean color.

The SIMBIOS MPL was deployed onboard the NOAA ship R/V Ronald H. Brown during ACE-Asia in order to determine the height of Asian aerosol plumes over the ocean. The MPL was operated from March 22 to April 20, 2001. Measurements were not continuous because of temperature stability problems in MPL van. The A/C unit on the van was damaged during a storm early in the cruise, and reliable temperature control was not possible for the remainder of the cruise. The MPL was operated only when the temperatures could be monitored manually, resulting in approximately 30% to 40% downtime over the whole cruise. The MPL ran continuously otherwise.

The MPL signals are stored at 1-minute time intervals, with a range resolution of 0.075 km from sea level up to a maximum altitude of 20 km. The raw data are converted into uncalibrated lidar signals, referred to as Normalized Relative Backscatter (NRB), using procedures discussed in *Campbell et al.* (2001) and *Welton and Campbell* (2001). The NRB signals are then analyzed to produce profiles of aerosol extinction and optical depth, and the layer averaged extinction-to-backscatter ratio, using techniques discussed in the Appendix of *Welton et al.* (2001a).

### *MPL Instrument Development*

The original MPL design used a fixed-place detector that was part of the optical path within the instrument. If the detector failed, it could not be replaced without performing a complete re-alignment of the MPL. This is not possible at sea. As a result, the health of the detector determined whether or not a particular cruise was a failure or a success. In order to overcome this problem, the MPL system was modified to incorporate a fiber-coupled detector. The detector itself is the same, however, it is no longer part of the optical path. It is connected to the optical path by a fiber cable. The detector can now be replaced by simply unscrewing the old detector from the fiber, and replacing it with a new one. This can be

accomplished at sea with a minimum of effort, and can be performed by anyone with a small amount of training.

## 21.3 RESEARCH RESULTS

Figure 21.1 shows a plot of the NRB signals vs. day of year during the ACE-Asia cruise. The gaps in data, due to the problems discussed in the previous section, are shown in black. Regions of higher signal indicate the presence of aerosols and clouds. The period around day 100, April 10, is of interest because the ship was in the Sea of Japan and positioned downwind of a massive dust storm that occurred a few days earlier over China. Preliminary aerosol optical data products have been generated for this time period. Figure 21.2 shows profiles of the NRB signal, extinction, and optical depth on April 10 at 0500 UTC. The aerosols are confined to two distinct layers. The lower layer extends from 0 to 2 km, and the upper from about 3.5 to 5.5 km. Cirrus is also present from 10 to 14 km, but is not included in the extinction retrieval because it is a cloud.

The aerosol extinction-to-backscatter ratio,  $S$ , for the lower and upper layers was 32 and 66 sr, respectively.  $S$  is proportional to the aerosol phase function at  $180^\circ$  and inversely proportional to the aerosol single scattering albedo. Layers with a high value of  $S$  tend to have a lower single scattering albedo, and therefore more aerosol absorption relative to layers with a lower value of  $S$ . The preliminary results shown here indicate that the upper aerosol layer was more absorbing than the lower layer. Therefore, the aerosols observed on this day may have influenced the retrieval of ocean color in this region.

This observation also serves as an example of the MPL's ability to distinguish aerosol layers from clouds. The microtops sunphotometer on the ship measured optical depths over 1 at 500 nm, at least 0.8 larger than the aerosol optical depth from the MPL. However, the NRB signal shows that a cirrus cloud was present during this time. The cirrus cloud optical depth was approximately 0.8 based on the difference between the microtops and MPL results.

## 21.4 FUTURE WORK

The results from the ACE-Asia cruise are still being analyzed. The NRB data has been fully processed and files are available on the SEABASS archive and also on the MPL-Net web-site (<http://virl.gsfc.nasa.gov/mpl-net/>). The remaining data products will be available only on the MPL-Net web-site. Some of these data are available now for the purpose of preparing papers, however the data are not quality assured. Final, quality assured extinction and optical depth data from ACE-Asia will be available by spring 2002 at the latest.

The results from the ACE-Asia cruise will be used together with other MPL-Net measurements made during the experiment to assess whether or not aerosol transport models predict the correct vertical distribution. This work will become

the focus of a paper over the course of the next several months. In addition, numerous publications, as co-authors, are planned with other researchers involved in ACE-Asia studies.

The MPL will be readied for the next series of deployments during 2002. A cruise is planned in the North Atlantic Ocean during the spring. This cruise will be aimed at studying the vertical distribution of Saharan dust over the ocean. Finally, the MPL will also be made available for a cruise scheduled in the summer. Our group will not participate directly in the cruise, but will help support the MPL measurements and analysis.

## REFERENCES

- Campbell, J.R., D.L. Hlavka, E.J. Welton, C.J. Flynn, D.D. Turner, J.D. Spinhirne, V.S. Scott, and I.H. Hwang. 2001: Full-time, Eye-Safe Cloud and Aerosol Lidar Observation at Atmospheric Radiation Measurement Program Sites: Instrument and Data Processing, *J. Atmos. Oceanic Technol.*, in press.
- Gordon, H. R., T. Du, and T. Zhang. 1997a: Remote sensing of ocean color and aerosol properties: resolving the issue of aerosol absorption, *Appl. Optics*, **36**, 8670-8684.
- Gordon, H. R., T. Zhang, F. He, and K. Ding. 1997b: Effects of stratospheric aerosols and thin cirrus clouds on atmospheric correction of ocean color imagery: Simulations, *Appl. Optics*, **36**, 682-697.
- Peppler, R.A., C.P. Bahrmann, J.C. Barnard, J.R. Campbell, M.D. Cheng, R.A. Ferrare, R.N. Halthore, L.A. Heilman, D.L. Hlavka, N.S. Laulainen, C.J. Lin, J.A. Ogren, M.R. Poellot, L.A. Remer, K. Sassen, J.D. Spinhirne, M. E. Splitt, and D.D. Turner. 2000: ARM Southern Great Plains Site Observations of the Smoke Pall Associated with the 1998 Central American Fires, *Bull. Amer. Meteor. Soc.*, **81**, 2563-2591.
- Spinhirne, J. D., Rall, J., and V. S. Scott. 1995: Compact eye-safe lidar systems. *Rev. Laser Eng.*, **23**, 26-32.
- Voss, K.J., E.J. Welton, P.K. Quinn, J. Johnson, A. Thompson, and H. Gordon. 2001: Lidar Measurements During Aerosols99, *J. Geophys. Res.*, **106**, 20821-20832.
- Welton, E.J., K.J. Voss, H.R. Gordon, H. Maring, A. Smirnov, B. Holben, B. Schmid, J.M. Livingston, P.B. Russell, P.A. Durkee, P. Formenti, M.O. Andreae. 2000: Ground-based Lidar Measurements of Aerosols During ACE-2: Instrument Description, Results, and Comparisons with other Ground-based and Airborne Measurements, *Tellus*, **B52**, 635-650.
- Welton, E.J., K.J. Voss, P.K. Quinn, P.J. Flatau, K. Markowicz, J.R. Campbell, J.D. Spinhirne, H.R. Gordon, and J.E. Johnson. 2001a: Measurements of aerosol vertical profiles and optical properties during INDOEX 1999 using micro-pulse lidars, *J. Geophys. Res.*, in press.
- Welton, E.J., J.R. Campbell, T.A. Berkoff, J.D. Spinhirne, S. Tsay, and B. Holben. 2001b: First Annual Report: The Micro-pulse Lidar Worldwide Observational Network, *Project Report*, <http://virl.gsfc.nasa.gov/mpl-net/>.
- Welton, E.J., and J.R. Campbell. 2001: Micro-pulse Lidar Signals: Uncertainty Analysis, *J. Atmos. Oceanic Technol.*, submitted.

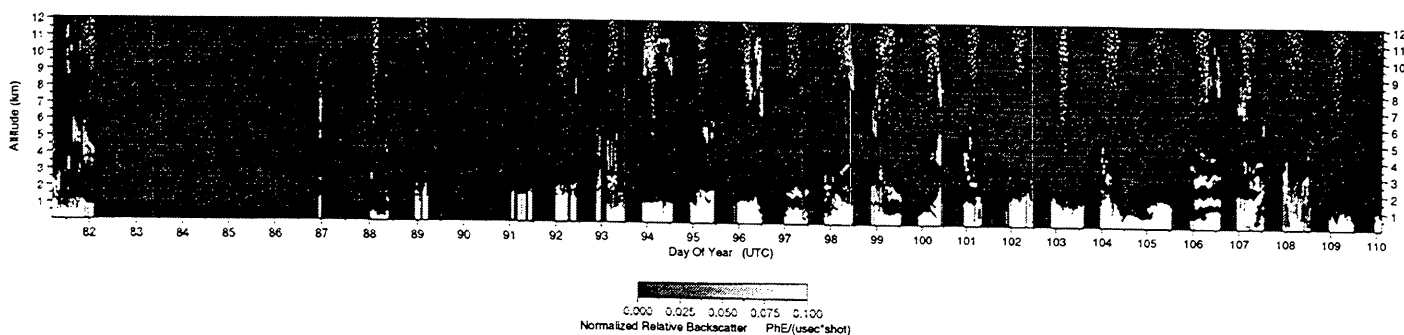


Figure 21.1: The Normalized relative backscatter (NRB) signals at 1-minute time resolution are plotted versus the day of the year during the ACE-Asia cruise.

0500 UTC.

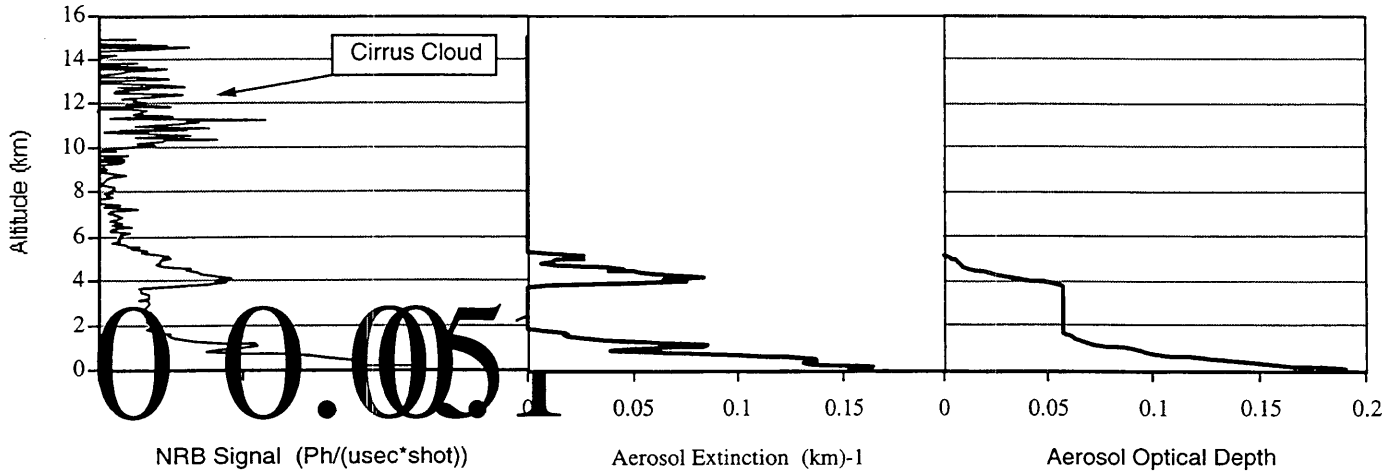


Figure 21.2: Profiles of the NRB signal, aerosol extinction, and aerosol optical depth are shown for 04/10/2001 at 0500 UTC

## Chapter 22

# Measurements and modeling of apparent optical properties of ocean waters in support to ocean color data calibration, validation, and merging

David Antoine, André Morel, Marcel Babin and Hervé Claustre

*Laboratoire d'Océanographie de Villefranche, CNRS-INSU, Villefranche sur Mer, France*

Stanford B. Hooker

*NASA/GSFC, Greenbelt, Maryland*

### 22.1 INTRODUCTION

This progress report does not show any results in terms of *in situ* data because the buoy deployment is only planned for late January 2002. The advancement of the buoy development and testing, of the instrument integration and testing, and of all other preparatory activities (in particular monthly cruises to the deployment site) are succinctly described here. The objectives and the analyses that are planned thanks to the data to be collected are also reminded. This project is supported by the European Space Agency (ESA/ESTEC contract N° 14393/00/NL/DC), the French Space Agency "Centre National d'Etudes Spatiales (CNES)", the "Centre National de la Recherche Scientifique (CNRS-INSU)" and the "Observatoire Océanologique de Villefranche sur mer". A prerequisite to building long-term (over decades) archives of ocean color, in response to the need for assessing the response of the oceanic biota to climate changes, is to accurately calibrate the top-of-atmosphere satellite observations, then to validate the surface geophysical parameters derived from these observations. Ensuring coherence between these geophysical products, as derived from different sensors, is also an important aspect to consider. When ocean color observations from different sensors are considered in view of data merging, their cross-calibration and validation might be facilitated if it could be "anchored" on continuous long-term *in situ* stations (IOCCG, 1999). Deploying and maintaining moorings that operate in a continuous way is, however, a difficult task.

In response to these concerns, we propose to carry out match-up analyses and vicarious calibration experiments, based on a data set to be built from a permanent marine optical buoy. This new type of marine optical buoy has been specifically designed for the acquisition of radiometric quantities, and has been already deployed in the Mediterranean sea in July 2000 (a deployment of 3 months for validating the mooring concept), between France and Corsica.

The vicarious calibration experiments should allow the top-of-atmosphere total radiance to be simulated and compared to the satellite measurements, in particular for the European MERIS sensor. By this way, the need for a change of the pre-flight calibration coefficients for a given sensor might be evaluated, and its amount quantified. From this data set, match-up analyses shall be also possible for chlorophyll concentration and water-leaving radiances, as well as algorithm evaluation (atmospheric correction and pigment retrieval). Because of a certain commonality in the band sets of the new-generation ocean color sensors, the data acquired with the buoy might be used for several of these sensors, and then contribute to the international effort of cross-calibrating them and of cross-validating their products, which are amongst the basic goals of SIMBIOS. In addition, some protocol issues (measurements) are specifically linked to the use of buoys, while others, of general concern to marine optics measurements, may find specific answers in the case buoys are used. We propose to examine these aspects, which, to our knowledge, have not been thoroughly investigated up to now.

#### *Description of the planned analyses*

Two main "vicarious" calibration paths exist to produce ocean color products of the desired accuracy, *i.e.*, water-leaving radiances within an error of about 5% in the blue for an oligotrophic ocean (Gordon, 1997, Antoine and Morel, 1999). The first one is usually referred to as "vicarious calibration", and consists in forcing the satellite-derived water-leaving radiances to agree with a set of *in situ* water-leaving radiances ("match-up analyses"). A set of "vicarious calibration coefficients" is therefore obtained, which is applied to the Top-of-atmosphere (TOA) total radiances measured by the sensor. The second procedure, which is also an indirect ("vicarious") calibration is sometimes referred to as a "radiometric calibration", and consists in simulating the TOA signal that the sensor should measure under certain conditions,

and to compare it to the measured signal. Inconveniences of the first type of “vicarious calibration” is that it is dependent upon the procedure used for the atmospheric correction of the TOA observations. The advantage of this technique is, however, and besides the fact that atmospheric measurements are not needed, that the marine signals delivered by several sensors that use different atmospheric correction algorithms can be cross-calibrated provided that the same set of *in situ* water-leaving radiances is used to perform the vicarious calibration. This is presently the case, for instance, for the SeaWiFS and OCTS sensors. Inconveniences of the vicarious “radiometric calibration” is that it requires a set of *in situ* measurements that is usually difficult to gather, among other things because a high accuracy is needed. In addition to the in-water measurements of the water-leaving radiances, this data set includes : sea state and atmospheric pressure, ozone concentration, aerosol optical thickness, aerosol type, and even aerosol vertical profile if the aerosols reveal to be absorbing. If this data set is successfully assembled, the great advantage of the vicarious “radiometric calibration” is that it is independent of the atmospheric correction algorithms, so that the TOA signals of various sensors can be cross-calibrated. Then it is up to any user to apply its preferred atmospheric correction to these TOA signals. The marine signals in that case might be inconsistent if significant differences exist in the various atmospheric corrections.

#### Match-up analyses

Match-up analyses should be possible for water-leaving radiances, as well as for chlorophyll concentrations, which are, however, only collected on a monthly basis (HPLC), during servicing to the mooring. The chlorophyll fluorescence is recorded in a continuous way, yet we cannot ascertain that its conversion into chlorophyll units, based on the monthly HPLC determinations, will be able to generate concentrations with an accuracy suitable for match-ups.

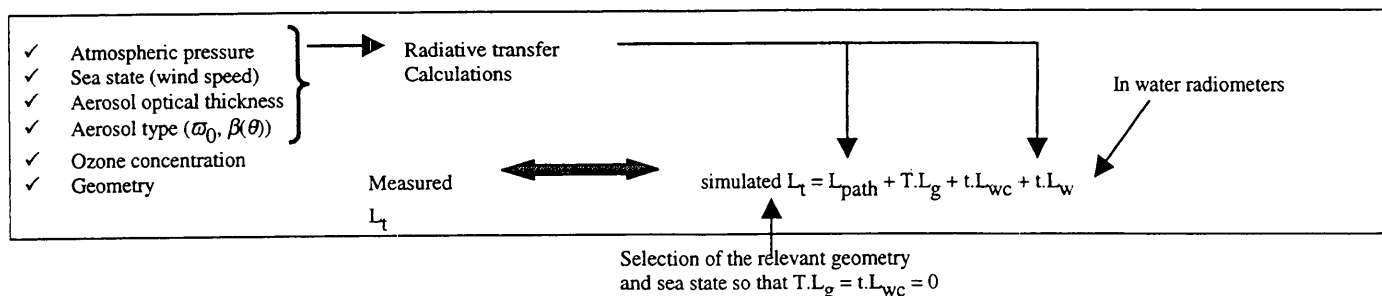
#### Vicarious calibration experiments

This is probably one of the most challenging parts of this project, aside from technological development. Indeed, we should have in hand all the necessary tools and data to generate TOA total radiances and to compare them to their “satellite equivalent” (e.g., see Gordon, 1998), yet it would be risky to warrant in advance that a 5% absolute accuracy (i.e., what is aimed at with the new-generation ocean color sensors, e.g., Gordon, 1997) will be reached.

The greatest difficulty, at least to our opinion, lies in a correct estimation of the aerosol optical thickness, phase function, and single scattering albedo. These parameters are accessible through the inversion of sun photometer measurements, yet uncertainties inevitably occur when applying such methods. Assembling all data needed for these vicarious calibration experiments will be often compromised only because aerosol parameters are not accurate enough. Nevertheless, we hope that over the 3 years of the project, enough relevant data will be gathered for that purpose. Therefore, we will set up a “toolbox” based on codes available at LOV, and which will be fed with all observation listed in the preceding sections, with the aim of generating the TOA radiances needed for vicarious calibrations. The error budget of these computations will be also examined. This may include, not exhaustively, the assessment of the impact of (1) the various ways of computing the water-leaving radiance from the below-water measurements of radiances and irradiances, (2) the uncertainties in the representation of surface roughness, and (3) the selection of a given RT code.

Inversion of the sun photometer measurements in order to get the aerosol optical thickness will follow the usual procedure, as described for instance in Frouin *et al.* (2000). There exist a variety of algorithms for the inversion of the sky radiance measurements (Wang and Gordon, 1993; Nakajima *et al.*, 1983, 1996; Dubovik and King, 2000; Dubovik *et al.*, 2000). Evaluation of these various algorithms is out of our scope, yet we will try to implement the most adapted ones in order to get some idea about the uncertainties attached to our retrievals. The routine processing performed by the AERONET will anyway already provide the necessary data, so that implementation of procedures at LOV will mostly be motivated by scientific purposes, which not necessarily intervene in the frame of the MERIS cal/val activities.

When the desired data are obtained, they will be used as inputs and boundary conditions to radiative transfer calculations. We can use several codes available at LOV, namely a Monte Carlo code (cross-validated with respect to other codes in Mobley *et al.*, 1995), the Hydrolight® code (Mobley, 1994), and the MOM code (Matrix Operator Method, developed by J. Fischer and collaborators at the Free University of Berlin). The simulated TOA total radiances will be then compared to their equivalent extracted from MERIS full resolution images. The principle is the following (L is for radiance, and the subscripts “t” for total TOA, “g” for sun glint, “wc” for white caps, and “w” for water-leaving; T and t and the direct and diffuse atmospheric transmittances, respectively):



*Preparatory activities: Buoy's design*

The design of the buoy, managed by the ACRI-in company, started in fall 1999 and led to a totally new type of optical buoy. The following paragraphs summarize the rationale for its design and the main characteristics of the system. Platforms developed for oceanographic purposes are rarely adapted to the deployment of radiometers at sea. Indeed, recording the light field within the ocean interior is difficult because the instruments themselves and, more dramatically, the platform onto which they are installed, inevitably introduce perturbations. Other difficulties originate from the need to keep the instruments as much horizontal as possible, either because a plane irradiance is aimed at (cosine sensor), or if a given direction (generally nadir) is aimed at. The actual measurement depth is also difficult to accurately assess, because rapid vertical displacements of the instruments sometimes occur, which prevent any precise estimation of pressure, thence of depth. Considering the above observations (among others), we have developed a new type of platform, dedicated to radiometry measurements, able to minimize shadowing effects, to minimize perturbation of the sub-marine light field, and to warrant the stability of the instruments.

The principle is that of a "reversed pendulum", with Archimedes thrust replacing gravity. A large sphere ( $\varnothing$  1.8 m) is stabilized at a 18 meters depth out of the effect of most swells (a cable goes down to the sea floor), and creates the main buoyancy. Above the sphere, a rigid, tubular, structure is fixed, which hosts the instrumentation onto horizontal arms (at 5 and 9 meters). An ~3 tons thrust ensures the stability of the system, which is subject to very limited forces from the so-called "transparent-to-swells" superstructure. With such a design, there is no large body at the surface generating shade.

*Reduced-scale model of the buoy and tests in an engineering pool*

A reduced scale model (scale 1/10) has been developed in order to verify the theoretical predictions, and it has been tested in an engineering pool (dimensions in meters 24x16x3, with a 10-meters shaft), by applying to it several types of swells and currents (mono chromatic or random swells, up to 5 meters real scale). Results of these tests have fully confirmed the theoretical predictions that were previously carried out, in terms of horizontal and vertical displacements (the latter are extremely low), as well as in terms of angular deviations from the vertical. For instance, the mean tilt of the buoy is  $\sim 4^\circ$  (with  $\pm 4^\circ$  of pitching), for a 4.6-meter swell of period 5.2 seconds. These tests have also confirmed that no "hidden defect", hardly discernible via calculations only, was compromising the feasibility of the system. The tests were fully conclusive and led to the construction of the first "beta version" of the buoy, in aluminum.

*Qualification by a 3-month test deployment of the buoy on site*

The full scale "beta version" was built in spring 2000 (Figure 22.1). The material was aluminum. It is made of two parts, the lower one which is from -20 meters to -9 meters below the surface and consists of the sphere and a simple tubular structure, and the upper one which goes from -9 meters below the surface to +4.5 meters above the surface, and which hosts the instrumentation. The full-scale beta version has been deployed on site during 3 months (20 of July to 20 of October, 2000), which allowed to encounter a variety of meteorological situations. The buoy was equipped with two inclinometers, a pressure sensor, an ARGOS beacon and a flashlight. The goal of this deployment was to qualify the new concept of buoy as well as to identify possible problems necessitating modifications. The results of the qualification deployment showed a certain lack of righting torque, with consequences on the behavior of the buoy when the swell becomes greater than about 2 meters. Although not dramatic, this behavior is not totally satisfactory, so that it was decided to introduce slight modifications in the design and construction of the buoy in order to improve the percentage of time for which the requirements in terms of inclination is satisfied.

*Modifications introduced in the buoy's design and construction*

One modification has been introduced in the design, by installing the sphere at 17 meters instead of 18 meters. By this way, the distance from the center of the sphere to the fixation of the buoy to the mooring cable is one meter greater (the righting torque is therefore much larger). Another modification has been introduced in the materials used to build the upper part of the buoy (the one hosting the instrumentation), from aluminum to carbon composite. A specific study has been conducted to check that this composite material was adapted to our problem, which is definitely the case.

The impacts of these 2 changes on the upper part of the system are : rigidity is improved, weight is diminished by the 2/3, corrosion is eliminated, the drag coefficient is reduced by the use of tubes with a lower diameter, and the elastic limit is larger than it was in comparison to the forces imposed by breaking waves. At the end, a net gain of 60% in the righting torque has been obtained for the full buoy. The first deployment of this modified version of the buoy, fully equipped, is planned for no later than the end of January 2002, weather permitting.

### *The instrumentation on the buoy*

The full system, developed by Satlantic Inc., has been delivered in Villefranche on the 24<sup>th</sup> of October, 2001. Its physical integration on the buoy and the subsequent testing will probably last until mid December 2001. It is reminded that the system comprises:

- Radiometers of the Satlantic 200 series, measuring  $E_s$  (at +4.5 meters above surface), and  $E_d$ ,  $E_u$ , and  $L_u$  (nadir) at 2 depths, namely 5 and 9 meters. The 2-axis tilt and the pressure are also recorded. The buoy orientation with respect to the sun is also recorded.
- Fluorometers, at the 2 same depths, for a proxy to Chl.
- Transmissometer, at the deepest sampling depth, *i.e.*, 9 meters, for a proxy to the particle load.
- CTD, at 9 meters, mainly for pressure and temperature.
- Backscattering meter for a proxy to  $b_b$  at 2 wavelengths (443 and 560 nm), at 9 meters.
- The set of parameters directly derived from the measurements is described in section 11.
- From these measurements, various AOPs or IOPs might be derived, as the water-leaving radiance,  $L_w$ , the diffuse attenuation coefficients for upwelling and downwelling irradiance,  $K_u$  and  $K_d$ , the attenuation coefficient for upwelling radiance,  $K_L$ , the diffuse reflectance just below the sea surface,  $R$ , the "nadir Q" factor,  $E_u/L_u$ , the attenuation and backscattering coefficients,  $c$  and  $b_b$ . The absorption coefficient,  $a$ , will be tentatively derived through inversion of the AOPs (using for instance  $K_d$  and  $R$ ).

All measurements will be simultaneously collected, and centralized by a unique (acquisition / storage / communication) system, that will merge the data and send them to the visiting ship via a RF link. Part of the data is transmitted in real time by an ARGOS link (only for checking that everything's working well and that batteries are Ok).

### *The coastal site for atmospheric measurements*

A coastal site (Cap Ferrat, in front of the laboratory) should be equipped with an automatic sun photometer station, introduced within the AERONET. This equipment should provide continuous record of the sky radiances at this site, from which information about aerosol types and aerosol optical thickness will be retrieved.

### *Atmospheric measurements : ship-of-opportunity*

In order to increase the number of determination of the aerosol optical thickness on the buoy site, a portable sun photometer shall be installed on the ships that daily cross from Nice to Corsica, and which go near the buoy site. The operation of such an instrument is simple enough to expect a significant percentage of good-quality measurement, if performed by trained crewmembers. These operations are under negotiation with the company that manages the ships.

### *Set up of the monthly additional measurements and BOUSSOLE site characterization*

Eighteen days of ship time have been obtained in 2001 from CNRS-INSU, as 6 campaigns of 3 days. They were initially planned for starting the monthly servicing of the buoy, in case it would have been deployed in July 2001 (initial plan). Because the buoy is still not deployed, the first 4 of these campaigns (end of July, beginning of September, October and November) have been used to prepare and organize most of the activities that will be necessary during monthly servicing to the buoy. These activities have included:

- Verification of the mooring line by divers (still on site; only the buoy has been removed).
- Deployment of several optical profilers (50 vertical profiles have been acquired), including the LOV' SPMR, the NASA' MicroNESS (collaboration Stan Hooker) and a new hyper-spectral profiler developed by Satlantic Inc. (collaboration M. Lewis).
- Pigment determination (HPLC; 35 surface samples).
- CTD profiles (25 profiles).
- Inter-comparison between above-water and below-water determination of the water-leaving radiances.
- Characterization of the spatial heterogeneity of the site, by following a grid pattern with a fluorometer, the pattern being then calibrated in terms of chlorophyll concentration by taking discrete samples along the grid.

The remaining two campaigns to be carried out until the end of 2001 (beginning and mid of December) will be devoted to the same kind of activities, and to the testing of the instrumentation of the buoy (using a rosette frame to be deployed from the ship). The other operations and measurements that will be progressively introduced in 2002 are :

- Replacement of radiometers by divers
- Cleaning/verification of the buoy

- IOP profiles (absorption, attenuation), IOP determination on the HPLC samples.

*Inter-comparison between above-water and in-water determination of the water-leaving radiance*

As part of the preparatory activities that we carry out in the frame of BOUSSOLE, we have pursued the comparative evaluation of the above-water determination of the water-leaving radiances against the under-water determination of this key parameter. The above-water data have been collected with a SIMBADA radiometer (developed and maintained by LOA in Lille, France; data processing also performed by LOA), and the in-water determination from our SPMR profiler and the MicroNESS profiler (NASA; only in July). The data are still under processing and the results of these inter-comparisons will be probably available in 2002. From these results, it will be decided whether or not it is useful to continue the above-water measurements.

*Plans for calibration of the radiometers*

The SQM-II (*i.e.*, the high stability lamp used for relative calibration) will be kept in the laboratory, and we will replace each month one set of instruments by a new, cleaned and calibrated, set of instruments. The recovered set of radiometers is brought back to the lab for calibration, cleaning, and repair if necessary. One month later, the exchange is again performed and so on. We first have set up the installation of the SQM-II and have worked towards establishing the routine operations that will be necessary each month on each set of radiometers (the so-called "SQM sessions").

*Bidirectionality of the ocean reflectance: Selection of adequate IOP for Case 1 waters*

A revision of the inherent optical properties of oceanic waters, which includes the consideration of the absorption values by pure waters (Pope and Fry, 1997), has been published (Morel and Maritorena, 2001). In addition, a new parameterization of the particle volume scattering function (VSF) has been developed, which allows the shape of the VSF to be regularly changing with the chlorophyll concentration (Chl). With these VSF, the backscattering ratio is decreasing, from 1.23 to 0.45 % when Chl increases from 0.01 to 10 mg m<sup>-3</sup>. These values are more realistic when introduced in a reflectance modeling, and when the modeled results are compared to actual reflectance spectra. They remove the weaknesses which previously resulted from the use of a single particle VSF (that of Petzold, with a backscattering ratio of 1.9%), whatever Chl. The shape and magnitude of the VSF are crucial in driving the angular pattern of the upward

radiance field, and thus the BRDF properties (and Tables). The recent radiative transfer computations and the production of the BRDF Lookup Tables have been performed by using these revisited IOPs.

*Raman scattering influence on the upward radiance field and bidirectional properties.*

In addition, the computations of these tables have been carried by accounting for the inelastic Raman scattering. The BRDF parameters are, as expected, sensitive to this emission for Chl values up to 0.3, even 1 mg m<sup>-3</sup> (in the red part of the spectrum). These Tables have been transferred to NASA. They are commented in detail in a Chapter of the revised version of the Ocean Optics Protocols for Satellite Ocean Color Sensor Validation (Version 3) prepared by J. Mueller (Chapter XIII « Normalized water-leaving radiance and remote sensing reflectance: Bidirectional reflectance and other factors »). This chapter describes the implication of bidirectionality onto ocean optics measurements, particularly in the frame of calibration of satellite data through in situ measurements (above and in-water determinations of water-leaving radiances). The bidirectional properties have also been summarized and their consequences examined when the merging of various satellite data is envisaged (Correction of bidirectional effects for an optimal binning of ocean color data). This will be a part of a document currently prepared by a Ad Hoc group, set up by IOCCG in January 2001 (D. Antoine, Chairman), with the aim of examining the binning issues of ocean color data.

## REFERENCES

- Antoine, D. and A. Morel, 1999: A multiple scattering algorithm for atmospheric correction of remotely-sensed ocean colour (MERIS instrument) : principle and implementation for atmospheres carrying various aerosols including absorbing ones, *Int. J. Remote Sensing* **20**, 1875-1916.
- Dubovik, O. and M.D.King, 2000: A flexible inversion algorithm for retrieval of aerosol optical properties from Sun and sky radiance measurements, *J. Geophys. Res.* **105**, 20673-20696.
- Dubovik, O., A.Smirnov, B.N.Holben, M.D.King, Y.J. Kaufman, T.F.Eck, and I.Slutsker, 2000: Accuracy assessments of aerosol optical properties retrieved from AERONET Sun and sky-radiance measurements, *J. Geophys. Res.* **105**, 9791-9806.

- Frouin R., B. Holben, M. Miller, C. Pietras, E. Ainsworth, J. Porter, and K. Voss, 2000: Sun and Sky radiance measurements and data analysis protocols, in "Ocean optics protocols for satellite ocean color sensor validation, revision 2", NASA/TM-2000-209966, NASA GSFC, 108-124.
- Gordon, H. R., 1997: Atmospheric correction of ocean color imagery in the Earth observing system era, *J. Geophys. Res.* **102**, 17081-17106.
- Gordon, H.R., 1998, In-Orbit calibration strategy for ocean color sensors, *Rem. Sens. Environ.* **63**, 265-278.
- IOCCG, 1999: Status and plans for satellite ocean-colour missions : considerations for complementary missions. Yoder, J.A. (ed.), Reports of the International Ocean-Colour Coordinating Group, No. 2, IOCCG, Dartmouth, Canada.
- Mobley, C.D., 1994: Light and water : radiative transfer in natural waters, Academic Press, London, 92 pp.
- Mobley, C. D., Gentili, B., Gordon, H. R., Jin, Z., Kattawar, G. W., Morel, A., Reinersman, P., Stamnes, K., and Stavn, R. H., 1993: Comparison of numerical models for computing underwater light fields, *Appl. Opt.* **32**, 7484-7504.
- Morel, A. and S. Maritorena, 2001: Bio-optical properties of oceanic waters : a reappraisal *J. Geophys. Res.* **106**, 7163-7180.
- Nakajima, T., M. Tanaka, and T. Yamauchi, 1983: Retrieval of the optical properties of aerosols from aureole and extinction data. *Appl. Opt.* **22**, 2951-2959.
- Nakajima, T., G. Tonna, R. Rao, P. Boi, Y. Kaufman, and B. Holben, 1996: Use of sky brightness measurements from ground for remote sensing of particulate polydispersions. *Appl. Opt.* **35**, 2672-2686.
- Pope R. M. and E. S. Fry. 1997: Absorption spectrum (380-700 nm) of pure water. II. integrating cavity measurements. *Appl. Opt.* **36**: 8710-8723.
- Wang, M. and H.R. Gordon, 1993: Retrieval of the columnar aerosol phase function and single scattering albedo from sky radiance over the ocean : simulations, *Appl. Opt.* **32**, 4598-4609.



Fig. 22.1: The “BOUSSOLE” buoy at sea (“beta version” deployed on site during 3 months in 2000 without instrumentation, for testing the principle) Once at sea, the top of the structure is at + 4.5 metres above the surface. The immersed part goes down to 20 metres, where it is linked to a Kevlar cable going down to the seafloor (2440 m). The cap of the buoy (here a fictitious one, just for tests) will host the radiometer for measurement of downwelling irradiance, solar panels, an ARGOS beacon and other equipment for transmission of data to the visiting ship.

## Chapter 23

# Contribution To A Global Climatology Of Surface Pigments From Ocean Color Sensors

Pierre-Yves Deschamps , Hubert Loisel, Jean Marc-Nicolas, Guislain Becu and François Thieuleux  
*LOA, Université de Lille 1, France*

Yves Dandonneau  
*LODYC, Université de Paris 6, France*

Cécile Dupouy  
*IRD, Nouméa, Nouvelle Calédonie*

Robert Frouin  
*Scripps Institution of Oceanography, University of California San Diego, California*

Cyril Moulin  
*LSCE, CEA, Gif-sur-Yvette, France*

Jacques Neveux  
*CNRS, Banyuls-sur-Mer, France*

### 23.1 INTRODUCTION

A group of French scientists concerned with the utilization of ocean color proposes to coordinate its efforts with the SIMBIOS program. The main objectives of this proposal are:

- to contribute to in-situ data collection effort centralized in SeaBASS, to be used for the CAL/VAL of different ocean color space sensors, including methodological improvement such as spectrofluorometry,
- to investigate the effect of biological variability on geophysical products (pigment concentration, marine reflectances) derived from ocean color,
- to assess the accuracy of the present processing of POLDER data vs SeaWiFS and others, by comparing Level-3 products, and by applying POLDER algorithms to SeaWiFS data,

- to improve the atmospheric correction in presence of absorbing aerosols.

*GeP&CO Cruises (LODYC, Banyuls, IRD, LOA)*

The GeP&CO cruises aim to describe the variability (quantitative, qualitative) of phytoplankton populations, and to estimate its impact on the ocean's biogeochemistry. The cruises use a merchant ship that sails quarterly from Le Havre (France) to Nouméa (New Caledonia), see Figure 23.2. The sampled areas include a large variety of oceanic conditions (temperate to equatorial, oligotrophic to eutrophic) which are observed using the same analytical instruments and methods, giving to GeP&CO a global character. The following measurements are made:

- Chlorophyll (mono and divinyl) and related pheopigments, carotenoids, and phycoerythrin, using HPLC and spectrofluorimetry

- Picoplankton (Prochlorococcus, Synechococcus, picoeucaryotes and bacteria) using flow cytometry
- Coccolithophorids, by microscope
- Light absorption spectra by the phytoplankton and by non-algal particles
- Light absorption spectra by dissolved organic matter
- Seawater reflectance using SIMBADA radiometer
- Nutrients (nitrate+nitrite, silicate, phosphate), TCO<sub>2</sub> and alkalinity, salinity and SST

To date, eight cruises have been made from October 1999 to August 2001. GeP&CO will stop in August 2002, i. e. a total of 12 cruises. Pigment data allowed to characterize the different populations in the phytoplankton communities (for instance: divinyl-chlorophyll *a* for Prochlorococcus sp., phycoerythrin for Synechococcus sp. or other cyanobacteria and cryptophyceae, 19'hexanoyloxyfucoxanthin for coccolithophorids and Phaeocystis sp., fucoxanthin for diatoms), and to use pigments ratios as proxies for the *f*-ratio (new production to net primary production). Validity of this approach can be tested using the identification and counts of cells by flow cytometry and microscopy. In addition, the GeP&CO data will also be used to validate algorithms that are being developed for the retrieval of geophysical parameters at sea. 2D (excitation, emission wavelength) fluorescence spectra are routinely measured in order to compute the concentration of chlorophylls (see above). We have also used these 2D spectra to "hindcast" the chlorophyll *a* and pheophytin *a* concentrations that would be obtained using the ancient fluorescence-acidification technique. Comparison of the results shows that the actual assemblages of pigments are dominated by chlorophyll *a* and divinyl-chlorophyll *a* everywhere, so that hindcasted ancient chlorophyll *a* values are tightly related to the sum chlorophyll *a* and divinyl-chlorophyll *a* ( $r^2=0.999$ ) and overestimate this sum by 5% (in preparation). It also shows that ancient pheophytin *a* results are not reliable. The results from this study may help to make a link between field chlorophyll data obtained before and after the introduction of modern techniques in pigments measurements.

We have also defined a protocol for the measurement of 2D fluorescence spectra on phytoplankton populations collected at the surface of membrane filters, in order to estimate the water soluble pigments, essentially phycoerythrins. The main difficulty arises when main fluorescence excitation and emission peaks are very close and the diffusion of excitation spectra are mixed. This difficulty seems to be solved by properly filtering out the blank in this method (in preparation). A cross checking of pigments determinations by HPLC in the GeP&CO program has been made recently by duplicating some measurements in collaboration with Charles Trees at San Diego State

University Foundation. Results from this comparison will be available by the end of November. For further information, see <http://www.lodyc.jussieu.fr/gepco>

#### *SIMBAD/SIMBADA network (LOA, SIO)*

The SIMBAD/SIMBADA optical radiometers have been specifically designed for to measure in situ the necessary parameters for the validation of ocean color sensors. They measure the aerosol optical thickness and the water leaving radiance/above-water reflectance; by aiming from the shipdeck successively to the Sun, then to the water surface at about the Brewster angle (a polarizer strongly reduces the reflected sky radiation). 10 SIMBAD radiometers with 5 spectral bands from 443 to 870 nm have been realized by LOA; 5 of them have been operated since 1996 by LOA, 3 by SIO, and 2 by the SIMBIOS project. A series of 25 SIMBADA radiometers with 11 wavelengths from 350 to 870 nm are under realization by LOA and SIO; their deployment has begun at the end of 2000 and it is expected that about 15 of them will be in operations by the end of 2001, and the others one by mid 2002. Further information on the SIMBAD/SIMBADA networks is available on:

<http://www-loa.univ-lille1.fr/simbada/>  
<http://polaris.ucsd.edu/~simbad/>

Figure 23.1 gives the statistics of the measurements by the LOA network from 1996. To avoid duplicates, clear sky measurements have been binned every 15 minutes. Fig. 23.1a gives the histogram of the monthly number of aerosol optical thickness measurements, Fig. 23.1a, and of the marine reflectance, Fig. 23.1b. Note that SIMBADA is replacing SIMBAD progressively from February 2001.

Next, SIMBAD measurements will be delivered to the SeaBASS data base. SIMBADA measurements will be continued in the future thanks to the support of CNES and the MERIS/ESA project.

#### *Validation of SeaWiFS geophysical products (LOA, LODYC, SIO)*

Figure 23.2 gives the location of SIMBAD/SeaWiFS matchups, during GeP&CO cruises in the North Atlantic and South Pacific, and during ACE-ASIA in the North Pacific.

#### *Validation of chlorophyll and marine reflectances during GeP&CO Cruises*

Figure 23.3a gives a comparison between the marine reflectances from SIMBAD and chlorophyll (TChla = Chla +

DivChla, measured by spectrofluorometry) measured during the 4 first GeP&CO cruises, 1999-2000, and the SeaWiFS geophysical products, Level 3b, daily data binned at 9 km spatial resolution. The matchups cover the North Atlantic and the South Pacific, with a range of in-situ values of the chlorophyll concentration measurements from 0.03 to 5 mg/m<sup>3</sup>. A matchup is declared when an in situ measurement has been done during the daylight coincident with the SeaWiFS acquisition. When comparing surface chlorophyll concentration, Fig. 23.3a, SeaWiFS slightly overestimate the chlorophyll by 11 %, and the rms of the difference is 37 %. The comparison between reflectance measurements at 443, 490, and 565 nm, Fig. 23.3b, gives similar results, biases less than 12 % and rms less than 20 %. These results are excellent and demonstrate the good quality of in-situ measurements and SeaWiFS estimates.

The final data set, 12 cruises, 1999-2001, will be further analyzed in an attempt to understand what are the weight of different error sources that may explain the differences shown in the comparison: in-situ or satellite? SeaWiFS radiometry or data processing? atmospheric correction or biooptical algorithm?

#### *Validation of aerosol products during ACE-ASIA*

During GeP&CO most of the measured aerosol optical thickness are very low, and the comparison with SeaWiFS products is not significant. But a very attractive data set has been acquired during ACE-ASIA 2001 and the results are shown in Fig. 23.4. They are matchups between SIMBADA measurements and SeaWiFS products, LAC when available, or Level 3b. The aerosol optical thickness, Fig. 23.4a, is accurately retrieved by SeaWiFS, but SeaWiFS underestimate strongly its wavelength dependence represented by its Angstrom coefficient, Fig. 23.4b. The reason of the discrepancy on the Angstrom coefficient seems to be linked to SeaWiFS algorithm. The consequence of an underestimate of the aerosol wavelength dependence by SeaWiFS should be an underestimate of the aerosol scattering, thus an overestimate of the marine reflectances at ocean color wavelengths. This is not what is shown in Fig. 23.5 showing a comparison of the spectra of marine reflectance during ACE-ASIA, measured in-situ by SIMBADA, and retrieved from SeaWiFS, for the 6 days. SeaWiFS derived reflectances are lower than the in situ ones in the blue region, and the effect is increasing toward the shorter wavelength. This is typical of the error committed by the SeaWiFS atmospheric correction algorithm in the presence of absorbing aerosols, mostly pollution aerosols in the ACE-ASIA case.

#### *POLDER (LOA, LSCE)*

POLDER-2 is now scheduled for launch in November 2002. For this perspective, we are developing an advanced data processing that will be used to process POLDER-2 and reprocess POLDER-1. The main improvements are:

- absorbing aerosol detection and improved atmospheric correction in their presence,
- improved atmospheric correction over turbid waters,
- inversion of marine reflectances to derive water absorption and scattering coefficients as products.

SeaWiFS data as well as POLDER-1 data are currently used to check the new algorithm.

Figure 23.6 gives an example of the detection of desert absorbing aerosol outflowing from the North Sahara, using POLDER data. More information on POLDER is available on

<http://www-projet.cst.cnes.fr:8060/POLDER/index.html>

and global images of chlorophyll, November 1996 to June 1997 are available on line on:

<http://www-projet.cst.cnes.fr:8060/POLDER/SCIEPROD/oc9611.htm>

POLDER-2 Level-3 products will include an additional product somewhat similar to the SeaWiFS L3 mapped product. Daily, 10-day and monthly global maps of the main marine parameters, projected on a regular 1/12° latitude-longitude grid, will be available in HDF-EOS format to ensure full compatibility with other ocean color data set. The final definition of this product will benefit of the recommendations of the IOCCG Working Group on Data Binning Issues.

#### *Atmospheric correction (LOA, LSCE)*

LSCE is working on alternative algorithms to improve atmospheric correction in the presence of absorbing aerosols, a situation that generally leads to the failure of current algorithms. An extensive work has been performed in collaboration with Howard Gordon (University of Miami) to adapt the Spectral Matching algorithm (Gordon et al., 1997) to the Atlantic dust-zone off the coast of Africa. Results show that significant improvements can be obtained in atmospheric correction by using such advanced algorithms. This algorithm has recently been implemented within SeaDAS and will be used to improve ocean color retrievals in the Eastern Mediterranean in the framework of a collaboration with researchers of the Middle East Technical University (Turkey). This basin is of particularly challenging in terms of atmospheric correction since it regularly experiences very

different aerosol influences, from desert dust to fire and pollution plumes within a few days.

LSCE is also exploring the capabilities of advanced numerical methods to speed up this kind of improved atmospheric correction algorithms. Neural network assemblages are currently being tested on the Spectral Optimization algorithm of Chomko and Gordon (1998). This work is performed within the framework of the NAOC (Neural Network for Advanced Ocean Color) project funded by the European Community, and we expect soon to be able to report on the results.

Pierre-Yves Deschamps and Jean-Marc Nicolas (LOA) participate to the comparison of atmospheric algorithms, sponsored by IOCCG, funded by SIMBIOS and organized by Menghua Wang, reported elsewhere in this report. They are working on the adaptation of the POLDER atmospheric correction to the SeaWiFS processing, and will report soon on the results.

Cyril Moulin (LSCE) participates to the Working Group on Data Binning Issues, sponsored by IOCCG and organized by David Antoine. These two activities are of particular importance since we are still actively working on the definition of both algorithm and products for POLDER-2.

This research is supported by the following French organisations: CEA, CNES, CNRS, IRD.

## PUBLICATIONS

- Dupouy C., H. Loisel, J. Neveux, C. Moulin, S. Brown, J. Blanchot, and A. Leboutteiller. Light-absorption and backscattering coefficients by microbial groups along 180° during an ENSO cold phase in the Pacific Ocean: a simulation test and an inversion of a POLDER image. *J. Geophysical Res.*, submitted.
- Frouin, R., S. F. Iacobellis, and P. Y. Deschamps, 2001: Influence of oceanic whitecaps on the global radiation budget. *Geophys. Res. Lett.*, **28**, 1523-1526.
- Loisel, L., E. Bosc, D. Stramski, K. Oubelker, and P-Y. Deschamps, 2001: Seasonal variability of the backscattering coefficients in the Mediterranean Sea based on Satellite SeaWiFS imagery. *Geophysical Res. Lett.*, **22**, 4203-4206.
- Mackay, D. J., J. Blanchot, H. W. Higgins, and J. Neveux, Phytoplankton community structure in the Equatorial Pacific. *Deep-Sea Res.*, in press.
- Moulin, C., H. R. Gordon, V. F. Banzon, R. H. Evans, 2001: Assessment of Saharan dust absorption in the visible from SeaWiFS imagery, *J. Geophys. Res.*, **106**, 18239-18250.
- Moulin, C., H. R. Gordon, R. M. Chomko, V. F. Banzon, R. H. Evans, 2001: Atmospheric correction of ocean color imagery through thick layers of Saharan dust, *Geophys. Res. Lett.*, **28**, 5-8.
- Nicolas, J. M., P. Y. Deschamps, and R. Frouin, Spectral reflectance of oceanic whitecaps in the visible and near infrared: Aircraft measurements over open ocean, *Geophys. Res. Lett.*, in press.
- Radenac, M.-H., C. Menkes, J. Vialard, C. Moulin, Y. Dandonneau, T. Delcroix, C. Dupouy, A. Stoens, and P. Y. Deschamps 2001: Modeled and observed impacts of the 1997-1998 El Niño on nitrate and new production in the equatorial Pacific. *J. Geophys. Res.*, **106**, C11, 26879-26898.

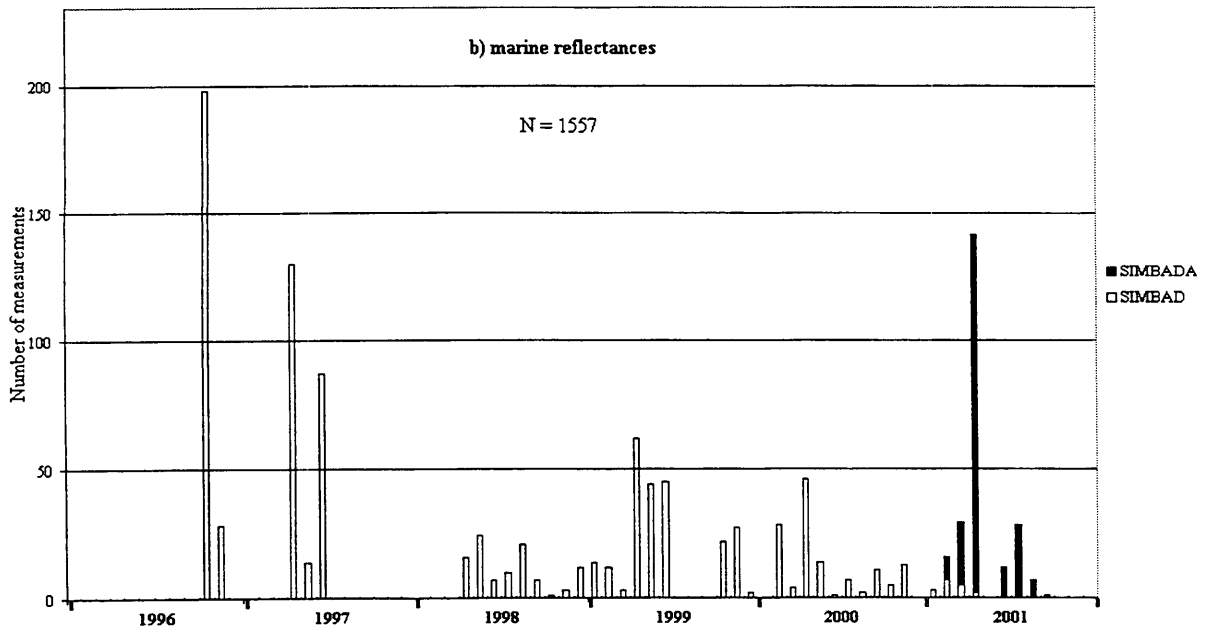
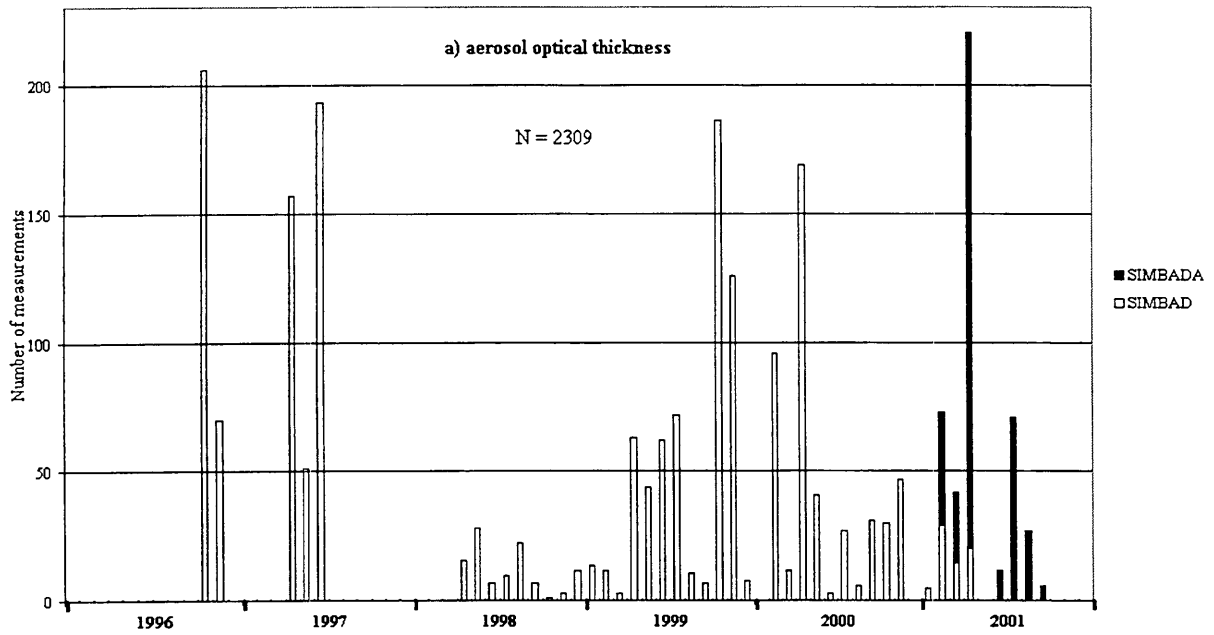


Figure 23.1: Histograms of the monthly number of SIMBAD(A) measurements of a) aerosol optical thickness, b) marine reflectances.

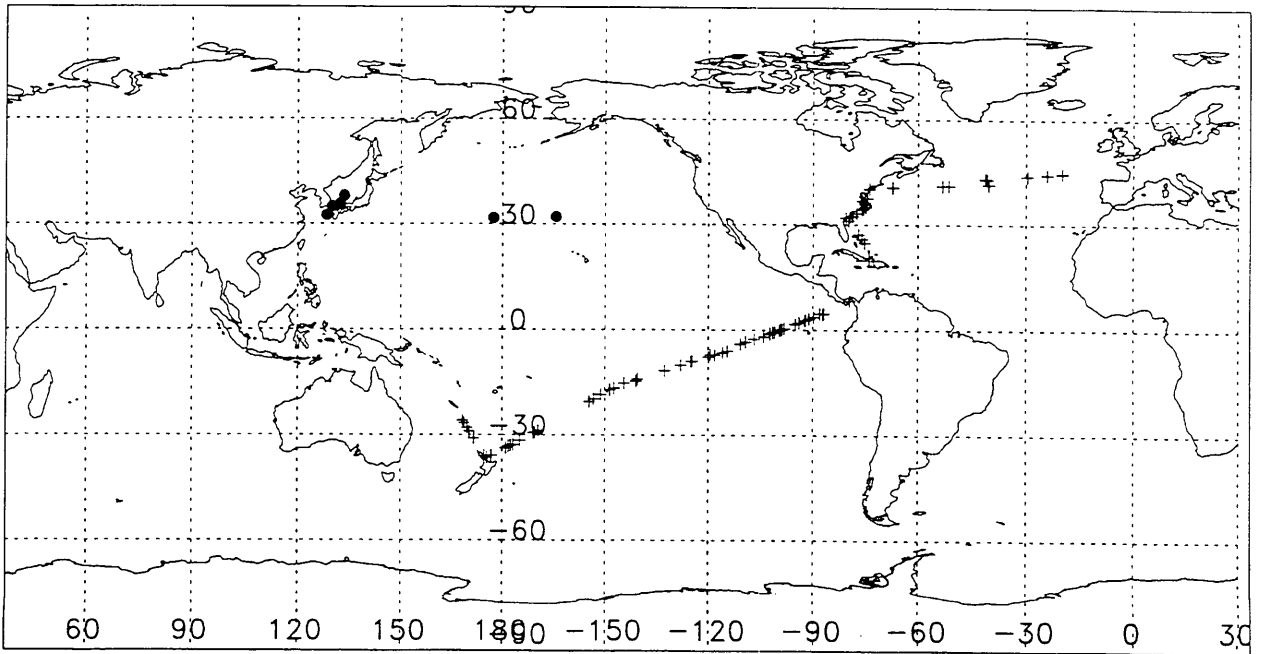


Figure 23.2: Location of SeaWiFS/SIMBAD(A) matchups during GeP&CO 1999-2000 (North Atlantic and South Pacific) and ACE-ASIA 2001 (North Pacific)

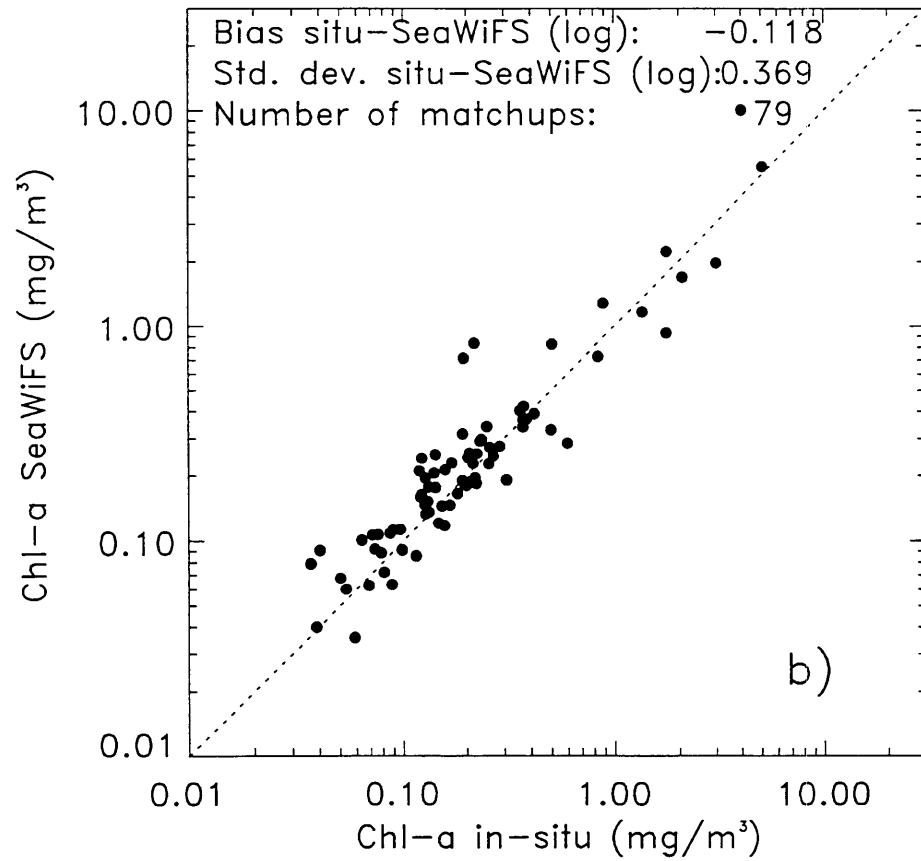


Figure 23.3a: SeaWiFS chlorophyll estimates (Level 3b) vs in-situ chlorophyll (TChla = Chla + DivChla) surface measurements by spectrofluorometry.

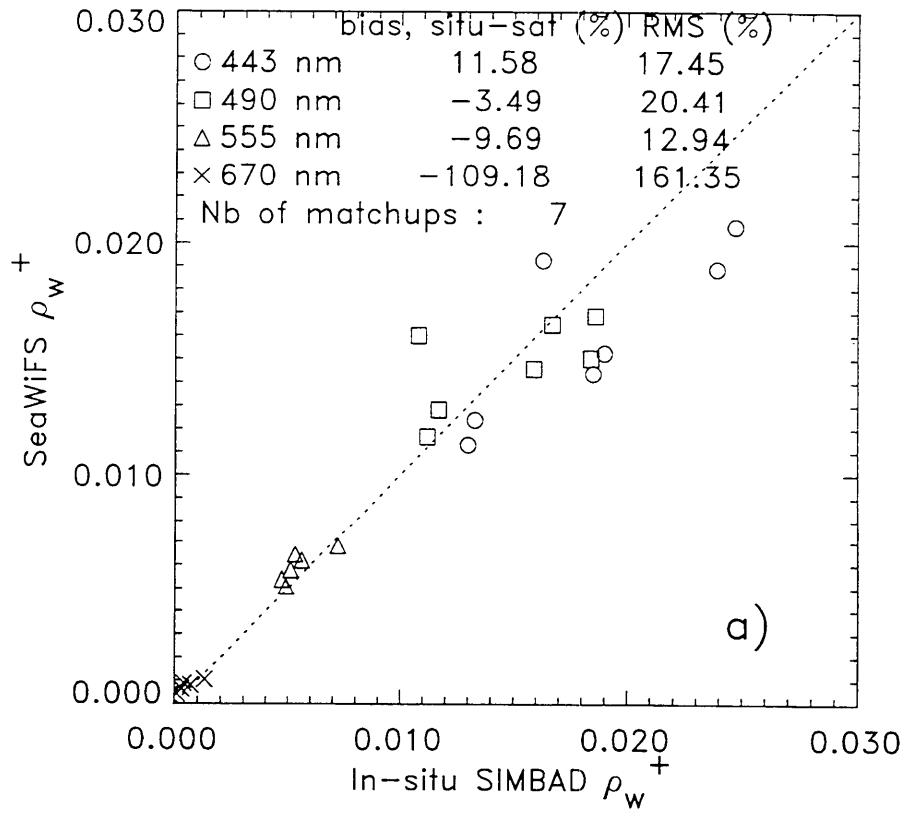


Figure 23.3.b: SeaWiFS marine above water reflectances (Level 3b, the water leaving radiances have been normalized by the solar downward surface irradiance) vs in-situ SIMBADA measurements during GeP&CO 1999-2000.

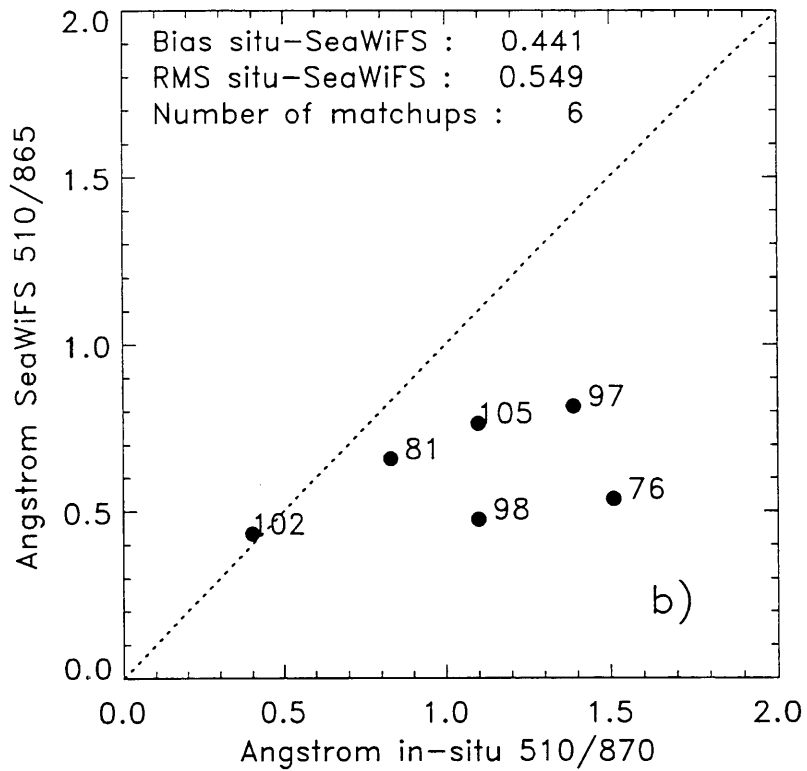


Figure 23.4a: SeaWiFS estimate vs in-situ SIMBADA measurements of the aerosol optical thickness at 870 nm.

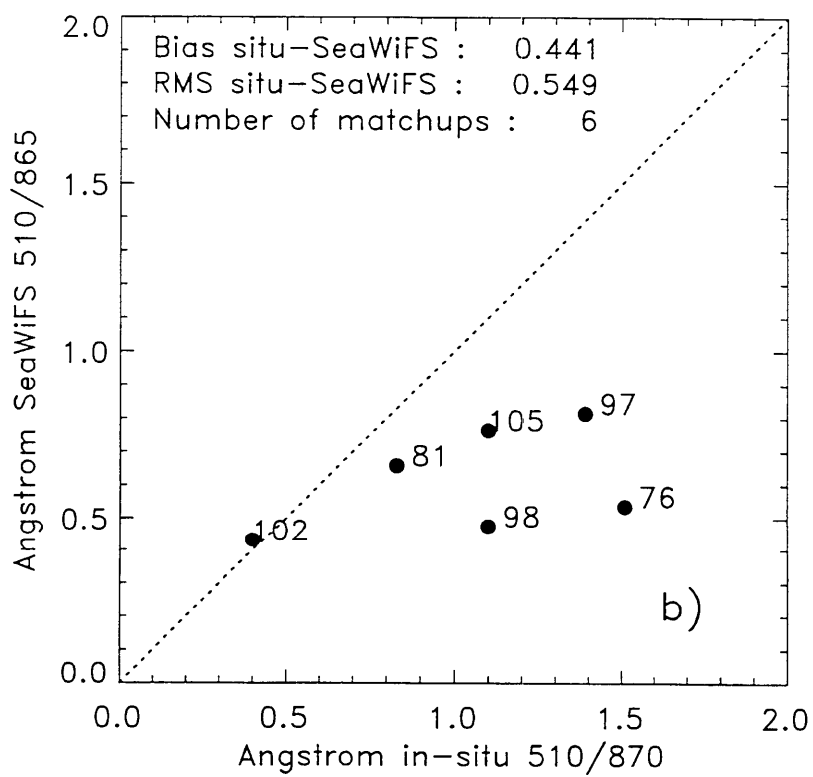


Figure 23.4b: SeaWiFS estimate vs in-situ SIMBADA measurements of the Angstrom coefficient.

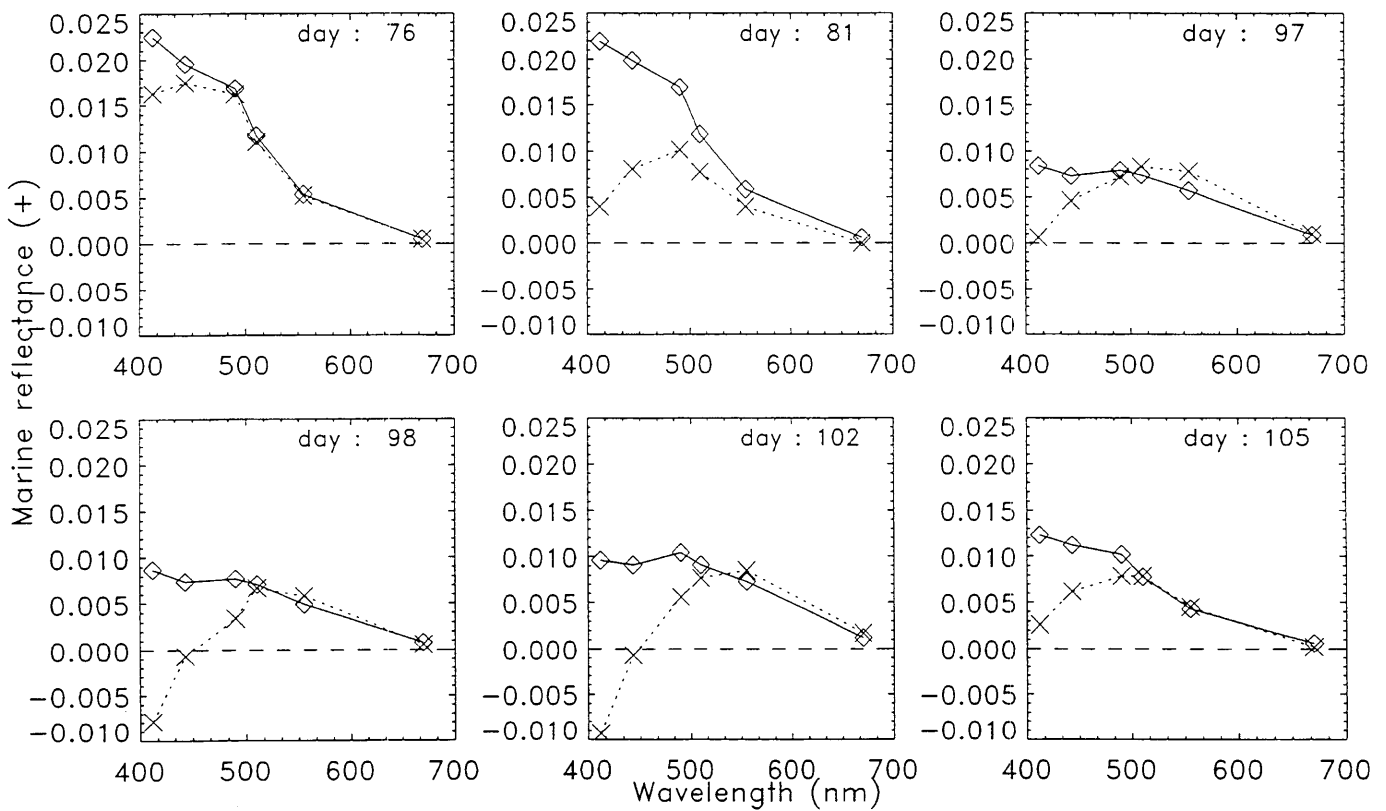


Figure 23.5: Spectral reflectances derived from SeaWiFS (LAC, Level 2) and measured in-situ by SIMBADA for some ACE-ASIA 2001 stations. The SeaWiFS underestimation increases when wavelength decreases, a typical effect of absorbing aerosols.

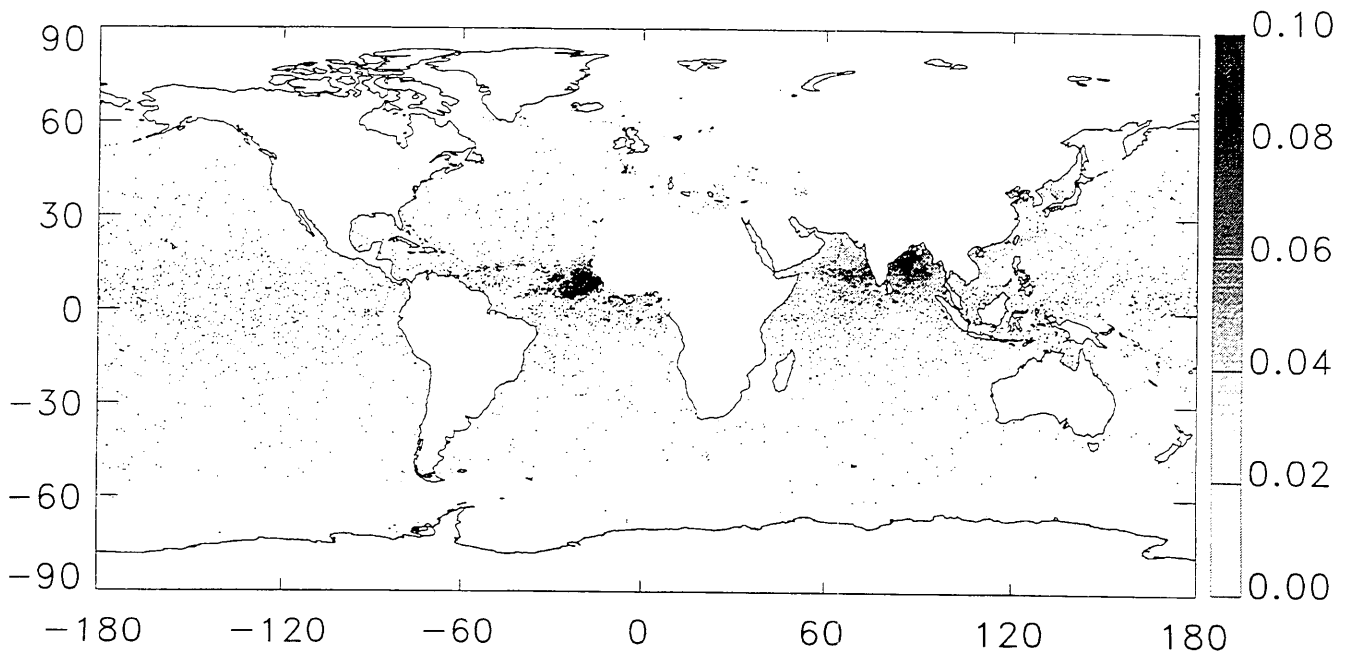


Figure 23.6: POLDER detection of absorbing aerosols over a decade, March 10-19 1997. The algorithm makes use of POLDER multiangle viewing. By this time, the two main sources of absorbing aerosols are located in India and the Sahara desert.

## Chapter 24

# CNES Contribution to Ocean Color Calibration : Multi-sensor Cross-Calibration over Desert Sites

Bertrand Fougnie, François Cabot, Olivier Hagolle, and Patrice Henry  
*Centre National d'Etudes Spatiales, Toulouse, France*

### 24.1 INTRODUCTION

Our proposal to the SIMBIOS project was a threefold investigation on calibration of ocean color sensors : i/ a multi-ocean color sensor cross calibration thanks to our rich database over desert sites spectrally and bidirectionnally characterized; ii/ a calibration of MERIS and MODIS over Rayleigh scattering which is a method successfully applied for various sensors like POLDER, *Végétation* or SPOT sensors; and iii/ a vicarious calibration of POLDER-2 using in-situ measurements. This report is focused on the multi-sensor cross-calibration over desert sites.

### 24.2 RESEARCH ACTIVITIES

Desert sites are terrestrial sites with remarkable properties. After a selection based on statistical description, 20 desert sites were carefully selected for

- large extent but with a good spatial homogeneity to minimize misregistration and various field-of-view impact
- temporal stability of the surface including low variation of the overlaying atmosphere and poor annual mean cloud coverage
- small bidirectional effects

These sites are located in Africa and Arabia and are 100\*100 km<sup>2</sup> and some in-situ measurements were conducted over some of them (see *Cosnefroy et al.*, 1996). Such terrestrial sites can be used as references for on-orbit sensors for different aspects : absolute calibration (which often requires additional in-situ measurements, see for instance *Henry et al.* 2000 for *Végétation*), large field-of-view multi-angular calibration (*Fougnie et al.*; 2000 for *Végétation* or *Hagolle et al.*, 1999 for POLDER/ADEOS). Another important application is the cross-calibration of two or more sensors. This method has the advantage to do not refer to the absolute calibration but only give a relative comparison of the calibration of the considered sensors.

The first step of this exercise was to build a consistent database with acquisitions of several sensors over the 20 selected desert sites. This was done in our team and these sites are now fully characterized in term of spectral and bidirectional signature (*Cabot et al.*, 1999). This database includes data from POLDER, *Végétation*, AVHRR, ATSR, SeaWiFS and now MISR and MODIS data. The earth observing sensors planned to be launched soon will be integrated in this database (MERIS, AATSR, *Végétation-2*, POLDER-2, GLI, MODIS-PM).

The data processing includes both spectral and bidirectional considerations. For this, the following processing is done : an atmospheric correction is made on the top-of-atmosphere radiances of the sensor-1 used as reference in order to estimate ground surface reflectance in the sensor-1 spectral bands. A spectral fit is applied afterwards to the surface reflectance of sensor-1 (see Cabot et al., 1998) and, considering the spectral response of sensor-2, the surface reflectance corresponding to the spectral band of sensor-2 are derived. This spectral fit is very accurate if the spectral bands of sensor-1 and 2 are nearly identical. The atmospheric contribution is finally added to compute the Top-of-Atmosphere radiances for sensor 2. It is important to take into account the fact that the sensor-1 aims the surface for a given viewing geometry that is not generally the same that the sensor-2's one. We usually consider POLDER as the reference sensor because of its enlarged field-of-view capabilities that allow a quasi-complete angular sampling of the BRDF of the site (in addition, reciprocity principle is used to extent geometric coverage). In this case we use two different approach : i/ a polynomial fit is performed on the BRDF and the reflectance corresponding to the viewing geometry of sensor-2 is calculated using this fit or ii/ we simply choose the closest POLDER geometry to compare to the sensor-2 geometry. These two methods provide nearly identical results. As a result POLDER can be used as a transfer radiometer allowing to cross-calibrate for instance two sensors with different viewing geometry. POLDER has provided acquisitions over desert sites from October 1996 to June 1997.

## 24.3 RESEARCH RESULTS

The first step was to update the POLDER-1 data in our base consequently to the last reprocessing of mid-2000 which includes a reappraisal of the POLDER-1 in-flight calibration after some algorithmic improvement (see *Fougnie et al.* 2001b) and a correction of a non linearity defect of the radiometric sensitivity (see *Fougnie et al.* 2001a).

The cross-calibration between POLDER and SeaWiFS previously published in *Cabot et al.* (1999) was therefore reevaluated and extended to a larger period (now nearly 4 years) as presented in Figures 24.1 and Table 24.1. The first important result is that multi-temporal evolutions of all the spectral bands are detected. The evolutions found for the large wavelengths, i.e. for 670, 765, and 865nm with decreases of respectively 1.6, 5.6, and 6.1%, corroborate those shown in *Barnes et al.* (2001) using lunar acquisitions and reminded in Table 24.1. On the other hand, decreases of typically 1 to 2% per year are detected for shorter wavelengths in the blue and green part of the spectrum. This is an important result because *Barnes et al.* (2001) suppose that bands 3 and 4 (490, and 510nm) are stable in time to normalize the lunar time correction made on the SeaWiFS level-1 data processing.

The second main result is an evaluation of the in-flight radiometric calibration coefficients. The coefficients estimated by this method and presented in Table 24.1 are referenced to the SeaWiFS in-flight official coefficients used to generate level-1 data : a value of 1.0 means that there is consistency with the official calibration coefficients. For bands 555, 670, 765 and 865 the results are consistent within 2% with those of *Barnes et al.* (2001). On the other hand, large discrepancies are found for 443, 490, and 510nm with variations of 5.6; 5.2, and 4.3%. Table 24.1, a consistent correction is given by *Eplee et al.* (2000a) using a vicarious adjustment at 490nm of 4.1%, and partly for 443 and 510nm with an adjustment of about 1%. It has to be considered that gains measured over desert sites are established for relatively high radiances and are representative to the radiometric sensitivity above bilinear knees described in *Barnes et al.* (2001) and in-flight calibrated in *Eplee et al.* (2000b). Consequently, it is necessary to transfer the results of Table 24.1 from above to under the bilinear knee for a further interpretation.

Finally, future investigations using Rayleigh scattering will be conducted and should be useful to complement these both aspects (calibration coefficients and multi-temporal evolutions).

The first cross-calibration of MODIS, MISR and SeaWiFS previously published in *Cabot et al.* (2001) was updated in Table 24.3. In order to be aware of some saturation over bright desert sites, the MODIS data considered were 412 and 443nm with a ground resolution of 1km (bands 8 and 9), 469 and 555nm with a ground resolution of 500meters (bands

3 and 4), 645 and 858nm with a ground resolution of 250meters (bands 1 and 2). For MISR, 7 cameras were considered and the first important point is that a strong dispersion of the behavior of each camera was clearly evidenced (*Cabot et al.*; 2001). Thus, variations up to 10% of the calibration coefficients were obtained over desert sites as shown in Table 24.2 where variations of each camera are given in reference to the nadir viewing camera, An. This variation of the cross-calibration with the camera should be considered in the future, particularly for ocean color applications for which calibration is a critical aspect. The calibration coefficients of the nadir An camera are given in Table 24.3 for the 4 spectral bands and a consistency within 3.5% is found with SeaWiFS. The multi-temporal evolution of the An camera is important and is found to be about 1% to 2% per month depending of the spectral band : this result is established for a period of 5 months in mid-2000. For MODIS, the accordance is within 3-4% with the exception of the 865nm spectral band for which a discrepancy of 7% is found. Our MODIS level-1 archive being limited to a short period of time, it was not possible to determine a multi-temporal variation of the radiometric sensitivity.

## 23.4 CONCLUSION

A cross-calibration of the POLDER-1, SeaWiFS, MODIS and MISR ocean color sensors has been performed. The main results are a possible decrease in time of the SeaWiFS bands 3 and 4 of typically 1 to 1.5% per year, a strong variation of the behavior of the MISR camera, a relatively good coherence within 3% between MISR and SeaWiFS, and finally an accordance within 3-4% between MODIS and SeaWiFS, except marginally for the 858nm band. These results are important informations available and helpful for discussion in the merging activities, complementary to vicarious calibration approach for instance using in-situ measurements. Other ocean color sensors will be soon available to complement this set of cross-calibration, such as MERIS and POLDER-2.

## REFERENCES

- Barnes, R. A., R. E. Eplee, G. M. Schmidt, F. S. Patt, and C. R. McClain, 2001: The Calibration of SeaWiFS, Part 1: Direct Techniques, *Appl. Opt.*, in press..
- Cabot, F., O. Hagolle, H. Cosnefroy, and X. Briottet, 1998: Inter-calibration using desert sites as a reference target, *Proc of IGARSS'98*, Seattle.
- Cabot, F., O. Hagolle, C. Ruffel, and P. Henry, 1999: Use of remote sensing data repository for in-flight calibration of

- optical sensors over terrestrial targets, Proceedings of SPIE'99, Denver.
- Cabot, F., O. Hagolle, and P. Henry, 2001: Calibration of MODIS and MISR over desertic sites, *Investigator Working Group*, Fort Lauderdale, Florida, January 30th - February 1st.
- Cosnefroy, H., M. Leroy, X. Briottet, 1996: Selection and characterization of Saharan and Arabian desert sites for the calibration of optical satellite sensors, *Remote Sensing of Environ.*, Vol. 58, N°1, pp 101-114.
- Eplee, R. E., and C. R. McClain, 2000a: MOBY data analysis for vicarious calibration of SeaWiFS bands 1-6, SeaWiFS Postlaunch Calibration and Validation Analyses, Part 1., *NASA Tech. Memo. 2000-206892*, Hooker and Firestone, Eds., NASA GSFC, vol. 9, 43-50.
- Eplee, R. E., and F.C. Patt, 2000b: Cloud-top radiance analysis for SeaWiFS bilinear gain knee calibration, SeaWiFS Postlaunch Calibration and Validation Analyses, Part 1., *NASA Tech. Memo. 2000-206892*, Hooker and Firestone, Eds., NASA GSFC, vol. 9, 13-16.
- Fougnie, B., P. Henry, F. Cabot, A. Meygret, and Marie-Christine Laubies, 2000: Végétation: In-flight Multi-angular Calibration, *45<sup>th</sup> SPIE annual Meeting*, San Diego, California.
- Fougnie, B., O. Hagolle, and F. Cabot, 2001a: In-flight measurement and correction of non-linearity of the POLDER-1'S sensitivity, *8th Symposium of the International Society for Photogrammetry and Remote Sensing*, Aussois, France.
- Fougnie, B., O. Hagolle, and F. Cabot, 2001b: POLDER In-flight Calibration : at <http://www-projet.cst.cnes.fr:8060/POLDER/index.html>.
- Hagolle, O., P. Goloub, P.-Y. Deschamps, H. Cosnefroy, X. Briottet, T. Bailleul, J.M.Nicolas, F. Parol, B. Lafrance, and M. Herman, 1999: Results of POLDER In-Flight Calibration," *IEEE Transactions on Geoscience and Remote Sensing*, vol. 37, 1550-1566.
- Henry, P., F. Cabot, B. Fougnie, O. Hagolle, F. Meunier, and A. Meygret, 2000: VEGETATION Absolute Calibration, *Végétation 2000*, Belgirate, Italy.

Table 24.1: Synthesis of results for SeaWiFS. [ $\alpha$ ] is the vicarious gain from *Eplee et al.* (2000a). [dAo/dt] is established for the period from 14/02/97 to 29/05/01, i.e. typically 1530 days. [dA] from *Barnes et al.* (2001). Results at 412nm are not reported.

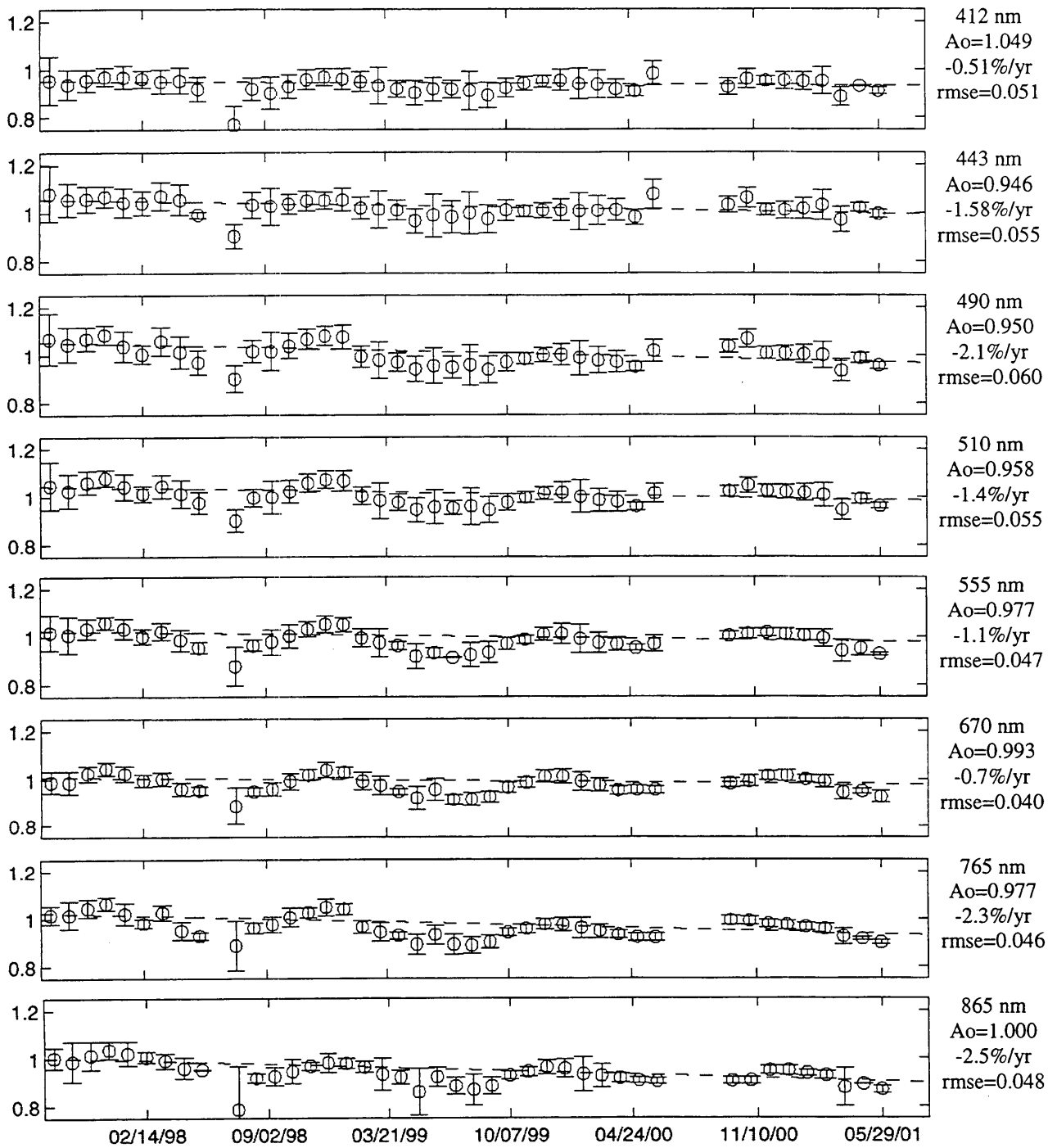
Band	Ao	dAo/dt (%/year)	dAo (860 days)	$\alpha$	dA (860 days)
443	0.946	-1.58	-3.77	0.991	-0.5
490	0.950	-2.16	-5.16	0.960	0.0
510	0.958	-1.49	-3.55	0.986	0.0
555	0.977	-1.19	-2.84	0.994	-0.3
670	0.993	-0.71	-1.69	0.95	-0.8
765	0.977	-2.37	-5.66	0.946	-3.4
865	1.000	-2.59	-6.18	1.000	-9.9

Table 24.2: Variation of the calibration coefficient for fore and aft cameras compared to the nadir viewing camera (An) and for the 4 MISR spectral bands. The last line gives the monthly evolution in percent for the An camera (established for 5 months in mid-2000).

Camera	Blue	Green	Red	NIR
Cf	2.00	4.67	-0.56	-1.04
Bf	11.74	1.74	3.75	-1.49
Af	10.33	5.10	4.81	-0.05
An	0.00	0.00	0.00	0.00
Aa	9.05	6.50	3.45	-1.62
Ba	11.59	11.36	6.29	3.64
Ca	6.16	8.62	-0.68	1.24
%/month				
An	-2.21	-1.35	-0.74	-0.85

Table 24.3. Cross-calibration between SeaWiFS and POLDER-1, MODIS, and MISR (nadir camera). <sup>(1)</sup> result for 412 are considered as not accurate. <sup>(2)</sup> result is not definitive because still in reprocessing.

POLDER / SeaWiFS							
412	443	490	510	555	670	765	865
<sup>(1)</sup>	0.946	0.950	0.958	0.977	0.993	0.977	1.000
MODIS/SeaWiFS							
412	443	469	555	645	858		
0.982	0.957	0.987 <sup>(2)</sup>	0.969	1.034 <sup>(2)</sup>	1.069		
MISR(nadir)/SeaWiFS							
BLUE	GREEN	RED	NIR				
0.999	0.964	0.977	1.010				



Figures 24.1.: Time series of the calibration coefficient estimated over desert sites for the 8 SeaWiFS spectral bands. The resulting  $A_0$  are given in reference to the official calibration parameters at the begin of the life. The mean annual variation in %/year (= slope of the dashed lines) and the root-mean square error are reported too.

## Chapter 25

# Summary of the OSMI Radiometric Calibration Efforts

Yongseung Kim, Donghan Lee and Sungu Lee

*Satellite Operation and Application Center, Korea Aerospace Research Institute, Korea*

### 25.1 INTRODUCTION

The ocean scanning multispectral imager (OSMI) aboard the KOREA Multi-Purpose SATellite (KOMPSAT) is designed to observe the global ocean color in support of biological oceanography. Since after the successful launch of OSMI on December 21, 1999, it has been collecting the global ocean color data in the six visible spectral bands centered at 412, 443, 490, 555, 765, and 865 nm. The level 1A data collection over worldwide oceans amounts to about 1.2 terabytes as of August 2001. The OSMI product processing is done through the OSMI data analysis system (OSMIDAS) that consists of several processing modules (Kim *et al.* 1999). One of OSMIDAS processing modules performs the conversion of the measured digital number (DN) for level 1A data to the physical quantity of radiance at the top of the atmosphere (TOA) and produces level 1B data. Such conversion is called the absolute radiometric calibration (Dinguirard and Slater, 1999) and requires the pre-launch sensor calibration information. The pre-launch sensor calibration is particularly important for the ocean color sensor because the ocean color information relies upon a 10% to 15% amount of measured total radiances. The KOMPSAT provider, TRW, delivered the pre-launch sensor calibration information. The OSMI sensor also has the capability of solar calibration. It is designed to monitor the post-launch sensor degradation and thus complements the pre-launch sensor characterization. We report the OSMI calibration anomalies that were seen from the initial radiometric calibration processing and summarize the ongoing calibration efforts.

### 25.2 RESEARCH ACTIVITIES

Figure 25.1 shows the OSMI level 1A image over Arabian Sea acquired on February 27, 2000. The image is not radiometrically corrected and reveals the bands and stripes extensively over the oceanic region. Dark and gray bands are interleaved in each scan of OSMI and narrow stripes periodically appear in gray bands. Banding is caused by differences of CCD detector responsivities between positive (1<sup>st</sup> to 48<sup>th</sup>) and negative (49<sup>th</sup> to 96<sup>th</sup>) fields. The above

periodic stripes result from low responsivities of along-track pixels 55, 56, 57, and 58, which cannot be expected from pre-launch calibration measurements. Since the measured digital numbers over land areas of high reflectivity exceed the saturation limit, they look white. A few sparse white areas near Oman and Pakistan are thought to be clouds and sand dust, respectively. We have applied the pre-launch calibration data of TRW to this image for radiometric calibration. The results are shown in Fig. 25.2. The radiometric calibration processing does not successfully remove the bands and stripes from the image illustrated in Fig. 25.1. More importantly, OSMIDAS with these calibrated radiances was not able to perform the subsequent processing to compute geophysical variables of level 2 products. We will describe the root cause of this problem shortly. Another way of performing the DN-to-radiance conversion may be to use solar calibration. To derive the radiometric calibration coefficients (slope and offset values), we have used the OSMI solar calibration data and the estimated incoming solar radiance at each pixel of given spectral bands. See the details of methods in Lee and Kim (2000). Figure 25.3 shows the results of the radiometric calibration processing using solar calibration. Bands and stripes are nearly invisible. However, it is clearly seen that there are lines between each scan of OSMI. In fact, these lines exist in Fig. 25.2. We found that such anomalous lines (hereinafter Venetian-Blind effect) between two neighboring scans are related to increases of pixel radiance values with along-track direction. Similar to the first method, we could not produce the level 2 products with this method for the reason below. A root cause of failure to produce the level 2 products is that the measured TOA radiance values at shorter wavelengths do not overcome the atmospheric Rayleigh scattering limit. Since the measured TOA radiance consists of Rayleigh, aerosol, sun glint, and water-leaving radiances, it should be greater than Rayleigh radiance alone. This is not true for the OSMI sensor as shown in Fig. 25.4. Regardless of the radiometric calibration method, the OSMI radiance values at band 412 nm and band 443 nm are shown to be smaller than the corresponding Rayleigh radiances and far less than the collocated SeaWiFS counterparts. It appears to be related to sensor design characteristics. However, we have not been told any analysis report regarding sensor anomalies from TRW.

### Cross-calibration with SeaWiFS Measurements

As mentioned in the previous section, the Rayleigh scattering limit basically inhibits the generation of the level 2 products. The cross-calibration method using other satellite measurements may be a solution of this problem. We have applied a simple method (hereinafter KARI method) to derive the radiometric calibration coefficients directly from the collocated match-ups of OSMI DNs and SeaWiFS radiances. The procedure is as follows: 1) Find the SeaWiFS image that matches well in time and space with the OSMI image. 2) Select the purely clear ocean areas from each image. 3) Resample the SeaWiFS image pixels for collocation, using the nearest-neighbor method. 4) For the collocated pixels, extract DNs from the OSMI level 0 data and radiances from the SeaWiFS level 1B data. 5) Offsetting the solar zenith angle differences between two data sets, calculate the calibration coefficients for each along-track pixel of a given spectral band. As an example, we have obtained the SeaWiFS image for the same area as shown in Fig. 25.1. The OSMI image was acquired 15:18 on February 27, 2000, while the SeaWiFS image was taken 16:42 on the same day. Time here is in Korean local hour. The solar zenith angles are  $37^\circ$  and  $26.5^\circ$  for the OSMI image and the SeaWiFS image, respectively. Following the above procedure, we derive the calibration coefficients and subsequently produce the level 2 products as discussed in the next section. Currently, the Korea Aerospace Research Institute (KARI) collaborates with NASA for the OSMI data merger as part of the SIMBIOS project. For this collaboration, the NASA SIMBIOS office is developing a cross-calibration method (hereinafter NASA method) using the collocated OSMI and SeaWiFS measurements over the region of MOBY. The preliminary results will be illustrated in the following section.

## 25.3 RESEARCH RESULTS

The KARI method of cross-calibration adequately overcomes the banding and striping problems as expected (Fig. 25.5) and resolves the Rayleigh limit issue. The resultant distribution of chlorophyll concentration, which is one of OSMI level 2 products, is depicted in Fig. 25.6. It displays the overall structure of ocean dynamics and reasonably agrees with the SeaWiFS pattern (not shown). For a few cases examined so far, including Argentinean coastal region, Great Australian Bight, and the Korean peninsula, the results are similar to the case of Arabian Sea. As part of validation efforts, we compare the TOA radiances of three different sources at ( $37.54^\circ\text{N}$ ,  $129.27^\circ\text{E}$ ) off the east coast of Korean peninsula on May 31, 2000 (Fig. 25.7). Calculation of OSMI TOA radiances uses the radiometric calibration coefficients

derived from the case of Arabian Sea. We resample the SeaWiFS data to collocate with OSMI measurements. Inputs for the model rstar5b run include the in-situ measurements of aerosol optical thickness and wind speed. The OSMI TOA radiances lie between the SeaWiFS measurements and model estimates. Apparently, the OSMI TOA measurements are in good agreement (5 ~ 17%) with the SeaWiFS measurements at this location. The model calculation with clear-sky assumption must have underestimated the radiance values because clouds reflect more shortwave radiation to the space. It was, in fact, partly cloudy on the day (May 31, 2000) when in-situ measurements were obtained. Figure 25.8 shows the level 1B image that was obtained from the NASA MSI12 program with the NASA derived cross-calibration coefficients. The banding and striping problems are fairly well treated. The similar analysis as shown in Fig. 25.7 will be made for the 2001 in-situ measurements.

## CONCLUSIONS

We have demonstrated two anomalous features in performing the OSMI data processing: Venetian-Blind effect and Rayleigh limit. To resolve these anomalies properly, we attempted two cross-calibration methods using the collocated match-ups of OSMI and SeaWiFS measurements. Both KARI and NASA methods seem to remove the bands and stripes fairly well and are successful to produce the ocean color (level 2) products. It is however necessary that further efforts should be made to validate the OSMI products.

## ACKNOWLEDGMENTS

We appreciate Prof. B. J. Sohn and Mr. D. H. Kim for their provision of rstar5b model results. The SeaWiFS data used in this study are obtained from the NASA Goddard DAAC.

## REFERENCES

- Dingirard, M. and P. N. Slater, 1999: Calibration of space-multispectral imaging sensors: A review, *Remote Sens. Environ.*, **68**, 194-205.
- Kim, Y., Y. S. Kim, H. Lim, D. Lee, C. Kang, 1999: KOMPSAT data processing system: An overview and preliminary acceptance test results, *J. of the Korean Society of Remote Sensing*, **15**(4), 357-365.
- Lee, D. H. and Y. Kim, 2000: Radiometric calibration of OSMI imagery using solar calibration, *J. of Astron. Space Sci.* **17**(2), 295-308.



Figure 25.1: Arabian Sea (OSMI Level 1A, 765 nm)

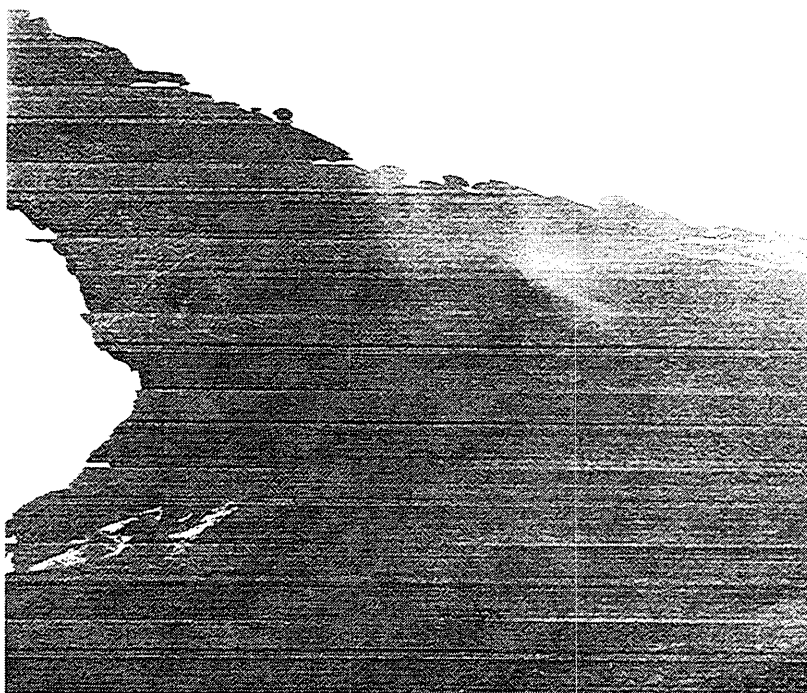


Figure 25.2: Same image as Fig.25.1 but radiometrically calibrated with TRW calibration data



Figure 25.3: Same image as Fig. 25.1 but radiometrically calibrated with solar calibration data

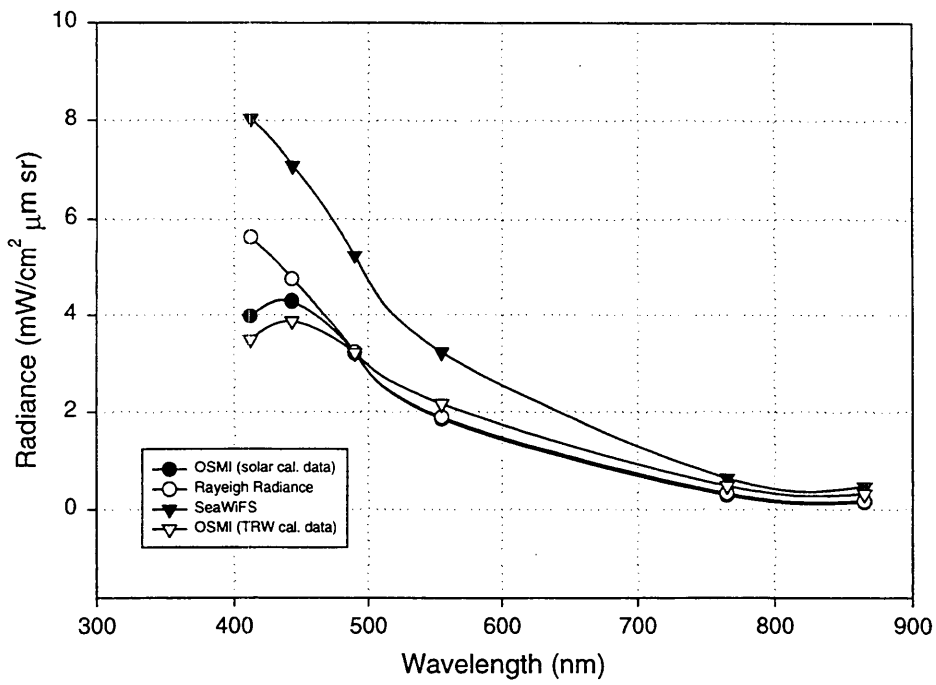


Figure 25.4: Comparison of TOA radiances at (20.01°N, 62.51°E) of Arabian Sea



Figure 25. 5: Same image as Fig. 25.1 but cross-calibrated with KARI method

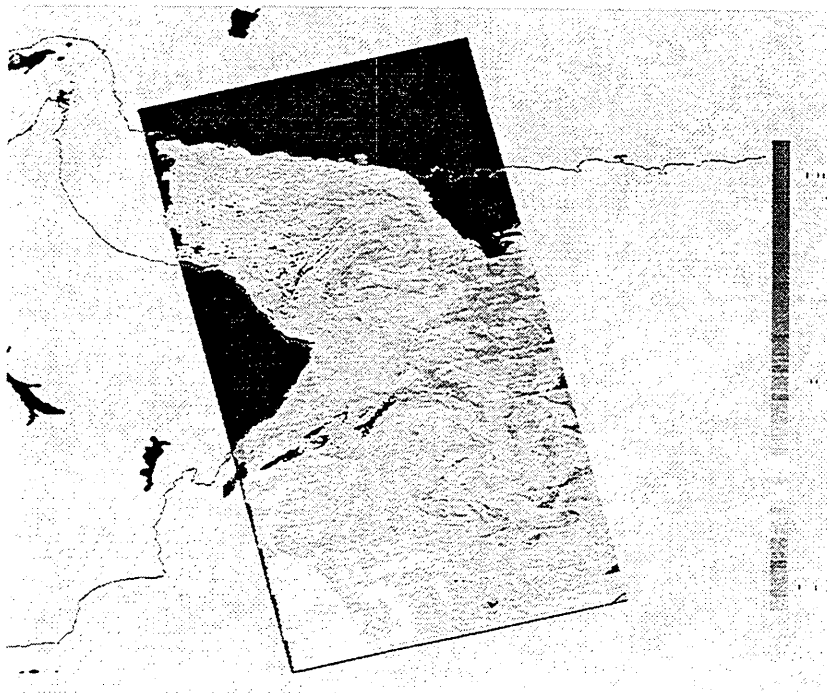


Figure 25. 6: Distribution of chlorophyll concentration ( $\text{mg}\cdot\text{m}^{-3}$ ) in Arabian Sea

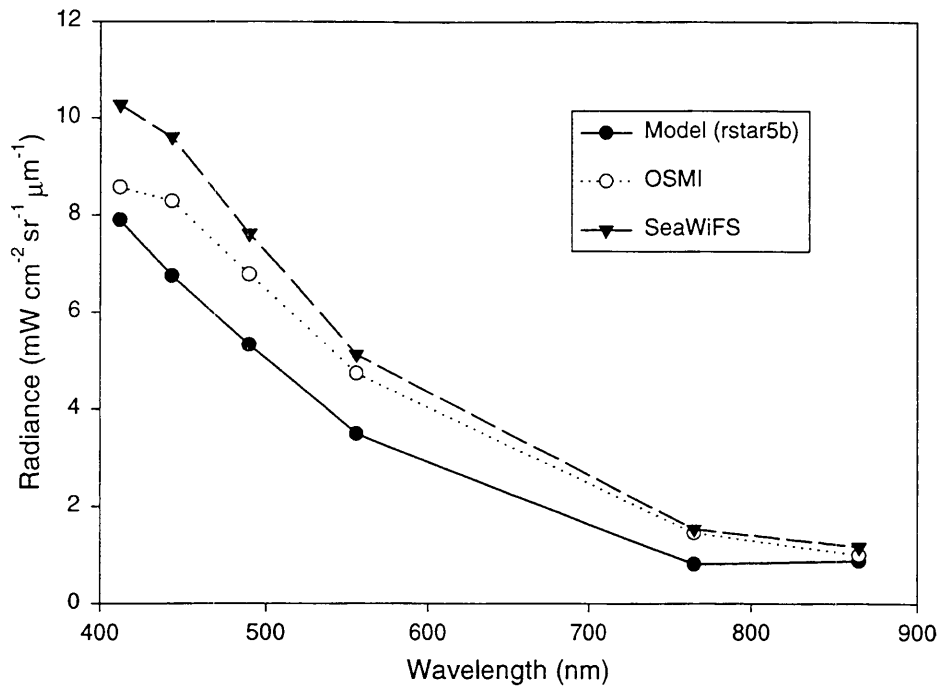


Figure 25.7: TOA radiances at (37.54°N, 129.27°E), May 31, 2000



Figure 25.8: Same image as Fig. 25.1 but cross-calibrated with NASA method

## Chapter 26

# Evaluation and Improvement of the Atmospheric Correction and Bio-optical Algorithms for the Black and Barents Seas

Oleg V. Kopelevich, Vladimir I. Burenkov, Svetlana V. Ershova, Marina A. Evdoshenko, Sergey V. Sheberstov

*Ocean Optics Laboratory, P.P.Shirshov Institute of Oceanology, Moscow, Russia*

### 26.1 INTRODUCTION

The overall objective of this research is to evaluate and improve the atmospheric correction and bio-optical algorithms for the Black and Barents Seas. The Black and Barents Seas are the regions currently subjected to increasing human activity, such as the oil-gas industries and fisheries in both of the regions; and also agriculture and tourism in the Black Sea. The operational monitoring of the environment state and processes in their waters is needed, and the data products derived from satellite ocean-color sensors can make important contribution to realization of such kind of monitoring. The problem is that the both regions qualify as Case 2 waters, with the Barents Sea falls within high-latitudes, and now there are no workable processing algorithms for such waters. The great errors in retrieval of the water-leaving radiances and chlorophyll concentration with the SeaWiFS operational algorithms have been detected in these regions as a result of our previous work done on the SIMBIOS project (Kopelevich 1999a, b, Kopelevich et al. 2001). Specific goals of the current project as follows:

- Evaluate the operational atmospheric correction and bio-optical algorithms for SeaWiFS, GLI and other ocean-color sensors;
- Develop and evaluate the new algorithms making possible to derive the standard data products with enhanced accuracy and to retrieve some new parameters such as the absorption coefficient of yellow substance and the backscattering coefficient of particulate matter;
- Estimate errors in water-leaving radiances, seawater optical characteristics, and chlorophyll concentration derived with different algorithms;
- Draw the conclusions concerning performance of the atmospheric correction and bio-optical algorithms in turbid (Case 2) waters and at high solar zenith angles.

### 26.2 RESEARCH ACTIVITIES

#### *Field studies*

The field studies were carried out in the White and Black Seas in August 2001. In Figure 26.1 the station locations of the cruise # 49 of RV *Professor Shtockman* in the White Sea are shown. The studies on ocean optics and biogeochemistry included measurements of spectral water-leaving radiance just beneath sea surface and down-welling irradiance just above sea surface by a floating spectroradiometer (Artemiev et al. 2000), vertical profiles of the beam attenuation coefficient by a submersible transmissometer, Secchi depth, underwater irradiance in the UV and PAR spectral ranges by a UV-PAR radiometer (Burenkov et al 2001), sampling and filtration of seawater samples from different depths, setting up the sediment traps, determination of size spectra of suspended particles by Coulter Counter, sampling aerosol particles by nets and pumps. Measurements of the spectral remote sensing reflectance were carried out at 8 drift stations, one of them (4 August 2001) was performed simultaneously with SeaWiFS pass under clear sky conditions.

The studies in the Black Sea included measurements of spectral water-leaving radiance above the sea surface, sky radiance and surface irradiance by a deck spectroradiometer, vertical profiles of the beam attenuation coefficient by a submersible transmissometer, sampling from different depth for determination of chlorophyll concentration. Ship measurements by the deck spectroradiometer were carried out onboard RV *Akwanavt* during its steaming and at drift stations off the Russian coast from Gelendjick to Yuzhnaya Ozereevka (44°31'-44°40'N, 37°36'-38°03'E) on 16, 18, 19 and 20 August 2001. On 23-29 August the instrument was mounted on the roof of the pier laboratory in the Blue Bay (near Gelendjick) and measured the surface irradiance and zenith

sky radiance with the aim of validation of the algorithm for retrieval of surface irradiance from SeaWiFS data under clear sky and cloud conditions (Ershova et al. 2001). A list of measurements by the deck spectroradiometer is given in Table 26.1. Since the beginning of October 2001 the ocean color collaborative US-Russia studies have been conducted onboard RV *Akademik Ioffe* as its transits the Atlantic Ocean and then during its tourist cruises in the Antarctic Regions. The ship left Kaliningrad (Russia) for Ushuoya (Argentina), the scientific equipment prepared by Robert Frouin (Scripps Institution of Oceanography) and Michael Reynolds (Brookhaven National Laboratory) was loaded in Kiel and Bremerhaven. On 17 November 2001 the ship came to Ushuoya; since 18 November it has made the tourist cruises from Ushuoya to Antarctica and back (duration of each cruise is 8-18days).

The various atmospheric and ocean characteristics have been studied during the cruises: the aerosol optical thickness and diffuse marine reflectance by the SIMBAD radiometer; the remote sensing reflectance by the deck spectroradiometer of the Shirshov Institute of Oceanology; the direct, diffuse and global irradiance with the Portable Radiation Package of the Brookhaven National Laboratory; chlorophyll-a concentration by a spectrophotometric method (Shirshov Institute of Oceanology); sampling, handling and storage in liquid nitrogen samples for HPLC pigment analyses (the equipment provided by Robert Frouin); seawater spectral absorption coefficient by the laboratory spectrophotometer of the Shirshov Institute of Oceanology; sampling, sample handling and determination of spectral absorption coefficients of particles, dissolved material and phytoplankton for surface water samples (the equipment provided by Robert Frouin).

The ship will leave Ushuoya for the return trip in the middle of March 2002. The studies performed are expected to provide data on spatial changeability of atmospheric and oceanic characteristics in the Atlantic Ocean between 55°N and 55°S in two different seasons as well as their mesoscale variability for poorly studied area south of 55°S from November to March, which will be compared with concurrent satellite data.

#### *Algorithm development*

The simplified algorithm to derive the particle backscattering coefficient  $b_{bp}$  has been developed. The  $b_{bp}$  values can be retrieved from ocean color data by the semianalytic bio-optical algorithm but the latter can not work in the cases of bad atmospheric correction, for example, of turbid waters or observations under conditions of large solar or viewing zenith angles (Burenkov et al. 2001). In such cases the errors of atmospheric correction are most great at 412 and 443 nm and much less at 510 and 555 nm (Kopelevich et al. 2000). The simplified algorithm uses only two SeaWiFS spectral bands 510 and 555 nm and allows to determine the

particle backscattering coefficient  $b_{bp}(555)$ . The  $b_b(555)$  value is derived through the values of the parameter  $X(555)=b_b(555)/[a(555)+b_b(555)]$  and the diffuse attenuation coefficient  $K_d(555)$ ; these quantities are determined from the normalized water-leaving radiances  $L_{wn}(510)$  and  $L_{wn}(555)$ ; the former is directly from  $L_{wn}(555)$ , the latter through the ratio of these radiances.

The regression equation between the  $b_{bp}(555)$  values and the suspended matter concentration  $SPM$  was derived from *in situ* measured data in the Barents Sea:  $SPM = 73.5 b_{bp}(555) + 0.016$ , where  $SPM$  in  $g \cdot m^{-3}$ ,  $b_{bp}(555)$  in  $m^{-1}$ .

Correlation between these quantities is reasonably good; the coefficient of determination  $R^2$  is equal to 0.83, the relative root-mean-square error is about 30%. The developed algorithms were used to derive the mean monthly distributions of the particle backscattering coefficient and the suspended matter concentrations in the Barents Sea from SeaWiFS data.

## 26.3 RESEARCH RESULTS

### *Results of field studies*

As a new result the measured data in the White Sea should be mentioned. This sea is located south to the Barents Sea and connected with it by the strait named Throat of the White Sea. The strong tidal streams through the strait (up to 2 m/s) promote the water exchange in upper layer between the basins. Several rivers (Northern Dvina, Mezen, Onega and others) flow into the White Sea, and it is interesting to make comparison between two neighboured basins. Three examples of the radiance reflectance spectrum measured in the White Sea are given in Figure 26.2. The similarity of the spectra to one another can be noticed, even though they were measured in different parts of the White Sea (see Fig.26.1). All of them have the maximum near 560-570 nm which is indicative of high concentration of colored organic matter ("yellow substance"). The above maximum is higher at St.4681 with larger value of the beam attenuation coefficient and probably with greater concentration of suspended matter. Also all spectra have the other maximum near 680 nm which is due to chlorophyll fluorescence and indicative of its high concentration. The data will be analyzed in detail in 2002.

### *Use of the simplified algorithm*

Figure 26.3 shows the mean monthly distributions of the particle backscattering coefficient  $b_{bp}(555)$ ,  $m^{-1}$  in the Black Sea in June and September derived from SeaWiFS data by the simplified algorithm. The highest values of  $b_{bp}$  (more than  $0.02 m^{-1}$ ) are caused predominantly by river runoff; the pronounced seasonal changeability can be noticed. The main source of suspended matter in the Black Sea is Danube; its

influence is seen the year round. The area of enhanced values of  $b_{bp}$  in the eastern part of the Black Sea is caused by runoff of many small rivers which dry up in summer.

Figure 26.4 shows the mean monthly distributions of the suspended matter concentration  $C_s$  in the Barents Sea in May and July 2000. The most turbid waters ( $C_s > 1-2$  mg/l) are observed in coastal zone and connected with river runoff, coastal erosion, resuspension of bottom sediments by tidal currents. The noticeable difference between May and July is seen. The area of turbid waters in the southern part of the Barents Sea is bigger in May when the river runoff is the greatest. The concentration of suspended matter in the central part of the Barents Sea is also higher in May, probably, due to spring phytoplankton bloom. In July the suspended matter concentration in the central part of the Barents Sea is lowest. The spatial distributions of suspended matter in the Barents Sea constructed from SeaWiFS data is in a good agreement with field data but satellite data provide us with much more information.

## 26.4 FUTURE WORK

Development of the new algorithms to improve an accuracy of the standard data products and retrieve some new parameters in such specific basins as the Black, Barents and White Seas is only possible on the base of *in situ* measured data. At the moment our future plans for the field studies are to be determined. The analysis of data obtained in 2001 and in January-April 2002 during the ongoing *Ioffe* cruise will be performed in 2002. Comparison between different regional algorithms will allow to understand which level of generality can be acceptable for Case 2 waters.

## REFERENCES

Artemiev, V.A., V.I.Burenkov, M.I.Vortman, A.V.Grigoriev, O.V.Kopelevich, and A.N.Khrapko, 2000: Sea-Truth

Measurements of Ocean Color: A New Floating Spectroradiometer and Its Metrology. *Oceanology*, Vol.40, 139-145. Translated from *Okeanologiya*, Vol.40, 148-155.

Burenkov, V.I., V.I.Vedernikov, S.V.Ershova, O.V.Kopelevich, S.V.Sheberstov, 2001: Use of Satellite Ocean Color Data for Assessment of Bio-Optical Characteristics in the Barents Sea. *Oceanology*, Vol.41. Translated from *Okeanologiya*, Vol.41, 485-492.

Ershova, S.V., O.V.Kopelevich, S.V.Sheberstov, V.I.Burenkov, and A.N.Khrapko, 2001: A Method for Estimating the Penetration of Solar Visual and Ultraviolet Radiation into the waters of the Arctic Seas Using Satellite Data: The Case of a Cloudless Atmosphere. *Oceanology*, Vol.41, 317-325.

Kopelevich, O.V., 1999a: Validation of the Water-Leaving Radiance Data Product .In: C. McClain, G. Fargion: SIMBIOS Project 1998 Annual Report. *NASA Tech. Memo. 208645*, NASA Goddard Space Flight Center, Greenbelt, Maryland, 88-93.

Kopelevich, O.V., 1999b: Validation of the Water-Leaving Radiance Data Product .In: C.R. McClain and G.S. Fargion: SIMBIOS Project 1999 Annual Report. *NASA Tech. Memo. 209486*, NASA Goddard Space Flight Center, Greenbelt, Maryland, 121-126.

Kopelevich, O.V., V.I.Burenkov, S.V.Ershova, S.V.Sheberstov, M.A.Evdoshenko, G.K.Karabashev, C.A.Pavlov, 2001: Validation of the Water-Leaving Radiance Data Product .In: G. Fargion and c. McClain: SIMBIOS Project 2000 Annual Report. *NASA Tech. Memo. 209976*, NASA Goddard Space Flight Center, Greenbelt, Maryland, 157-162.

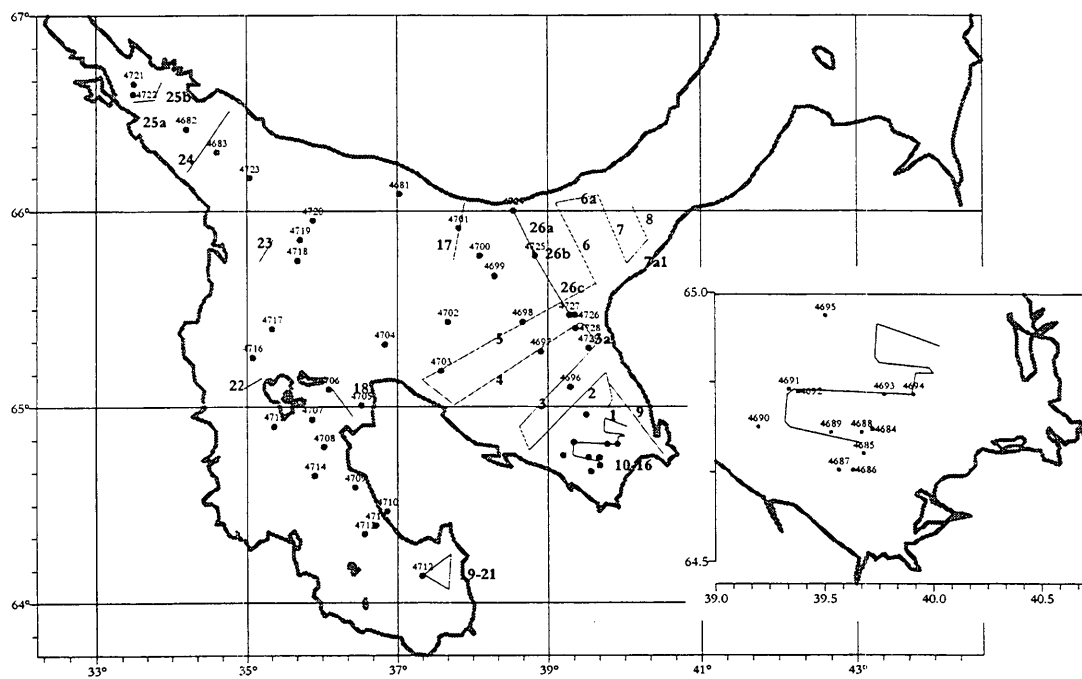


Figure 26.1: The station locations of the cruise # 49 of RV *Professor Stockman* in the White Sea. The station locations in the south part of the Dvina Bay are shown on the setting-in.

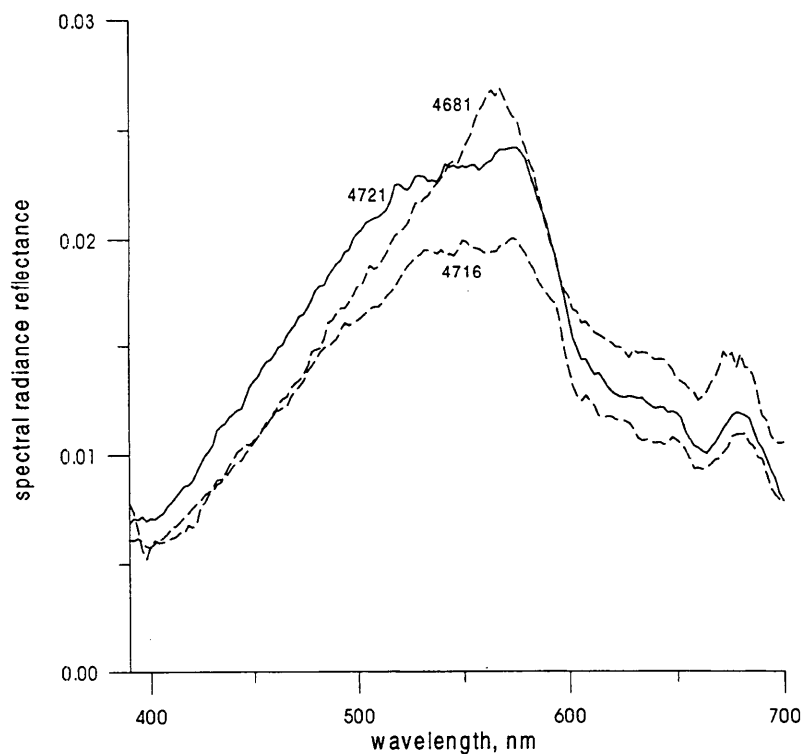


Figure 26.2: Radiance reflectance spectra measured in the White Sea at different stations. The values of the beam attenuation coefficient were  $0.97 \text{ m}^{-1}$  at St.4681,  $0.76 \text{ m}^{-1}$  at St.4716, and  $0.73 \text{ m}^{-1}$  at St.4721.

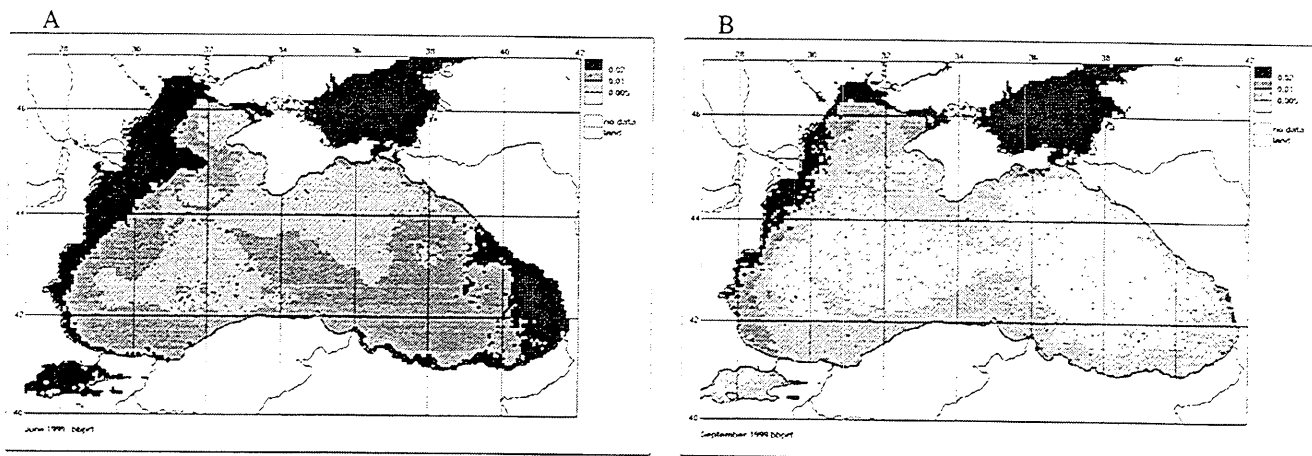


Figure 26.3: The mean monthly distributions of the particle backscattering coefficient  $b_{bp}(555)$ ,  $m^{-1}$  in the Black Sea in June (A) and September (B) derived from SeaWiFS data in 1999.

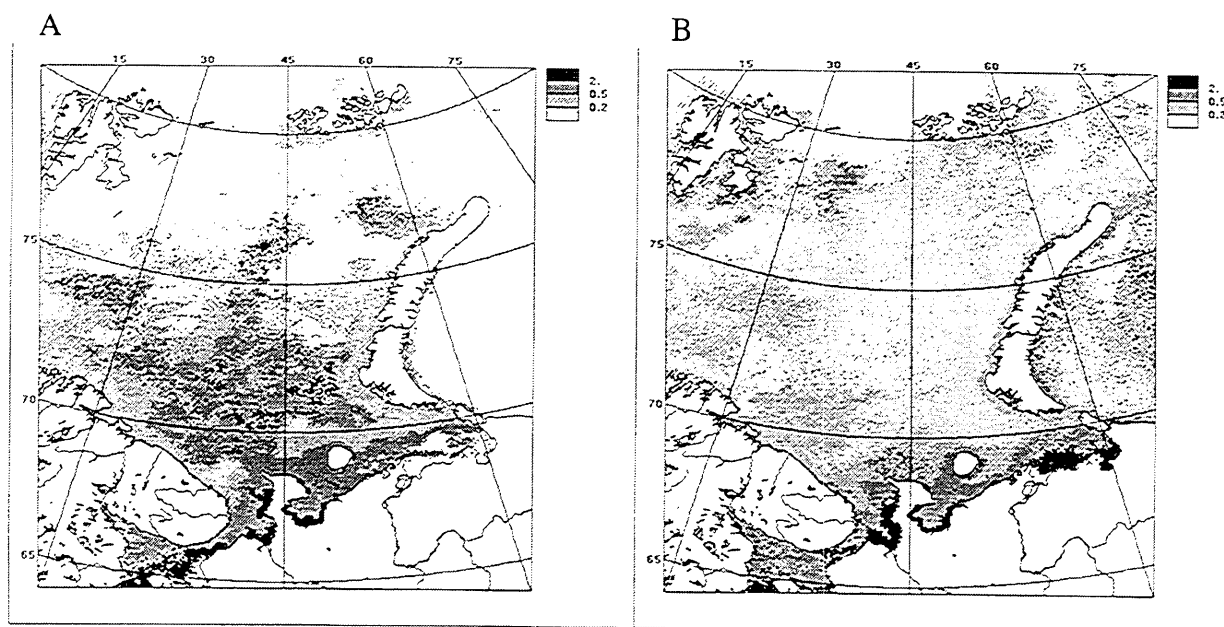


Figure 26.4 : The mean monthly distributions of the suspended matter concentration (mg/l) in the Barents Sea in May (A) and July (B) derived from SeaWiFS data in 2000.

Table 26.1: Measurements by the deck spectroradiometer in the Black Sea in August 2001

Date	Local time of measurements*	SeaWiFS		Location	Sky condition
		Time of the pass	Elevation, deg		
16 Aug 01	13:34 – 18:59	13:40	51.5	Near Gelendjick	Clear
18 Aug 01	11:06 – 18:50	13:26	38.4	Blue Bay- Novorossisk	Clear
19 Aug 01	09:30 – 19:43	14:09	82.5	Near Yuzhnaya Ozereevka	Clouds
20 Aug 01	11:51 – 16:55	14:51	33.0	Near Blue Bay	Clouds, rain
23 Aug 01	07:49 – 19:43	13:43	55.5	Blue Bay	Clouds
24 Aug 01	07:27 – 19:41	14:25	57.6	Blue Bay	Clouds
25 Aug 01	07:33 – 19:39	13:30	41.2	Blue Bay	Clear
26 Aug 01	07:28 – 19:37	14:13	77.1	Blue Bay	Clouds
27 Aug 01	07:22 – 19:34	13:16	31.0	Blue Bay	Clouds
28 Aug 01	07:24 – 19:34	14:00	80.3	Blue Bay	Clear
29 Aug 01	07:39 – 15:43	14:41	40.4	Blue Bay	clouds

\*the time difference between the local time and GMT is + 4 hours

## Chapter 27

# VALIDATION OF SEAWIFS OCEAN AND ATMOSPHERIC PRODUCTS IN THE MEDITERRANEAN SEA

R. Santoleri, G.L. Liberti, G.P. Gobbi and F. Barnaba

*Istituto di Scienze dell'Atmosfera e del Clima – ISAC, Italy*

M. Ribera d'Alcalà, F. D'Ortenzio, M. Ragni, G.L. Volpe and E. Bohm

*Stazione Zoologica A. Dorn di Napoli – SZN, Italy*

S. Marullo

*Ente Nazionale per le Nuove tecnologie l' Energia e l'Ambiente – ENEA, Italy*

### 27.1 INTRODUCTION

The objective of this report is to describe the activities linked to the SIMBIOS project carried out during the year 2001 by the joint ISAC and SZN group. The goal of this research was: 1) to assess the accuracy of satellite ocean color products in the Mediterranean Sea. 2) to develop new regional ocean color algorithms for the Mediterranean Sea that include improved atmospheric correction (Mediterranean aerosols) and retrieval of bio-optical parameters. 3) to design and execute oceanographic campaigns to investigate particularly the relationship between mesoscale features and biological response over selected areas and validate Mediterranean algorithms.

The Mediterranean Sea is a mid-latitude, predominantly oligotrophic and ultra-oligotrophic basin. However, higher biomass may locally and seasonally occur in regions affected by river runoff or by deep convection events (Antoine et al., 1996). This basin is a good oceanographic test area both for its complex ocean dynamics, which mimics several basic processes of ocean functioning and for its intensive anthropogenic pressure. From the atmospheric point of view, the Mediterranean area is strongly affected by anthropogenic emissions from the highly industrialized northern border and desert dust from the south. Aerosols transported to the Mediterranean Sea may be considered to consist of anthropogenic-rich "background" materials supplied continuously from Europe, upon which sporadic pulses of Saharan crust-rich dust are superimposed. Schematically, the latter represent more than 90% of the mass of particulate atmospheric deposition, though they occur 10% of the time in the Mediterranean atmosphere, whereas the inverse figures

apply to anthropogenic aerosols. The very peculiar aerosol composition makes more difficult the use of routine remote sensing procedures for atmospheric correction (Moulin et al., 1997). In parallel, previous study on CZCS data in this basin (Morel and André, 1991; Antoine et al., 1996) showed that the global ocean-color bio-optical algorithm often results in a poor estimate of the chlorophyll-a.

All the considerations above imply the need of a special validation effort for the Mediterranean Sea and eventually the development of new regional ocean color algorithms. Development of specific regional algorithms requires, as a starting point the evaluation of current SeaWiFS standard products to identify and understand areas possible sources of errors and design activities for their handling. Within this frame, the following strategy was adopted in this first year activity. Firstly, independent teams with specific experience analysed separately the SeaWiFS current atmospheric correction scheme and the bio-optical algorithms. At the same time, a joint effort in collecting data to enlarge the available data set for studies was carried out by both teams with a dedicated effort in data acquisition both from land based instrumentation as well as from specific oceanographic campaigns. In the following a brief description of activities is reported.

### 27.2 RESEARCH ACTIVITIES

#### *In situ data acquisition*

During the 2001 oceanographic in situ data acquisition consisted in: a major oceanographic cruise, Norbal 2001, carried out in December in the Western Mediterranean Sea,

three additional cruises in which only SIMBAD measurements were performed and weekly measurements in the Gulf of Naples.

During the NORBAL 2001 cruise, 62 hydrological profiles (CTD casts) have been carried out along transects covering different region of the West Mediterranean: North Tyrrhenian, the Ligurian Sea and the Gulf of Lion. In a selected number of stations, samples for Winkler determination of dissolved organic and inorganic nutrients were collected to characterize water mass properties and associated fluxes. Around mid-day bio-optical stations were performed. In this station in water bio-optical profiles were acquired by means of a Satlantic SPMR radiometer, vertical profiles of PAR and variable fluorescence were performed. In the bio-optical stations phytoplackton lipophilic pigment distribution (HPLC and spectrofluorometer analysis) and ancillary biological data were also acquired. Moreover, during the daytime several measurements of upwelling radiances at ocean colour wave length and solar irradiance and sky irradiance were measured using SIMBAD instrument. Finally, meteorological parameters, sea surface temperature, salinity and fluorescence were measured continuously along the ship track. Vertical profiles of horizontal velocities were also acquired continuously (surface-to 300 m) by means of two on board ADCP currentmeters. In figure 1 the position of the CTD station were reported.

Thanks to an agreement with other Italian research Institution we take the opportunity to carried out SIMBAD measurements during three addition cruises carried out in March, September and October 2001. Actually a total of 45 days of measurements of water leaving radiances, atmospheric aerosol load and type were acquired in the Mediterranean Sea during 2001. Data are currently under processing at LOD (Laboratoire d'Optique Atmospherique) and will be available at the SIMBAD web site.

In addition a weekly station in which CTD profile, water samples and bio-optical measurements were taken in the Gulf of Naples. Using the fact that the Gulf of Naples station is reached with a relatively fast motorboat an experiment was designed based on frequent atmospheric measurements with SIMBAD to evaluate the variability of the AOT from land to coast. Results from such an experiment would be used to have a first estimate of uncertainties derived from the use of land based coastal site for the validation of off-shore aerosol optical properties. Unfortunately, the first attempt of such experiment failed because of problems with the SIMBAD instrument. The experiment will be repeated, as often as possible, during the next year depending on SIMBAD availability.

### *Land Observations*

Giving the relatively high frequency of occurrence anomalous stratification in the vertical aerosol distribution, in the Mediterranean basin, as for example in the case of desert dust transport events and the expected impact on remotely sensed ocean colour, a particular effort have been concentrated in the description of the vertical distribution of aerosol extinction. A technique to derive aerosol extinction profiles from single-wavelength (532 nm) lidar measurements have been improved by adding continental aerosol types to the aerosol types already accounted for (stratospheric volcanic (Gobbi, 1995); maritime and desert dust (Barnaba and Gobbi, 2001, Gobbi et al., 2000).

At the same time we are collecting a yearly record (Feb. 2001-Feb.2002) of coincidental lidar and sunphotometer (AERONET site Rome Tor Vergata) observations to validate such inversion schemes and to study the impact of aerosols (in particular desert dust) on solar radiation. The outcome of these studies will have an impact on all lidar and photometric activities relevant to SIMBIOS.

## **27.3 RESEARCH RESULTS**

### *Evaluation of the performances of the atmospheric correction scheme in the case of Mediterranean basin*

Preliminary results of a validation exercise aimed to evaluate the SeaWiFS aerosol products goodness over the Mediterranean Basin are presented in this section, (see also Liberti et al., 2000). The validation data set is based on observations from AERONET (Holben et al., 1998) ground-based CIMEL sun-photometers measurements made in sites around the Mediterranean within 100 km from the coast. The following sites were selected: Avignon, El Arenosillo, Erdemli, Lampedusa, Nes Ziona, Oristano, Venezia. Data from the EU campaign ADMIRA in Nea Michaniona (Webb et al.2002) were also used.

The data analyzed derive from single SeaWiFS orbit data collected at the receiving station of Roma Tor Vergata (41°50'N 12°39'E), during the whole year 2000, and successively processed to level 2.0 geophysical products using SEADAS processing Version 4.0b (Gordon and Wang 1994, Wang 2000) with the following options that are the ones adopted for the standard NASA products: Multi-scattering atmospheric corrections; Aerosol model selection based on the analysis of the 765 and 865 nm radiances; Siegel (Siegel et al. 2000) NIR iterations; land and straylight flags were activated. Level 2 processed data were successively remapped on a Cylindrical Equirectangular Projection with a reduced ground

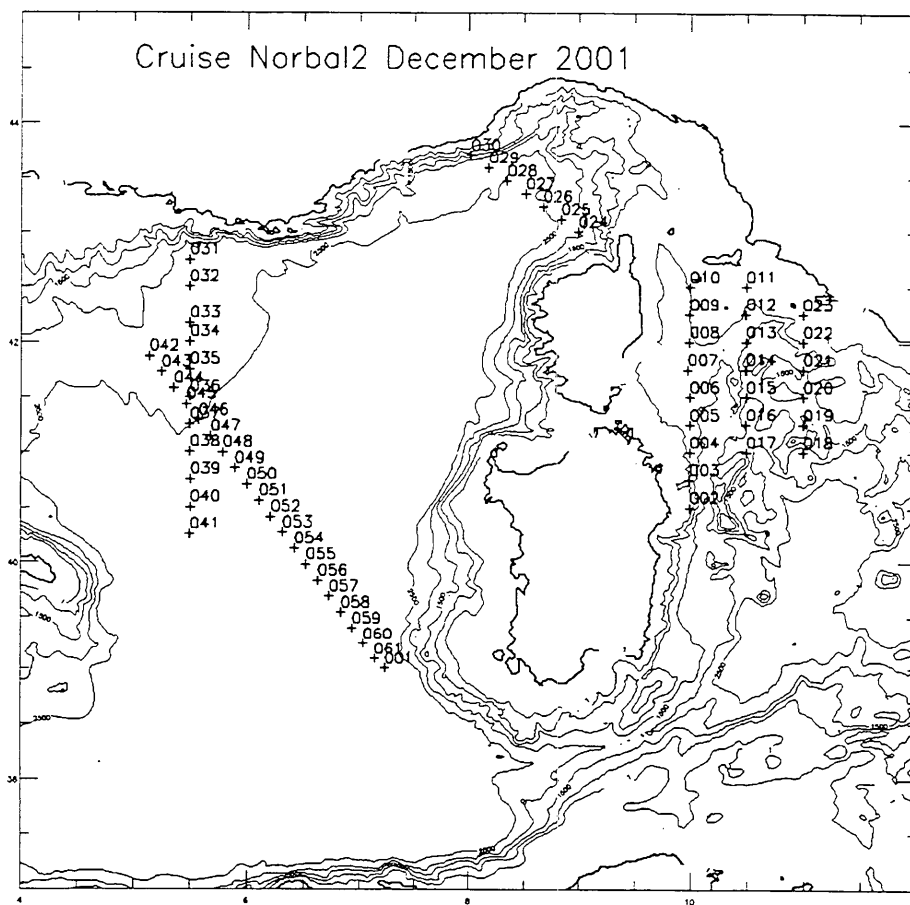


Figure 27.1: Area of Norbal 2001 cruise measurements and position of CTD stations.

resolution of about 4 km obtained with a nearest neighbour sampling. The resulting data set consists into about 670 single orbit images with very few data gaps, mostly occurring between September and October.

CIMEL-AERONET instruments and the SeaWiFS radiometer have only three common wavelengths: 440, 670 and 875 nm. Therefore, as a preliminary analysis, aerosol optical thickness at 670 nm ( $\lambda$ ) and the Ångström coefficient between 670 and 875 nm were compared. The evaluation of the SeaWiFS products have been performed with several parallel activities:

- the first type of evaluation is based on a subjective analysis of each single orbit product map as well as monthly and seasonal composites ones. From such an analysis it is expected to identify evident algorithm behaviours such as the occurrence of clearly not-physical features/values, consequence, for example, of calibration, observation geometry and cloud screening.
- a second type statistical or pseudo-climatological comparison of SeaWiFS aerosol derived products against ground truth derived ones. The rationale for this comparison is that climatologies of geophysical parameters for the same areas and periods, should compare also if areas and periods do not match exactly but refer to the same climatological regime.
- Finally, a match-up comparison was performed. The matching criteria have been determined by analysing spatial and temporal variability characteristics of the aerosol products. Fig. 27.2 shows the comparison of match-up results obtained using ground truth data in a  $\pm 0.5$  hr time window from the satellite overpass and in a space window of 40 km around the ground truth data. A relatively good agreement for the aerosol optical thickness is found. On the contrary, the comparison of  $\alpha$  shows a very poor agreement between AERONET in situ and SeaWiFS estimations. On the other hand, part of the relatively large in situ values of  $\alpha$  come from the

Oristano station, which we suspect to have a calibration problem which produces larger values of  $\alpha$  at local noon.

The main conclusions from such preliminary comparison are:

- relatively good agreement for the aerosol optical thickness at NIR wavelengths.
- underestimation of the Angstrom coefficients because of lack of models covering part of the commonly observed values in the Mediterranean Sea.

On the basis of the analysis of ground truth data and recent literature on characterization of aerosols in the Mediterranean Area, it seems that the SeaWiFS candidate aerosol models are somehow too maritime. In fact, Mediterranean Sea is relatively a close basin, with low wind intensity regimes and under the influence of strong continental-like, both anthropogenic and natural, sources of aerosols. An interesting feature is the selection of tropospheric aerosol for relatively polluted area. Giving the fact that the aerosol model selection is based on the spectral dependence of a signal in a relatively narrow region of the NIR spectrum (760 and 870 nm) there may be more than one aerosol having in such region the same spectral dependence. This is roughly true for the two main components of the Tropospheric (i.e. the water soluble) and the Urban (i.e. the soot). Similarly the Sea Salt shows in the NIR a spectral dependence relatively similar to that of the Desert Dust or of the Clouds.

On the other hand, the relatively good agreement in retrieving NIR aerosol optical thickness may be explained by the fact that the two wavelengths used for the aerosol model selection (i.e. 760 and 870 nm) are relatively close so that the optical characteristics other than the aerosol optical thickness (representative somehow of the amount of aerosol) i.e. the single scattering albedo and the phase function (specific of the aerosol model) are relatively similar among the ones of the candidate models. In such a way the main source of variability in the measured radiance is the optical thickness.

In terms of chlorophyll retrieval a wrong estimate of the Angstrom coefficient may have a strong impact. In fact, the Angstrom coefficient is responsible for the colour of the atmosphere and wrong evaluation of the spectral dependence of the aerosol component may introduce in the water leaving reflectances undesired spectral behaviour.

Validation of SeaWiFS aerosol products has been already performed (Wang et al. 2000). Although, there are few differences in the match up criteria that are aimed to select relatively clear ( $\tau < 0.2$ ) and stable days, the results are similar: i.e. a good agreement between AOT's at the NIR wavelengths while an underestimation going to shorter wavelengths. This is consistent with our results. Although, the sites are not in the Mediterranean Sea, they still are on coasts of the Northern Hemisphere. It is interesting to notice that

similar results were obtained in the validation POLDER aerosol products over ocean (Goloub et al. 1999).

#### *Evaluation of empirical SeaWiFS bio-optical algorithms for chlorophyll-a retrieval in the Mediterranean*

The major aim of this section is the validation of some representative empirical algorithms to determine their performance in retrieving chlorophyll-a concentration in the Mediterranean Sea from SeaWiFS data (see also D'Ortenzio et al. 2001). We selected three algorithms: OC2v4 and OC4v4 as NASA's operational algorithms, and GIT (Gitelson et al., 1996), as an example of a regional Mediterranean algorithm.

In view of the SeaWiFS ocean color algorithms' validation in the Mediterranean Sea, a specific data set of bio-optical and pigment concentration measurements has been built by SZN group in the period 1998-2000 in the framework of the SYMPLEX (SYnoptic Mesoscale and PLankton EXperiment) Project of the Italian Space Agency (ASI). During SYMPLEX project four oceanographic cruises were performed on board the R/V Urania of the Italian Research Council. During each cruise, water samples were taken from Niskin bottles mounted on a General Oceanics Rosette equipped with a SBE 911 CTD profiler and a SeaTech Fluorometer. Sub-samples to measure chlorophyll-a (C) and phaeophytin-a (P) were filtered on board on GF/F filters (low vacuum) and immediately deep-frozen. Pigment concentrations were subsequently determined at the SZN on 90% acetone extracts within few weeks of the sampling using a SPEX Fluorolog spectrofluorometer with an estimated coefficient of variation for chlorophyll-a concentration of ca. 10% (Neveux and Panouse, 1987). For each cruise, we merged and linearly fitted spectrofluorometrically derived chlorophyll-a concentrations with data acquired by the SeaTech in situ fluorometer. Therefore, the data set consists of 582 chlorophyll-a profiles derived from the calibrated fluorescence profiles. We also conducted optical measurements at selected sites during each cruise, totally 45 stations. In water downwelling irradiance (Ed) and upwelling radiance (Lu) profiles were taken in 32 stations using a Satlantic SPMR (SeaWiFS Profiling Multichannel Radiometer). The data were acquired following the standard SeaWiFS protocols (Mueller & Austin, 1995). The instrument had been calibrated at Satlantic Inc. just prior to each cruise. The above water measurements were made in the remaining 13 stations (when SPMR were not available) using the SIMBAD radiometer. SIMBAD data were then processed at LOA of the University of Lille (Fougnie et al., 1998). The final data set covers a relatively wide range of conditions in Case 1 waters of the Mediterranean Sea, spanning from oligotrophic (Sicily Channel and Ionian Sea) to moderately

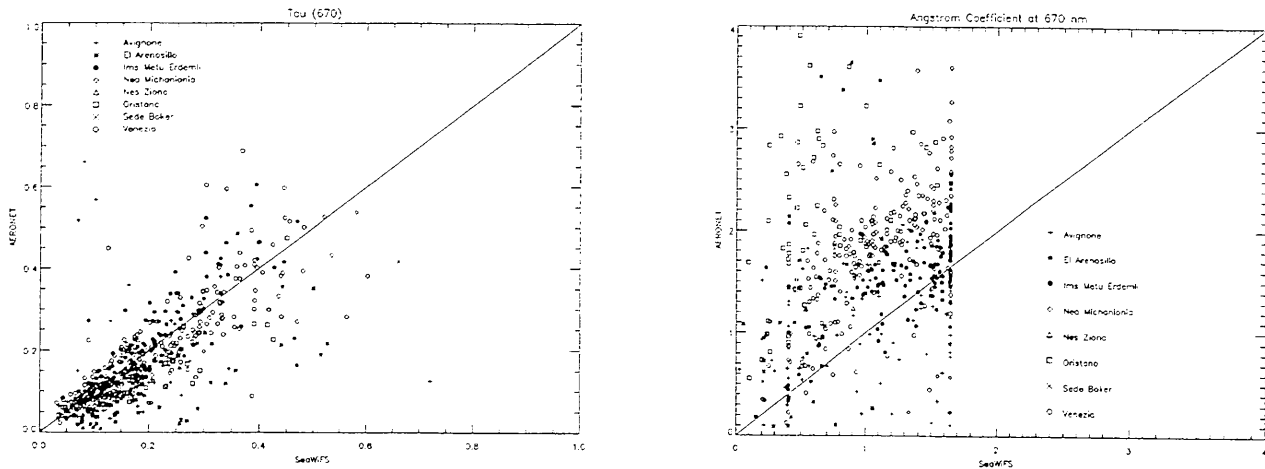


Figure 27.2: SeaWiFS products (X-axis) vs Ground Truth ones (Y-axis):  $\tau$  (left) and  $\alpha$  (right). Measurements have been matched using the  $\pm 0.5$  hr time window for the ground truth data and the closest not-empty distance class for SeaWiFS products

eutrophic regimes (North-Western Mediterranean). Chlorophyll-a concentrations vary between 0.03 and 2.75 mg/m<sup>3</sup>, though low values ( $< 0.1$  mg/m<sup>3</sup>) are definitely more numerous ( $\approx 70\%$ ). Most of them were sampled during the stratified season at sites exhibiting one, or seldom two, Deep Chlorophyll Maxima (DCM) located in the 55-85 m depth interval. To test the performance of different algorithms in retrieving chlorophyll-a concentrations independently from atmospheric correction errors, we used only situ optical measurements (Rrs) and concurrent in situ chlorophyll-a data. Bio-optical estimates of chlorophyll-a (Cmod) were obtained by introducing the in situ Rrs measurements in the three selected algorithms. For algorithms requiring data at wavelengths different from those available from in situ optical measurements (i.e. GIT and OC4v4 when applied to SIMBAD data), Rrs estimates have been generated using the interpolation procedure suggested by O'Reilly et al. (2000). The results of this validation are shown in Figure 27.2. The analysis revealed a systematic overestimation of chlorophyll-a concentration by NASA global algorithms (OC2v4 and OC4v4). The error appears to be correlated with chlorophyll-a concentration, by exhibiting marked differences at low values ( $C < 0.15$  mg/m<sup>3</sup>). In particular at low concentration, the bias observed for OC2v4 is about twice that observed for OC4v4. The same analysis made using the Gitelson et al. (1996) CZCS regional algorithm revealed that this model underestimate the pigments concentration but it does not exhibit a correlation between the error and the measures. The algorithm validation suggests that a regional algorithm is needed for the Mediterranean Sea. Even if the bio-optical data set presented above consists of a limited number of data (45 stations), they represent most of the Mediterranean conditions ranging from

oligotrophic to moderately eutrophic regimes. It is then possible to use this dataset to develop a preliminary version of a Mediterranean ocean color algorithm. Two new Mediterranean algorithms are then proposed by fitting our Mediterranean bio-optical data set with a linear (L-DORMA) and an OC2-like functional forms (NL-DORMA):

$$C = 10^{(0.217 - 2.728R + 0.704R^2 + 0.297R^3)} - 0.035$$

$$C = 1.49 * 10^{(-2.51R)}$$

where  $R = \log_{10}(Rrs_{490}/Rrs_{555})$

Finally, we performed a validation of the algorithms by comparing satellite estimates with concurrent in situ chlorophyll-a observations. The validation procedure was applied to the selected algorithm as well as to the new Mediterranean algorithm. Moreover, we considered also the Neural Network Algorithm (NNA), to complete the list of the algorithms provided by NASA's standard processing system (Gross et al., 2000). We opportunely modified the SeaDAS code to allow the application of the tested bio-optical algorithms, which are not present in the used SeaDAS software version. Chlorophyll maps have been flagged by applying all of the 24 masks provided by SeaDAS (Baith et al., 2001). This implies that Saharan dust events have been implicitly excluded by our analysis. The scatter plots of satellite chlorophyll estimates versus in situ measurements are shown in figure 4. In this case, the OC2v4 algorithm exhibits better estimates than OC4v4, which is probably more affected by atmospheric correction problems. When applied to satellite data, the GIT algorithm performs better than the NASA global

algorithms, even though the estimates are very poor in the high chlorophyll-a range. The new algorithms perform well when applied either to the bio-optical measurements or to satellite data. The main conclusions of the work are: the actual SeaWiFS algorithms selected are not able to give chlorophyll-a estimates for the Mediterranean Sea satisfying NASA requirements (i.e. 35% error in chlorophyll-a concentration). The analysis of bio-optical measurements revealed a systematic overestimation of chlorophyll-a concentration by NASA global algorithms. The error appears to be correlated with chlorophyll-a concentration, by exhibiting marked differences at low values ( $C < 0.15$  mg/m<sup>3</sup>). In particular at

low concentration, the bias observed for OC2v4 is about twice that observed for OC4v4. The different behaviour of the same algorithm when applied to bio-optical measurements or to remotely sensed data demonstrates that the atmospheric correction is still the main source of error in ocean color data. Due to the relatively small number of available in situ data, the algorithms that we generated have to be considered very preliminary, but clearly reveal the necessity of the development of a Mediterranean regional algorithm. A discussion on the reasons of the global algorithms misfit, providing possible explanations and some preliminary result can be found in D'Ortenzio et al., (2001).

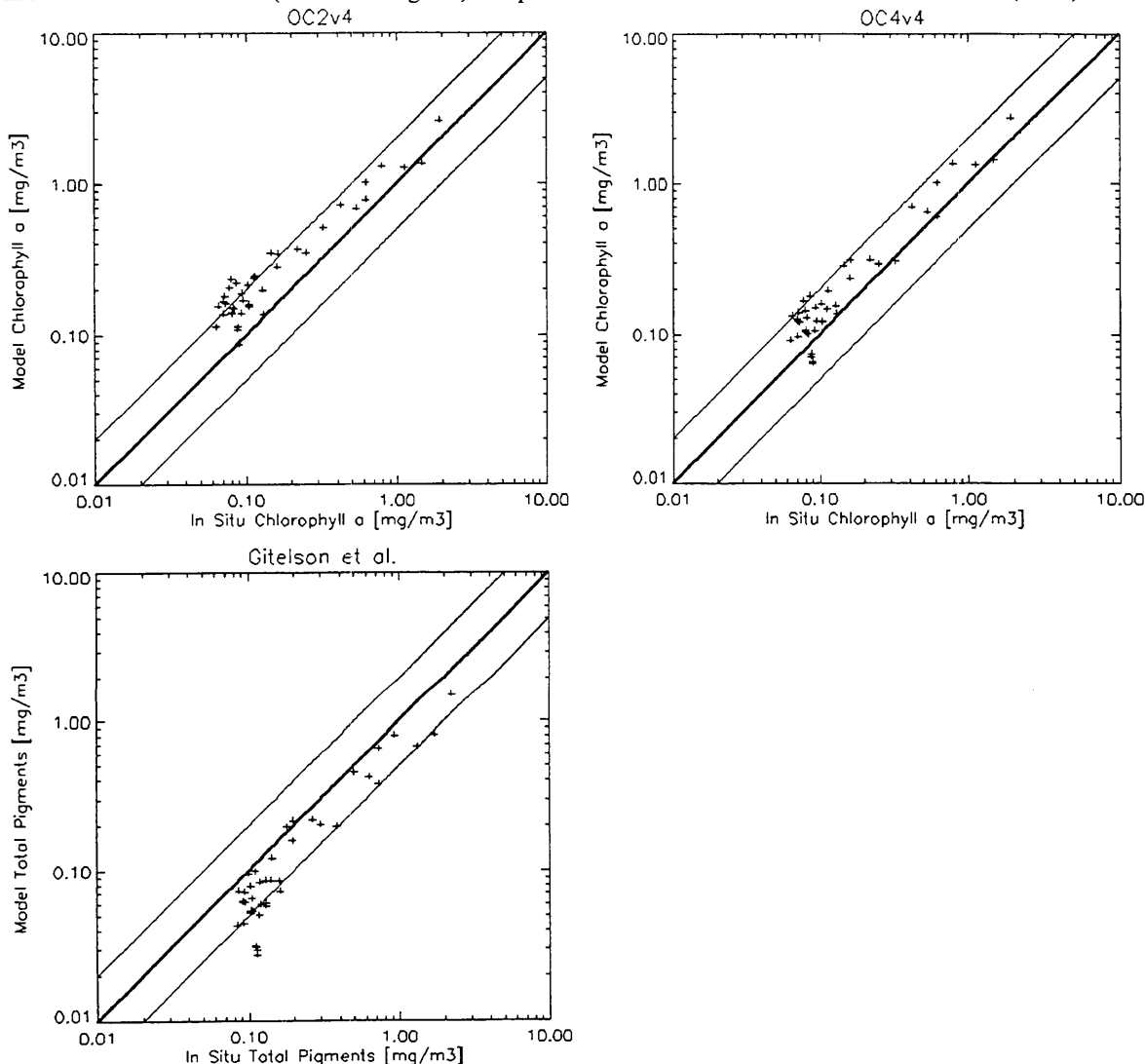


Figure 27.3: Algorithm validation using *in situ* bio-optical measurements and concurrent *in situ* chlorophyll-a data  $C_M$  : (a) scatter plot of OC2v4 model values versus  $C_M$ ; (b) scatter plot OC4v4 model values versus  $C_M$ ; (c) scatter plot of GIT model values versus  $C_M$ . The 1:1 (center thick line) 1:2 (bottom thin line) and the 2:1 (top thin line) lines are also plotted.

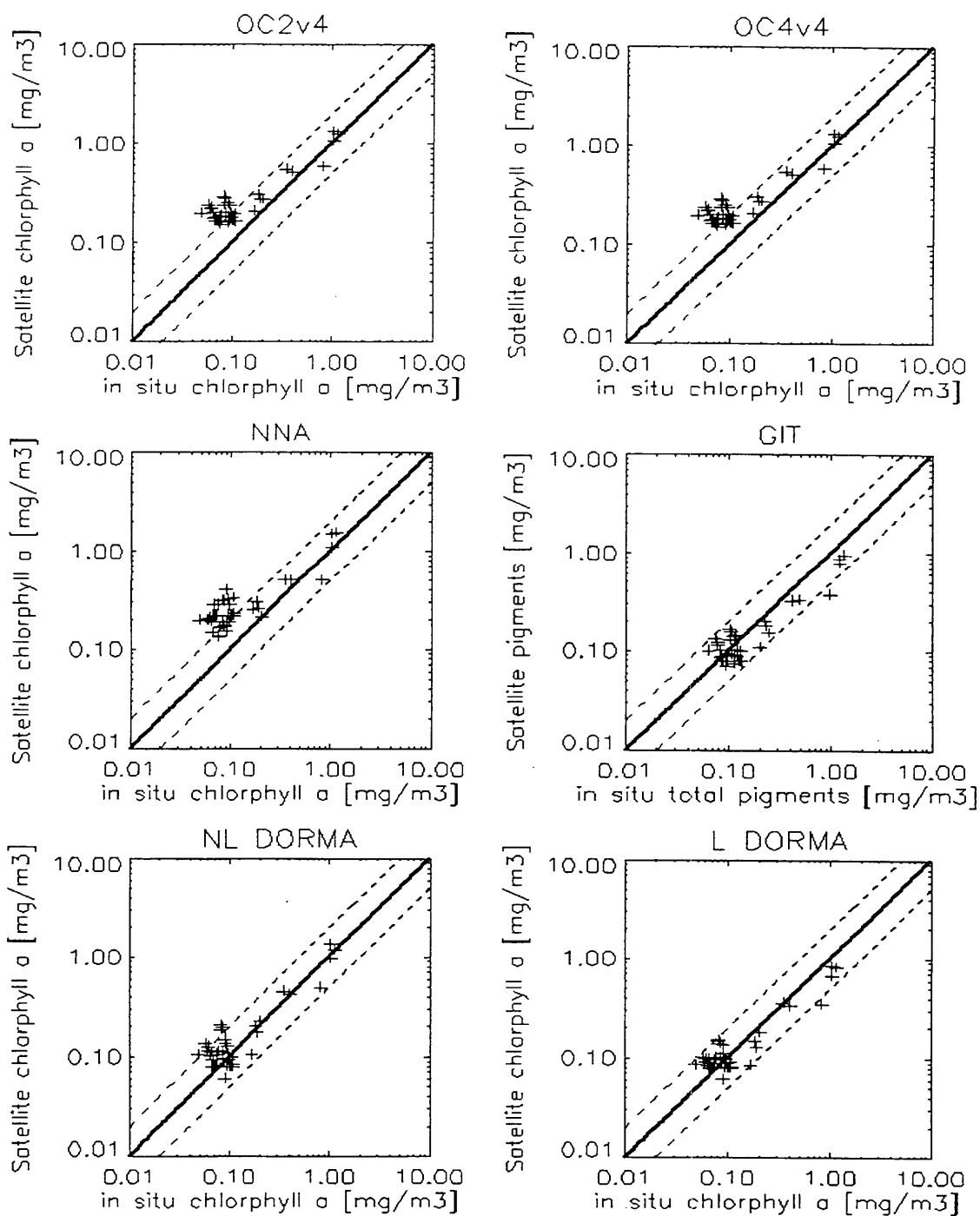


Figure 27.4: SeaWiFS chlorophyll-*a* estimates ( $C_{sat}$ ) validation against concurrent in situ chlorophyll-*a* data  $C_{situ}$ : (a) scatter plot of SeaWiFS estimate using OC2v4 model values versus  $C_{situ}$ ; (b) scatter plot of SeaWiFS estimate using OC4v4 model values versus  $C_{situ}$ ; (c) scatter plot of SeaWiFS estimate using Neural Network model values versus  $C_{situ}$ ; (d) scatter plot of SeaWiFS estimate using GIT model values versus  $C_{situ}$ ; (e) scatter plot of SeaWiFS estimate using NL-DORMA model values versus  $C_{situ}$ . (f) scatter plot of SeaWiFS estimate using L-DORMA model values versus  $C_{situ}$ . The 1:1 (center thick line) 1:2 (bottom thin line) and the 2:1 (top thin line) lines are also plotted.

## REFERENCES:

- Antoine, D., Morel, A. and André, J.-M. 1996: Algal pigment distribution and primary production in the eastern Mediterranean as derived from coastal zone color scanner observations. *J. Geophys. Res.* **100**, 16,193-16,209
- Baith, K., R. Lindsay, G. Fu, and C. R. McClain, 2001: SeaDAS: Data Analysis System Developed for Ocean Color Satellite Sensors, *Eos, Trans. AGU*, **82** (18), 202.
- Barnaba F. and Gobbi. G.P., 2001: Lidar estimation of tropospheric aerosol extinction, surface area and volume: Maritime and desert-dust cases, *Journal of Geophysical Research*, **106**-D3, 3005-3018.
- D'Ortenzio, S. Marullo, M. Ragni, M. Ribera, 2001: Validation of empirical SeaWiFS algorithms for chlorophyll-a retrieval in the Mediterranean Sea: a case study for oligotrophic seas, in press *Rem. Sens. Environ.*
- Gitelson A., Karnieli A., Goldman N., Yacobi Y.Z., Mayo M. 1996: Chlorophyll estimation in the SE Mediterranean using CZCS images: adaptation of an algorithm and its validation, *J. Marine Sys.*, **9**, 283-290
- Gobbi, G.P., 1995: Lidar estimation of stratospheric aerosol properties: Surface, volume, and extinction to backscatter ratio, *Journal of Geophysical Research*, **100**, 11,219-11,235, 1995.
- Gobbi, G. P., F. Barnaba, R. Giorgi and A. Santacasa, 2000: Altitude-resolved properties of a Saharan dust event over the Mediterranean, *Atmospheric Environment*, **34**, 5119 - 5127.
- Goloub P, D. Tanré, J.L. Deuzé, M. Herman, A. Marchand, F.M. Bréon, 1999: Validation of the first algorithm applied for deriving the aerosol properties over the ocean using the POLDER/ADEOS measurements, *IEEE Transactions on Geoscience and Remote Sensing*, **37**, 1586-1596.
- Gordon, H.R., and M. Wang, 1994: Retrieval of water-leaving radiance and aerosol optical thickness over the oceans with SeaWiFS: A preliminary algorithm, *Appl. Opt.*, **33**, 443-452.
- Gross, L., Thiria, S., Frouin, R. and Mitchell, B. G. 2000: Artificial neural networks for modeling the transfer function between marine reflectance and phytoplankton pigment concentration, *J. Geophys. Res.*, **105**, 3483-3495.
- Holben B.N., T.F Eck, I. Slutsker, D. Tanré, J.P. Buis, A. Setzer, E. Vermote, J.A. Reagan, Y.J. Kaufman, T. Nakajima, F. Lavenu, I. Jankowiak and A. Smirnov, 1998: AERONET - A federated Instrument Network and Data Archive for Aerosol Characterization, *Rem. Sens. Environ.*, **66**, 1-16.
- Liberti G. L., F. D'Ortenzio, R. Santoleri, C. McClain, M. Wang, G. Volpe, 2001: Validation of the SeaWiFS aerosol products over the Mediterranean Sea". The EUMETSAT meteorological satellite data users' conference. 1-5 October 2001, Antalya Turkey.
- Morel, A. and André, J.-M. 1991: Pigment distribution and primary production in the western Mediterranean as derived and modeled from Coastal Zone Color Scanner observations, *J. Geophys. Res.*, **96**, 12,685-12,698.
- Moulin, C., F. Dulac, C. E. Lambert, P. Chazette, I. Janowiak, B. Chatenet and F. Laven 1997b: Long-term daily monitoring of Saharan dust load over ocean using Meteosat ISCCP-B2 data, 2, Accuracy of the method and validation using Sun photometer measurements, *J. Geophys. Res.*, **102**, 16959-16970.
- Mueller, J. L. and Austin, R. W. 1995: Ocean Optics Protocols for SeaWiFS Validation, Revision 1, SeaWiFS Technical Report Series, Vol. 25, S. B. Hooker, E. R. Firestone and J. G. Acker (eds.), NASA Technical Memorandum 104566, Greenbelt, Maryland.
- O'Reilly, J. E., S. Maritorena, D. Siegel, D., M.C. O'Brien, D. Toole, B.G. Mitchell, M. Kahru, F. Chavez, et al. 2000: Ocean color chlorophyll a algorithms for SeaWiFS, OC2, and OC4: Version 4, SeaWiFS Postlaunch Technical Report Series, edited by Hooker, S. B and Firestone, E. R. Volume 11, SeaWiFS Postlaunch Calibration and Validation Analyses, Part 3. NASA, Goddard Space Flight Center, Greenbelt, Maryland. 9-23.
- Siegel, D.A., M. Wang, S. Maritorena, and W. Robinson, 2000: Atmospheric correction of satellite ocean color imagery: the black pixel assumption, *Appl. Opt.*, **39**, 3582-3591.
- Wang, M., 2000: SeaWiFS atmospheric correction algorithm updates, The SeaWiFS Postlaunch Technical Report Series, Vol. 9, NASA Tech. Memo. 2000-206892, S.B. Hooker and E.R. Firestone, Eds., NASA Goddard Space Flight Center, Greenbelt, Maryland, p57-63.

- Wang, M., S. Bailey, C. Pietras, C. R. McClain, and T. Riley, 2000: SeaWiFS aerosol optical thickness matchup analyses, The SeaWiFS Postlaunch Technical Report Series, Vol. 10, NASA Tech. Memo. 2000-206892, S.B. Hooker and E.R. Firestone, Eds., NASA Goddard Space Flight Center, Greenbelt, Maryland, 39-44.
- Webb, A.R., A.F. Bais, M. Blumthaler, G-P. Gobbi, A. Kylling, R. Schmitt, S. Thiel, F. Barnaba, T. Danielsen, W. Junkermann, A. Kazantzidis, P. Kelly, R. Kift, G.L. Liberti, M. Misslbeck, B. Schallart, J. Schreder and C. Topaloglou, 2001: Measuring Spectral Actinic Flux and Irradiance: Experimental Results. from the ADMIRA (Actinic Flux Determination from Measurements of Irradiance). In press *J. Atm Oc. Tech.*.



# REPORT DOCUMENTATION PAGE

*Form Approved*  
OMB No. 0704-0188

Public reporting burden for this collection of information is estimated to average 1 hour per response, including the time for reviewing instructions, searching existing data sources, gathering and maintaining the data needed, and completing and reviewing the collection of information. Send comments regarding this burden estimate or any other aspect of this collection of information, including suggestions for reducing this burden, to Washington Headquarters Services, Directorate for Information Operations and Reports, 1215 Jefferson Davis Highway, Suite 1204, Arlington, VA 22202-4302, and to the Office of Management and Budget, Paperwork Reduction Project (0704-0188), Washington, DC 20503.

<b>1. AGENCY USE ONLY (Leave blank)</b>		<b>2. REPORT DATE</b> March 2002	<b>3. REPORT TYPE AND DATES COVERED</b> Technical Memorandum	
<b>4. TITLE AND SUBTITLE</b> SIMBIOS Project 2001 Annual Report			<b>5. FUNDING NUMBERS</b> 970	
<b>6. AUTHOR(S)</b> Giulietta S. Fargion and Charles R. McClain				
<b>7. PERFORMING ORGANIZATION NAME(S) AND ADDRESS (ES)</b> Laboratory for Hydrospheric Processes Goddard Space Flight Center Greenbelt, Maryland 20771			<b>8. PERFORMING ORGANIZATION REPORT NUMBER</b> 2002-01288-1	
<b>9. SPONSORING / MONITORING AGENCY NAME(S) AND ADDRESS (ES)</b> National Aeronautics and Space Administration Washington, DC 20546-0001			<b>10. SPONSORING / MONITORING AGENCY REPORT NUMBER</b> TM—2002—210005	
<b>11. SUPPLEMENTARY NOTES</b> G.S. Fargion, Science Applications International Corporation, Beltsville, Maryland				
<b>12a. DISTRIBUTION / AVAILABILITY STATEMENT</b> Unclassified—Unlimited Subject Category: 48 Report available from the NASA Center for AeroSpace Information, 7121 Standard Drive, Hanover, MD 21076-1320. (301) 621-0390.			<b>12b. DISTRIBUTION CODE</b>	
<b>13. ABSTRACT (Maximum 200 words)</b> The purpose of this technical report is to provide current documentation of the Sensor Intercomparison and Merger for Biological and Interdisciplinary Oceanic Studies (SIMBIOS) Project activities, NASA Research Announcement (NRA) research status, satellite data processing, data product validation, and field calibration. This documentation is necessary to ensure that critical information is related to the scientific community and NASA management. This critical information includes the technical difficulties and challenges of validating and combining ocean color data from an array of independent satellite systems to form consistent and accurate global bio-optical time series products. This technical report is not meant as a substitute for scientific literature. Instead, it will provide a ready and responsive vehicle for the multitude of technical reports issued by an operational project. The SIMBIOS Science Team Principal Investigators' (PIs) original contributions to this report are in chapters four and above. The purpose of these contributions is to describe the current research status of the SIMBIOS-NRA-96 funded research. The contributions are published as submitted, with the exception of minor edits to correct obvious grammatical or clerical errors.				
<b>14. SUBJECT TERMS</b> SIMBIOS, ocean color data, bio-optical time series.			<b>15. NUMBER OF PAGES</b> 184	
			<b>16. PRICE CODE</b>	
<b>17. SECURITY CLASSIFICATION OF REPORT</b> Unclassified	<b>18. SECURITY CLASSIFICATION OF THIS PAGE</b> Unclassified	<b>19. SECURITY CLASSIFICATION OF ABSTRACT</b> Unclassified	<b>20. LIMITATION OF ABSTRACT</b> UL	